

# Design, synthesis and characterisation of rigid rod conjugated organometallic polymers and their molecular precursors

Al-Suti, Mohammed K.

*Award date:*
2005

*Awarding institution:*
University of Bath

# Design, Synthesis and Characterisation of Rigid Rod Conjugated Organometallic Polymers and their Molecular Precursors

Submitted by Mohammed K. Al-Suti
For the Degree of Doctor of Philosophy
of the Department of Chemistry of the University of Bath
July 2005.

## COPYRIGHT NOTICE



Mohammed K. Al-Suti





ProQuest LLC
789 East Eisenhower Parkway
P.O. Box 1346
Ann Arbor, MI 48106-1346

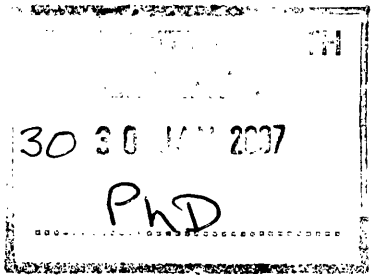
30 3 0 2007
PhD

# ACKNOWLEDGEMENTS

Many thanks with obeisance to my supervisor in the Department of Chemistry at the University of Bath, Professor Paul R. Raithby, DSc. for his valuable advice and help during the past four years. Professor Raithby encouraged me to continue my Ph. D. after the M. Phil and made things so smooth for me to register, conduct my Ph.D. work at Bath and complete my Ph. D. in a very enjoyable environment.

I also profusely thank my supervisor in the Department of Chemistry at Sultan Qaboos University, Professor Muhammad S. Khan for looking after me so very well over the years as well as funding my Ph.D. project. Professor Khan had unlimited patience to listen to my multi-facet problems at home and abroad and always came up with brilliant ideas to solve my problems.

Special thanks go to Professor Sir Richard H. Friend FRS, Dr. Anna Köhler and their students Joanne S. Wilson, Clare Boothby, Ning Zhang and Lakshmi S. Devi for their wonderful contribution to the optical spectroscopy of conjugated materials.

Many thanks go to Drs. Mary F. Mahon, Birte Ahrens, Louise Male, J. Bjernemose and Ms. Hazel Sparkes for solving the crystal structures reported in this thesis.

Thanks to the Chemistry Departments at the University of Bath, UK and Sultan Qaboos University, Oman for providing excellent working environments and logistic supports for the work.

Finally, I would like to thank all members of my family. Without their support, I could not survive the long struggle of my doctoral study.

# ABSTRACT

The thesis contains a description of the synthesis, characterisation and optical spectroscopy of rigid rod conjugated Pt(II) di-ynes and poly-ynes and their molecular precursors. Pt(II) di-ynes of the general formula, *trans*-[$(Et_3P)_2PhPt$-C≡CRC≡C-$PtPh(PEt_3)_2$] and that of the Pt(II) poly-ynes, *trans*-[-$Pt(P^nBu_3)_2$-C≡C-R-C≡C-]$_n$ where R = aromatic or heteroaromatic spacer group, have been synthesised with various R groups by the dehydrohalogenation polycondensation reaction of *trans*-$[(P^nBu_3)_2PtCl_2]$ with the diterminal alkynes.

The thesis contains six chapters: Chapter One gives a brief introduction to metal-containing polymeric poly-ynes and their molecular precursors.

Chapter Two contains details of the synthesis, thermal stability, X-ray crystallographic studies and optical spectroscopy of the organic ligands, rigid-rod conjugated di-ynes and poly-ynes with derivatised benzene linkers as the spacer groups. Those include the fused naphthalene and anthracene spacers as well as amino, flouro, and alkoxy substituted benzene compounds.

Chapter Three contains details of the synthesis, thermal stability, X-ray crystallographic studies and optical spectroscopy of the organic ligands, rigid-rod conjugated di-ynes and poly-ynes with oligopyridiyl linkers as the spacer groups. Comparisons were made among the two and three fused pyridine spacers as well as with the poly-yne and di-yne containing a mono-pyridine as the spacer.

Chapter Four contains details of the synthesis, thermal stability, X-ray crystallographic studies and optical spectroscopy of the organic ligands, rigid-rod conjugated di-ynes and poly-ynes with fused oligothienyl linkers as spacer groups. Those include thienothiophene and di-thienothiophene spacer groups and comparisons were made with the poly-ynes and di-ynes containing non-fused bi-thiphene and terthiophene spacers.

Chapter Five: contains details of the synthesis, X-ray crystallographic studies and optical spectroscopy of the organic ligands, rigid-rod conjugated di-ynes and poly-ynes with various aromatic, hetero-aromatic and mixed hereocyclic spacer groups.
Chapter Six lists the details of experimental procedures for the synthesis of all compounds reported in chapters 2-5.

# LIST OF ABBREVIATION

| | |
|---|---|
| $^{n}$Bu | n-Butyl |
| $^{n}$BuLi | n-Butyllithium |
| Et | Ethyl |
| X | Halogen |
| THF | Tetrahydrofuran |
| Me | Methyl |
| TMS | Trimethylsilyl |
| TMSA | Trimethylsilyl acetylene |
| M | Metal |
| MPYs | Metallo-poly-ynes |
| DMF | N,N-dimethylformamide |
| L | Ligand |
| LDA | Lithium diisopropylamide |
| NBS | N-Bromosuccinimide |
| R | Aromatic or hetero-aromatic spacer group |
| Ph | Phenyl |
| Py | Pyridyl |
| Bipy | Bipyridine |
| $^{i}$Pr | *Iso*-propyl |
| $^{i}Pr_2NH$ | Diisopropylamine |
| Th | Thienyl |
| mmol | Millimol |
| mg | Milligram |
| min | Minute |
| h | Hour |
| rt | Room temperature |
| NLO | Non linear optical |
| P | Polarisation |
| $\chi$ | Non-linear optical susceptibility |
| $\beta$ | Second order non-linear optical term |

| | |
|---|---|
| $\gamma$ | Third order non-linear optical term |
| $\gamma'$ | Hyperpolarizability (real component) |
| $\gamma''$ | Hyperpolarizability (imaginary component) |
| Å | Angstrom |
| HOMO | Highest occupied molecular orbital |
| LUMO | Lowest unoccupied molecular orbital |
| A | Acceptor |
| D | Donor |
| D. P. | Degree of polymerisation |
| TLC | Thin layer chromatography |
| IR | Infrared |
| GPC | Gel permission chromatography |
| UV | Ultraviolet |
| vis | Visible |
| eV | Electron-volt |
| TGA | Thermogravemetric analysis |
| $S_0$ | Ground state (singlet) |
| $S_1$ | First singlet excited state |
| $T_1$ | First triplet excited state |
| LCD | Liquid crystal display |
| PL | Photoluminescence |
| OA | Optical absorption |
| LED | Light emitting diode |
| br | Broad |
| sh | Shoulder |
| NMR | Nuclear magnetic resonance |
| $\delta$ | Chemical shift |
| ppm | Parts per million |
| s | Singlet |
| d | Doublet |
| dd | Doublet of doublets |
| td | Triplet of doublet |
| t | Triplet |
| m | Multiplet |

| | |
|---|---|
| brs | Broad singlet |
| J | Coupling constant |
| Hz | Hertz |
| $\{^1H\}$ | Proton-decoupled |
| MS | Mass spectrometry |
| EI | Electron impact |
| FAB | Fast atomic bombardment |

# TABLE OF CONTENTS

# LIST OF TABLES

# LIST OF FIGURES

# LIST OF SCHEMES

# CHAPTER 1

# INTRODUCTION

## 1.1 Brief History

Extensive studies in the area of π-conjugated materials have been carried out over the last two decades. Research in this area has produced a wide variety of new and important results, that has lead to the development of "conducting polymers", "light emitting materials", and "synthetic metals"[1]. Synthetic developments in the areas of organic, inorganic and organometallic chemistry have been paralleled by developments in new electronic techniques, that have occurred during the second half of the 20th century, and which have lead to the development of new smart materials[2].

The development of polymer science has been largely in the area of organic chemistry and one of the most valued properties of synthetic polymers has been their ability to act as excellent electrical insulators, e.g., polyethylenes and teflon. However, the preparation and characterization of some conjugated organic polymers containing aryl groups (aromatic and heteroaromatics) e.g., poly(*p*-phenylene)[3] (PPP), poly(pyridine-2,5-diyl)[4] (PPy), poly(thiophene-2,5-diyl)[5] (PTh) and some linear conjugated polymers with alternating aryl and vinyl or ethynyl groups in the backbone, poly(phenylenevinylene)[6] (PPV) and poly(*para*phenylenethynylene)[7] (PPE) have led to systems with extensive electronic delocalization. It is these conjugated polymer backbones that are responsible for the conducting/optical properties of these materials[8] **(Figure 1.1).**

In the late 1970s, two important developments in this field were brought to the public domain. The first was the discovery of the concept of doping and applying that to poly-acetylenes by MacDiarmid et. al.[9], while the second was the synthesis and characterization of high molecular weight metal acetylide polymers by Hagihara and co-workers[8,10]. The first discovery facilitated the preparation and processing of what was believed to be the first examples of "conducting polymers" (CP) which gave incentive to the manufacture of low-cost disposable plastic electronic devices.

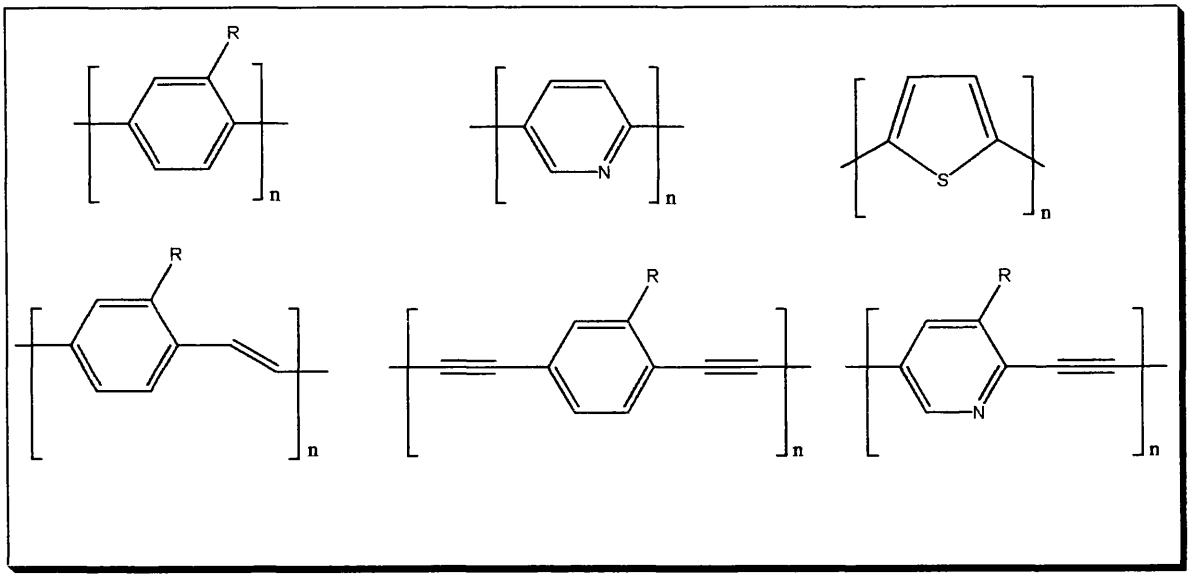


**Figure 1.1: Some examples of conjugated organic polymers**

The second result illustrated the possibility of preparing soluble rigid-rod high molecular weight conjugated polymers with metal moieties in the main chain (**Figure 1.2).** It has long been recognized that introducing transition metals into organic polymeric structures is an efficient way for preparing new materials with diverse backbone structures and new properties that differ from the carbon based materials[11]. In addition, it was observed in 1990 that when passing an electric current through certain conjugated polymers it was possible to produce light emission (electroluminescence)[12]. Thus, properties of transition metals like variable oxidation states, colour, coordination numbers and geometry can be combined with the properties of organic compounds like solubility in organic solvents and processability to give novel materials with interesting redox, magnetic, optical and electrical characteristics as well as other properties like mechanical deformation into various forms. Such properties have led these materials to have potential as active components in applications such as light emitting diodes (LEDs) [13], lasers[14], photocells[15], field effect transistors (FETs)[16], electroluminescence[17], non-linear optics and optical information storage[18], *etc*...

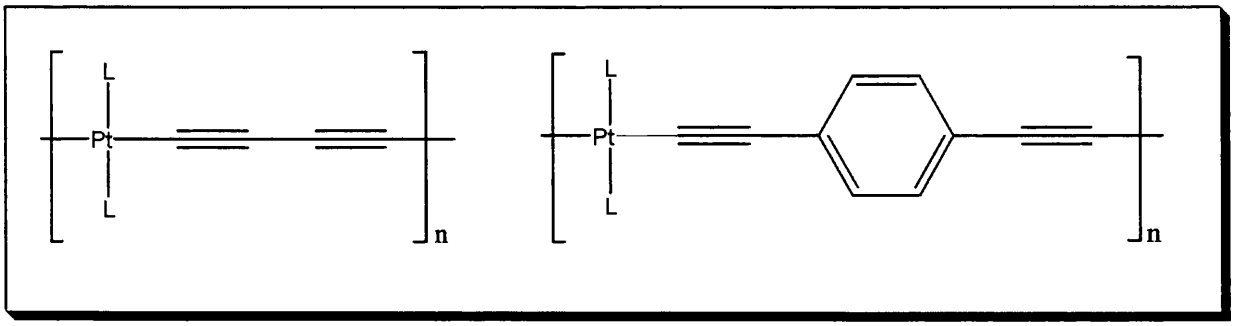


**Figure 1.2: Some Pt(II) poly-yne polymers synthesized by Hagihara's group**

It was against the backdrop of such information that a significant worldwide research effort has been dedicated to develop the theoretical and practical aspects of transition metal based organic polymer chemistry[19]. The motivation was based on the synthetic flexibility of these materials where the polymer can be structurally modified by changing the metal, organic spacer group and the ancillary ligands attached to the metals as well as the novel properties and potential applications demonstrated by these polymers.

A variety of synthetic strategies have been developed to assemble the molecular precursors into macromolecules, hence, a number of metals have been incorporated in the polymer structures and various types of organic ligands have been utilized to link the different metals to form various novel metallo-organic π-conjugated macromolecules[20] (**Figure 1.3**).

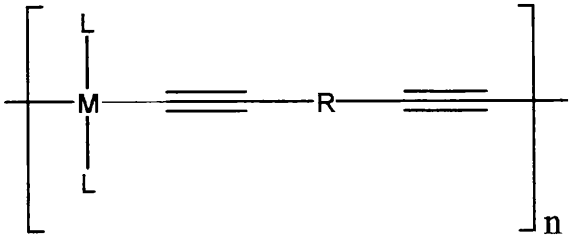


M = Gr. 10 metals

L = Tertiary phosphines or arsines

R = None, aromatic or hetero-aromatic ring

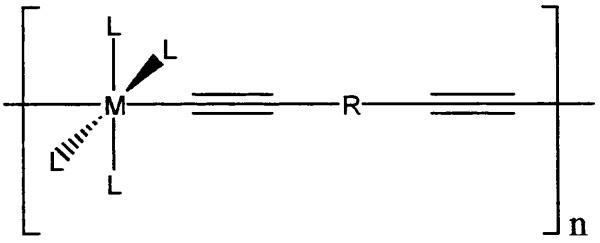


M = Gr. 8-9 metals

L = Phosphines, carbonyls

R = None, aromatic or hetero-aromatic ring

**Figure 1.3: General formulae of group 8-10 transition metal poly-ynes**

# 1.2 Synthesis

## 1.2.1 Ligand precursors

The cross-coupling reaction of organometallic reagents with organic halides and other electrophiles represents the most straightforward method for the carbon-carbon bond formation[21]. Various cross-coupling reactions have been utilized to synthesize alkynyl-functionalized aromatic ligands such as the reaction between lithium, magnesium and sodium alkynyls with active halides[21]. Conjugated terminal acetylenes can be prepared from acetylene gas or acetylenes with protecting groups like trimethylsilyl (TMS) group. The general synthesis of the acetylene ligands used in the preparation of the metal complexes in this project is outlined in **Scheme 1.1**, where Sonogashira-type metal catalyzed cross-coupling reaction was applied to introduce the acetylenic moieties on the aromatic ring. The cross-coupling reaction between dihalo-arene and trimethylsilylacetylene (TMSA) introduces the acetylene moieties in the aromatic ring. This reaction requires a set of catalysts and an amine solvent for neutralizing the acidic by-product (HX). Amine solvents also act as proton acceptors and form a complex with the halide anion, thus playing a dual role in such reactions. Dibromo arenes need longer time and higher temperatures (24h / 80 °C) than the diiodo analogues (2 h/ r.t). The diterminal alkynyl ligand is prepared by a smooth removal of the trialkylsilyl group by a mixture of aqueous KOH in MeOH/THF by a proto-desilylation reaction. The reaction is smooth and run in almost 1h at room temperature.

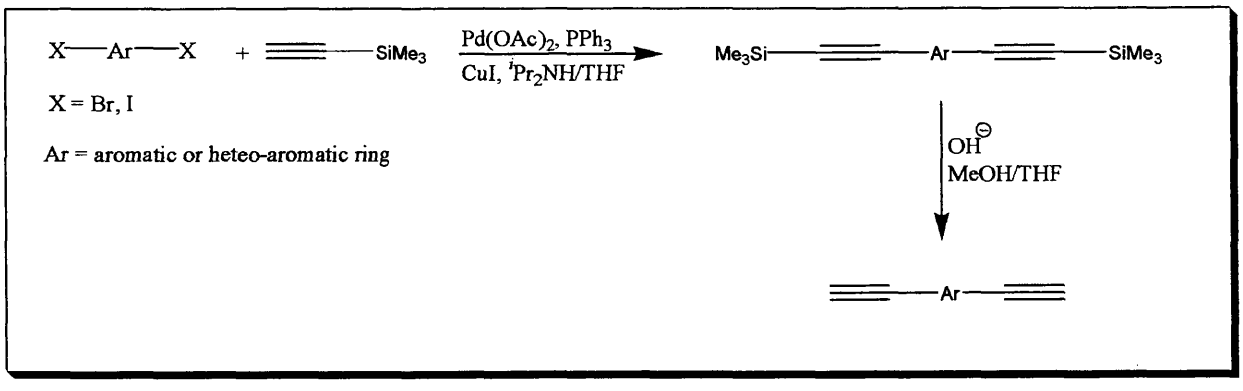


**Scheme 1.1: Synthesis of di-terminal alkynes**

## 1.2.2 Mechanism of the cross-coupling reaction

The palladium/copper-catalyzed cross coupling of terminal alkynes with aryl halides is the most powerful method for introducing the carbon-carbon triple bond into the arene spacer group. T. B. Marder[22] and co-workers showed by some quantitative analysis experiments that the catalyst initiation proceeds via reduction of $Pd^{II}$ to $Pd^0$. If air is present, the catalyst mixture and the amine solvent become a very effective system for catalyzing the terminal alkynes into a homocoupled products (diynes) and thus air must be excluded from the cross-coupling reaction.

## Catalyst initiation and homo-coupling process

A generally accepted mechanism for the cross-coupling reaction was proposed initially by Hagihara and co-workers[23], in which $PdCl_2(PPh_3)_2$ is the catalyst precursor. **Scheme 1.2** shows the whole process, which can be divided into two parts: 1) catalyst initiation; and 2) the catalytic cycle. A small amount of di-yne was observed in the reaction which might be the by-product resulting from the initial formation of bis(triphenylphosphine)bis(trimethylsilylethynyl)palladium(II) when $PdCl_2(PPh_3)_2$ reacts with an alkynyl cuprate complex in the presence of a base. Reductive elimination of bis(trimethylsilyl)butadiyne would give $Pd(PPh_3)_2$. Thus reduction of $Pd^{II}$ to $Pd^0$ is accomplished via the oxidative coupling of two equivalents of $Me_3SiC{\equiv}CH$. $Pd(PPh_3)_2$ undergoes oxidative addition with aryl halide to form $Pd(PPh_3)_2(Ar)(X)$, *trans*-metallation gives $Pd(PPh_3)_2(Ar)(C{\equiv}CR)$, followed by reductive elimination giving ethynylarenes and regenerating $Pd(PPh_3)_2$.

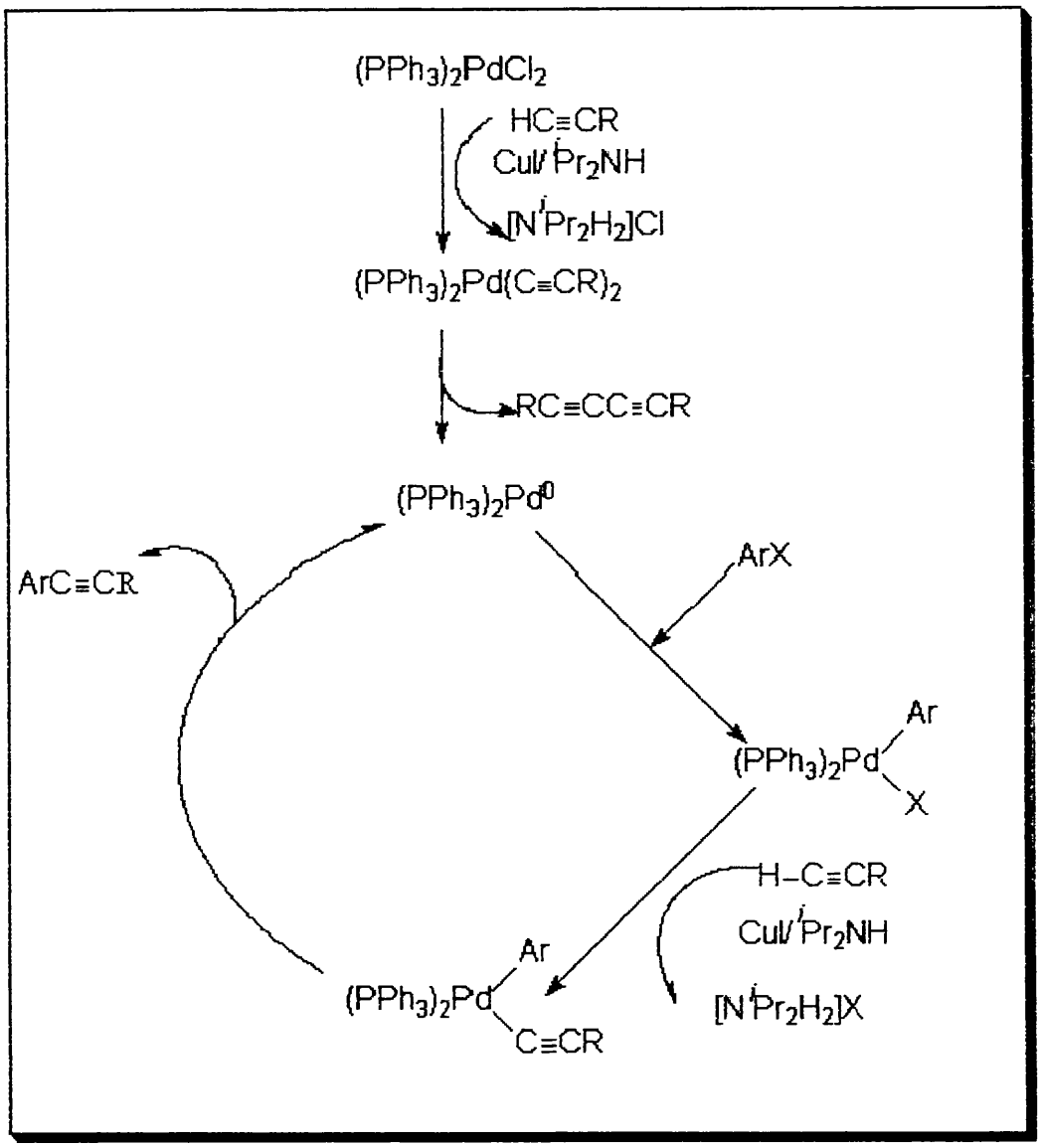


**Scheme 1.2**. Mechanism of the cross-coupling reaction

## 1.2.3 Metal acetylides

A wide range of synthetic methods has been utilized for the synthesis of metal acetylides. Some methods can be widely applied, while others are specific to a particular metal. **Condensation** reactions involve the elimination of small molecules e.g. $H_2O$, HX (X = Br, Cl, or I) from two precursors. The resultant polymer contains repeat units with fewer atoms than the sum of the two precursors. The likihood of this reaction giving a high molecular weight polymer lies in the

exact ratio of 1:1 between the two precursors, which should be of high purity. **Oxidative coupling** could be utilized to obtain polymers from metal acetylides that contain terminal ≡CH groups. This reaction produces polymers with a high degree of polymerization, as the process is dependent upon only a single monomer type. The degree of polymerization using condensation reactions approach, on the other hand, is dependent upon the exact ratio of the reacting species. Another attractive feature of oxidative coupling is the lengthening of the conjugated organic spacer in that varying the inter-metal distance may result in slightly different polymer properties.

The first platinum σ-acetylide complexes were reported in 1959 by Chatt and Shaw[24], who applied transmetallation reactions to react compounds like *cis*-$L_2PtCl_2$ (L =$PEt_3$ or $AsEt_3$) with metal acetylide reagents (Na or Mg phenylacetylides) in basic media to yield *trans*-$L_2Pt(C{\equiv}C\text{-}C_6H_5)_2$ materials (**Scheme 1. 3**).

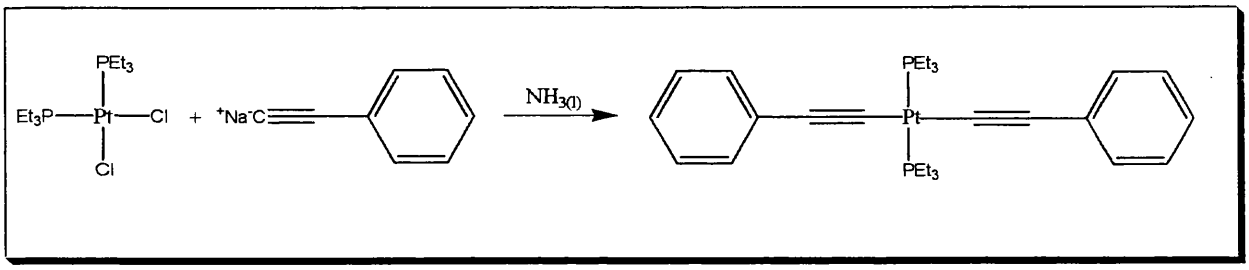


**Scheme 1.3: Synthesis of Pt(II) acetylides by trans-metallation reactions**

Transmetallation was the major method for the synthesis of metal acetylides but the drawbacks of this method led chemists to think about alternative types of reactions. Many difunctionalised acetylenes would react at both ends leading to side reactions. In addition, the monomers are sensitive to moisture and air and pure samples are extremely difficult to obtain.

As early as 1960, the synthesis of the first metal acetylide polymers was reported, however, they were not soluble and thus further characterization was not possible[25](**Figure 1.4**). The insolubility resulted from the exposed nature of the conjugated organic portions, which presumably results in strong lattice interaction and poor interaction with solvent molecules.

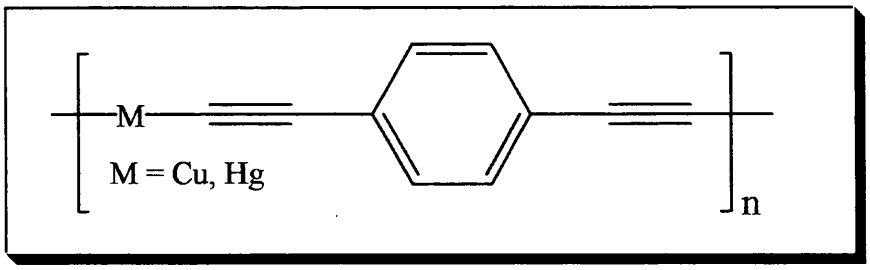


**Figure 1.4: Examples of insoluble polymers**

In late 1970s, Hagihara synthesized the first soluble σ-acetylide polymers containing group 10 metals (**Scheme 1.4**). Hagihara and co-workers used three different types of reactions (i) **dehydrohalogenation** between bis-ethynyl metal complexes and metal halides, catalyzed by cuprous halide, which provided the first soluble polymers containing transition metal-carbon σ-bond in the main chain. (ii) **oxidative coupling** of terminal acetylides using CuI and $O_2$ as in Hay coupling and (iii) **alkynyl ligand exchange**, catalyzed by cuprous iodide in amines was used to prepare nickel complexes, which were difficult to prepare, by the other methods. The nickel halides required for dehydrohalogenation are unstable in the presence of amines and the nickel-bis-acetylide complex required for oxidative coupling is unstable to the oxidant. The starting material in this process, $L_2Ni(C{\equiv}CH)_2$, was prepared by treating $L_2NiX_2$ (X = halide) with HC≡CMgBr in diethyl ether.

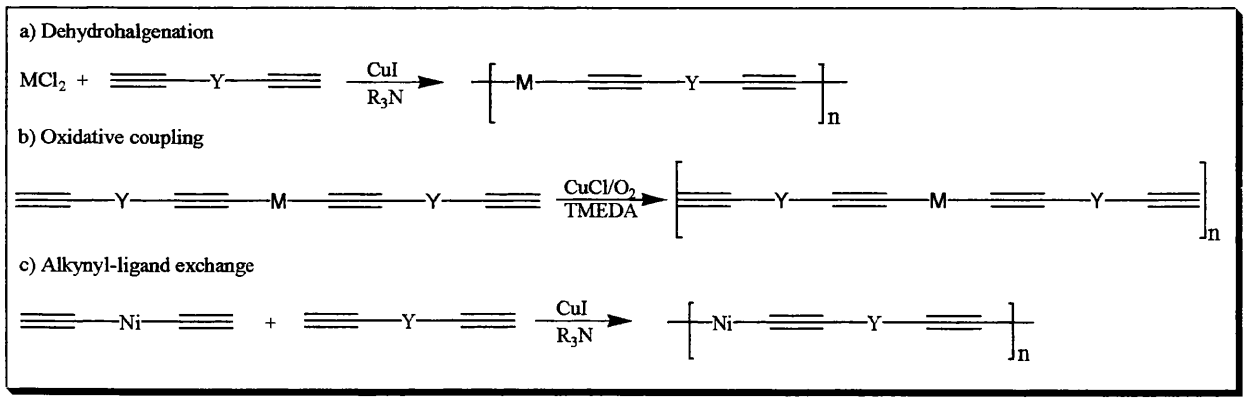


**Scheme 1.4: Hagihara's methods for group 10 metal-based polymers**

**Scheme 1.5** shows the possible mechanism for the Cu-catalyzed dehydrohalogenation reaction between terminal acetylides and metals halides[26]. A copper-amine complex is formed during

the reaction which then reacts with the terminal acetylide to yield a copper-acetylide complex.

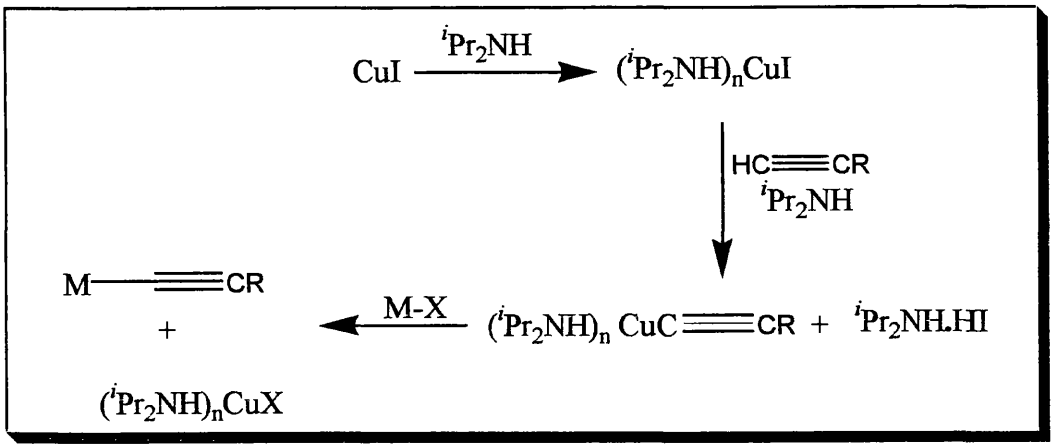


**Scheme 1.5: Possible mechanism for the Cu-catalyzed dehydrohalogenation reaction**

This then undergoes transmetallation with the metal halide to yield the metal acetylide at the end.

Polycondensation has been mostly used in the preparation of metal containing poly-ynes and it works very well for the production of materials with high purity and molecular weights. The condensation reactions used were i) dehydrohalogenation (**Scheme 1.4**) ii) metathesis method involving trimethyltin reagents and metal halides, developed by Lewis and co-workers[27] and iii) C-H bond activation involving reaction between diterminal alkynes and coordinatively unsaturated metal alkyl complexes[28] (**Scheme 1.6**). Although the condensation reactions were applied for some syntheses, which led to low molecular weight and insoluble materials[29]; an exception to that are the platinum-containing poly-ynes with butyl phosphines groups [30].

The metathesis method using the stannyl derivative has advantages over the dehydrohalogenation method in that i) higher molecular weights were achieved and ii) a wide variety of transition metals (group 8,9 and 10) could be incorporated as a wide range of organic solvents could be used including $CH_2Cl_2$, THF, toluene, *etc.* The method is not restricted to amines whereas in dehydrohalogenation, amines are essential components for the synthesis. With group 8 and 9 metals using this reaction conditions, the amines react with metals and form metal amides complexes rather than metal acetylides. The major disadvantage of the tin route is the handling of the toxic trimethyltin reagents.

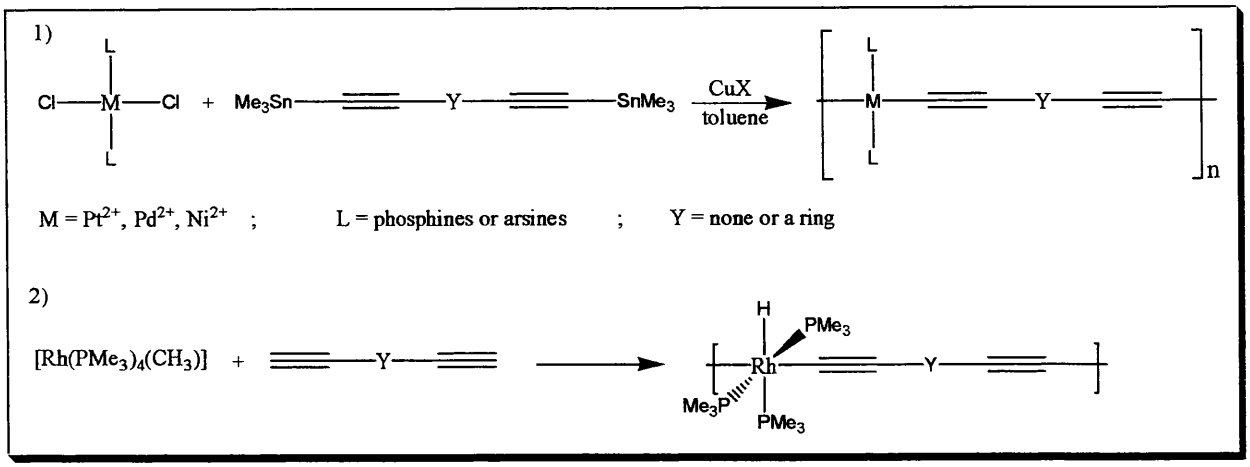


**Scheme 1.6: 1) metathesis and 2) C-H bond activation polymerizations**

# 1.3 Structural consideration

Alkynyl groups possess linear geometry, structural rigidity, extended electronic delocalization and the ability to interact with the metal centers *via* pπ-dπ frontier orbital overlap which made them attractive candidates as building blocks for the high molecular weight materials. These materials hold promise for the synthetic, structural, and materials chemists alike. Linear chains of carbon atoms with alternating single and triple bonds, i.e., $(-C\equiv C-)_n$, are known as poly-ynes. The problem with these one-dimensional rods is the lack of processability and the thermal and environmental instability makes them less attractive than conventional materials[31], hence in order to use these ligands for linking transition metals a spacer group is necessary. These compounds are most stable when they are protected with end groups such as $R_3Si$ (trialkylsilyl groups). However, acetylene materials with stannyl end groups are more stable than the tertiary silyl derivatives and these may be used in reactions without spacer groups.

The spacer groups most generally used include aromatic/ heteroaromatic rings that impart enhanced thermal stability to the acetylene ligands and to the polymers. In addition to thermal and environmental stability they also provide the versatility for modification leading to studies of the structure/property relationship. They can be functionalised with various electron donating/withdrawing substituents to generate a huge number of materials where properties can be explained in terms of the structure.

A comparative study of how the variation of the chemical structure affects the physical

properties and electronic structure shows that conjugation is increased by the electron rich thiophene units while this is reduced for the pyridine units compared to the neutral phenylene units[32].

The donor-acceptor interaction has an effect in controlling the HOMO-LUMO band gap in these polymers, which is a key feature for conductivity. Hence, the organic ligands may be modified in the polymer backbone either by using derivatised spacers or by altering the spacer itself. The spacers used have ranged from electron rich to electron deficient systems and this may be enhanced by substitution on the ring by electron donating / withdrawing groups (**Figure 1.5**). A summary of the band gaps for a series of platinum(II) poly-ynes showing the difference that the spacer group makes is given in **Table 1.1.**

**Table 1.1: Band gaps of some platinum(II) poly-ynes as a function of the organic ligand[8-15]**

| Compound | Band gap/eV |
|---|---|
| $[-Pt(P^nBu_3)_2-C\equiv C-C\equiv C-]_n$ | 2.70 |
| $[-Pt(P^nBu_3)_2-C\equiv C-C\equiv C-C\equiv C-]_n$ | 2.33 |
| $[-Pt(P^nBu_3)_2-C\equiv C-p-C_6H_4-C\equiv C-]_n$ | 3.28 |
| $[-Pt(P^nBu_3)_2-(C\equiv C)_2-p-C_6H_4-(C\equiv C)_2-]_n$ | 3.01 |
| $[-Pt(P^nBu_3)_2-C\equiv C-2,5-C_4H_2S-C\equiv C-]_n$ | 2.80 |
| $[-Pt(P^nBu_3)_2-C\equiv C-(C_4H_2S)_2-C\equiv C-]_n$ | 2.55 |
| $[-Pt(P^nBu_3)_2-C\equiv C-(C_4H_2S)_3-C\equiv C-]_n$ | 2.40 |

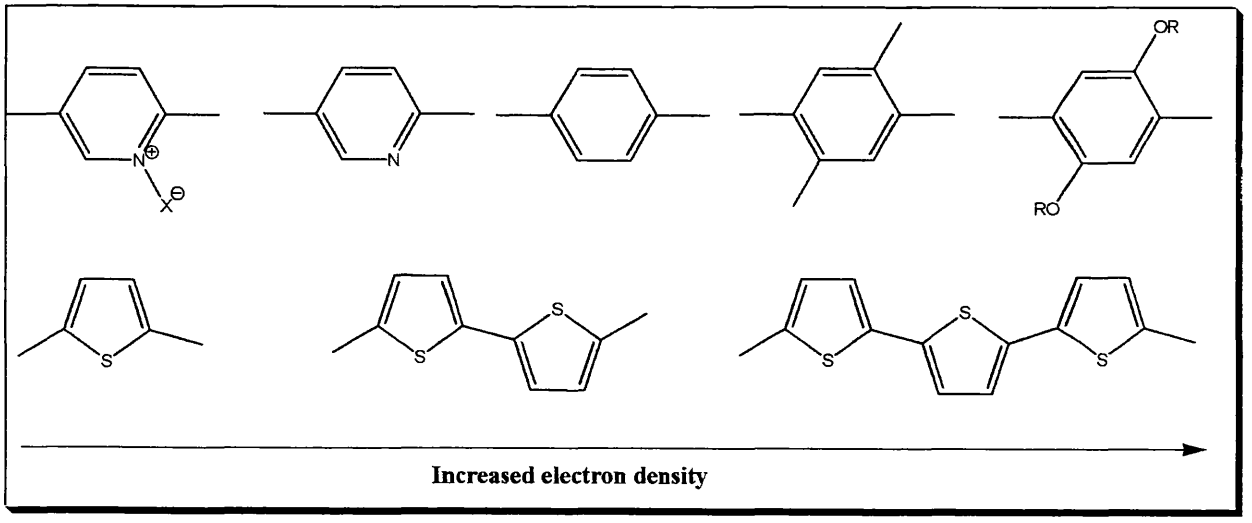


**Figure 1.5: Tailored spacer groups for organo-metallic polymers**

Solubility puts great emphasis on precursor design where a soluble polymer may result. The solubility of these polymers (**Scheme 1.6** and **Table 1.1**) is due to the tri-$^{n}$butylphosphine groups attached to the square planar platinum centres, since the butyl groups are large enough to shield the conjugated backbone allowing strong interaction with solvent molecules. An alternative method for increasing the solubility involves the alkylation of the aromatic rings, and this has the added advantage of tailoring the electronic properties. The alkyl chains used included hexyls, octyls or alkyloxy groups.

The *trans* square planar geometry at the platinum centre coupled with the linear geometry of the acetylene groups and the *para*-substituted aromatic rings provide the polymer with linearity and rigid-rod morphology. Organometallic polymers can be modified by changing the metal, the auxiliary ligands, the spacer group and the substituents on the spacer. With respect to the position of the metal, there are two types of metal containing polymers, (i) main-chain polymers where the metal is an integral part of the polymer backbone and (ii) side-chain polymers where the metal is at a side-chain. The diversity of these polymers can be extended by combining side-chain/main-chain polymers by using N- based spacers such as 2,2'-bipy units in the backbone. These compounds could also be electronically tuned by quaternization on the nitrogen atoms[19] **(Figure 1.6)**.

Various transition metal fragments have been incorporated into these poly-ynes including group 10 (Ni, Pd, Pt), group 9 (Co, Rh), and 8 (Fe, Ru, Os) metals[33]. It has been shown that $d^8$ square planar configuration presents a larger conduction bandwidths then the $d^6$ octahedral configuration, offering a better chance for electrical conduction[37].

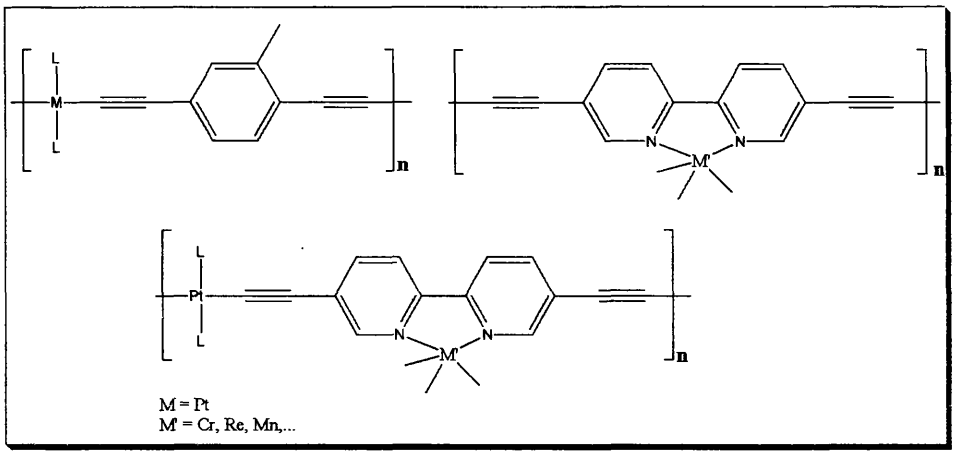


**Figure 1.6: Types of polymers**

The inclusion of metals in the main chain allows emission from the triplet state (phosphorescence)[34]. The spin-orbit coupling associated with heavy atoms like platinum allows significant mixing of singlet and triplet states, so that the spin-forbidden triplet emission are readily accessible. At low temperatures this emission is extremely dominant[35]. This is in contrast to organic polymers in which the triplet emission is difficult to access. The knowledge gained from the study of the photophysics of organometallic polymers can be extended to conjugated hydrocarbon polymers. In addition, as model compounds for physical phenomena these materials have shown promise for opto-electronic applications. For example, if electron withdrawing groups are attached to the aromatic spacer then a high thermal stability is achieved together with the reduction of the band gap and induced charge transfer. Theoretical calculations and experimental evidence have shown that the triplet excited state is localized within the spacer group while the singlet state may be extended over a number of repeat units. Thus, the energy gap between the singlet and triplet can be reduced by altering the nature of the spacer group.

# 1.4 Structure and bonding

As mentioned in earlier sections, these materials possess rigid-rod like structure, which may be linear if the spacer is 6-membered ring such as *para*-substituted benzene or pyridine or bent if

the spacer ring is a 5-memebered heterocycle such as 2,5-substituted thiophene, pyrrole and their derivatives. In all cases, the stability of the M-C σ-bond is dependent on the nature of the

transition metal, the spacer group and the ancillary ligands attached to the metal. *Tertiary* phosphines are able to stabilize the M-C σ-bond by π-backbonding with the metal. The M-C bond does not involve a σ-component only but also an overlap of metal d- and π-orbitals and the π- and π* orbitals of the acetylenes[36]. Various spectroscopic techniques have been exploited to establish the nature of bonding and orbital overlaps in these materials.

## 1.4.1 Vibrational spectroscopy

IR spectral data provide an excellent means of monitoring the reactions as well as qualitative determination of the extent of π-conjugation in the polymer chain. Trimethylsilylethynylarene compounds have a sharp IR peak at *ca.* 2140-2159 $cm^{-1}$ that can be assigned to the C≡C triple bond. The deprotected compounds have a sharp peak at 3300 $cm^{-1}$ that may be assigned to the $C_{sp}$–H bond, while the triple bond in platinum polymers and complexes can be detected at *ca.* 2080-2095 $cm^{-1}$.

The extent of π-conjugation has also been studied by IR spectroscopy. The C≡C absorption frequencies in the organometallic monomer units are higher than that in the polymers and both are lower than that in the organic ligand precursors. Often a red shift is observed in going from the ligand to monomer to polymer. The fact that platinum materials have lower absorption frequencies than the organic ligands could be attributed to metal-to-alkynyl-backbonding or polarization of metal-carbon bond as $M^{\delta+}$-$C^{\delta-}$. A recent investigation by Markwell *et. al.*, showed that ν(C≡C) frequencies are considerably lower for platinum-containing alkyne polymers than the platinum-ethynylaryl polymers. This may suggest greater π-conjugation with an increase in the conjugation length of the organic spacer group.

IR spectroscopy could also be used to determine the isomeric configuration of the metal complexes. *Cis*-$[Pt(PBu_3)_2(C{\equiv}CC{\equiv}CH)_2]$, for example, which has $C_{2v}$ symmetry, has two stretching C≡C IR bands at 2153 and 2145 $cm^{-1}$, and two C–H stretching bands at 3315 and 3295 $cm^{-1}$. The *trans* isomer with $D_{2h}$ symmetry gives only one stretching band at 2147 $cm^{-1}$ for C≡C and one at 3312 $cm^{-1}$ for C–H.

## 1.4.2 Nuclear magnetic resonance spectroscopy

NMR studies have been used to assign the electronic environment of various atoms in the platinum containing poly-yne polymers. $^{1}H$ and $^{13}C$ NMR spectra show various aromatic, heteroaromatic and aliphatic protons and carbon nuclei. As with IR spectroscopy, the $^{31}P$-{$^{1}H$} NMR is used to assign the configuration around the metal centre. The *trans* metal *bis* acetylide monomer $[Pt(P^{n}Bu_3)_2(C{\equiv}C\text{-}R)_2]$ (R = aromatic ring) shows a $^{31}P$ signal in the range +3.0 to +5.0 ppm, while a *cis* monomer gives a signal at -2.0 to -4.0 ppm with respect to 85% phosphoric acid standard.

**Table 1.2: Spectral data of some Platinum acetylide complexes**

| Complex | $\nu_{C\equiv C}/cm^{-1}$ | $\nu_{C\text{-}H}/cm^{-1}$ | $^{31}P$ NMR/ppm[a] $^{1}J$(Pt-P), Hz |
|---|---|---|---|
| *cis*-$[(Bu_3P)Pt(\text{-}C{\equiv}CC{\equiv}CH)_2]$ | 2153, 2145 | 3315, 3295 | + 3.7 (2269) |
| *trans*-$[(Bu_3P)Pt(C{\equiv}CC{\equiv}CH)_2]$ | 2174 | 3307 | - 4.7 (2279) |

[a] referenced to $H_3PO_4$

## 1.4.3 Electronic and optical studies

Several research groups have conducted theoretical and experimental studies of the electronic structures of organometallic conjugated polymers in order to establish structure/property correlations and to improve their electrical and optical properties. The development of different synthetic approaches has made possible the preparation of a large number of materials with different components for reliable comparison of structure/property relationship. Frapper *et. al.*[37] used extended Hückel calculations to study the effect of changing the metal and its coordination geometry and number, the nature of the ligands attached to the metal and the organic spacer groups on the conduction properties of conjugated systems. The bonding properties are accounted for by the usual 16 and 18 electron rules for the square planar and octahedral geometries. When ligands are phosphines, both $ML_2^{2+}$ square planar and $ML_4^{2+}$ octahedral fragments have phosphine lone pairs interacting with metal orbitals of the corresponding

symmetry giving bonding and antibonding molecular orbitals, which are stabilized and destabilized, respectively. Metal d-π orbitals interact also with empty phosphines π-symmetry orbitals, which are much higher in energy. These interactions give rise to the weak π-acceptor ability and σ-donor ability of the phosphine ligands.

In the square planer geometry, the two phosphine lone pairs, which have $a_1$ and $b_1$ symmetry, interact with their symmetry match, M (s + $x^2$-$y^2$) and M (x) orbitals, respectively. The introduction of the alkynyl group forming the M-C σ- bond results in interactions between alkynyl sp-σ orbitals with the metal $p_z$ and $d_{z2}$ empty orbitals. The summary of their conclusion is that (i) π- interactions extend over the polymer chain resulting from continuous overlap of the π-orbitals of the alkynyls and the metal d-orbitals along the whole chain; ii) the band gap decreases with increasing polymer length and (iii) 4-coordinated $d^8$ metals have a greater conduction band width by 0.4 eV than in the 6-coordinated $d^6$ metals.

Lhost et. al.[36] performed Hückel calculations on some platinum-acetylene polymers and concluded the following (i) the platinum atom does not interrupt conjugation and participates in the electronic delocalization to a significant extent; (ii) the decrease in the band gap is due to the stabilization of the HOMO, where as it is found that the LUMO remains approximately at the same energy as chain length increases.

It was also found that the π* orbital of the acetylene ligands is the LUMO for these kinds of complexes, with a slight interaction with the metal $p_z$ orbital, while calculations on the HOMO suggest that it shows metal d orbital character with some contribution of the ligand π orbital.

Extensive optical studies have been carried out on these materials as the luminescence produced by either optical or electrical excitations is a very sensitive probe of the electronic structure[30-33]. **Figure 1.7** summarizes the different processes that occur in the electronic transitions of these materials. The strong absorption and luminescence peaks in these materials are assigned to π-π* transitions. The first absorption band due to absorption of visible or ultraviolet radiation by a molecule causes an electronic transition from the singlet ground state ($S_0$) to an excited singlet state ($S_1$, $S_2$,...). The spins of electrons in $S_0$ and $S_1$ are paired which agree with the quantum mechanical selection rules for electronic transitions.

The photophysical processes mainly occur from the lowest excited singlet state ($S_1$). Since the rate of internal conversion from the upper excited states to the lowest excited singlet state is a very fast process, transitions from the upper excited states are rarely observed

From the excited state a variety of processes may occur. Internal conversion, which is a radiationless process, is the movement of an electron between states of same multiplicity. The movement of the electron from the singlet excited state to the ground state by internal conversion is followed by vibrational relaxation and the process is irradiative, however the electron may relax directly from $S_1$ to $S_0$ and emit light. The $S_1 \rightarrow S_0$ transition is called fluorescence. The electron may also jump from the singlet excited state to a triplet state by a radiationless process called inter-system crossing. From this point the electron will relax to the lowest vibrational level of the triplet state and then two processes may occur, either another intersystem crossing to $S_0$ and then vibrational relaxation to the lowest vibrational level of $S_0$ (irradiative transition), or that electron may relax directly from $T_1 \rightarrow S_0$ through a radiative process (phosphorescence). The lifetime of florescence is short ($10^{-8}$-$10^{-12}$ s), while phosphorescence has a much longer lifetime ($10^{-2}$-$10^{2}$ s) and is a spin forbidden transition. However, the introduction of a heavy metal atom in the polymer backbone enhances the spin orbit coupling and thus the intersystem crossing from singlet to triplet manifolds increases and emission from the triplet state is observed in conjugated organometallic systems.

Usually, the triplet states of conjugated polymers are investigated by using indirect methods such as triplet-triplet absorption measurements, energy transfer, optically detected magnetic resonance or delayed fluorescence. Such measurements give partial information on the triplet states, whereas direct measurements of the triplet state give access to the energies, vibrational structure, temperature dependence and lifetimes.

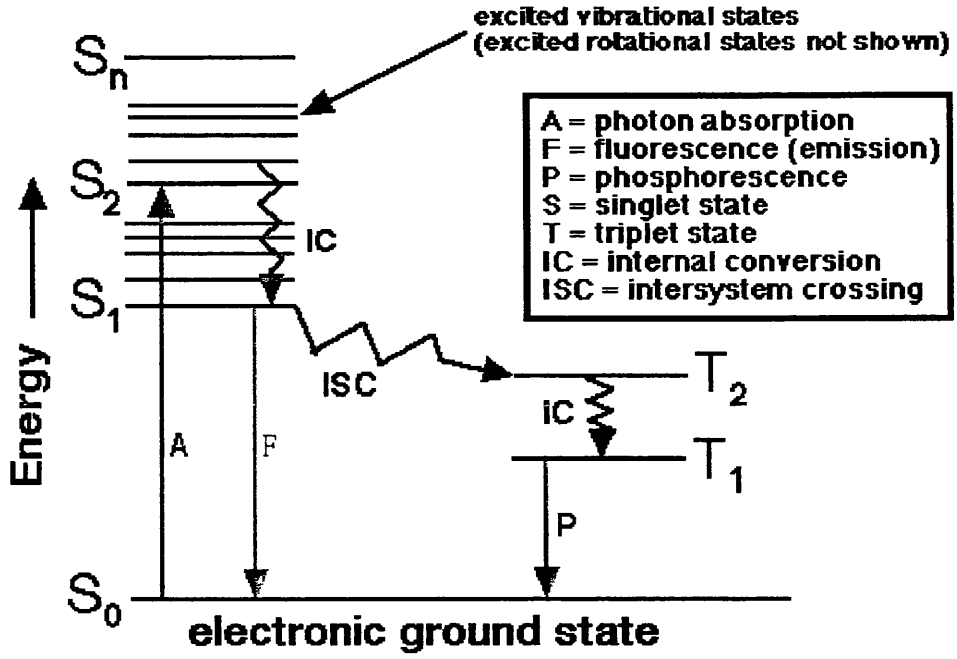


Figure 1.7: The Jablonski diagram

# 1.5 Applications

## 1.5.1 Non linear optics

Metal-containing polymers have been studied by laser spectroscopy in order to explore their non-linear optical properties. Materials that possess non-linear properties have applications in optical data storage, optical communications, optical switching, image processing and computing[18].

These properties are measured in terms of polarization of the material by the formula:

$$P = \alpha E + \beta E^2 + \gamma E^3 + .....$$

which is analogous to

$$P = P_0 + \chi^{(1)}E + \chi^{(2)}E^2 + \chi^{(3)}E^3 + ... + \chi^n E^n$$

where $P_0$ is the static dipole of the sample, E is the electric field and $\chi^n$ is the $n^{th}$ order non-linear optical susceptibility. A material is said to show second order non-linear optical properties if

$\beta$ is non-zero. Materials that show second order non-linearity have asymmetric charge distribution e.g., donor and acceptor groups in both ends of the molecule. Thus, such properties can only be observed in noncentrosymmetric molecules. However, for third order nonlinear properties, the asymmetric charge distribution is not a must and metal containing conjugated polymers show such property. A material is said to show third order non-linear optical properties if $\gamma$ is non-zero. Organometallic and coordination compounds have metal to ligand or ligand to metal charge transfer bands and this may lead to large non linear optical response in such compounds.

Studies by Fraizer[38] using four-wave mixing show that metal containing polymers exhibit hyperpolarizabilities, $\gamma'$ (real component) and $\gamma''$ (imaginary component) that are significantly larger than in similar organic systems and are comparable to the $\gamma$ values of inorganic semiconductors such as InSb ($1700 \times 10^{-36}$ esu) or Ge ($1300 \times 10^{-36}$). Non-linear properties for group 10 metal poly-yne polymers have been also studied by Blau[39] and the imaginary and the real portions of the hyperpolarizability were recorded for Pt and Ni. Pt polymers have been shown to be good materials for optical thresholding. These polymers are transparent at visible light and exhibit large $\chi^3$ parameter values even in solution, which is important for device applications

It was shown by experimental and theoretical results that polarizability could be enhanced by extending the conjugation length and the use of donor acceptor groups in the molecule[40]. This is mainly for enhancing the second order non-linearity. For third order non linearity the structure-property relationship might not be as clear as in the second order but the conjugated poly-yne polymers have been shown to have such a property. The electronic communication between the metal and the organic ligand, the nature of the metal and the ligands themselves may lead to such properties. More effort is being undertaken to explore such properties in these materials.

## 1.5.2 Liquid crystals

Liquid crystals or mesogens have applications in liquid crystalline displays (LCD) and communications. These are found in many everyday devices, such as watches and calculators. Liquid crystallinity is defined as the fourth state of matter, in which it is between the ordered solid state and the disordered fluid state. The liquid crystalline phase can be achieved by either

changing the temperature (thermotropic liquid crystals) or by changing the concentration of a solution in a specific solvent (lyotropic liquid crystals). To date all commercial applications have involved organic liquid crystalline molecules. Each liquid crystal type has a different chemical structure. Some have linear rod-like structure; others form disks with long chains. The two most important conditions for achieving the liquid crystalline phase are that the structure should be anisotropic and should have a high susceptibility for polarizability. Metallomesogens have recently gained more interest because of applications. Such compounds may have advantages over the purely organic analogues due to the following.

i) The incorporation of transition metals into organic liquid crystalline materials may provide a wide range of new liquid crystalline compounds.

ii) The high polarizability of transition metal atom electrons may enhance properties such as dielectric constants and viewing quality of the displays used.

iii) The possibility of designing displays, which are based on magnetic rather then electric fields may have more potential in metallomesogens rather then purely organic analogues. Transition metals often form stable paramagnetic complexes with one or more unpaired electrons where organic molecules do not form radicals and thus all are diamagnetic.

iv) Transition metal compounds are strongly coloured because of either ligand to metal or metal to ligand charge transfer bands, so coloured displays could be made without dyes or filters.

Metal acetylide polymers form lyotropic liquid crystals and align either parallel or perpendicular to the electric field. A new class of thermotropic and lyotropic crystals has been discovered[41] for these complexes and the investigation continues to study the effect of chemical structure on these properties.

## 1.6 Aims and objectives

Extensive studies have been carried out in the last few decades in order to establish the synthetic strategies for metal-containing conjugated polymers and also to explore the origins of electronic transitions that occur upon electrical or optical excitations[1-15]. I have carried out the work in this thesis as an extension of previous work in order to establish (i) the possibility of making large conjugated molecules while they remian, stable, and are soluble and processible for further characterisation, (ii) the effect of the heavy Platinum atom in promoting the triplet emission state ($T_1$), and hence (iii) study the relative energies of the singlet ($S_1$) and triplet ($T_1$) emissions which is not possible in purely organic analogues due to non-emissive triplets, (iv) provide

information on how the chemistry affects the opto-electronic properties and (v) the potential for applications in light emitting diodes and other opto-electronic devices.

In all cases the general formula of the poly-ynes is $[-(P^nBu_3)_2Pt\text{-}C{\equiv}CRC{\equiv}C-]_n$, where the properties can be explained and compared as a function of the spacer group. These systems described in chapters 2-5 have provided the reliable comparison between the chemical structure and the electronic processes associated with them.

Chapter two describes the synthesis and properties of metal containing different arene derivatives including fused ring systems e.g., naphthalene and anthracene. Chapter three describes the synthesis and properties of metal containing 6-membered heterocyclic spacers, the oligopyridines. Chapter four is concerned about metal containing 5-membered hereocyclic system, the fused oligothiophenes and in chapter five, metal containing aromatic, heteroaromatic and mixed heterocyclic spacers are described. The information derived from all these are useful for designing future materials that can be more efficient, more stable and ideal for real life applications

# 1.7 References


1) (a) T. A. Stokheim, Ed., "*Handbook of Conducting Polymers*", Vols. I and II, Marcel Dekker, New York **1986**; (b) W. R Salaneck, D. L. Clark and E. J. E. Samuelsen, "*Science and Application of Conducting Polymers*", Adam Hilger, New York **1990**.
2) (a) J. L. Breads and R. R. Chance, Eds., "*Conjugated polymeric materials: Opportunities in electronics, optoelectronics and molecular electronics*", Kluwer Academic Publishers, Dordrecht **1990**; (b) U. H. F. Bunz, *Chem. Rev.*, **2000**, 100, 1605; (c) R. Giesa, *J. Macromol. Sci.-Rev. Maromol. Chem.* **1995**, C36(4), 631; (d) V. W-W Yam, *Acc. Chem. Res.*, **2002**, 35, 555; (e) P. Nguyen, P. Gómez-Elipe and I. Manners, *Chem. Rev.* **1999**, 99, 1515; (f) R. P. Kingsborough and T. M. Swager, *Prog. Inorg. Chem.*, **1999**, 48, 123,
3) T. Morimoto and K. Sonogashira, *J. Chem. Soc., Chem. Commun.*, **1984**, 3.
4) M. Delamar, P. Lacaze, J. Dumousseau, E. Dubois, *Electrochim. Acta.* **1982**, 27, 61.
5) T. Yamamoto, Y. Hayashi and A. Yamamoto, *Bull. Chem. Soc. Jpn.* **1978**, 51, 2091.
6) A. F. Diaz, *Chem. Scr.* **1981**, 17, 142.

7) G. Gustafasson, Y. Cao, G. M. Treacy, F. Klavetter, N. Colaneri and A. J. Heeger, *Nature*. **1992**, 357, 477.

8) K. Sonogashira, Y. Tohada, N. Hagihara, *Tetrahedron Lett.* **1975**, 4467.

9) (a) C. K. Chiang, C. R. Fincher Jr, H. Shirakawa, E. J. Lewis, S. C. Gau and A. G. MacDiarmid, *Phys. Rev. Lett.* **1977**, 39, 1098; (b) W. P. Su, J. R. Schrieffer and A. J. Heeger, *Phys. Rev. Lett.* **1979**, 42, 1698; (c) W. P. Su, J. R. Schrieffer and A. J. Heeger, *Phys. Rev. B.* **1979**, 22, 2099.

10) (a) K. Sonogashira, S. Kataaoka, S. Takahashi and N. Hagihara, *J. Organomet. Chem,* **1978**, 160, 319, (b) N. Hagihara, K. Sonogashira, and S. Takahashi, *Adv. Polym. Sci.*, **1981,** 41, 149.

11) R. Nast, *Coord. Chem. Rev*, **1982**, 47, 89-124.

12) J. H. Burroughes, D. D. Bradley, A. R. Brown, R. N. Marks, K. Mackay, R. H. Friend, P. L. Burn and A. B. Holmes, *Nature*, **1990**, 347, 539.

13) D. Beljonne, H. F. Wittmann, A. Kohler, M. Younus, J. Lewis, P. R. Raithby, M. S. Khan, R. H. Friend and J. L. Bredas, *J. Chem. Phys.*, **1996**, 105, 3868.

14) J. Manna, K. John, and M. Hopkins, *Adv. Organomet. Chem.*, **1995**, 38, 79.

15) (a) N. L. Long, *Angew. Chem.*, **1995**, 5, 2041; (b) T. B. Marder, G. Lesely, Z. Yuan, H. B. Fyfe, P. Chow, G. Stringer, I. R. Tobe, N. J. Taylor, I. D. Williams and S. Kurtz, *ACS Symp. Ser.*, **1991**, 455, 605

16) D. W. Bruce and D. O'Hare 'Inorganic Materials' eds., Wiley, London, **1992**.

17) (a) J. Roncali; *Chem. Soc. Rev.*, **2005**, 34(6), 483-495 (b) U. Mitschke and P. Bauerle, *J. Mat. Chem.*, **2000**, 10, 1471-1507.

18) (a) D. J. Williams, *Angew Chem. Int. Ed. Engl.* **1984**, 23, 690-703, (b) J. W. Perry, *Materials for non-linear optics*, ACS, Washington D. C. **1991**, Vol. 455; *Non-linear optical properties of organic molecules and crystals.*, Academic press, New York, **1987**, Vol. 1,2.

19) K. Bunten and A. Kakkar, *Macromolecules*, **1996**, 29, 2885.

20) (a) G. Gustafasson, Y. Cao, G. M. Treacy, F. Klavetter, N. Colaneri and A. J. Heeger, *Nature*. **1992**, 357, 477, (b) A. Montali, C. Bastiaansen, P. Smith and C. Weder, *Nature*, **1998**, 392, 261.

21) F. Diederich and P. Stang"*Metal Catalyzed Cross-coupling Reactions*" Eds., Wiley **1999**

22) P. Nguyen, Z. Yuan, L. Agocs, G. Lesley and T. B. Marder, *Inorganica Chimica Acta*, **1994**, 220(1-2). 289-96.

23) N. Hagihara, K. Sonogashira, and S. Takahashi, *Adv. Polym. Sci.*, **1981,** 41, 149.

24) J. Chatt and B. L. Shaw, *J. Chem. Soc.*, **1959**, 4020.

25) V. V. Korshak, A. M. Sladkov and Y. P. Kurdyavtesev. *Vysokomol. Soedin.* **1960,** 2, 1824.

26) K. Sonogashira, T. Yatake, T. Tohda, S. Takahashi and N. Hagihara, *J. C. S. Chem., Commun.*, **1977**, 291.

27) Z. Atherton, C. Faulkner, S. Ingham, A. Kakkar, M. S. Khan, J. Lewis, N. J. Long and P. R. Raithby, *J. Organomet. Chem.*, **1993**, 462, 264.

28) H. B. Fyfe, M. Mlekuz, D. Zargarian, N. J. Taylor and T. B. Marder, *J. Chem. Soc. Chem. Commun*, **1991**, 188.

29) J. E. Sheats, C. E. Carraher, Jr. and C. Pittman, 'Metal Containing Polymers', Plenum Press, New York, **1985**.

30) M. S. Khan, S. Davies, A. Kakkar, D. Schwartz, B. Lin, B. F. G. Johnson and J. Lewis, *J. Organomet. Chem.* **1992**, 424, 87.

31) F. Diedrich and Y. Rubin, *Angew. Chem. Int. Ed. Engl.* **1992**, 31, 1101.

32) N. Chawdhury, A. Kohler, R. H. Friend, M. Younus, N. J. Long, P. R. Raithby and J. Lewis, *Macromlecules*, **1998**, 31, 722.

33) (a) M. S. Khan, N. Pasha, A. Kakkar, S. Davies, P. R. Raithby, J. Lewis, K. Fuhramann and R. H. Friend, *J. Mater. Chem.*, **1992**, 2, 759; (b) R. Crescenzi and C. L. Sterzo, *Organometallics*, **1992**, 11, 4301., (c) A. Sebald, C. Stader and B. Wrackmeyer, *J. Organomet. Chem.*, **1986**, 311, 233.

34) H. Wittmann, R. Friend, M. Khan and J. Lewis, *J. Chem. Phys.* **1994**, 101 (4), 2693

35) H. F. Wittmann, PhD thesis, Cambridge, **1994**.

36) O. Lhost, J. M. Toussaint, J. L. Bredas, H. F. Wittmann, K. Fuhrmann, R. H. Friend, M. S. Khan and J. Lewis, *Synth. Met.*, **1993**, 55-57, 4525-4530.

37) G. Frapper and M. Kertesz, *Inorg. Chem.*, **1993**, 32, 732-740.

38) P. L. Porter, H. Guha, K. Kang and C. C. Frazier, *Polymer*, **1991**, 32, 1756.

39) W. J. Blau, H. J. Byrne, D. J. Cardin, A. P. Davey, *J. Mater. Chem.*, **1991**, 1, 245.

40) S. J. Lalama and A. F. Garito, *Phys. Rev. A*, **1979**, 20,1179.

41) (a) A. Kimura and S. Tabata, *Macromolecules*, **1991**, 24, 6238; (b) T. Kuharu, H. Matsubara and S. Takahashi; *J. Mater. Chem.*, **1991**, 1, 145

# CHAPTER 2

## Rigid-Rod Pt(II) Poly-ynes and Di-ynes Incorporating Derivatised Aromatic Linker Groups in the Backbone

# 2.1 Introduction

Conjugated polymers, that have potential electronic and photonic applications have sparked off an ever-increasing interest in the scientific community[1-10]. Of particular interests are a series of poly-ynes composed of alternating aryl and ethynyl units, e.g., polyarylene ethynylenes (PAEs) that have been the focus of much research with respect to material science applications[2]. The ease of preparation of PAEs, their photophysical stability and wide usage can be combined with the features of transition metals to give metallo-poly-ynes (MPYs) with novel properties, such as optical nonlinearity[1], liquid crystallinity[2], luminescence[3], electrical and photoconductivity.[4] In the organic polymers, light emission occurs from the singlet excited state ($S_1$) but emission in LEDs occurs from both the excited singlet ($S_1$) and triplet ($T_1$) manifolds. Normally, the triplet state is not optically accessible in organic polymers, and as there are three triplet states per each singlet state, the device efficiency is limited to 25%. It is desirable to understand the photophysics of the triplet excited states and how they change with the chemical structure in order to manipulate the relative separation of the energy bands and hence, increase the efficiency of the devices. The triplet state can be detected readily by inclusion of platinum atoms in the polymer backbone that introduces sufficient spin-orbit coupling to allow light emission from the triplet excited state, by allowing spin-crossover processes to occur.[5]

Within the family of platinum(II) poly-ynes, spacers involving condensed aromatic ring systems have received little attention although the use of fused-ring spacers has been found to be a powerful approach to the production of some low band gap conjugated polymers.[6] Among the fused aromatic systems, naphthalene and anthracene units (**Figure 2.1**) are particularly interesting because of their fluorescence, photo- and electroluminescence, liquid crystal, photochromic and hole-transporting properties.[7] Some reports have been concerned with the incorporation of naphthalene and anthracene as bridging chromophores into conjugated poly-yne frameworks and studies in intra-molecular electron and energy transfer.[8] The incorporation of the relatively electron-rich

anthracene units into PAEs has been found to have a marked influence on the luminescence properties of the materials,[9] and they are particularly effective in promoting π-electron delocalisation along the backbone of long-chain Pt(II) poly-ynes.

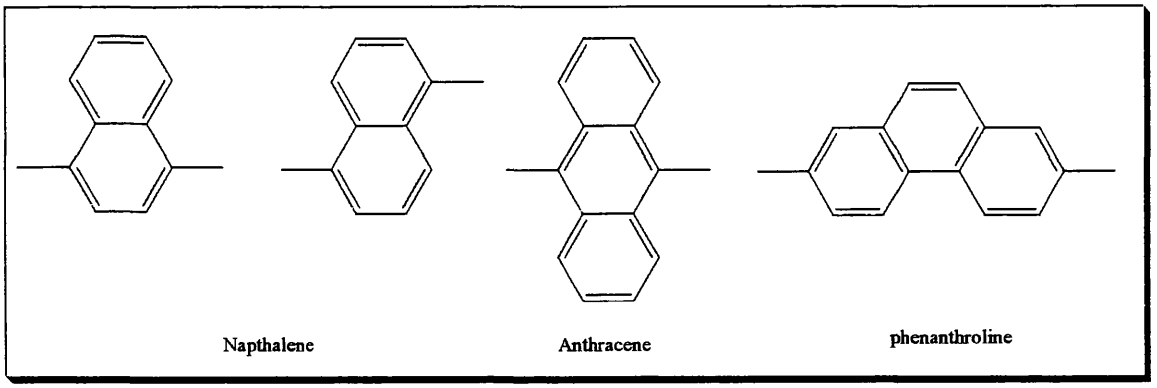


**Figure 2.1. Examples of fused carbo-cyclic rings**

This background triggered the interest to investigate Pt(II) poly-ynes incorporating naphthalene and anthracene rings in the backbone (**Figure 2.2**). The motivation for their synthesis was to extend the range of organometallic poly-ynes and establish in what way the incorporation of fused aromatic spacer unit affects the optical, electronic and thermal properties of the Pt(II) poly-ynes.

Furthermore, the systematic study of the related di-ynes allows direct correlation of physical properties with chemical structures, and enables the generation of useful and predictive structure-property relationship in these poly-ynes. Di-ynes are often more crystalline, allowing for a detailed structural analysis.

In addition, the solid state arrangement of the molecules is an important factor in determining their optical behaviour.[11] While the π–π stacking interaction between adjacent oligomer molecules or polymer chains has been identified as a key 'interchain' interaction in solids[12], it is possible that hydrogen bonding can also play an important rôle in this context. Hydrocarbon groups are generally poor donors of hydrogen bonds, but the ethynyl moiety with its acidic H atom is an exception.[13] Furthermore, the concentration of electron density in the triple bond can act as an acceptor, albeit a rather weak one, of

an H-bond.[14] Thus ethynyl groups can form co-operative H-bonds,[15] similar to OH groups.[16] Such a cooperative effect is evident in the crystal structure[14] of 1,4-diethynylbenzene **1b**[17].

The single crystal structure of protected dialkynes, 1,4-bis(trimethylsilylethynyl)naphthalene, **2a** and 9,10-bis(trimethylsilylethynyl)anthracene, **3a** and of two dinuclear Pt(II) complexes, *trans*- [$(Ph)(Et_3P)_2Pt$-C≡C-R-C≡C-$Pt(Et_3P)_2(Ph)$] (R = benzene-1,4-diyl, **1c**; napthalene-1,4- diyl, **2c**) are described. The related protected, deprotected, Pt(II) di-yne and poly-yne (**1a-1d**)[10] with benzene spacer were also prepared and characterised for comparison. A description of the spectroscopic, thermal and optical properties of theses materials is described in this chapter.

In order to investigate the effect of various substituents on the crystalline architecture of these poly-yne precursors, particularly the stability of the C≡CH···$\pi_{C\equiv C}$* H-bonding in competition[18] with other intermolecular interactions, e.g. X-H···$\pi_{C\equiv C}$ (X = N, C) and C-H···Y (Y= N, O, F)[19], a series of amino-, fluoro- and alkoxy-derivatives of 1,4-diethynylbenzene **4b-9b** were synthesised (**Figure 2.3**) and structurally characterised by single crystal and powder X-ray diffraction. The structure of **1b** is also included for comparison. The structures **6b** and **7b** were determined at variable temperature, to investigate the supposed effects of the latter on weak hydrogen bonds.[20] The substituted diethynylbenzene ligands have been incorporated into rigid-rod platinum(II)-containing poly-ynes **4d-9d** and their thermal and opto-electronic properties investigated systematically.

---

* $\pi_{C\equiv C}$ is the midpoint of the C≡C bond

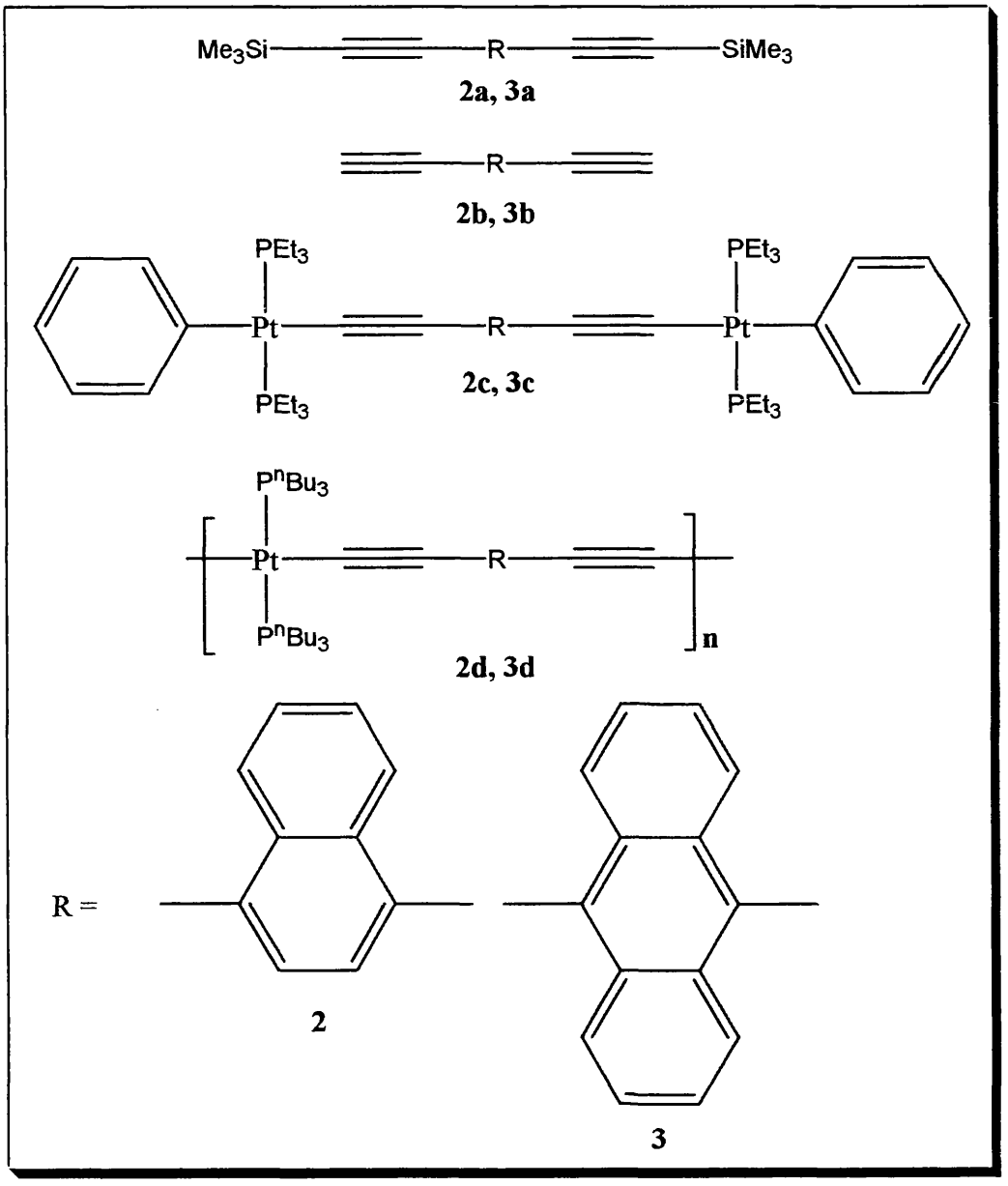


**Figure 2.2. Rigid-rod materials with naphthalene and anthracene condensed spacers**

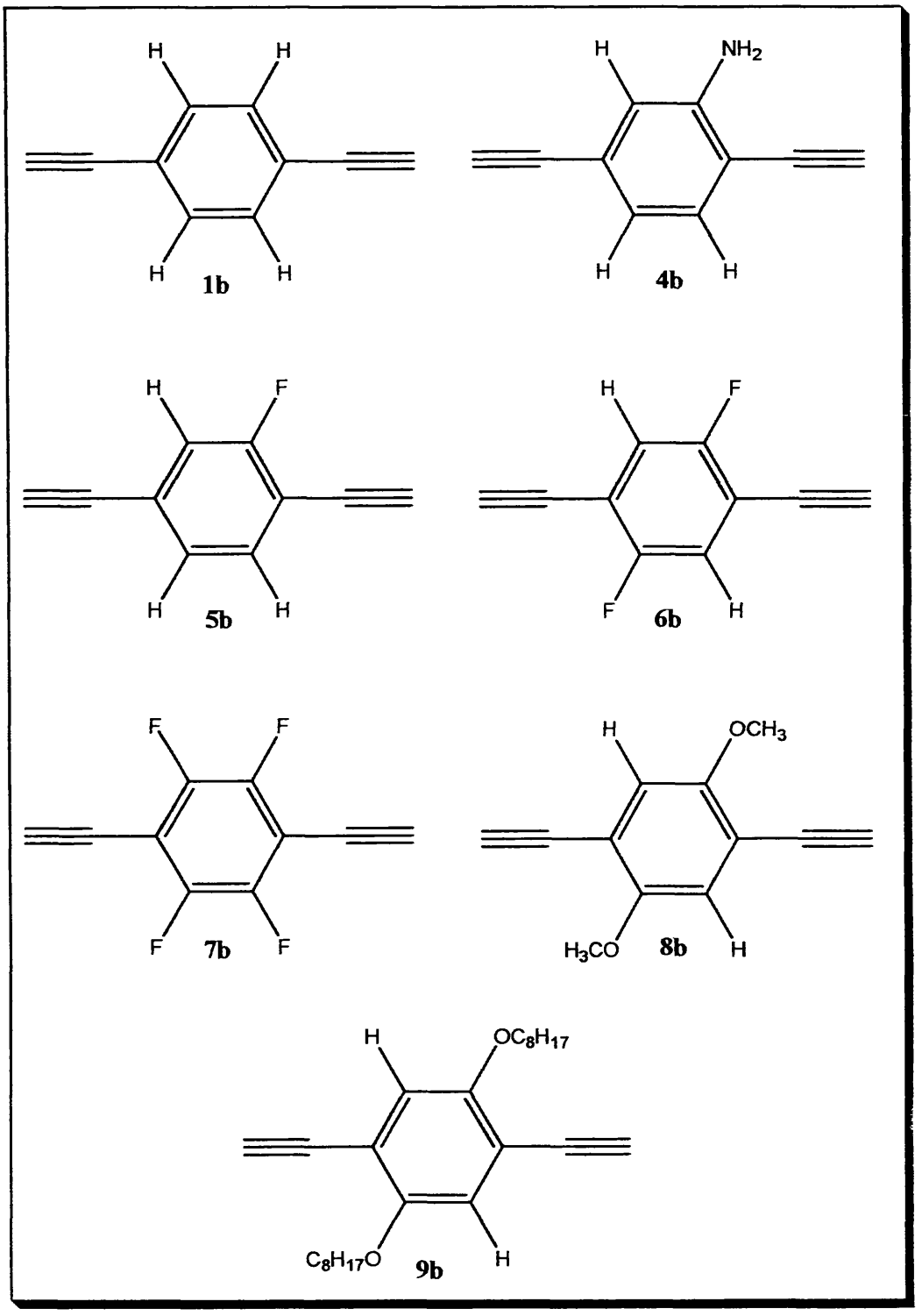
H
H
H
H
1b
H
NH2
H
H
4b
H
F
H
H
5b
H
F
F
H
6b
F
F
F
F
7b
H
OCH3
H3CO
8b
H
H
OC8H17
C8H17O
H
9b

**Figure 2.3.**

## 2.2 Results and discussion

## 2.2.1 Synthesis

1,4-Dibromonapthalene and 9,10-dibromoanthracene were converted into the diiodo-derivatives by lithiation with $^{n}$BuLi followed by iodination with iodine in diethylether[21]. This conversion is preferred whenever possible due to the enhanced reactivity of the iodo-arenes compared to the bromo derivatives. The use of the diiodo derivatives gave improved yields (80-85%) of the desired bis(trimethylsilylethynyl) ligands with minimum homo-coupling that would lead to the formation of the side product bis(trimethylsilylethynyl) butadiyne.

The bis-ethynyl ligands were then synthesized by a sequence of coupling and proto-desilylation reactons. The protected alkynyl ligand precursors, 1,4-bis(trimethylsilylethynyl) benzene, **1a** 1,4- bis(trimethylsilylethynyl)naphthalene **2a**, 9,10-bis(trimethylsilylethynyl)anthracene **3a,** 1,4-bis(trimethylsilylethynyl)-2-aminobenzene **4a**, 1,4-bis(trimethylsilylethynyl)-2-flourobenzene **5a**, 1,4-bis(trimethylsilylethynyl)-2,5-diflourobenzene **6a**, 1,4-bis(trimethylsilylethynyl)-2,3,5,6-tetraflourobenzene **7a**, 1,4-bis(trimethylsilylethynyl)-2,5-dimethoxybenzene **8a** and 1,4-bis(trimethylsilylethynyl)-2,5-dioctyloxybenzene **9a**, were prepared by palladium(II)/copper(I)-catalysed cross-coupling reactions of trimethylsilylethyne with the dibromo/diiodo derivatives in $^{i}Pr_2NH$-THF solvent mixture as illustrated in **Scheme 2.1**.

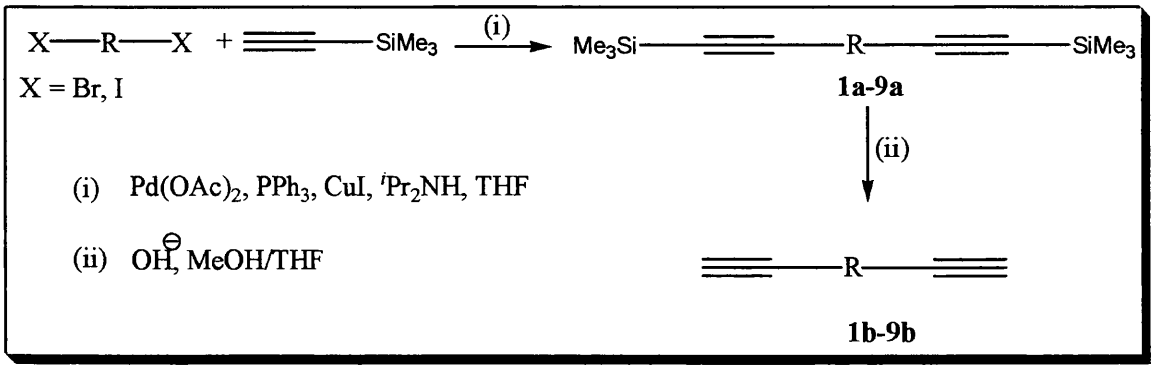


**Scheme 2.1.**

The protected alkynes are indefinitely stable towards light and air at ambient temperature. The IR spectra show a strong peak in the region 2140-2155 $cm^{-1}$ due to the acetylenic moieties. The protected compounds **4a-9a** were not isolated but converted directly into their diterminal alkyne derivatives. Conversion of the protected dialkynes into the diterminal ones was accomplished by cleavage of the trimethylsilyl groups with dilute aqueous KOH in MeOH-THF system (**Scheme 2.1**). These diterminal alkynes show characteristic peaks at 2010 $cm^{-1}$ for the acetylenic moieties and at 3300 $cm^{-1}$ for the $C_{sp}$—H bond. The ligands were purified by silica gel column chromatography and isolated in 78–85% yields. The diterminal alkynes described here are among the most stable and the single crystal structures of **1b, 4b-7b** were determined and that of **8b** and **9b** were determined by powder diffraction.

The dehydrohalogenation reactions between *trans*-[(Ph)$(Et_3P)_2PtCl$] and **1b**, **2b**, and **3b** in a 2:1 stoichiometry, in $^{i}Pr_2NH$-$CH_2Cl_2$, in the presence of CuI at room temperature gave the dinuclear Pt(II) di-ynes **1c-3c,** while the polycondensation reactions between *trans*-[$(P^{n}Bu_3)_2PtCl_2$] and **1b-9b**, in a 1:1 ratio, under similar reaction conditions, readily afforded the platinum(II) poly-ynes **1d-9d** (**Scheme 2.2**). It was not possible to isolate the dinuclear Pt(II) di-ynes of **4b-9b** due to the side reactions that led to the formation of many side products. The poly-ynes were obtained as off-white for **1d, 2d** and **4d-7d**, light yellow for **8d** and **9d** and red for **3d** in yields of 80-90%, pointing to a very high conversion. The IR spectra of both di-ynes and poly-ynes show a single sharp $\nu_{C\equiv C}$ absorption at around 2095 $cm^{-1}$ consistent with a *trans*-configuration of the ethynylenic units around the Pt(II) centre. Furthermore, the Pt(II) di-ynes and poly-ynes display lower $\nu_{C\equiv C}$ values than those in the corresponding protected or terminal dialkynes. This may be attributed to either metal-yne $\pi$-backbonding or the $M^{\delta+}$-$C^{\delta-}$ polarity.[22] Purification of the Pt(II) di-ynes was accomplished by column chromatography or preparative TLC on silica while the poly-ynes were purified by chromatography on an alumina column followed by repeated precipitation into methanol from dichloromethane.

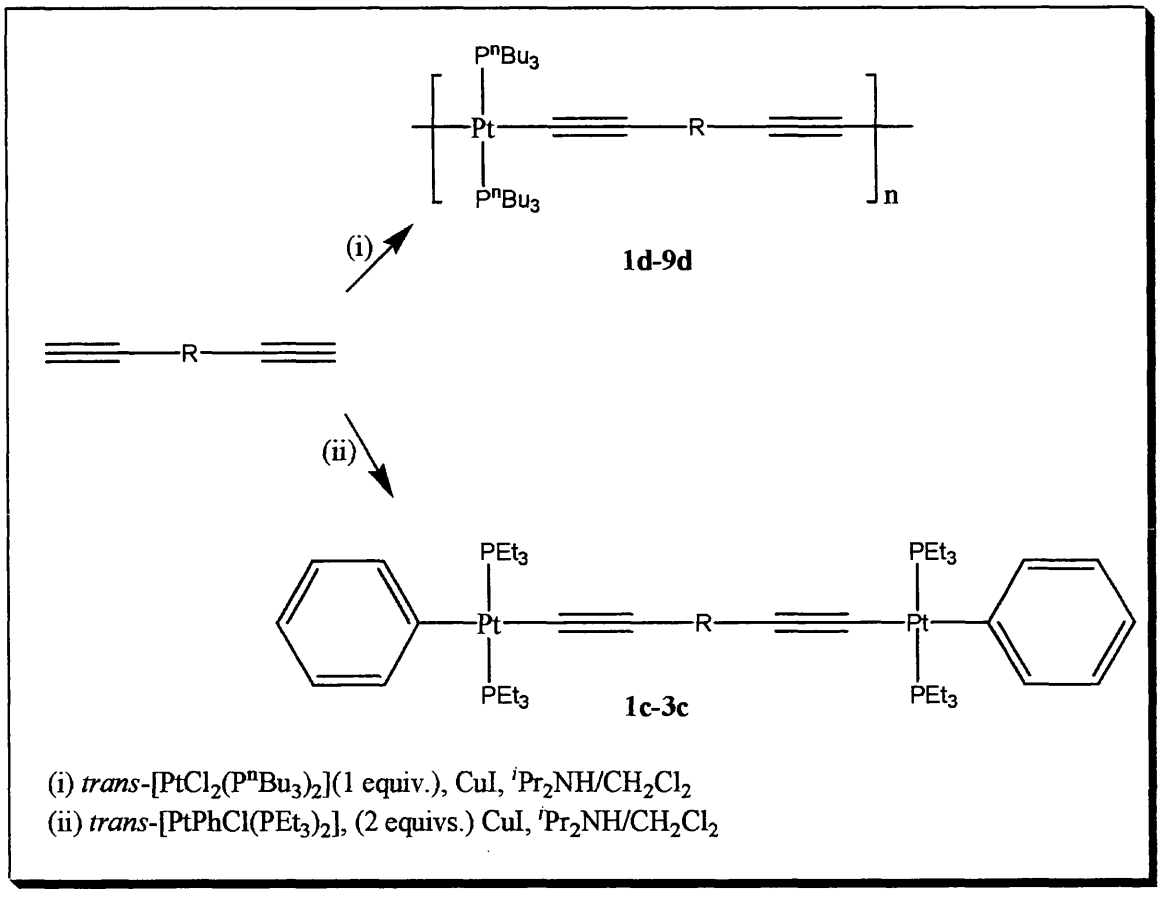


**Scheme 2.2**

NMR analyses indicate a rigid structure for the Pt(II) di-ynes and poly-ynes. In all cases, $^1$H NMR resonances arising from the protons of the aromatic ring systems were clearly observed. **Figure 2.4** shows the aromatic region of **1c**. The protons of the $C_6H_4$ spacer appeared as a singlet at around 7.13 ppm and those of the terminal arene ones at 7.35, 6.95 and 6.78 ppm indicting a high degree of symmetry in the complex. In most cases, it was difficult to get a clear picture of the individual ethynylenic carbons in the $^{13}$C NMR especially with the naphthalene and anthracene containing di-ynes and poly-ynes. The aromatic region of the $^{13}$C NMR spectra of **1c** reveals a high degree of structural regularity for the main-chain skeleton (**Figure 2.5**). For example, only 6 well-defined peaks appear in the region between 115-160 ppm related to the 18 aromatic carbon atoms of **1c**. The ethynylenic carbons appeared at the region between 105-110 ppm. The single resonance in the $^{31}$P NMR spectra of the Pt(II) diynes and poly-ynes confirms the *trans* arrangement of the phosphine ligands (**Figure 2.6**). The $^1J_{Pt\text{-}P}$ values range from 2628 to 2645 Hz for the di-ynes and 2363-2377 Hz for the poly-ynes.

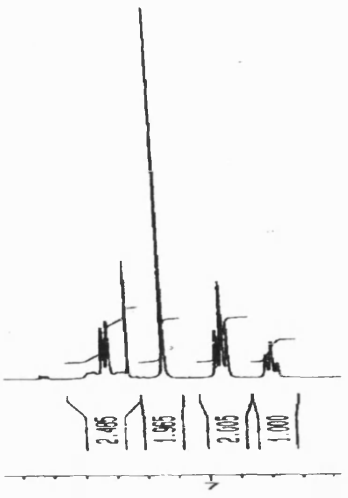


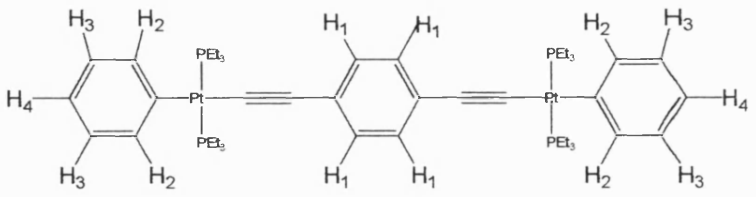


δ: 7.13 ppm (s, 4H, $H_1$)

δ: 7.35 ppm (d, 4H, $H_2$)

δ: 6.95 ppm (t, 4H, $H_3$)

δ: 6.78 ppm (t, 2H, $H_4$)

δ: 7.24 ppm $CHCl_3$ solvent

**Figure 2.4: $^1$H NMR spectrum of the aromatic region of 1c**

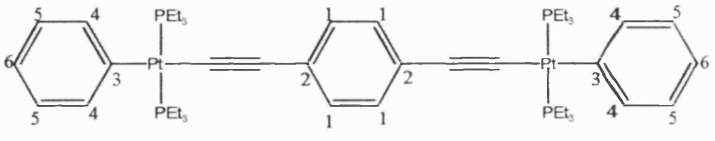


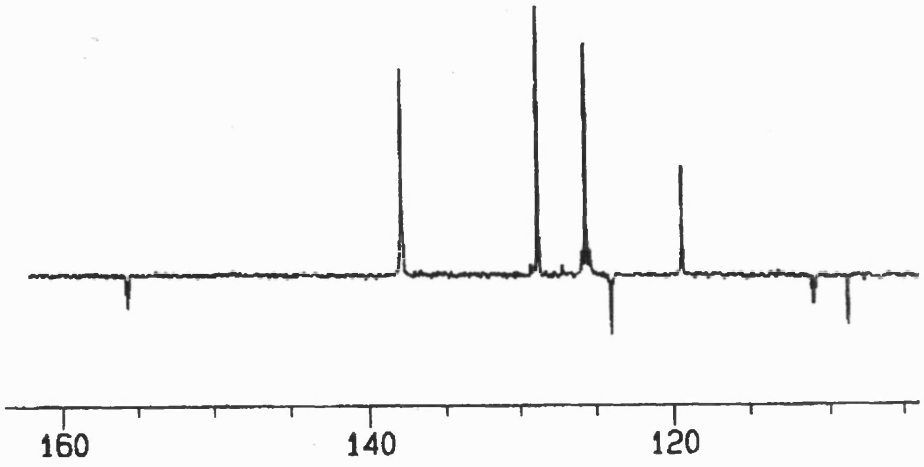


**Figure 2.5: DEPT $^{13}$C NMR spectrum of the aromatic region of 1c. Carbons 1-6 at 115-160 ppm, acetylenic carbons at 105-115 ppm. Quatenary carbons appear inverted**

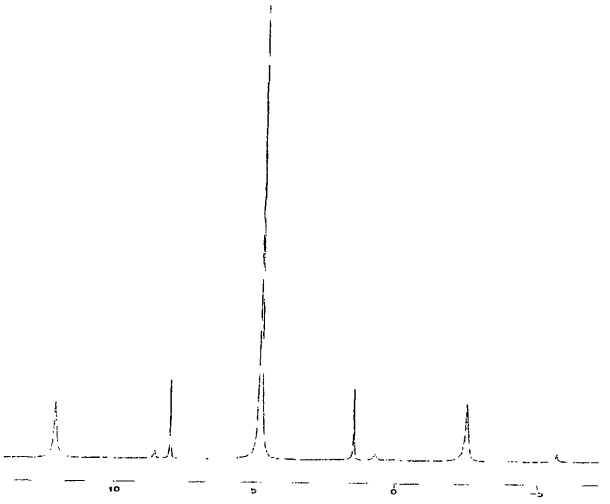

**Figure 2.6: $^{31}P$ NMR spectrum of 2d**

The mass spectrometric results confirm the molecular assignments for the compounds. Gel permeation chromatography (GPC), using a polystyrene (PS) standard shows that the number-average molecular weights is 41,000 $gmol^{-1}$ for **2d** and 28,000 $gmol^{-1}$ for **3d** corresponding to degrees of polymerisation of between 34 and 53 repeat units, respectively and in the range of 74,000-95,000 g $mol^{-1}$ for **4d-9d** corresponding to degrees of polymerisation of between 95-128 repeat units. The value of poly dispersity index (PDI) varied between 1.8 and 1.9. The narrow poly dispersity index (PDI < 2) in the molecular weights is indicating reasonably homogenous polymer chain lengths and consistent with the proposed linear structure[23].

GPC data indicate that the number of repeat unit per chain for the naphthalene-based poly-yne ($n$ = 53) is higher than that for the anthracene-based poly-yne ($n$ = 34) and the degree of polymerization is significantly reduced in both cases as compared to that found for the related phenylene-based poly-yne[10,24] ($n$ ~ 95). This reduction in chain length with the increasing size of the spacer group may reflect a reduction in the solubility of the larger species.

**Table 2.1: Synthetic and other characterization data for 1a-3a and 1b-9b**

| Compound | Color | Yield (%) | $M^+(gmol^{-1})$ | $\upsilon_{C\equiv C}(cm^{-1})$ | $\upsilon_{Csp\text{-}H}(cm^{-1})$ |
|---|---|---|---|---|---|
| **1a** | White | 90 | 270.3 | 2150 | - |
| **2a** | Salmon | 85 | 320.4 | 2155 | - |
| **3a** | Deep red | 78 | 370.5 | 2152 | - |
| **1b** | White | 85 | 126.1 | 2100 | 3300 |
| **2b** | Orange | 80 | 176.2 | 2107 | 3299 |
| **3b** | Red | 76 | 226.3 | 2107 | 3299 |
| **4b** | Pale yellow | 76 | 141.1 | 2108 | 3300 |
| **5b** | off-white | 82 | 144.1 | 2107 | 3300 |
| **6b** | off-white | 95 | 162.1 | 2107 | 3299 |
| **7b** | off-white | 82 | 198.1 | 2106 | 3297 |
| **8b** | off-white | 86 | 186.2 | 2107 | 3299 |
| **9b** | pale yellow | 79 | 382.1 | 2107 | 3299 |

The molecular weight values should be viewed with caution in view of the difficulties associated with utilizing GPC for rigid-rod polymers. GPC does not give absolute values of molecular weights but provides a measure of hydrodynamic volume. Rod-like polymers in solution possess very different hydrodynamic properties to flexible polymers. Therefore, calibration of the GPC with PS standards could inflate the values of the molecular weights of the poly-ynes to some extent. However, the lack of discernable resonances that could be attributed to end groups in the $^1H$ NMR spectra e.g., -C≡CH groups, provides support for the view that a high degree of polymerization has been achieved in these organometallic polycondensation reactions.

**Table 2.2: Synthetic and other characterization data for 1c-3c and 1d-9d**

| Compound | Color | Yield (%) | $M^+$ ($gmol^{-1}$) | $M_n$ ($gmol^{-1}$) | $M_w$ ($gmol^{-1}$) | PDI | $\upsilon_{C\equiv C}$($cm^{-1}$) ($CH_2Cl_2$) | $^{31}P\{^1H\}$NMR (300 MHz) (ppm)[a] |
|---|---|---|---|---|---|---|---|---|
| **1c** | Pale yellow | 70 | 1141 | - | - | - | 2095 | –131.17 ($^1J_{Pt-P}$ = 2628 Hz) |
| **2c** | Orange | 65 | 1191 | - | - | - | 2095 | –131.17 ($^1J_{Pt-P}$ = 2643 Hz) |
| **3c** | Orange | 65 | 1241 | - | - | - | 2094 | –131.17 ($^1J_{Pt-P}$ = 2645 Hz) |
| **1d** | Off-white | 85 | - | 75,000 | 150,000 | 1.8 | 2095 | –138.17 ($^1J_{Pt-P}$ = 2335 Hz) |
| **2d** | Off-white | 85 | - | 41,020 | 78,000 | 1.9 | 2095 | –138.03 ($^1J_{Pt-P}$ = 2363 Hz) |
| **3d** | Red | 90 | - | 28,000 | 50,500 | 1.8 | 2094 | –138.03 ($^1J_{Pt-P}$ = 2373 Hz) |
| **4d** | off-white | 85 | - | 94,700 | 151,500 | 1.9 | 2094 | -138.08 ($^1J_{Pt-P}$ = 2330 Hz) |
| **5d** | Off-white | 82 | - | 94,650 | 160,900 | 1.7 | 2095 | -138.50 ($^1J_{Pt-P}$ = 2330 Hz) |
| **6d** | Off-white | 78 | - | 88,230 | 158,810 | 1.8 | 2094 | -138.50 ($^1J_{Pt-P}$ = 2330 Hz) |
| **7d** | Off-white | 72 | - | 82,500 | 156,770 | 1.9 | 2095 | -138.50 ($^1J_{Pt-P}$ = 2330 Hz) |
| **8d** | Light yellow | 85 | - | 74, 100 | 111,200 | 1.5 | 2095 | -138.10 ($^1J_{Pt-P}$ = 2330 Hz) |
| **9d** | Light yellow | 90 | - | 94,850 | 151,750 | 1.6 | 2095 | -138.10 ($^1J_{Pt-P}$ = 2330 Hz) |

[a] referenced to $P(OMe)_3$

## 2.2.2 Thermal analysis

The thermal stability was determined by simultaneous differential thermal analysis

(DTA) and thermogravimetry (TG). Decomposition onset was defined as a mass loss of 2%. The first decomposition step might be due to the removal of trialkylphosphine groups from the di-ynes and the poly-ynes. TG traces show that the Pt(II) diynes and poly-ynes have decomposition temperatures of over 300 °C, indicative of good thermal stability. Poly-yne **3d** exhibits higher decomposition onset and peak temperatures than **2d**, which in turn, exhibits higher thermal stability than the phenylene-containing poly-yne **1d**. Similar trend in thermal stability was also observed for the Pt(II) di-ynes where **1c** showed the lowest and **3c** the highest onset and peak decomposition temperatures. The diynes exhibited slightly higher onset and peak decomposition temperatures than the corresponding Pt(II) poly-ynes. The results are shown in **Table 2.3**.

Polymers **4d** and **8d** exhibited the lowest decomposition temperature among the substituted benzene polymers, while the fluorinated polymers **5d-7d** exhibited increasing decomposition temperatures with increasing fluorination. Polymer **9d** also exhibited one of the highest decomposition temperatures, since the octyloxy groups likely encourage stronger interchain van der Waals bonding (**Table 2.3**).

**Table 2.3: Thermal analysis results for decomposition temperatures: all temperatures in °C. Uncertainties are approximately ±8 °C.**

| Compound | $T_{decomp}$ (onset) | $T_{decomp}$ (peak) |
|---|---|---|
| **1d** | 302 | 335 |
| **2d** | 308 | 342 |
| **3d** | 315 | 354 |
| **1c** | 309 | 345 |
| **2c** | 312 | 349 |
| **3c** | 319 | 362 |
| **4d** | 248 | 336 |
| **5d** | 300 | 333 |
| **6d** | 304 | 337 |
| **7d** | 312 | 345 |
| **8d** | 254 | 314 |
| **9d** | 310 | 353 |

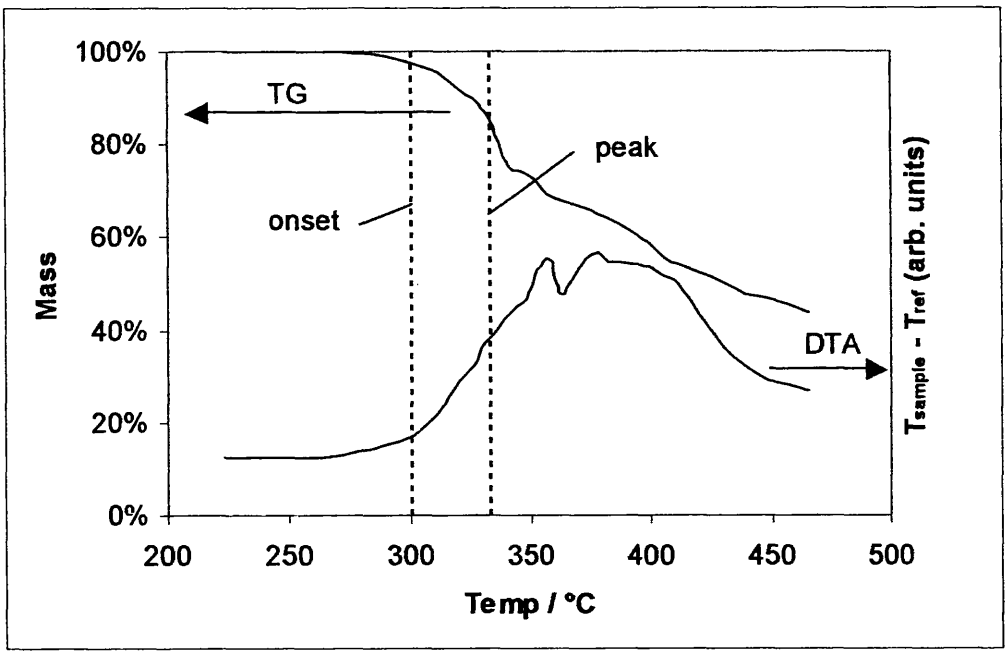


**Figure 2.7. Simultaneous thermogravimetric (TG) curve (above) and differential thermal analysis (DTA) curve (below) for 5d. The onset and peak decomposition temperatures, as defined in the text are marked.**

## 2.2.3 Crystal structural analysis

Single crystals of compounds **2a**, **3a**, **1c** and **2c** were obtained by diffusion techniques using dichloromethane and either hexane or methanol co-solvents. The molecular structures of these materials were determined in order to confirm the spectroscopic assignments, and investigate the intermolecular interactions in the solid state, with a view to correlating the structure/property relationships in these systems.

The molecular structure of 1,4-*bis*(trimethylsilylethynyl)naphthalene **2a** is shown in **Figure 2.8** while selected bond parameters are listed in **Table 2.4**. The molecules show the expected linear geometry (average Si-C≡C, 177.9(2)°, and average C≡C-C, 179.2(2)°) along the two acetylene groups on either side of the planar naphthalene group. The C-C bond lengths within the central naphthalene ring is 1.358(3) – 1.438(3) Å, and the two C≡C bonds have an average length of 1.206(3) Å, consistent with values found in a range of *bis*-trimethylsilylethynyl derivatives.[25] For the trimethylsilyl groups the

(Me)C-Si-C(Me) angles (average 110.83°) are somewhat larger than the (≡C)C-Si-C(Me) angles (average 108.07°), and the geometry around Si is distorted tetrahedral.

The compound 9,10-*bis*(trimethylsilylethynyl)anthracene, **3a**, crystallises in the monoclinic space group $P2_1/c$, with one unique whole molecule, and two independent half molecules, sitting on centres of symmetry, in the asymmetric unit. The structure is illustrated in **Figure 2.9** while selected bond parameters are presented in **Table 2.5**. Within the structure the four independent C≡C triple bonds lie in the expected range of 1.187(6) – 1.207(8) Å, and the acetylene units are essentially linear with Si-C≡C and C≡C-C angles of 175.6° and 176.1°, respectively. The anthracene rings are planar, with a maximum deviation from planarity of 0.03 Å, and within the ring systems the C-C bond lengths lie in the range 1.334(11) – 1.451(7) Å.

**Table 2.4: Bond Lengths (Å) and Angles (°) for 1,4-*bis*(trimethylsilylethynyl)naphthalene 2a**

| | | | |
|---|---|---|---|
| Si(1)-C(4) | 1.834(2) | C(18)-Si(2)-C(17) | 107.93(15) |
| Si(1)-C(1) | 1.842(2) | C(18)-Si(2)-C(19) | 111.5(3) |
| Si(1)-C(3) | 1.846(2) | C(17)-Si(2)-C(19) | 108.24(12) |
| Si(1)-C(2) | 1.858(2) | C(18)-Si(2)-C(20) | 112.8(3) |
| Si(2)-C(18) | 1.827(4) | C(17)-Si(2)-C(20) | 107.98(13) |
| Si(2)-C(17) | 1.835(2) | C(19)-Si(2)-C(20) | 108.23(18) |
| Si(2)-C(19) | 1.837(3) | C(5)-C(4)-Si(1) | 178.0(2) |
| Si(2)-C(20) | 1.857(3) | C(4)-C(5)-C(6) | 179.0(2) |
| C(4)-C(5) | 1.205(3) | C(7)-C(6)-C(11) | 119.88(18) |
| C(5)-C(6) | 1.436(3) | C(7)-C(6)-C(5) | 119.64(19) |
| C(6)-C(7) | 1.376(3) | C(11)-C(6)-C(5) | 120.48(18) |
| C(6)-C(11) | 1.432(3) | C(6)-C(7)-C(8) | 120.9(2) |
| C(7)-C(8) | 1.396(3) | C(9)-C(8)-C(7) | 121.3(2) |
| C(8)-C(9) | 1.380(3) | C(8)-C(9)-C(10) | 119.63(18) |
| C(9)-C(10) | 1.432(3) | C(8)-C(9)-C(16) | 119.89(19) |
| C(9)-C(16) | 1.438(3) | C(10)-C(9)-C(16) | 120.48(19) |
| C(10)-C(15) | 1.416(3) | C(15)-C(10)-C(11) | 118.38(19) |
| C(10)-C(11) | 1.424(3) | C(15)-C(10)-C(9) | 122.51(18) |
| C(11)-C(12) | 1.415(3) | C(11)-C(10)-C(9) | 119.09(18) |
| C(12)-C(13) | 1.358(3) | C(12)-C(11)-C(10) | 118.90(19) |
| C(13)-C(14) | 1.404(3) | C(12)-C(11)-C(6) | 121.90(18) |
| C(14)-C(15) | 1.360(3) | C(10)-C(11)-C(6) | 119.19(18) |
| C(16)-C(17) | 1.207(3) | C(13)-C(12)-C(11) | 120.9(2) |
| C(4)-Si(1)-C(1) | 107.99(11) | C(12)-C(13)-C(14) | 120.2(2) |
| C(4)-Si(1)-C(3) | 108.54(10) | C(15)-C(14)-C(13) | 120.7(2) |
| C(1)-Si(1)-C(3) | 111.00(11) | C(14)-C(15)-C(10) | 120.9(2) |
| C(4)-Si(1)-C(2) | 107.71(11) | C(17)-C(16)-C(9) | 179.3(2) |
| C(1)-Si(1)-C(2) | 109.62(12) | C(16)-C(17)-Si(2) | 177.8(2) |
| C(3)-Si(1)-C(2) | 111.85(11) | | |

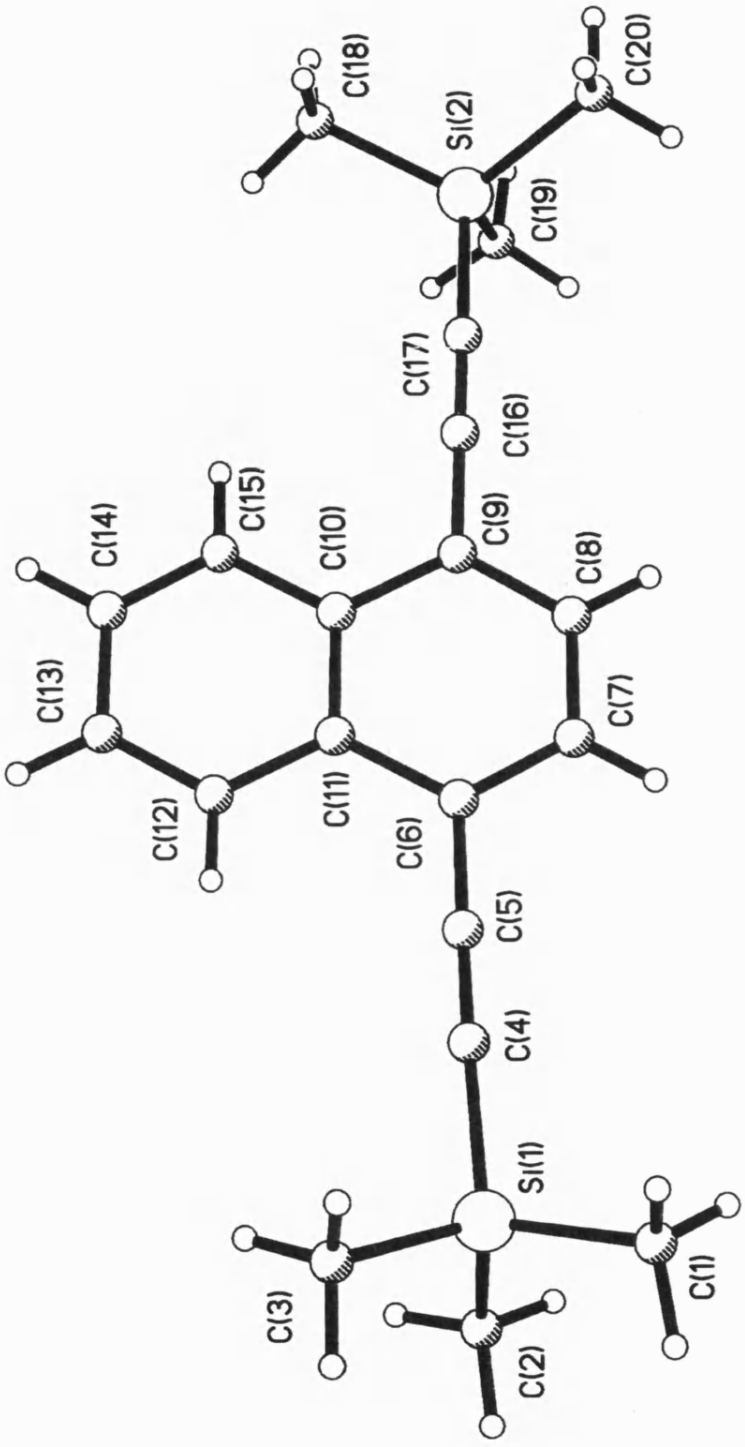


**Figure 2.8 The molecular structure of 1,4-*bis*(trimethylsilylethynyl)naphthalene 2a showing the atom numbering scheme adopted.**

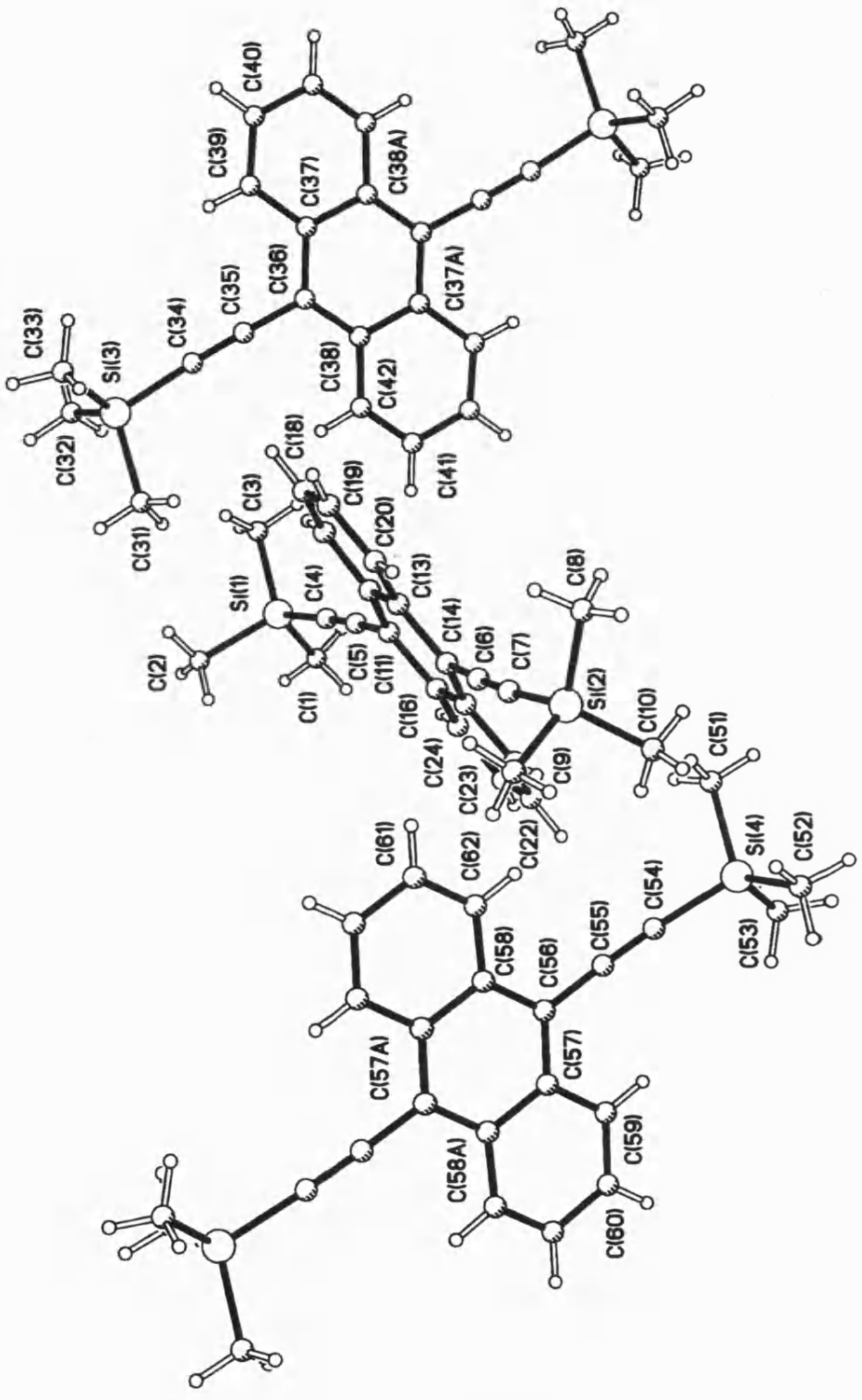


**Figure 2.9: The molecular structure of 9,10-*bis*(trimethylsilylethynyl)anthracene 3a showing the atom numbering scheme adopted. The asymmetric unit contains one whole molecule and two half molecules located on crystallographic centres of symmetry.**

**Table 2.5: Bond Lengths (Å) and Angles (°) for 9,10-bis(trimethylsilylethynyl)anthracene 3a**

| | | | |
|---|---|---|---|
| Si(1)-C(1) | 1.722(10) | C(20)-C(13)-C(12) | 120.0(6) |
| Si(2)-C(10) | 1.829(7) | C(15)-C(14)-C(13) | 121.2(4) |
| Si(3)-C(32) | 1.854(8) | C(11)-C(16)-C(24) | 120.7(5) |
| C(4)-C(5) | 1.191(7) | C(11)-C(16)-C(15) | 118.1(6) |
| C(13)-C(14) | 1.423(9) | C(24)-C(16)-C(15) | 121.1(6) |
| C(13)-C(20) | 1.424(10) | C(18)-C(17)-C(12) | 122.3(7) |
| C(14)-C(15) | 1.379(10) | C(17)-C(18)-C(19) | 120.9(8) |
| C(15)-C(16) | 1.437(8) | C(20)-C(19)-C(18) | 120.7(8) |
| C(34)-C(35) | 1.205(8) | C(42)-C(38)-C(37a) | 115.8(5) |
| C(54)-C(55) | 1.207(8) | C(40)-C(39)-C(37) | 119.9(7) |
| C(55)-C(56) | 1.434(8) | C(39)-C(40)-C(41a) | 121.4(7) |
| C(56)-C(58) | 1.387(8) | C(42)-C(41)-C(40a) | 119.1(7) |
| C(56)-C(57) | 1.406(7) | C(41)-C(42)-C(38) | 124.6(6) |
| C(61)-C(62) | 1.328(9) | C(55)-C(54)-Si(4) | 175.8(6) |
| C(1)-Si(1)-C(3) | 120.7(6) | C(54)-C(55)-C(56) | 176.5(6) |
| C(10)-Si(2)-C(7) | 106.8(3) | C(58)-C(56)-C(57) | 121.2(5) |
| C(33)-Si(3)-C(32) | 112.9(4) | C(58)-C(56)-C(55) | 120.0(5) |
| C(54)-Si(4)-C(51) | 108.9(3) | C(57)-C(56)-C(55) | 118.8(5) |
| C(5)-C(4)-Si(1) | 176.3(6) | C(56)-C(57)-C(59) | 121.2(5) |
| C(4)-C(5)-C(11) | 175.4(6) | C(56)-C(57)-C(58b) | 118.7(5) |
| C(7)-C(6)-C(14) | 175.9(6) | C(59)-C(57)-C(58b) | 120.1(5) |
| C(6)-C(7)-Si(2) | 173.9(4) | C(56)-C(58)-C(62) | 124.0(5) |
| C(11)-C(12)-C(17) | 124.9(6) | C(56)-C(58)-C(57b) | 120.0(5) |
| C(11)-C(12)-C(13) | 119.1(6) | C(59)-C(60)-C(61b) | 120.5(6) |
| C(17)-C(12)-C(13) | 116.0(7) | C(62)-C(61)-C(60b) | 120.3(6) |
| C(14)-C(13)-C(20) | 121.0(6) | C(61)-C(62)-C(58) | 123.3(6) |
| C(14)-C(13)-C(12) | 118.9(6) | | |

In the crystal structure of [PhPt($PEt_3$)$_2$C≡C($C_6H_4$)C≡CPt($PEt_3$)$_2$Ph] **1c** The metal complex sits on a crystallographic centre of symmetry, situated at the centre of the central arene ring, and co-crystallises with two chloroform solvent molecules. The molecular structure of **1c** is shown in **Figure 2.10** which also shows the hydrogen bond between the hydrogen atom of one of the chloroform molecules and the centre of one of the acetylenic C≡C triple bonds. The hydrogen bond parameters are H...C≡C(centroid) 2.517 Å, C-H...C≡C(centroid), 171.0°, and C...C≡C(centroid), 3.508 Å.

The complex **1c** can be viewed as the archetypal platinum "rigid rod" di-yne system on which much of the chemistry of the organometallic di-ynes, [PhPt($PEt_3$)$_2$C≡C-R-C≡CPt($PEt_3$)$_2$Ph], and poly-ynes, [-Pt($P^nBu_3$)$_2$-C≡C-R-C≡C-]$_n$, has been based.[5,25] The alkynylic units are essentially linear, with Pt-C≡C and C≡C-C angles within a few degrees of 180°. The Pt(1)-C(1) (alkynyl) bond, at 2.040(7) Å. The Pt-P distances (*av.* 2.294 Å) also lie in the expected range 2.27 – 2.32 Å by comparison to other structurally characterised systems[5,25]. The Pt(1)-C(6) (phenyl) distance is 2.074(7) Å, also falls in the previously determined range 2.05(2) – 2.09(3) Å. As expected the geometry at the platinum centre is distorted square planar, and this plane makes an angle of 60.36° with the plane of the central arene ring, and an angle of 82.54° degrees with the terminal phenyl ring. The terminal and central arene rings make an angle of 37.10° with each other (**Table 2.6**).

**Table 2.6: Selected Bond Lengths (Å) and Angles (°) for $[PhPt(PEt_3)_2C{\equiv}C(C_6H_4)C{\equiv}CPt(PEt_3)_2Ph]$ 1c**

| | | | |
|---|---|---|---|
| Pt(1)-C(1) | 2.040(7) | C(1)-Pt(1)-C(6) | 173.5(2) |
| Pt(1)-C(6) | 2.074(7) | C(1)-Pt(1)-P(1) | 93.4(2) |
| Pt(1)-P(1) | 2.2934(19) | C(6)-Pt(1)-P(1) | 87.7(2) |
| Pt(1)-P(2) | 2.295(2) | C(1)-Pt(1)-P(2) | 87.6(2) |
| C(1)-C(2) | 1.210(10) | C(6)-Pt(1)-P(2) | 91.1(2) |
| C(2)-C(3) | 1.449(9) | Pt(1)-C(1)-C(2) | 172.9(6) |
| C(3)-C(4) | 1.393(10) | C(1)-C(2)-C(3) | 175.3(8) |
| C(3)-C(5) | 1.393(10) | C(4)-C(3)-C(5) | 117.3(6) |
| C(4)-C(5a) | 1.369(9) | C(4)-C(3)-C(2) | 122.0(7) |
| C(5)-C(4a) | 1.369(9) | C(5)-C(3)-C(2) | 120.7(7) |
| P(1)-Pt(1)-P(2) | 178.39(6) | C(3)-C(4)-C(5a) | 121.0(7) |
| | | C(3)-C(5)-C(4a) | 121.7(7) |

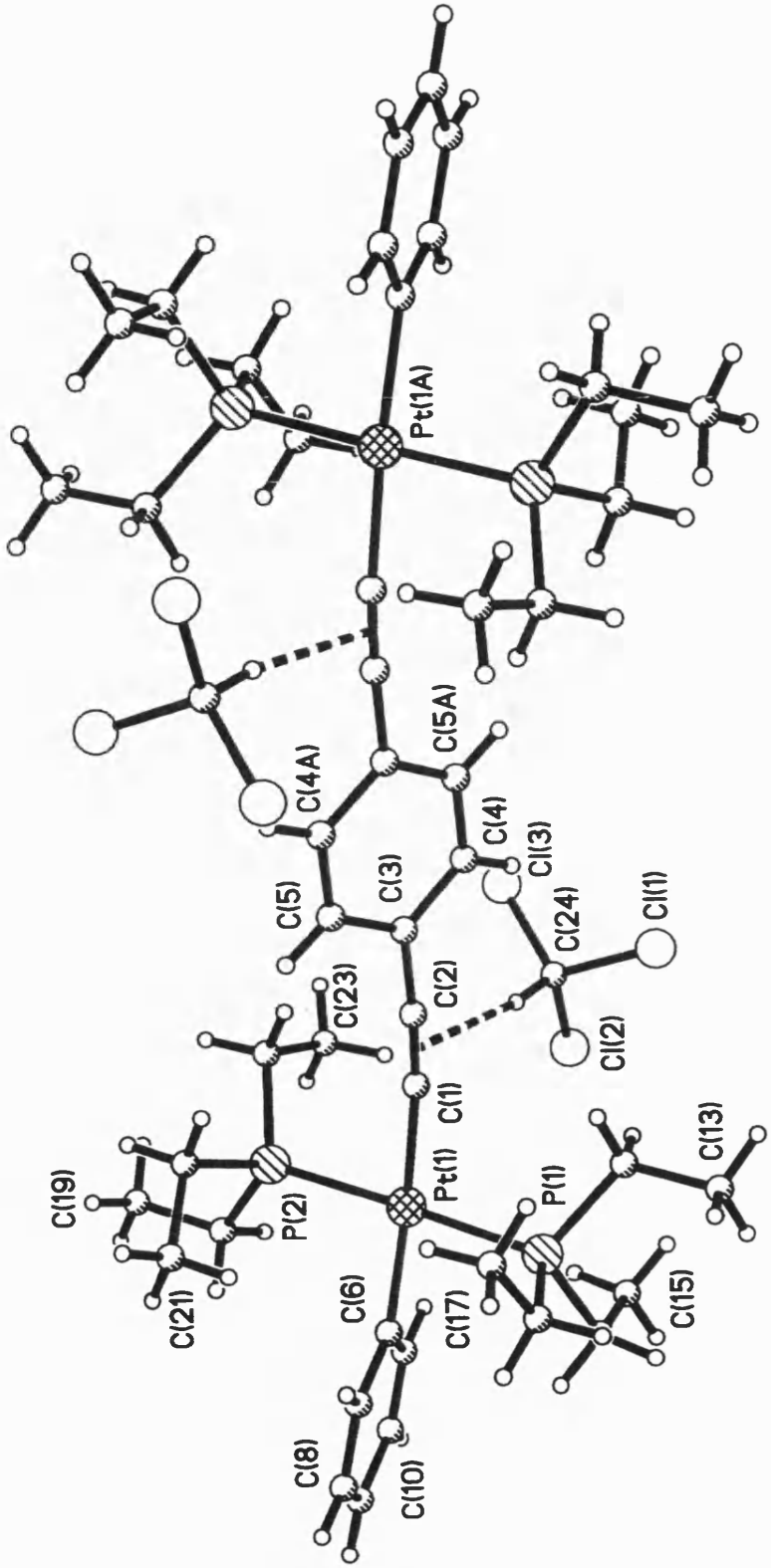
Pt(1A)
C(5A)
C(4A)
C(4)
Cl(3)
C(5)
C(3)
C(24)
Cl(1)
C(23)
C(2)
Cl(2)
C(1)
Pt(1)
P(2)
P(1)
C(13)
C(19)
C(21)
C(6)
C(17)
C(15)
C(8)
C(10)

**Figure 2.10**

The complex $[PhPt(PEt_3)_2C{\equiv}C\text{-}(C_{10}H_6)\text{-}C{\equiv}CPt(PEt_3)_2Ph]$ **2c** crystallises in the triclinic space group P-1 (no. 2) with one unique molecule of the di-platinum species and half a molecule of dichloromethane in the asymmetric unit. The molecular structure is displayed in **Figure 2.11** while selected bond lengths and angles are listed in **Table 2.7**. Unlike **1c**, there is no short contact between the solvent molecules and the acetylinic triple bonds. The shortest contacts involve hydrogen atoms from the disordered ethyl groups and the chlorine atoms of the dichloromethane molecule {H(22O)...Cl(61), 2.739 Å; H(21I)...Cl(62), 2.711 Å; H(16B)...Cl(61), 2.186 Å}. The molecular geometry of **2c** is related to that of **1c**. The terminal phenyl rings make angles of 87.4° and 88.5° with the two platinum-centred square planes. The central naphthalene unit is essentially planar, with a dihedral angle of 3.6°, between the two fused six-membered rings. The linked ring (C(1), C(2), C(3), C(4), C(5), C(10)) makes angles of 61.9° and 63.9° with the Pt(1)-centred and Pt(2)-centred square planes, respectively.

**Table 2.7 Selected Bond Lengths (Å) and Angles (°) for $[PhPt(PEt_3)_2C{\equiv}C\text{-}(C_{10}H_6)\text{-}C{\equiv}CPt(PEt_3)_2Ph]$ 2c**

| | | | |
|---|---|---|---|
| Pt(1)-C(12) | 2.001(4) | Pt(2)-C(201) | 2.067(4) |
| Pt(1)-C(101) | 2.064(4) | Pt(2)-P(21) | 2.2923(11) |
| Pt(1)-P(11) | 2.2892(11) | Pt(2)-P(22) | 2.2976(12) |
| Pt(1)-P(12) | 2.2865(10) | C(12)-Pt(1)-C(101) | 177.21(19) |
| C(11)-C(12) | 1.214(6) | P(11)-Pt(1)-P(12) | 174.84(4) |
| C(11)-C(1) | 1.436(6) | P(11)-Pt(1)-C(12) | 90.37(13) |
| C(1)-C(2) | 1.387(7) | P(11)-Pt(1)-C(101) | 91.31(12) |
| C(2)-C(3) | 1.402(6) | P(12)-Pt(1)-C(12) | 86.47(13) |
| C(3)-C(4) | 1.391(7) | P(12)-Pt(1)-C(101) | 91.70(12) |
| C(4)-C(5) | 1.431(6) | Pt(1)-C(12)-C(11) | 174.9(4) |
| C(5)-C(10) | 1.415(6) | C(12)-C(11)-C(1) | 176.5(5) |
| C(5)-C(6) | 1.428(6) | C(4)-C(41)-C(42) | 175.5(5) |
| C(6)-C(7) | 1.358(7) | C(41)-C(42)-Pt(2) | 177.1(4) |
| C(7)-C(8) | 1.412(7) | C(42)-Pt(2)-C(201) | 178.68(17) |
| C(8)-C(9) | 1.361(7) | P(21)-Pt(2)-P(22) | 173.97(5) |
| C(9)-C(10) | 1.438(7) | P(21)-Pt(2)-C(42) | 87.88(14) |
| C(4)-C(41) | 1.433(6) | P(21)-Pt(2)-C(201) | 90.81(11) |
| C(41)-C(42) | 1.217(6) | P(22)-Pt(2)-C(42) | 94.34(14) |
| C(42)-Pt(2) | 2.024(4) | P(22)-Pt(2)-C(201) | 86.97(11) |

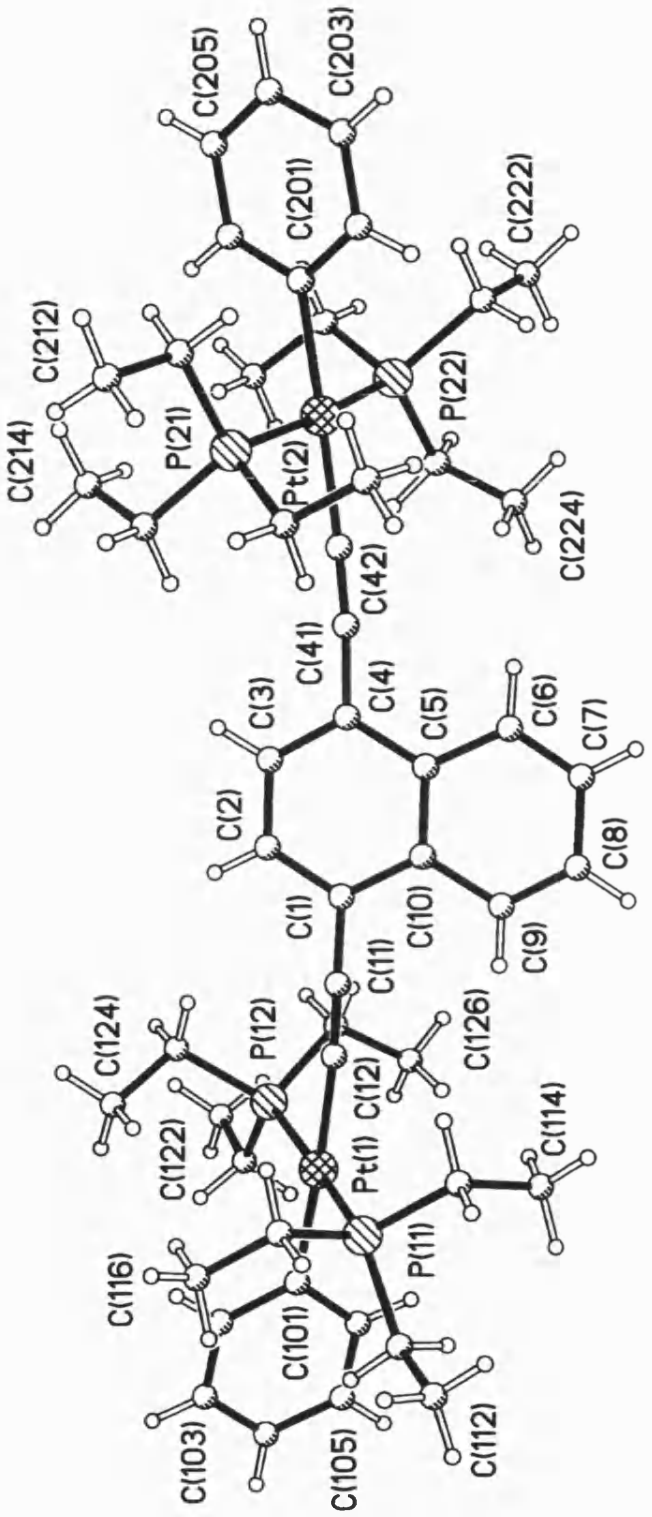


**Figure 2.11: The molecular structure of [PhPt($PEt_3$)$_2$C≡C-($C_{10}H_6$)-C≡CPt($PEt_3$)$_2$Ph] 2c. Only one orientation of the disordered $PEt_3$ groups is shown for clarity, and the $CH_2Cl_2$ solvent is also omitted.**

**Table 2.8. Crystallographic data**

| Compound | 2a | 3a | 1c | 2c |
|---|---|---|---|---|
| Formula | $C_{20}H_{24}Si_2$ | $C_{24}H_{26}Si_2$ | $C_{46}H_{74}P_4Pt_2.2CHCl_3$ | $C_{50}H_{76}P_4Pt_2$. 0.5 $CH_2Cl_2$ |
| $M_r$ | 320.57 | 370.6 | 1379.85 | 1233.63 |
| Crystal habit | Colourless block | Colourless prism | Yellows plate | Yellow plate |
| Crystal size [mm] | 0.18x0.16x0.09 | 0.18x0.08x0.04 | 0.30x0.24x0.06 | 0.50x0.12x0.03 |
| Crystal system | Orthorhombic | Monoclinic | Triclinic | Triclinic |
| Space group | *Pbca* | *$P2_1/c$* | *P-1 (No. 2)* | *P-1 (No. 2)* |
| Cell dimensions | | | | |
| *a* [Å] | 17.6525(15) | 22.511(16) | 9.615(2) | 9.2606(1) |
| *b* [Å] | 12.6498(12) | 16.794(18) | 11.356(4) | 16.6595(2) |
| *c* [Å] | 18.3731(15) | 11.829(10) | 13.277(4) | 18.7419(2) |
| α [°] | 90 | 90 | 83.84(2) | 112.549(1) |
| β [°] | 90 | 90.00(7) | 84.89(2) | 95.470(1) |
| γ [°] | 90 | 90 | 79.79(2) | 94.400(1) |
| *U* [$Å^3$] | 41027.(6) | 4472(7) | 1414.9(7) | 2637.82(5) |
| *Z* | 8 | 8 | 1 | 2 |
| $\mu$ [$mm^{-1}$] | 0.169 | 0.163 | 5.365 | 5.501 |
| *T* [°C] | -103 | -123 | -93 | -123 |
| $\theta_{max}$ [°] | 25.01 | 25.00 | 24.97 | 30.09 |
| Wavelength [Å] | 0.71073 | 0.6941 | 0.71069 | 0.71073 |
| No. of reflections | | | | |
| Measured | 6797 | 24363 | 9296 | 96643 |
| Independent | 3610 | 8424 | 4969 | 15448 |
| $R_{Int}$ | 0.034 | 0.056 | 0.031 | 0.084 |
| Parameters | 205 | 480 | 271 | 602 |
| Restraints | 12 | 327 | 0 | 18 |
| *wR2*($F^2$, all refl.) | 0.115 | 0.266 | 0.1173 | 0.0949 |
| *R1[F>2σ(F)]* | 0.045 | 0.085 | 0.0287 | 0.0357 |
| GoF | 1.045 | 1.022 | 1.252 | 1.063 |

## 2.2.4 Crystal structures of 4b-9b

Structures of compounds **4b-7b** were determined by single-crystal X-ray diffraction and those of the alkoxy derivatives **8b** and **9b** by powder X-ray diffraction. In **1b** the potential donor (ethynyl H) and acceptor (C≡C bonds) H-bonding favour the formation of a two-dimensional net of co-operative H-bonds, linking molecules into a puckered layer **(Figure 2.12, Table 2.9).**

**Table 2.9. Intermolecular interactions in crystals of 1b and its fluorinated derivatives**

| Compound | **1b**[17b] | **1b**[17c] | **5b** | **6b** | **6b** | **7b** | **7b** | **7b** |
|---|---|---|---|---|---|---|---|---|
| **T, K** | 295 | 125 | 180 | 180 | 120 | 273 | 180 | 150 |
| (i)[a] H···π, Å | 2.68 | 2.60 | 2.75 | 2.87 | 2.85 | 2.94 | 2.93 | 2.89 |
| (i) C–H···π, ° | 176 | 175 | 168 | 161 | 160 | 129 | 127 | 127 |
| (ii) H···F, Å | | | 2.66 | 2.60 | 2.58 | | | |
| (ii) C–H···F, ° | | | 121 | 122 | 122 | | | |
| (iii) H···F, Å | | | 2.86 | 2.94 | 2.88 | 2.49 | 2.41 | 2.41 |
| (iii) C–H···F, ° | | | 90 | 116 | 117 | 132 | 136 | 134 |
| $d$[b], Å | 3.71[b] | 3.53 | 3.47 | 3.43 | 3.41 | 3.63 | 3.60 | 3.59 |

[a]See notation in Figures 2.8 and 2.11. [b]Mean interplanar distance in the π-π stack.

Introduction of a polar (amino) group in **4b** contributes two additional "active" H atoms, but only one potential acceptor site (the lone pair of N). The prominent feature of this structure (**Figure 2.14**) is a ring system of co-operative H-bonds, involving four molecules. The ring (having crystallographic $C_i$ symmetry) includes two relatively strong C≡CH···$\pi_{C\equiv C}$ bonds (H···π = 2.51 Å, C–H···π = 145°)[‡] and two C≡CH···N bonds (H···N = 2.44 Å, C–H···N = 159°), directed towards the lone pair of the substantially pyramidalised N atom.

[‡] All hydrogen bond parameters are calculated for idealized bond lengths C–H 1.08 Å and N–H 1.01 Å

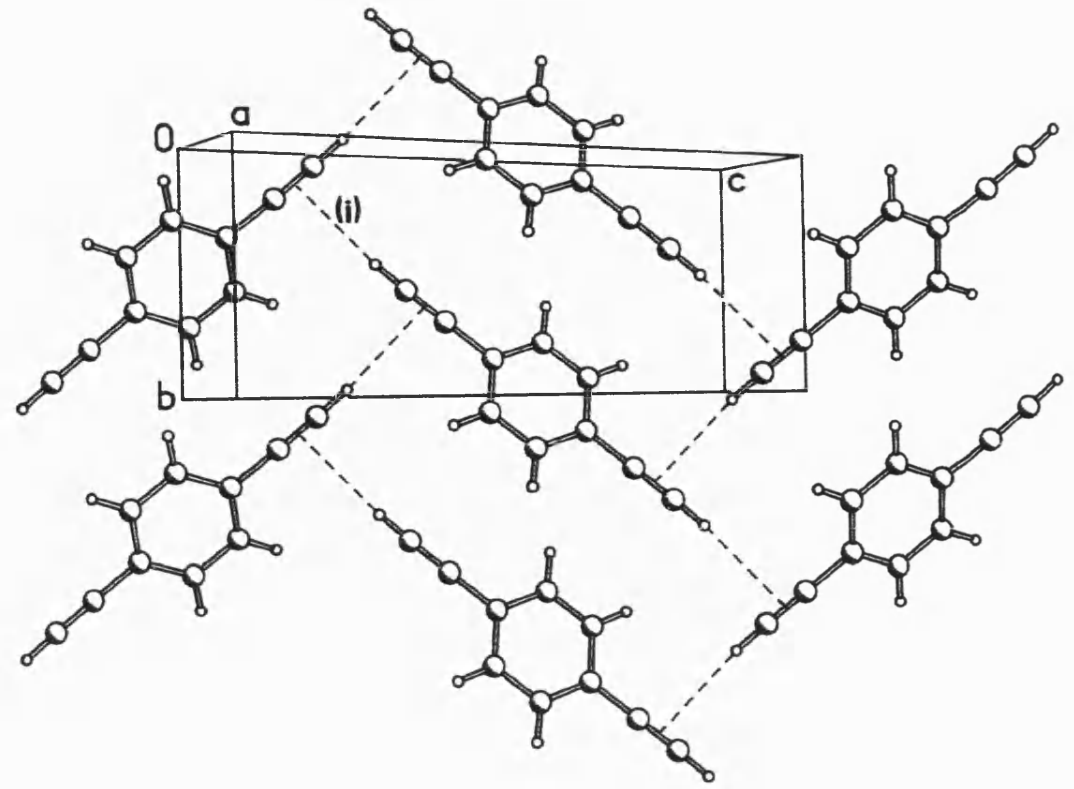
0
a
c
b
(i)

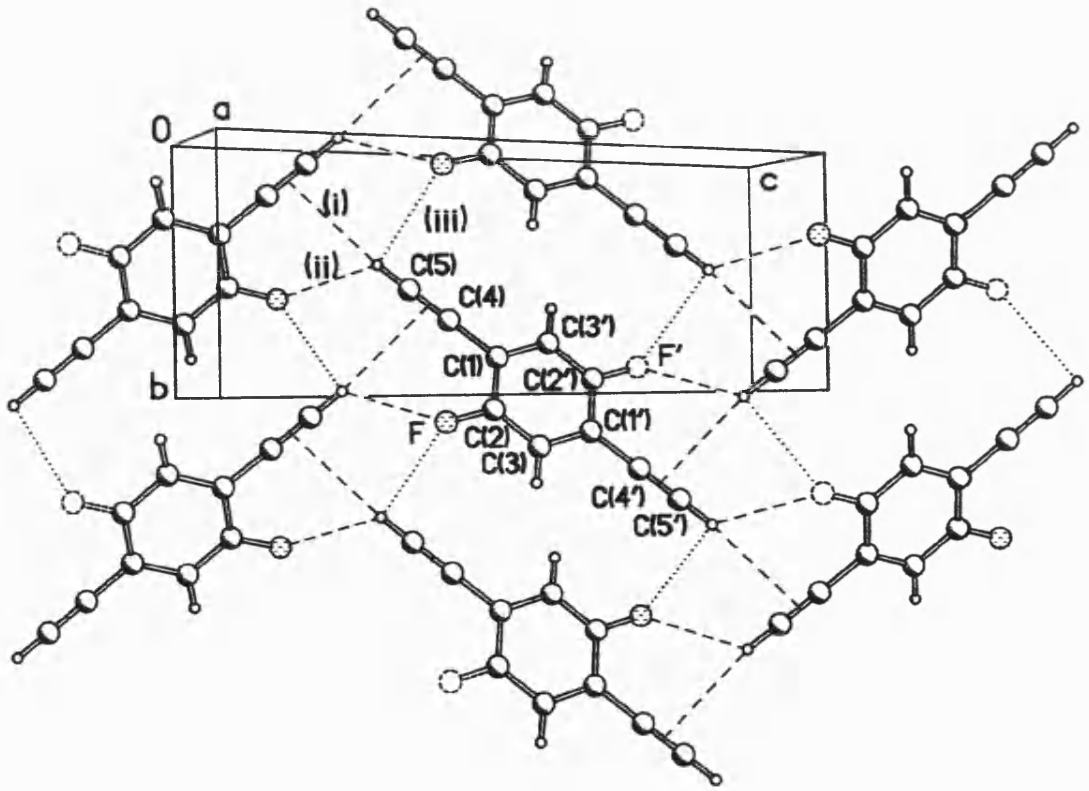
0
a
c
b
(i)
(ii)
(iii)
C(5)
C(4)
C(3')
C(1)
C(2')
F'
F
C(2)
C(3)
C(1')
C(4')
C(5')

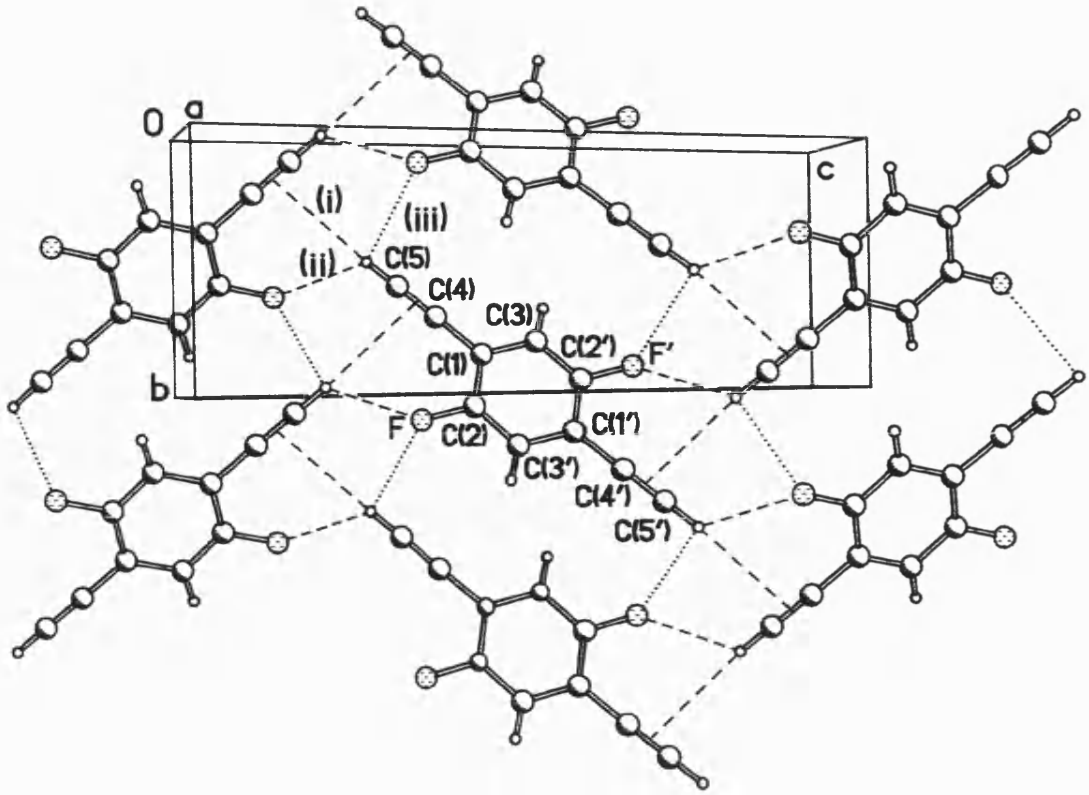


**Figure 2.12. Crystal structures of 1b, 5b and 6b; projections on the (1 0 –2) plane.**

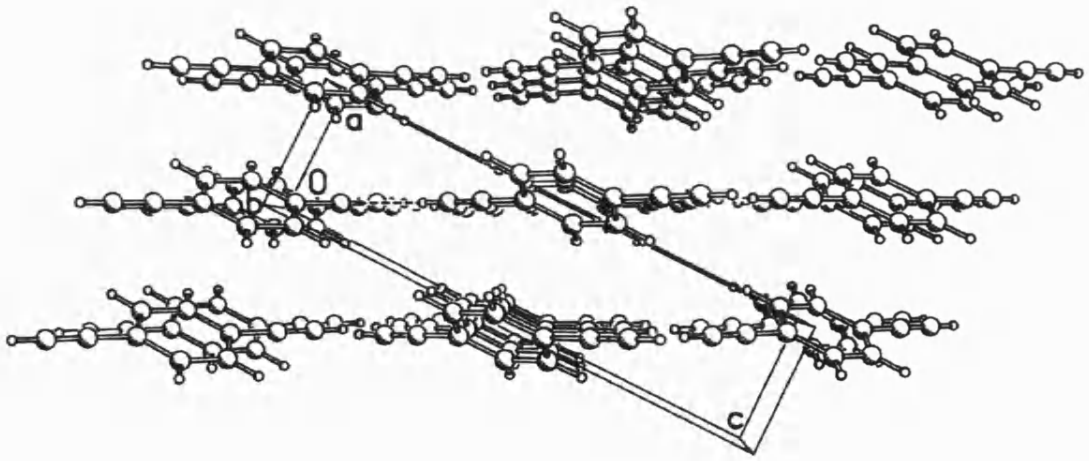


**Figure 2.13. Crystal structure of 1b, viewed down the *y* axis.**

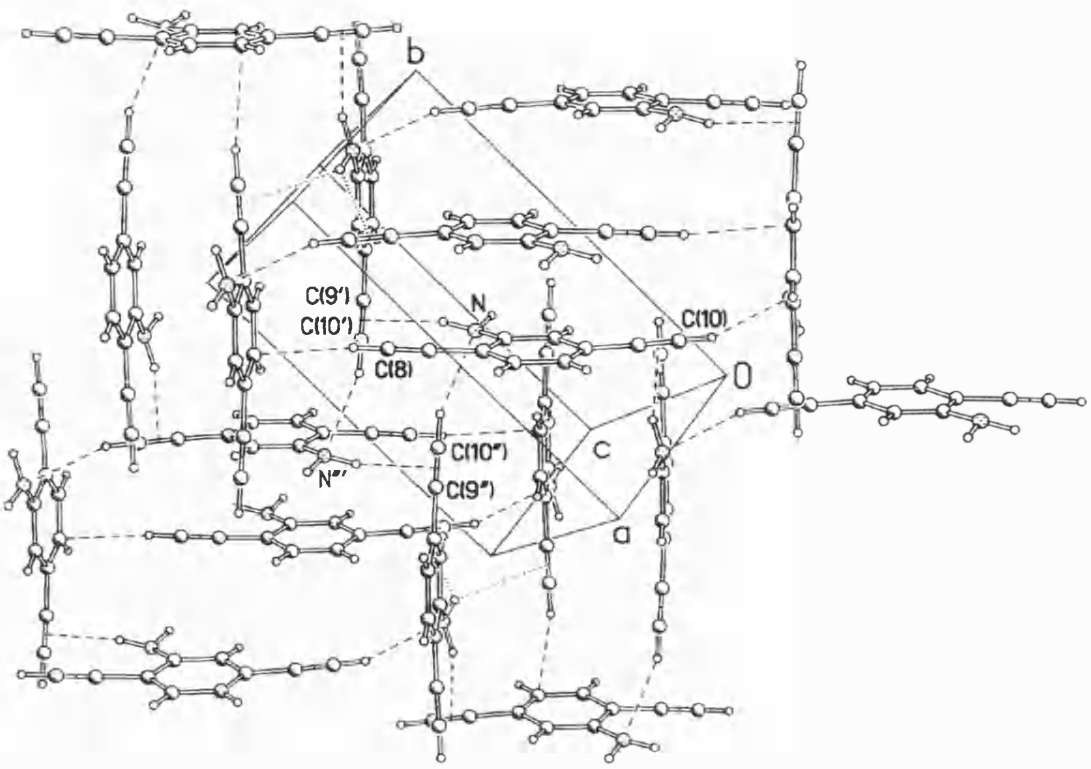


**Figure 2.14. Crystal structure of 4b, projected on the (1 0 –2) plane**

The H atoms are bonded to $sp^2$ or *sp*-hybridised C atoms. In **5b** and **6b** the C≡CH···$\pi_{C\equiv C}$ H-bond of **1b** is weakened, or rather replaced by a bifurcated H-bond to both the C≡C group and the fluorine atom of the same molecule, the C≡CH···F interaction being the stronger of the two. Thus, the H···π distance increases by *ca.* 0.2 Å from that in **1b** to that in **6b**. Comparison of the structure of **6b** at different temperatures (180 and 120 K) shows similar (*ca.* 0.02 Å) thermal expansions of the H-bonds (i) and (ii) and the interplanar separations (*d*) in the π–π stack, but a larger extension of contact (iii). The layers in all three structures are similarly puckered: the dihedral angles between H-bonded molecules are 48° (**1b**), 52° (**5b**) and 54° (**6b**).

The increased degree of fluorination in compound **7b** gives rise to completely different crystal packing (**Figure 2.15**). The molecule also possesses crystallographic $C_i$ symmetry, but the principal synthon in structure **7b** is the pair of inversion-related, parallel and nearly coplanar molecules, linked by two C≡CH···F hydrogen bonds (iii),

shorter than in **5b** and **6b** (see **Table 2.9**). Thus molecules are linked into an infinite 'ribbon', parallel to the (1 0 −1) direction. There are no continuous π–π stacks of molecules, although each molecule has one neighbour contacting it in a π–π fashion. These molecules, related by an inversion centre, have a longitudinal (parallel to the C≡C bond) shift of *ca.* 4.3 Å, so that a C≡C bond of one molecule overlaps with the benzene ring of another. The interplanar separation contracts from 3.63 Å at 273 K to 3.59 Å at 150 K.

This double ribbon is surrounded on all sides by four other ribbons, propagating in the same direction but with perpendicular molecular planes. Each ethynyl H atom participates in a rather long inter-ribbon C≡CH···$\pi_{C\equiv C}$ contact (i) (**Table 2.9**); the interaction thus can be interpreted as a very asymmetric bifurcated H-bond. Structure determinations at 273, 180 and 150 K did not reveal any substantial change, although thermal expansion in the direction of the strongest H-bond (iii) is somewhat greater than in other directions.

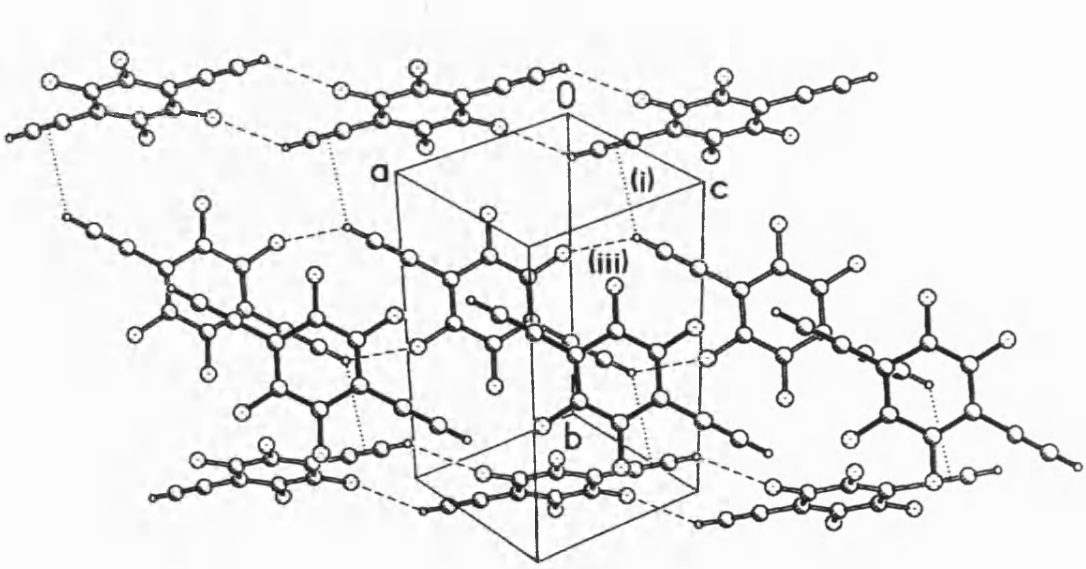


**Figure 2.15. Crystal structure of 7b.**

The crystal packing of di-alkoxy derivatives **8b** and **9b** are shown in **Figures 2.16** and **2.17**. Both molecules have crystallographic $C_i$ symmetry and adopt planar (**8b**) or nearly planar(**9b**) conformations. Structure **8b** comprises puckered layers, parallel to the (1 0 −2) plane and broadly similar to those observed in structures **5b** and **6b**, in which the

molecules are linked by C≡CH···O hydrogen bonds (H···O = 2.34 Å, C–H···O = 146°), while the C≡CH···$\pi_{C\equiv C}$ interaction between the same molecules is much weaker than in structures **5b** and **6b** (H···π = 3.07 Å, C–H···π = 137°). Unlike **1b** and **4b**–**6b**, structure **8b** contains no π–π stacks, molecules of adjacent layers contacting in a herring-bone fashion.

Structure **9b** contains nearly-flat layers, in which a synthon, broadly similar to that of structure **7b** can be identified: a centrosymmetric pair of molecules, linked by two C≡CH···O hydrogen bonds. These, however, are much weaker than in **8b** (H···O = 2.80 Å, C–H···O = 167°). Probably, the crystal structure of **9b** is dominated by the close packing of (all-*trans*) *n*-alkyl chains, to which the H-bonding pattern has to adjust

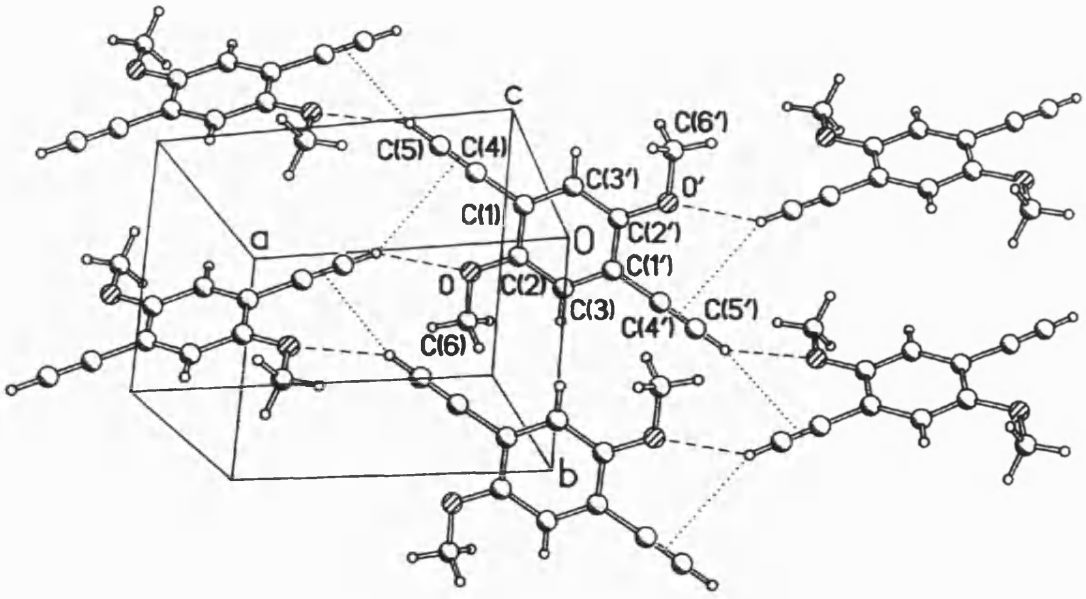


**Figure 2.16. Crystal structure of 8b.**

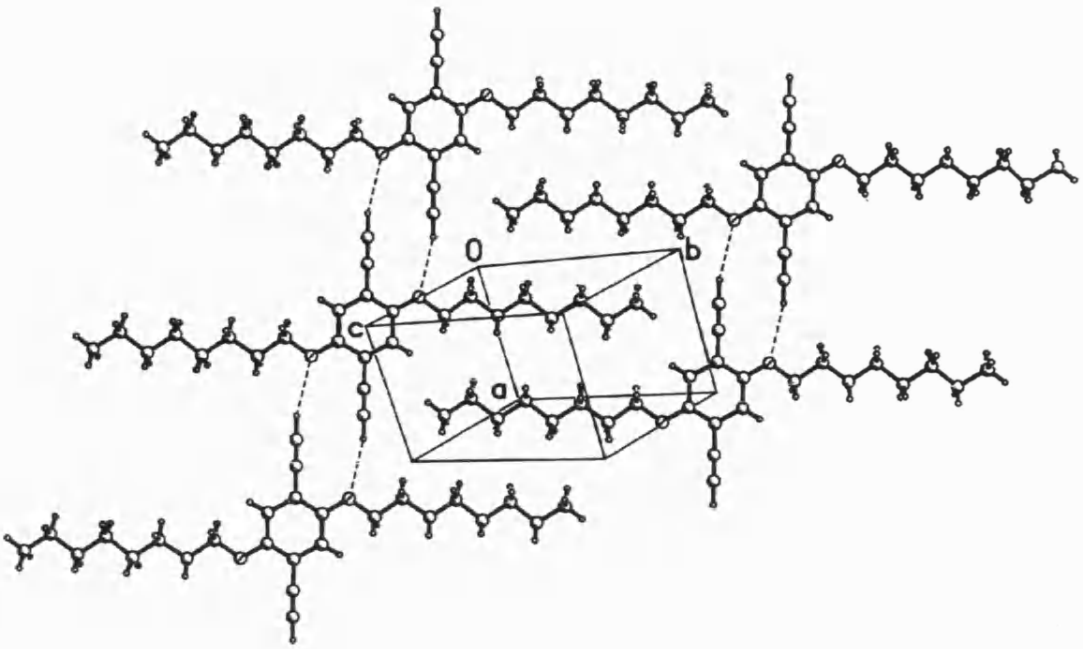


**Figure 2.17. Crystal structure of 9b.**

## 2.2.5 Optical spectroscopy

The results of optical spectroscopy of all the systems described in this thesis have been carried out by the group of Professor Sir Richard R. Friend and Dr. Anna Köhler from the Cavendish Laboratory, University of Cambridge. Their effort in measuring and providing us with these results is gratefully acknowledged. **Figure 2.18** shows the room temperature absorption spectra and photoluminescence spectra taken at room temperature and at 10 K for the Pt(II) poly-ynes **1d-3d** and di-ynes **1c-3c**. For **1d** and **1c**, the first absorption band has been assigned to transitions between the mixed ligand $\pi$ and platinum 5d orbitals and the ligand $\pi^*$ and platinum 6p orbitals.[5,26] This band shifts to lower energies along the series that suggests an increase in donor-acceptor interaction between the Pt(II) centre and the conjugated ligand. Along the series, the absorption of the poly-ynes is shifted to the red compared to the corresponding di-ynes, which indicates that the conjugation of the ligand continues through the metal centre.

The band gaps, taken as the onset of absorption, are 3.4 eV for **1c**, 3.0 eV for **2c** and

2.40 eV for **3c**, and are 3.0 eV for **1d**, 2.85 eV for **2d** and 2.30 eV for **3d**, which can be considered as insulators or high band gap semiconductors. The relatively high band gaps compared to some systems with less than 2.0 eV[5c] might be due to less electronic interactions in these systems.

The photoluminescence spectra of **1d** and **1c** show two emission bands which have previously been assigned to a singlet $S_1$ state (fluorescence) and a triplet $T_1$ state (phosphorescence) by lifetime and photoinduced absorption measurements.[5,10,11] The emission bands centered around 2.8 eV in **2d** and **2c** and around 2.2 eV in **3d** and **3c** are attributed to the singlet $S_1$ state since this emission is located just beneath the $S_1$ absorption band and shows little temperature dependence, while the emission peaking at 1.96 eV in **2d** and **2c** could be assigned to a triplet $T_1$ state. It is a temperature dependent peak and it is at the expected energetic position for the triplet emission,[5e] and shows vibronic structure that excludes it from being an excimer state that appear as structureless, broad and weakly emissive band.

For compounds **3d** and **3c** that contain an anthracene unit no phosphorescence was observed in thin films. The $T_1$ state is expected to be at around 1.5 eV. The platinum atom mainly determines the spin-orbit coupling in these compounds and thus the radiative decay rate $k_r$ should be similar throughout the series. The loss of phosphorescence might be due to the increase of the organic nature of **3d** compared to the smaller spacer groups in **1d** and **2d**. It has been shown by previous studies that the non-radiative decay rate $k_{nr}$ increases exponentially with decreasing $T_1$ energy and is expected to be three orders of magnitude larger in **3d** than in **1d**,[27b] so that the detection of the phosphorescence becomes very difficult.

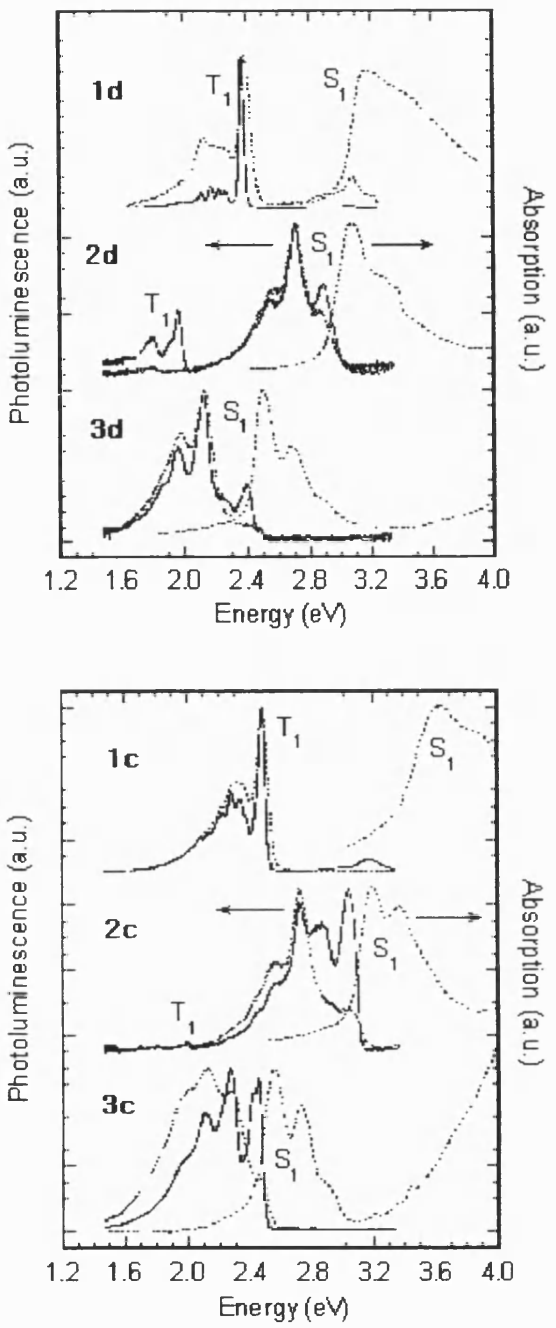


**Figure 2.18: Thin film photoluminescence and absorption spectra of (a) Pt(II) polyynes 1d-3d and (b) the diynes 1c-3c at room temperature (dotted lines) and at 10 K (solidlines). The spectra are normalised to unity at the peak of the emission or absorption.**

Poly-ynes **4d-9d** provided an opportunity to investigate the effect of substituents on the aromatic spacer group on the electronic properties of the materials. Having the absorption and emission spectra taken at room temperature from thin films, of polymers **7d** and **8d** as well as that for **1d,** for comparison, are shown in **Figure 2.19**. Substitution by fluorine or by methoxy groups leads to a weak red shift of 0.05 eV and 0.15 eV, respectively, from that in **1d** indicating only slightly more conjugated backbones. Substitution with less than four fluorines, as in **5d** and **6d**, leads to correspondingly smaller red shift (**Figure 2.20**).

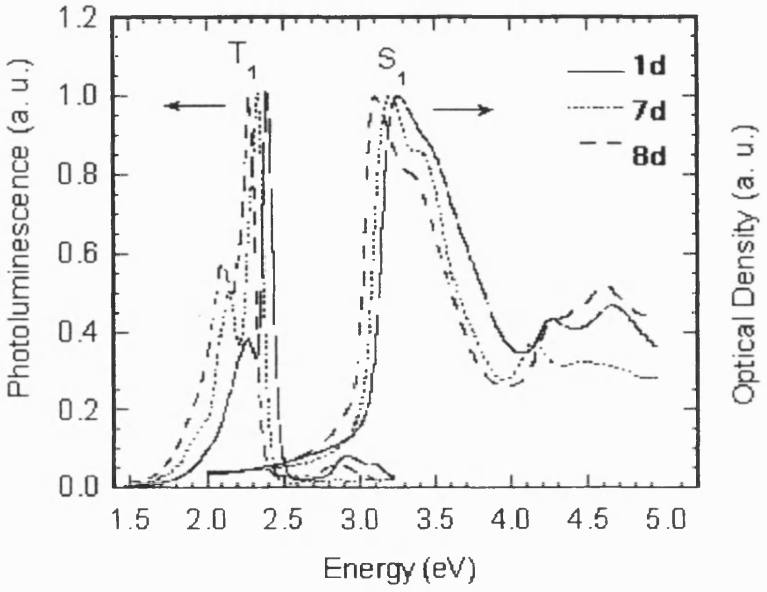


**Figure 2.19. Absorption and luminescence spectra of the platinum(II) poly-ynes 1d, 7d and 8d taken from thin films at room temperature with excitation at 3.4 eV.**

The emission spectra also consist of two bands in this system. The band just below the onset of absorption at 3.0 eV is emission from the $S_1$ state (fluorescence). The band below 2.5 eV is assigned to emission from the triplet excited state $T_1$ (phosphorescence). Substitution of the aromatic ring shifts the energy of the $T_1$ emission by about the same amount as the $S_1$ emission, so that the $S_1$-$T_1$ energy difference remains constant. The constant $S_1$-$T_1$ energy gap has been observed for these organometallic and analogous organic polymers that is controlled by the exchange energy which is determined by the $\pi$-$\pi^*$ orbital overlap

The emission spectra normalised to the fluorescence peak for the polymers with one, two and four fluorine substituents (polymers **5d**, **6d** and **7d**, respectively) are shown in **Figure 2.20**. The relative intensity of phosphorescence increases strongly with the fluorine content.

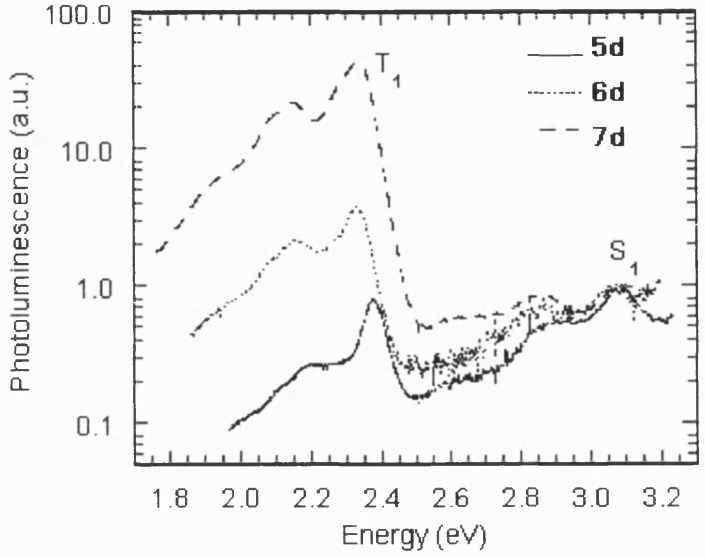


**Figure 2.20. Room temperature thin-film luminescence spectra of platinum(II) poly-ynes 5d, 6d and 7d normalised to the peak of the $S_1$ emission and shown on a logarithmic scale.**

**Table 2.10: Optical data for some poly-ynes[a].**

| Compound | $S_0 \rightarrow S_1$ (Onset) | $S_1 \rightarrow S_0$ (Peak) | $T_1 \rightarrow S_0$ (Peak) | $T_1$-$S_1$ gap |
|---|---|---|---|---|
| **1d** | 3.0 | 2.95 | 2.35 | 0.60 |
| **2d** | 2.85 | 2.70 | 2.0 | 0.70 |
| **3d** | 2.30 | ~ 2.40 | - | |
| **5d** | - | 3.10 | 2.35 | 0.75 |
| **6d** | - | 3.10 | 2.30 | 0.80 |
| **7d** | 2.95 | - | 2.30 | |
| **8d** | 2.85 | 2.85 | 2.25 | 0.60 |

[a] Energies in eV

## 2.3 Conclusion

The work described in this chapter provides a convenient entry to a series of Pt(II) di-ynes and poly-ynes incorporating condensed carbocyclic spacer groups in the backbone. Attempts have been made to evaluate how the nature of the central linking unit would influence their spectroscopic, optical, thermal, and structural properties. From the optical spectroscopic measurements it is apparent that the electron-rich anthracene spacer creates strong donor-acceptor interactions between the Pt(II) centres and conjugated ligands along the rigid backbone of the polymers. Thermogravimetry shows that the di-ynes possess a somewhat higher thermal stability than the corresponding poly-ynes. Both the Pt(II) di-ynes and the poly-ynes exhibit increasing thermal stability along the series of spacers from phenylene through naphthalene to anthracene. In addition, a number of substituted derivatives of 1,4-diethynylbenzene with electron donating and accepting substituents have been studied, and their structural characterisation performed by both single-crystal and powder X-ray diffraction. An interesting result of this work has been the ability to obtain comparable structural information from conventional techniques (single crystal) and from powder X-ray diffraction.

The packing analysis of the structures of the polymer precursors has also thrown light on the co-presence of weak hydrogen bonding in model compounds of polymers that are of technological interest. In summary the ethynylenic moiety provides a good hydrogen bond donor and acceptor, which is able to compete in terms of intermolecular interactions and as structure defining synthons, with more electronegative atoms, such as nitrogen. C≡CH···$\pi_{C\equiv C}$ hydrogen bonds dominate the crystal structure **1b**, and are gradually replaced by C≡C–H···F ones with the increase of fluorination (**5b**→**7b**), or completely replaced by C≡CH···N and NH···$\pi_{C\equiv C}$ bonds in **4b**, and C≡CH···O in **8b** and **9b**. A C–H···$\pi_{C\equiv C}$ bond in **1b** has been estimated being of *ca.* 4 kJ mol$^{-1}$.[25] When alkoxy substituents are present, C–H···O interactions occur, but the presence of long alkyl chains in the structure can impede the formation of these short contacts.

The substituted 1,4-diethynyl benzene ligands have also been incorporated into rigid-rod

Pt(II) polymers and their thermal and opto-electronic properties investigated. The substituents on the aromatic spacer have a major effect on the thermal stability of the polymeric complexes but their electronic properties are affected only to a limited extent.

## 2.4 References


1) (a) A. J. Heeger and J. Long Jr., *Optics & Photonics News*, **1996**. 7(8), 24; (b) H. S. Nalwa, in *Nonlinear Optics of Organic Molecules and Polymers*, Eds. H. S. Nalwa and S. Miyata, CRC, New York, **1997**, pp 611-787; (c) S. R. Marder, B. Kippelen, A. K.-Y. Jen and N. Peyghambarian, *Nature*, **1997**, 388, 845.
2) (a) A. Montali, C. Bastiaansen, P. Smith and C. Weder, *Nature*, **1998**, 392, 261; (b) D. Steiger, P. Smith and C. Weder, *Macromol. Rapid Commun.*, **1997**, 18, 643; (c) C. Weder, C. Sarwa, A. Montali, C. Bastiaansen and P. Smith, *Science*, **1998**, 279, 835.
3) N. J. Long and C. K. Williams, *Angew. Chem., Int. Ed. Engl.*, **2003**, 42, 2.
4) M. A. Baldo, M. E. Thompson and S. R. Forrest, *Nature*, **2000**, 403, 750; V.
5) (a) Y. Liu, S. Jiang, K. Glusac, D. H. Powell, D. F. Anderson and K. S. Schanze, *J. Am. Chem. Soc.*, **2002**, 124, 12412; (b) V. W-W Yam, *Acc. Chem. Res.*, **2002**, 35, 555; (c) M. Younus, A. Kohler, S. Cron, N. Chawdhury, M.R.A. Al-Mandhary, M.S. Khan, J. Lewis, N.J. Long, R.H. Friend and P.R. Raithby, *Angew. Chem. Int. Ed. Engl.*, **1998**, 37, 3036; (d) N. Chawdhury, A. Kohler, R.H. Friend, W.-Y. Wong, M. Younus, P.R. Raithby, J. Lewis, T.C. Corcoran, M.R. A. Al-Mandhary and M.S. Khan, *J. Chem. Phys.*, **1999**, 110, 4963; (e) J. S. Wilson, A. Kohler, R. H. Friend, M. K. Al-Suti, M. R. A. Al-Mandhary, M. S. Khan and P.R. Raithby, *J. Chem. Phys.*, **2000**, 113, 7627; (f) N. Chawdhury, A. Kohler, R.H. Friend, M. Younus, N. J. Long, P. R. Raithby and J. Lewis, *Macromolecules*, **1998**, 31, 722.
6) (a) K. Ogawa and S. Rasmussen, *J. Org. Chem.*, **2003**, 68, 2921; (b) J. Roncali, *Chem. Rev.*, **1997**, 97, 173.
7) (a) N. G. Pschirer, T. Miteva, U. Evans, R. S. Roberts, A. R. Marshall, D.

Neher, M. L. Myrick and U. H. F. Bunz, *Chem. Mater.*, **2001**, 13, 2691; (b) T. M. Swager, C. J. Gil and M. S. Wrighton, *J. Phys. Chem.*, **1995**, 99, 4886; (c) D. J. Fatemi, H. Murata, C. D. Merritt and Z. H. Kafafi, *Synth. Met.*, **1997**, 85, 1225; (d) M. Hirohata, K. Tada, T. Kawai, M. Onoda and K. Yoshino, *Synth. Met.*, **1997**, 85, 1273; (e) N. G. Pschirer, M. E. Vaughn, Y. B. Dong, H-C. Zur Loye and U. H. F. Bunz, *Chem. Commun.*, **2000**, 85; (f) G. McSkimming, J. H. R. Tucker, H. Bouas-Laurent and J-P. Desvergne, *Angew. Chem. Int. Ed.*, **2000**, 39, 2167; (g) S. A. Manhart, A. Adachi, K. Sakamaki, K. Okita, J. Ohshita, T. Ohno, T. Hamaguchi, A. Kunai and J. Kido, *J. Organmet. Chem.*, **1999**, 592, 52; (h) M. E. Wright and D. A. Schorzman, *Macromolecules*, **2001**, 34, 6550; (i) M. E. Wright, D. A. Schorzman and A. M. Berman, *Macromolecules*, **2002**, 35, 4768.

8) (a) A. P. Davey, S. Elliot, O. O'Connor and W. Blau, *J. Chem. Soc. Chem. Commun.*, **1995**, 1433; (b) W. E. Douglas, D. M. H. Guy, A. K. Kar and C. Wang, *Chem. Commun.*, **1998**, 2125; (c) J. G. Rodriguez and J. L. Tejedor, *J. Org. Chem.*, **2002**, 67, 7631; (d) W. Y. Wong, A. W. M. Lee, C. K. Wong, G. L. Lu, H. Zhang, T. Mo and K. T. Lam, *New J. Chem.*, **2002**, 26, 354; (e) N. G. Pschirer, T. Miteva, U. Evans, A. R. Marshall, C. Stanley, H. W. Beckham and U. H. F. Bunz, *Macromol. Rapid. Commun*, **2000**, 21, 493; (f) P. N. Taylor, A. P. Wylie, J. Huuskonen and H. L. Anderson, *Angew. Chem. Int. Ed.*, **1998**, 37, 986; (g) A. El-Ghayoury and R. Ziessel, *Tet. Lett.*, **1997**, 38, 2471; (h) A. El-ghayoury, A. Harriman, A. Khatyr and R. Ziessel, *J. Phys. Chem. A* **2000**, 104, 1512; (i) A. El-ghayoury, A. Harriman, A. Khatyr and R. Ziessel, *Angew. Chem. Int. Ed.*, **2000**, 39,185; (j) K. Kilsa, J. Kajanus, J. Märtensson and B. Albinsson, *J. Phys. Chem. B* **1999**, 103, 7329; (k) K. Kilsa, J. Kajanus, A. N. Macpherson, J. Märtensson and B. Albinsson, *J. Am. Chem. Soc.*, **2000**, 122, 1749.

9) K. Tada, M. Onoda, M. Hirohata, T. Kawai and K. Yoshino, *Jpn., J. Appl. Phys.*, **1996**, 35, L251.

10) (a) S. J. Davies, B. F. G. Johnson, M. S. Khan and J. Lewis, *J. Chem. Soc., Chem. Commun.*, **1991**, 187; (b) J. Lewis, M. S. Khan, A. K. Kakkkar, B. F. G. Johnson, T. B. Marder, H. B. Fyfe, F. Wittmann, R. H. Friend and A. E.

Dray, *J. Organomet. Chem.*, **1992**, 425, 165; (c) S. Takahashi, Y. Ohyam, E. Murata, K. Sonogashira and N. Hagihara, *J. Polym. Sci.: Poym. Chem. Ed.*, **1980**, 18, 349.

11) (a) N. Chawdhury, A. Köhler, R. H. Friend, W.-Y. Wong, J. Lewis, M. Younus, P. R. Raithby, T.C. Corcoran, M.R.A. Al-Mandhary and M. S. Khan, *J. Chem. Phys.*, **1999**, 110, 4963. (b) K. Mullen and G. Wegner, 'Electronic Materials: the Oligomer Approach', Wiley-VCH, **1998**.

12) J. Cornil, D. A. dos Santos, X. Crispin, R. Silbey and J. L. Bredas, *J. Am. Chem. Soc.*, **1998**, 120, 1289.

13) (a) G.R. Desiraju, *J. Chem. Soc., Chem. Commun.*, **1990**, 454; (b) P.J. Langley, J. Hulliger, R. Thaimattam and G.R. Desiraju, *New J. Chem.*, **1998**, 1307; (c) J.M.A. Robinson, D. Philp, B.M. Kariuki and K.D.M. Harris, *Chem. Commun.*, **1999**, 329.

14) (a) T. Steiner, *J. Chem. Soc., Chem. Commun.*, **1995**, 95; (b) D. Philp and J.M.A. Robinson, *J. Chem. Soc., Perkin Trans. 2*, **1998**, 1643.

15) S. Kumar, K. Subramanian, R. Srinivasan, K. Rajagopalan, A. M. M. Schreurs, J. Kroon, G. Koellner, and T. Steiner, *J. Mol. Struct.*, **1998**, 448, 51.

16) T. Steiner, B. Lutz, J. van der Maas, N. Veldman, A.M.M. Schreurs, J. Kroon and J. A. Kanters, *Chem. Commun.*, **1997**, 191.

17) a) N.A. Ahmed, A.I. Kitaigorodsky and M. Sirota, *Acta Cryst.*, **1972**, B28, 2875; b) J.M.A. Robinson, B.M. Kariuki, R.J. Gough, K.D.M. Harris and D. Philp, *J. Solid State Commun.*, **1997**, 134, 203; c) H.-C. Weiss, D. Bläser, R. Boese, B.M. Doughan and M.M. Haley, *Chem. Commun.*, **1997**, 1703.

18) T. Steiner, E.B. Starikov and M. Tamm, *J. Chem. Soc. Perkin Trans. 2*, **1996**, 67.

19) V. N. Vangala, A. Nangia and V. M. Lynch, *Chem. Commun.*, **2002**, 1304.

20) T. Steiner, *J. Chem. Soc., Chem. Commun.*, **1994**, 101.

21) B. F. Duerr, Y-S Chung and A.W. Czarnik, *J. Org. Chem.*, **1988**, 53, 2120.

22) J. Manna, K. D. John, M. D. Hopkins, *Adv. Organomet. Chem.*, **1995**, 38, 79.

23) G. Odian, *Principles of Polymerization*, 3rd ed.; John Wiley & Sons, New York, **1991**.

24) S. Takahashi, Y. Kuroyama, K. Sonogashira and N. Hagihara, *Synthesis*,

**1980**, 627.

25) (a) M. S. Khan, M. R. A. Al-Mandhary, M. K. Al-Suti, A. K. Hisham, P. R. Raithby, B. Ahrens, M. F. Mahon, L. Male, E. A. Marseglia, E. Tedesco, R. H. Friend, A. Köhler, N. Feeder and S. J. Teat, *J. Chem. Soc., Dalton Trans.*, **2002**, 1358; (b) M. S. Khan, M. R. A. Al-Mandhary, M. K. Al-Suti, N. Feeder, S. Nahar, A. Köhler, R. H. Friend, P. J. Wilson and P. R. Raithby, *J. Chem. Soc., Dalton Trans.*, **2002**, 2441; (c) M. S. Khan, M. R. A. Al-Mandhary, M. K. Al-Suti, T. C. Corcoran , J. P. Attfield, N. Feeder, W. I. F. David, K. Shankland, R. H. Friend, A. Köhler, E. A. Marseglia, E. Tedesco, C. C. Tang, P. R. Raithby, J. C. Collings, K. P. Roscoe, A. S. Batsanov, L. M. Stimson and Todd B. Marder, *New J. Chem.*, **2003**, 27, 140.

26) H. F. Wittmann, R. H. Friend, M. S. Khan, and J. Lewis, *J. Chem. Phys.*, **1994**, 101, 2693.

27) (a) J. S. Wilson, A. S. Doot, A. J. A. B. Seeley, M. S. Khan, A. Kohler, R. H. Friend, *Nature*, **2001**, 413, 828; (b) J. S. Wilson, N. Chawdhury, A. Kohler, R. H. Friend, M. R. A. Al-Mandhary, M. S. Khan, M. Younus and P. R. Raithby, *J. Am. Chem. Soc.*, **2001**, 123, 9412; (c) D. Beljonne, H. F. Wittmann, A. Kohler, S. Graham. M. Younus, J. Lewis, P. R. Raithby, M. S. Khan, R. H. Friend, J. L. Bredas, *J. Chem. Phys.*, **1996**, 105, 3868.

# CHAPTER 3

## Rigid-Rod Pt(II) Poly-ynes and Di-ynes Incorporating Ologopyridiyl Linker Groups in the Backbone

# 3.1 Introduction

A few recent reports have concerned the incorporation of pyridine and its derivatives into conjugated polymeric frameworks.[1] Compared to benzene or thiophene, pyridine is considered to be electron-deficient. Consequently, the derived polymers have increased electron affinity and improved electron transporting properties.[2] The increase in the number of pyridine units may enhance the electron-accepting ability of the polymers making the oligopyridyl-containing polymers more suited for applications in electronic devices.

In addition, oligopyridines have the ability to chelate metal centres forming metal complexes which offer the possibility of the fabrication of photo/electroactive multinuclear systems.[3] It was, therefore, envisaged that oligopyridines would constitute an interesting class of spacer units in the novel platinum(II) poly-ynes, and the synthesis and characterisation of these is the subject of this chapter.

# 3.2 Results and Discussion

## 3.2.1 Syntheses

The key starting material for the preparation of 6,6'-dibromo-2,2'-bipyridine and the terpyridines is 6-bromo-2-lithiopyridine. It was prepared by reaction of 2,6-dibromopyridine with one equivalent of $^{n}$BuLi.[4] 6,6'-Dibromo-2,2'-bipyridyl was then synthesized by coupling 6-bromo-2-lithiopyridine *in situ* by anhydrous cupric chloride at –80 °C, followed by oxidation with dry compressed air at –60 °C **(Scheme 3.1)**[4]. 5,5'-Dibromo-2,2'-bipyridyl was prepared from 2,5-dibromopyridine *via* 5-bromo-2-methylsulfenylpyridine and 5-bromo-2-methylsulfinylpyridine by following a literature method developed by Yamamoto *et. al*[5] **(Scheme 3.1)**.

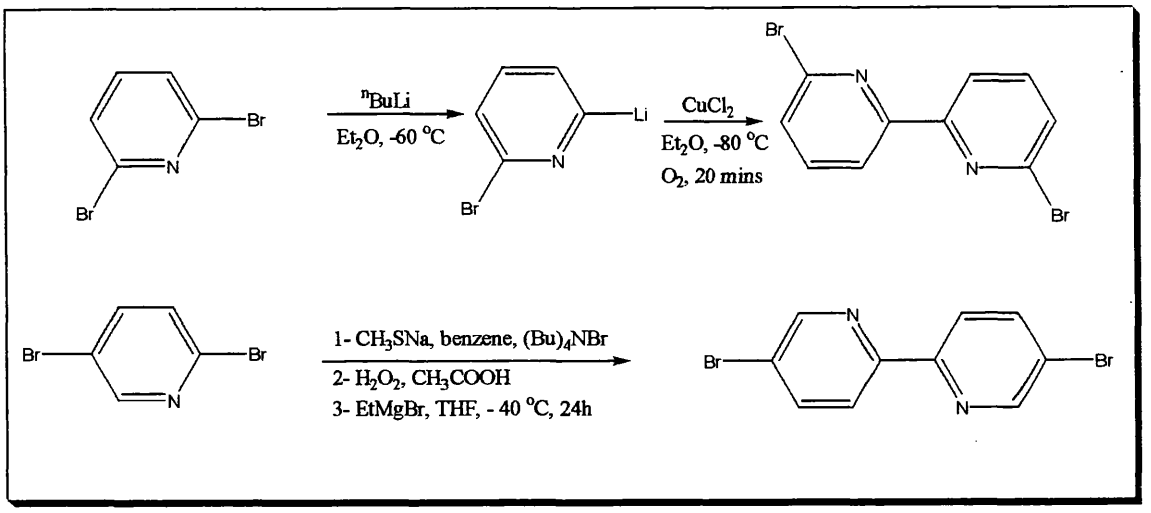


**Scheme 3.1**

For the phenylterpyridine spacer, 6-bromo-2-acetylpyridine was prepared by reacting 6-bromo-2-lithiopyridine with *N,N'*-dimethylacetamide at –80 °C. This was then reacted with benzaldehyde under basic conditions to afford 1-(2-bromopyridyl)-3-phenyl-2-propenone, and then with iodine in refluxing pyridine to afford 1-(2-bromopyridylcarbonylmethyl) pyridinium iodide[6]. The two precursors were then coupled with ammonium acetate and heated to reflux in acetic acid to afford 6,6''-dibromo-4'-phenyl-2,2':6',2''-terpyridine. For 6,6''-dibromo-2,2':6',2''-terpyridine, 6-bromo-2-acetylpyridine was reacted with dimethylammonium chloride and paraformaldehyde in refluxing ethanol/ HCl mixture to yield 2-bromo-6-[3-dimethylamino-1-oxopropyl]pyridinehydrochloride which was then reacted with 1-(2-bromopyridylcarbonylmethyl) pyridinium iodide and ammonium acetate in refluxing MeOH to afford the desired compound[6](**Scheme 3.2**).

The bis(ethynyl)oligopyridine ligands were synthesised by a sequence of coupling and proto-desilylation reactions. The bis-(trimethylsilyl)-protected ligand precursors **1a-4a** were synthesised by the palladium-catalyzed coupling of trimethysilylethyne with dibromo-oligopyridines (**Scheme 3.3**). The IR spectra show a distinctive peak around 2159 $cm^{-1}$ due to the acetylenic moieties, and the expected peak for the molecular weight in mass spectrometry was found (**Table 3.1**). The materials are indefinitely stable towards light and air and could be stored for long period without any apparent change.

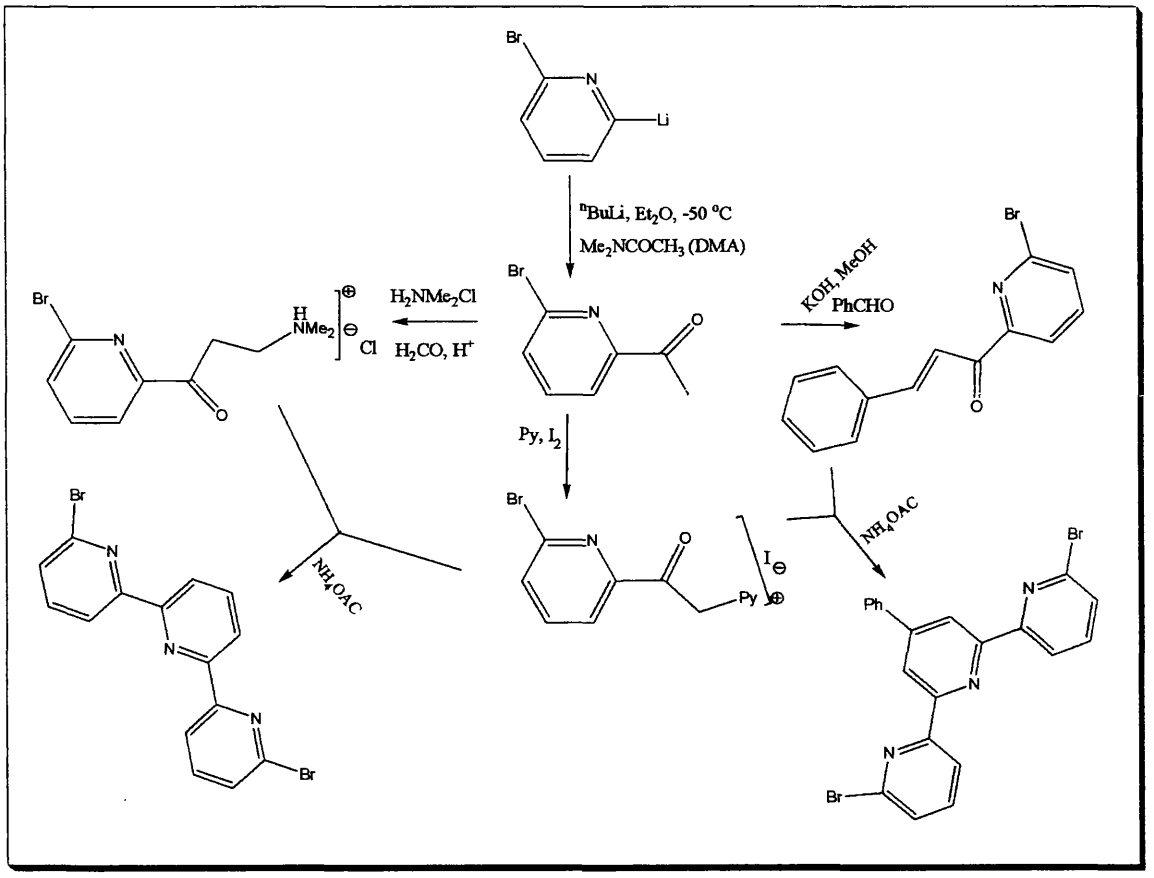


**Scheme 3.2**

Conversion of the protected ligand precursors into the terminal di-ynes **1b-4b** was accomplished by smooth removal of the trimethylsilyl protecting groups with dilute aqueous KOH in MeOH/THF (**Scheme 3.3**). These diterminal alkynes show a distinctive peak at 2010 $cm^{-1}$ for the C≡C acetylenic moieties and at 3300 $cm^{-1}$ for the $C_{sp}$—H bond of the terminal acetylene, and the mass spectra gave the expected peaks for their molecular weight. Both the protected and the terminal di-ynes were purified by silica column chromatography and isolated in 65-85% yields.

The terminal di-ynes are relatively stable at low temperature in the absence of light and air; however, in the presence of light and/or air they undergo a slow colour change. Long storage times at ambient temperature and under aerobic conditions led to the formation of some insoluble material (<5%), which was presumed to be a polymerisation product.

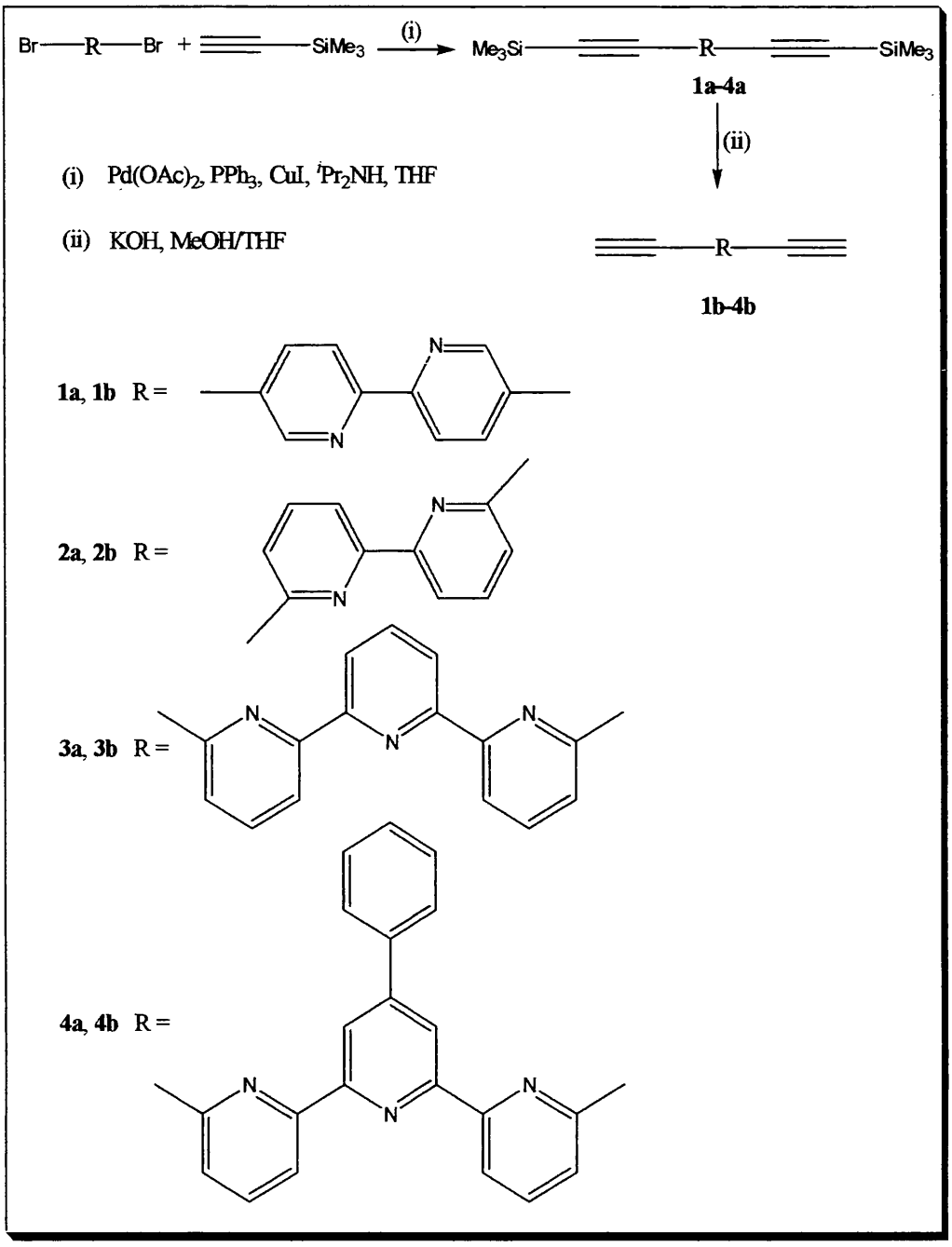


**Scheme 3.3**

The reaction of each of the terminal di-ynes **1b-4b** with two equivalents of *trans*-[Pt(Ph)($PEt_3$)$_2$Cl], in $CH_2Cl_2$/$NHPr^i_2$, in the presence of CuI, at room temperature, readily affords the dinuclear complexes *trans*-[($Et_3P$)$_2$(Ph)Pt-C≡C-R-C≡C-Pt(Ph)($Et_3P$)$_2$] (**1M-4M**), in 60-70% yields (**Scheme 3.4 and Table 3.2**).

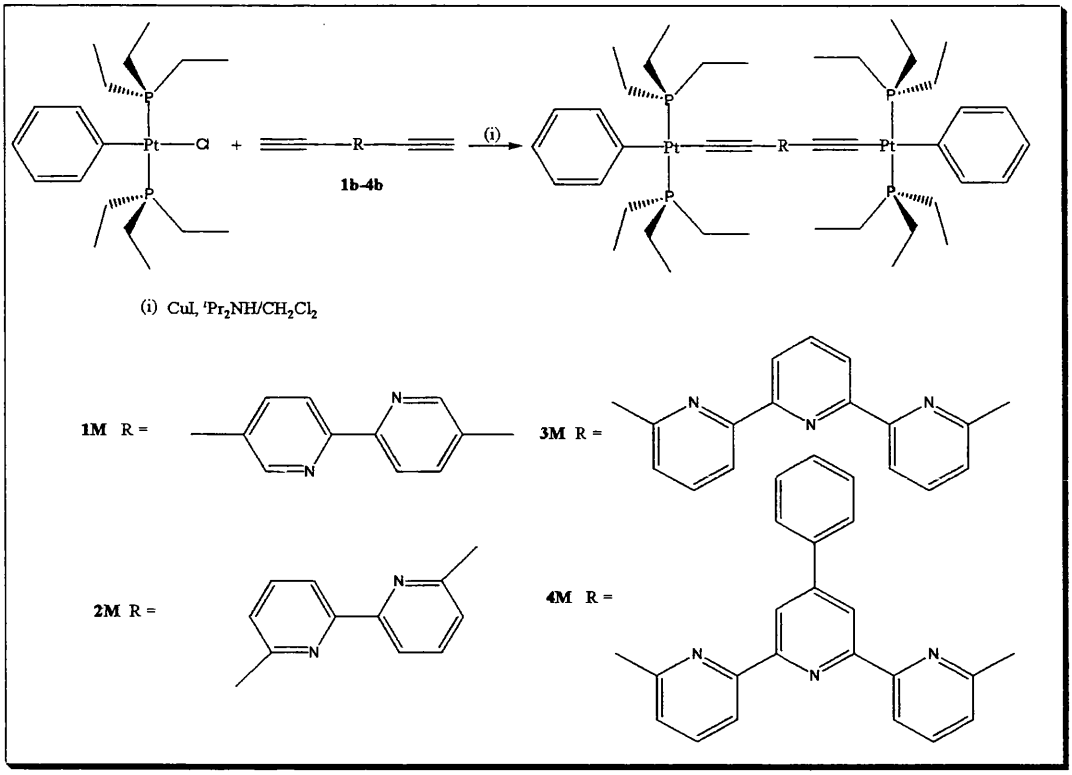


**Scheme 3.4**

The corresponding polymers *trans*-$[Pt(P^nBu_3)_2\text{-}C{\equiv}C\text{-}R\text{-}C{\equiv}C\text{-}]_n$ **(1P-4P)** were prepared by the reaction of one equivalent of *trans*-$[(Bu_3P)_2PtCl_2]$ with the appropriate di-yne under similar reaction conditions and were isolated in 70-85% yield **(Scheme 3.5 and Table 3.2)**. Purification of **1M-4M** was accomplished by silica column chromatography, while the polymers **1P-4P** were purified by alumina column chromatography followed by precipitation from dichloromethane solution into methanol.

The IR spectra of the Pt(II) di-ynes and poly-ynes show a single sharp $\nu_{C\equiv C}$ absorption at around 2095 $cm^{-1}$ consistent with a *trans*-configuration of the acetylenic units around the Pt(II) centre. As expected these stretching frequencies appear at lower wavenumbers than the ligand precursors which is an indication of higher conjugation in the former. The $^1H$ and $^{13}C$ NMR spectra show the expected structures and confirm the symmetry and the *trans* configuration of the poly-ynes and di-ynes. **Figure 3.1** shows the aromatic region of $^1H$ NMR spectrum of **1M**. Three peaks appeared for the six aromatic hydrogens of the bipyridine spacer at 8.57, 8.18 and 7.60 ppm and that of the terminal benzene rings at 7.31, 6.95 and 6.80 ppm. The resonance expected for any of the terminal acetylenic protons (C≡C—H) were absent in all spectra. In poly-ynes this indicates a

polymeric nature of the chains. The observed ethynyl carbons were deshielded in the $^{13}C\{^{1}H\}$ NMR spectra from ligands

(~ 90-100 ppm) to Pt(II) di-ynes and poly-ynes (~ 110-120 ppm). This might be attributed to the higher conjugation in the former. The single resonance in the $^{31}P$ NMR spectra of **4M** is shown in **Figure 3.2** which confirms the *trans* arrangement of the phosphine ligands around platinum.

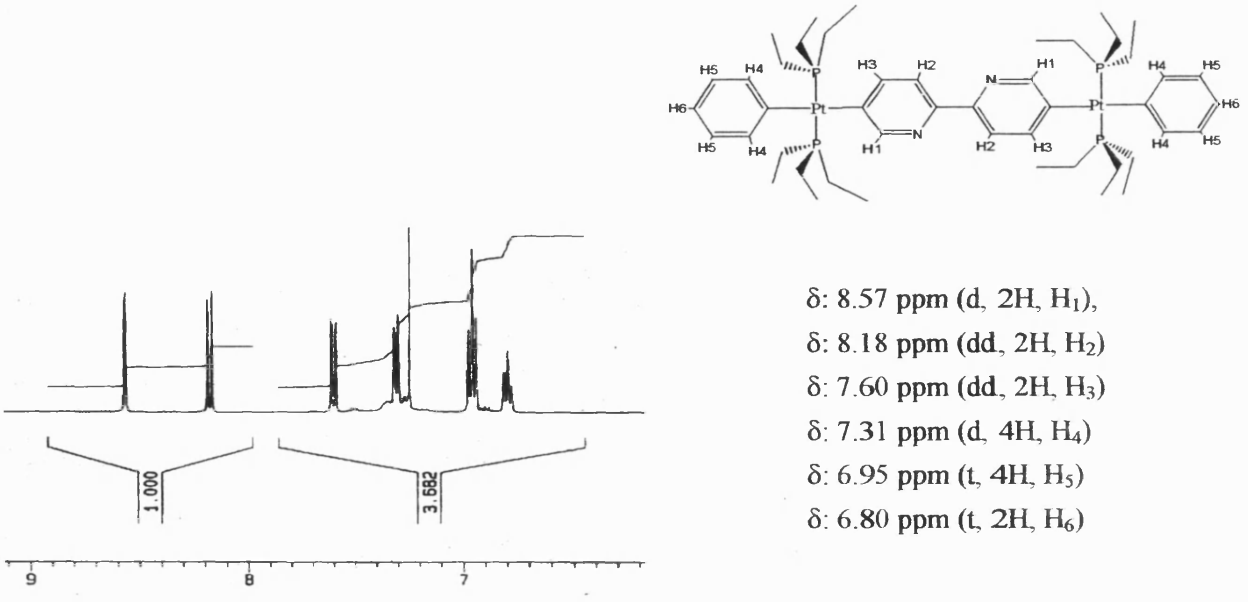


δ: 8.57 ppm (d, 2H, $H_1$),
δ: 8.18 ppm (dd, 2H, $H_2$)
δ: 7.60 ppm (dd, 2H, $H_3$)
δ: 7.31 ppm (d, 4H, $H_4$)
δ: 6.95 ppm (t, 4H, $H_5$)
δ: 6.80 ppm (t, 2H, $H_6$)

**Figure 3.1: The aromatic region of the $^{1}H$ NMR spectrum of 1M.**

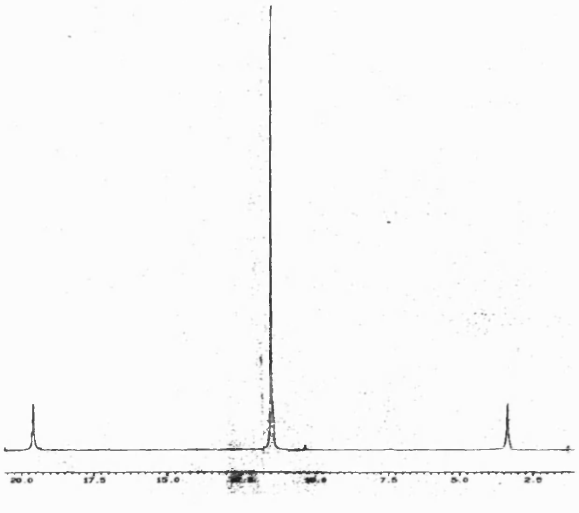

**Figure 3.2: $^{31}P$ NMR spectrum of 4M.**

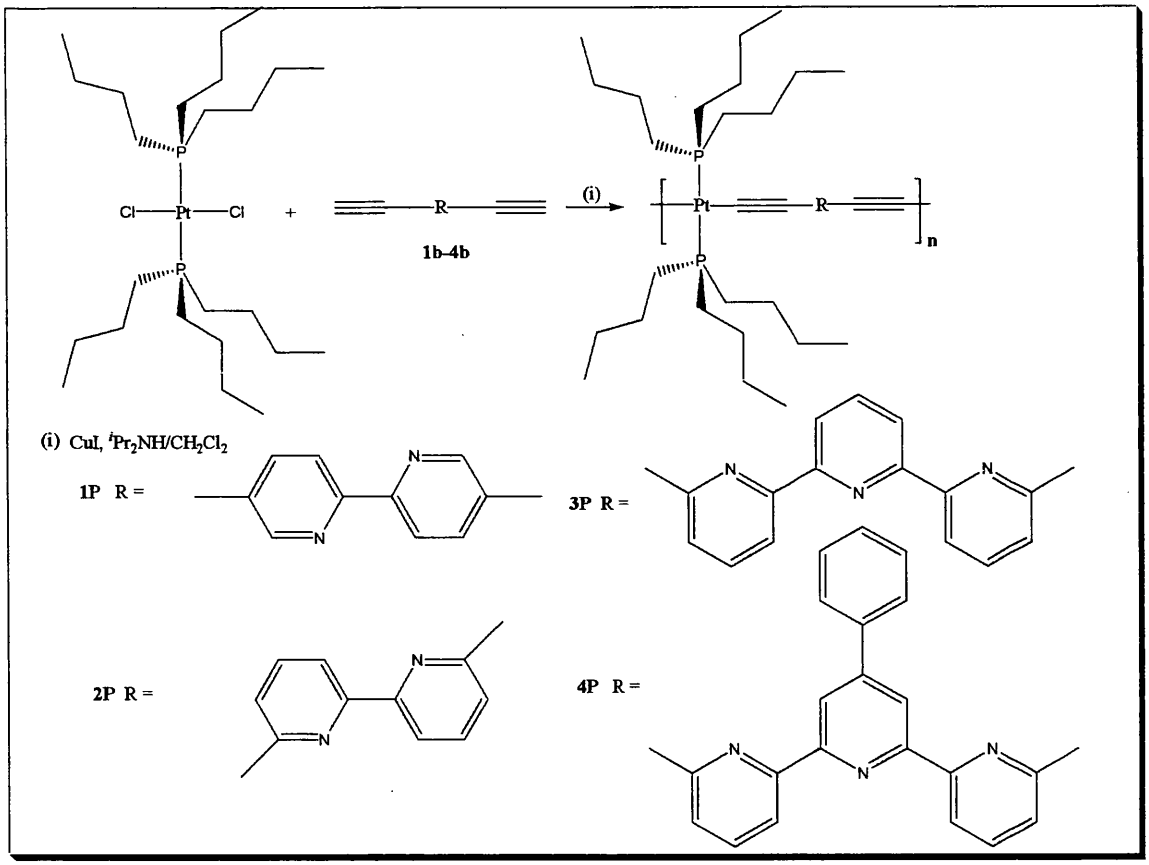


**Scheme 3.5**

The number-average molecular weight ($M_n$) values for the polymers are in the range of 60,000 to 87,000 g/mol, corresponding to between 75 and 91 repeating units per chain. The polydispersity ($M_w/M_n$) varies between 1.3 and 1.8 indicating reasonably homogenous polymer chain lengths.

**Table 3.1: Synthetic and other characterization data for 1a-4a and 1b-4b**

| Compound | Color | Yield (%) | $M^+(gmol^{-1})$ | $\upsilon_{C\equiv C}(cm^{-1})$ | $\upsilon_{Csp-H}(cm^{-1})$ |
|---|---|---|---|---|---|
| **1a** | Pale yellow | 80 | 348.4 | 2159 | - |
| **2a** | Off-white | 72 | 348.4 | 2159 | - |
| **3a** | Off-white | 75 | 425.5 | 2159 | - |
| **4a** | White | 90 | 501.6 | 2159 | - |
| **1b** | White | 76 | 204.2 | 2107 | 3300 |
| **2b** | White | 60 | 204.2 | 2107 | 3299 |
| **3b** | White | 65 | 281.3 | 2105 | 3298 |
| **4b** | White | 85 | 357.4 | 2106 | 3298 |

**Table 3.2: Synthetic and other characterization data for 1M-4M and 1P-4P**

| Compoud | Color | Yield (%) | $M^+$ ($gmol^{-1}$) | $M_n$ ($gmol^{-1}$) | $M_w$ ($gmol^{-1}$) | PDI* | $\upsilon_{C\equiv C}$ ($cm^{-1}$) | $^{31}P\{^1H\}$NMR (ppm)[a] |
|---|---|---|---|---|---|---|---|---|
| **1M** | Off-white | 70 | 1219.2 | - | - | - | 2093 | –131.17 ($^1J_{Pt-P}$ = 2677 Hz) |
| **2M** | Pale yellow | 70 | 1219.2 | - | - | - | 2095 | –131.10 ($^1J_{Pt-P}$ = 2657 Hz) |
| **3M** | Off-white | 65 | 1296.3 | - | - | - | 2096 | –131.27 ($^1J_{Pt-P}$ = 2659 Hz) |
| **4M** | White | 55 | 1372.4 | - | - | - | 2095 | –131.12 ($^1J_{Pt-P}$ = 2659 Hz) |
| **1P** | Off-white | 85 | - | 68,900 | 89,570 | 1.3 | 2096 | –137.87 ($^1J_{Pt-P}$ = 2353 Hz) |
| **2P** | Off-white | 85 | - | 60,100 | 102,170 | 1.7 | 2095 | –138.07 ($^1J_{Pt-P}$ = 2357 Hz) |
| **3P** | Off-white | 80 | - | 72,100 | 129,780 | 1.8 | 2095 | –138.28 ($^1J_{Pt-P}$ = 2350 Hz) |
| **4P** | Off-white | 70 | - | 86,800 | 156,240 | 1.8 | 2095 | –137.58 ($^1J_{Pt-P}$ = 2357 Hz) |

* PDI = Poly-dispersity Index

## 3.2.2 Thermal Characterisation

The Thermal stability was determined by simultaneous differential thermal analysis (DTA) and thermogravemetry (TG). A clear trend of decreasing decomposition temperature was observed as the number of pyridine units was increased from two to three. Polymer **2P** with a kinked backbone was more stable to increasing temperature than the linear analogue **1P**. The mass loss in **3P** was sharp and over 50% of the sample mass was lost as the temperature rose from 170 to 250°C. Decomposition onset was defined as a mass loss of 2%. The results are shown in **Table 3.3**.

**Table 3.3: Results of thermal analysis; temperatures in °C**

| Compound | $T_{decomp}$ (onset) | $T_{decomp}$ (peak) DTG | $T_{decomp}$ (peak) DTA |
|---|---|---|---|
| **1P** | 274 | 325 | 326 |
| **2P** | 287 | 343 | 344 |
| **3P** | 169 | 236 | 234 |
| **4P** | - | 212 | - |

## 3.2.3 Structural characterisation

The molecular structures of the compounds **2a – 4a** and **2M** are shown in **Figures 3.3 –3. 6** respectively, and selected intra-molecular bond parameters are listed in **Tables 3.4 – 3.7**.

The nitrogen-carbon bond lengths in **2a, 3a** and **4a** are in the range of 1.331(3) to 1.351(5) Å. These bond lengths are similar to those in 6,6′-bis(2-phenyl-1-ethynyl)-2,2′-bipyridine (= ph-A-bipy), (1.337(4) and 1.351(4) Å), [7] or in 2,2′:6′,2″:6″,2‴-quaterpyridine (1.333(2) to 1.340(2) Å).[8] The C-N-C angles in **2a-4a** (116.9(4), 117.7(3)°) are equivalent to those in the uncoordinated ph-A-bipy compound (117.6(3)°)[7] or in quaterpyridine (117.3(2), 118.5(1)°).[8]

The carbon-carbon bonds between the pyridine rings in **2a-4a** are in order of 1.482(7) to 1.496(6) Å) typical for a single bond between $sp^2$-hybridized carbons, as in quaterpyridine (1.485(2),1.482(3) Å),[8] in terpy (1.474(9) to 1.479(9) Å).[9] The carbon-carbon bonds between the $sp^2$-hybridized pyridine ring and the sp-hybridized ethynyl group are shorter (1.447(7) to 1.457(4) Å in **2a-4a**. The carbon-carbon triple bonds in **2a-4a** correspond to the expected value (1.195(4) to 1.212(6) Å[8]. The ethynyl groups in **2a-4a** show the expected linear arrangement (C-C≡C 176.0(5) to 178.9(6)°, Si-C≡C 171.6(2) to 178.0(5)°.

The bond parameters within the organic spacer groups in the diplatinum complex **2M** does not show significant differences from those in the organic precursors. The Pt-C(acetylenic) distances lie in the range 2.022(9) – 2.026(10) Å, which is within the range of values, 1.96(2) – 2.05(2) Å, found in related platinum di-yne complexes when the spacer group consists of one or two thiophene rings.[10]

However, the distances are consistently longer than the Pt-C(acetylenic) distances of 1.940(19) and 1.947(17) Å in the *cis*-complex $[Pt(C{\equiv}CC_6H_4Me)_2(^tBu_2bipy)]$.[11] The Pt-C(Ph) distances, range 2.074(9) – 2.086(10) Å, and the Pt-P(phosphine) distances, range 2.286(7) – 2.292(3) Å, are also quite similar to those observed in the thiophene derivatives. **2a, 3a** and **4a**, and the metal complex, **2M**, showed the expected transoid conformation for uncoordinated oligo-pyridines (torsion angles N-C-C-N 162.2(4) to 180.0°).

**Table 3.4. Selected bond lengths [Å] and angles [°] for 2a**

| | | | |
|---|---|---|---|
| N(1)-C(6) | 1.341(4) | N(1)-C(7) | 1.344(4) |
| C(4)-C(5) | 1.195(4) | C(5)-C(6) | 1.457(4) |
| C(7)-C(7)#1 | 1.482(7) | N(11)-C(16) | 1.346(4) |
| N(11)-C(17) | 1.346(4) | C(14)-C(15) | 1.199(4) |
| C(15)-C(16) | 1.457(4) | C(17)-C(17)#2 | 1.485(7) |
| | | | |
| C(6)-N(1)-C(7) | 117.7(3) | C(5)-C(4)-Si(1) | 177.5(3) |
| C(4)-C(5)-C(6) | 178.9(3) | C(16)-N(11)-C(17) | 117.3(3) |
| C(14)-C(15)-C(16) | 178.2(4) | C(15)-C(14)-Si(11) | 175.5(4) |

Symmetry transformations used to generate equivalent atoms: #1 -x+1,-y+1,-z+2 #2 -x+2,-y+2,-z+2

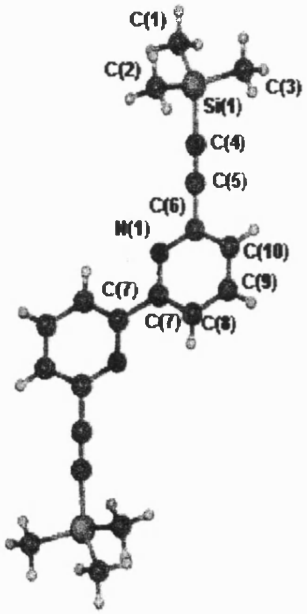


**Figure 3.3: The molecular structure of one of the two independent half molecules of 2a (with the symmetry related half). Only one orientation of the disordered trimethylsilyl fragment is shown for clarity.**

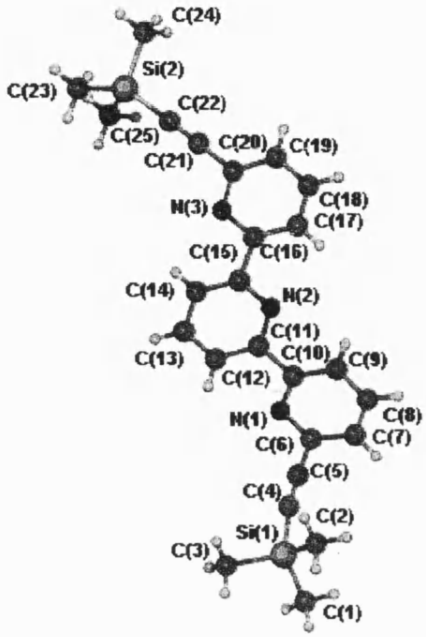


**Figure 3.4: The molecular structure of 3a showing the atom numbering scheme adopted.**

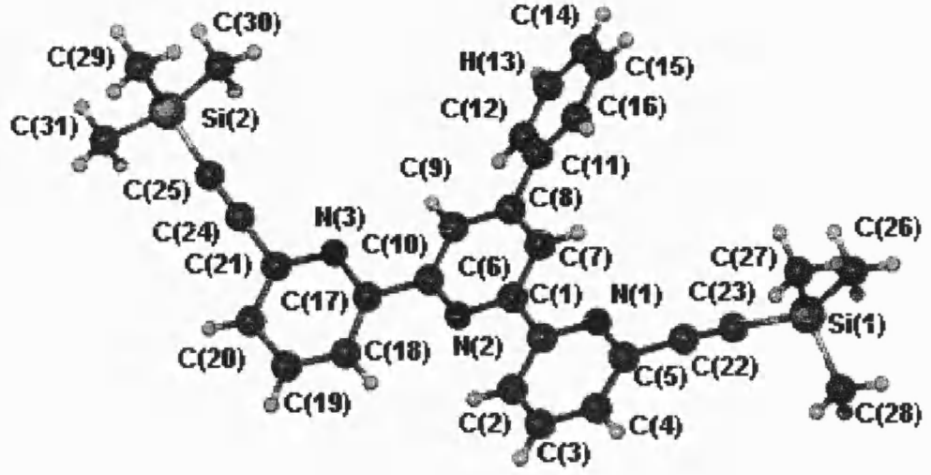


**Figure 3.5: The molecular structure of one of the two independent molecules of 4a showing the atom numbering scheme.**

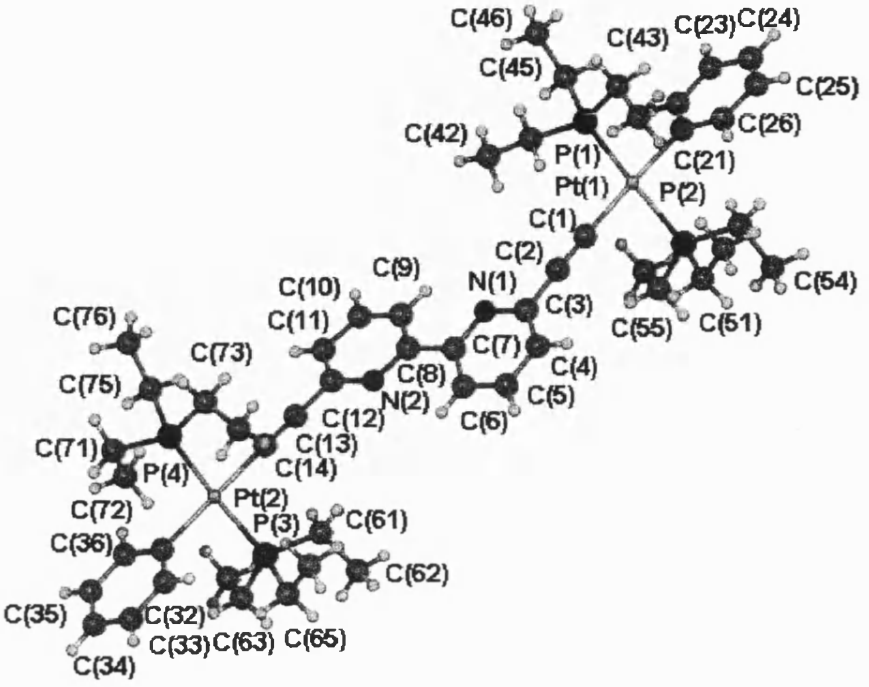


**Figure3.6: The molecular structure of 2M showing the atom numbering scheme.**

**Table 3.5. Selected bond lengths [Å] and angles [°] for 3a.**

| | | | |
|---|---|---|---|
| C(4)-C(5) | 1.206(3) | C(5)-C(6) | 1.457(3) |
| N(1)-C(10) | 1.343(3) | N(1)-C(6) | 1.345(3) |
| C(10)-C(11) | 1.494(3) | N(2)-C(11) | 1.343(3) |
| N(2)-C(15) | 1.343(3) | C(15)-C(16) | 1.489(3) |
| N(3)-C(20) | 1.338(3) | N(3)-C(16) | 1.347(3) |
| C(20)-C(21) | 1.453(3) | C(21)-C(22) | 1.199(3) |
| | | | |
| C(5)-C(4)-Si(1) | 171.6(2) | C(4)-C(5)-C(6) | 176.6(2) |
| C(10)-N(1)-C(6) | 117.43(18) | C(11)-N(2)-C(15) | 117.72(19) |
| C(20)-N(3)-C(16) | 118.0(2) | C(21)-C(22)-Si(2) | 177.2(3) |
| C(22)-C(21)-C(20) | 177.8(3) | | |

**Table 3.6. Selected bond lengths [Å] and angles [°] for 4a**

| | | | |
|---|---|---|---|
| N(1)-C(1) | 1.344(5) | N(1)-C(5) | 1.347(5) |
| N(2)-C(6) | 1.338(5) | N(2)-C(10) | 1.343(5) |
| N(3)-C(17) | 1.338(5) | N(3)-C(21) | 1.351(5) |
| N(4)-C(36) | 1.343(5) | N(4)-C(32) | 1.343(5) |
| N(5)-C(41) | 1.337(5) | N(5)-C(37) | 1.349(5) |
| N(6)-C(48) | 1.344(5) | N(6)-C(52) | 1.345(5) |
| C(5)-C(22) | 1.449(6) | C(1)-C(6) | 1.496(6) |
| C(10)-C(17) | 1.492(6) | C(8)-C(11) | 1.480(6) |
| C(21)-C(24) | 1.447(7) | C(22)-C(23) | 1.204(6) |
| C(24)-C(25) | 1.208(6) | C(39)-C(42) | 1.486(6) |
| C(32)-C(37) | 1.491(6) | C(52)-C(55) | 1.451(7) |
| C(36)-C(53) | 1.445(7) | C(41)-C(48) | 1.495(6) |
| C(53)-C(54) | 1.203(6) | C(55)-C(56) | 1.212(6) |
| | | | |
| C(1)-N(1)-C(5) | 117.3(3) | C(6)-N(2)-C(10) | 117.8(3) |
| C(17)-N(3)-C(21) | 116.9(4) | C(36)-N(4)-C(32) | 117.6(4) |
| C(41)-N(5)-C(37) | 117.0(3) | C(48)-N(6)-C(52) | 117.6(3) |
| C(23)-C(22)-C(5) | 176.0(5) | C(22)-C(23)-Si(1) | 176.3(4) |
| C(25)-C(24)-C(21) | 178.9(6) | C(24)-C(25)-Si(2) | 177.3(5) |
| C(54)-C(53)-C(36) | 177.3(6) | C(53)-C(54)-Si(3) | 178.0(5) |
| C(56)-C(55)-C(52) | 176.4(5) | C(55)-C(56)-Si(4) | 175.1(5) |

**Table 3.7. Selected bond lengths [Å] and angles [°] for 2M**

| | | | |
|---|---|---|---|
| Pt(1)-P(1) | 2.291(2) | Pt(1)-P(2) | 2.287(2) |
| Pt(1)-C(1) | 2.022(9) | Pt(1)-C(21) | 2.074(9) |
| Pt(2)-P(3) | 2.292(3) | Pt(2)-P(4) | 2.286(3) |
| Pt(2)-C(14) | 2.026(10) | Pt(2)-C(31) | 2.086(10) |
| C(1)-C(2) | 1.199(13) | C(13)-C(14) | 1.195(14) |
| C(2)-C(3) | 1.433(13) | C(12)-C(13) | 1.452(12) |
| C(3)-N(1) | 1.352(13) | C(12)-N(2) | 1.354(12) |
| C(3)-C(4) | 1.387(15) | C(11)-C(12) | 1.398(14) |
| C(4)-C(5) | 1.384(14) | C(10)-C(11) | 1.377(13) |
| C(5)-C(6) | 1.396(15) | C(9)-C(10) | 1.375(14) |
| C(6)-C(7) | 1.386(13) | C(8)-C(9) | 1.387(13) |
| N(1)-C(7) | 1.357(11) | N(2)-C(8) | 1.356(11) |
| C(7)-C(8) | 1.498(13) | | |
| | | | |
| P(1)-Pt(1)-P(2) | 173.70(9) | C(1)-Pt(1)-C(21) | 177.5(4) |
| C(1)-Pt(1)-P(1) | 94.7(3) | C(1)-Pt(1)-P(2) | 86.4(3) |
| C(21)-Pt(1)-P(1) | 87.3(3) | C(21)-Pt(1)-P(2) | 91.7(3) |
| P(3)-Pt(2)-P(4) | 173.24(10) | C(14)-Pt(2)-C(31) | 177.1(4) |
| C(14)-Pt(2)-P(3) | 89.9(3) | C(14)-Pt(2)-P (4) | 87.4(3) |
| C(31)-Pt(2)-P(3) | 88.7(3) | C(31)-Pt(2)-P(4) | 94.3(3) |
| Pt(1)-C(1)-C(2) | 174.4(8) | C(1)-C(2)-C(3) | 176.8(10) |
| Pt(2)-C(14)-C(13) | 178.7(9) | C(12)-C(13)-C(14) | 176.2(11) |
| N(1)-C(7)-C(8) | 115.4(8) | C(6)-C(7)-C(8) | 121.3(8) |
| N(1)-C(7)-C(6) | 123.2(9) | C(7)-C(8)-N(2) | 115.7(8) |
| C(7)-C(8)-C(9) | 122.5(8) | N(2)-C(8)-C(9) | 121.7(8) |

## 3.2.4 Crystal packing

From the nature of the molecules **2a** to **4a** one could expect to find C-H···N hydrogen bonds or $\pi\cdots\pi$ interactions in the crystal packing. A proposed upper value for C···N distances for this type of hydrogen bond is 3.5 Å,[12] *c.f.* sum of the van der Waals radii 3.25 Å.[13] Except for **2a** $\pi\cdots\pi$ interactions were present in the crystal packing (interlayer distances smaller than 3.5 Å).[14]

The molecules in **2a** form criss-crossed, interlinked layers perpendicular to (0 0 1). Within the layers weak C-H···N hydrogen bonds are present (N···H 2.80, 2.91 Å). The combination of those two hydrogen bonds forms a chain, motif $C_2^2(8)$.[15] The smallest interlayer distance between parallel aromatic systems within one of the layers perpendicular to (0 0 1) is 5.581(12) Å.

In **3a** the shortest C···N distance of 3.624(3) Å (angle 160.2°) is in direction of the stacks parallel to (1 0 0). Those stacks also show small interplanar distances of 2.397(5) Å. Between neighboured stacks only weak forces are present. The interplanar distance of 5.838(5) Å shows no indication of $\pi\cdots\pi$ interactions. On the other hand, two stacks could be considered to be linked by weak C-H···N hydrogen bonds ($C_{Me}$···N 3.683(3) Å, $C_{Ph}$···N 3.761(4) Å, angles 131.7 and 149.4°). These hydrogen bonds show ring motifs [$N_1$: $R_2^2(26)$ and $R_2^2(12)$, respectively]. The combination of these hydrogen bonds results in the motif $R_2^2(13)$.

In **4a** the combination of $\pi\cdots\pi$ interactions and weak non-conventional hydrogen bonds results in a zigzag ribbon arrangement parallel to the plane with trace (1 1 0) on the *a*/*b*-plane. Within this ribbons small interplanar distances of 3.297(9) and 3.302(10) Å between symmetry related phenyl rings of the two independent molecules could be found. Additional, those dimers are stabilised by C-H···N hydrogen bonds (C···N 3.593(6), 3.554(6) Å, angles 148.9, 143.4°, motif $R_2^2(20)$. Between two dimers additional, weak, non-conventional hydrogen bonds are present, linking not symmetry related molecules [C···N 3.522(6), 3.774(6) Å, angles 129.8, 157.1°, combined motif $R_2^2(18)$].

In the crystal structure of **2M** weak C-H...N hydrogen bonds are also observed (**Table 3.8**). However, the presence of the bulky platinum-phosphine groups prevents $\pi\ldots\pi$ interactions from occurring.

**Table 3.8 C-H···N hydrogen bonds and contacts, not corrected**

| Structure | Bond | D-H [Å] | H···A [Å] | D···A [Å] | D-H···A [°] |
|---|---|---|---|---|---|
| **2a** | C20-H20···N1 | 0.95 | 2.80 | 3.619(4) | 144.8 |
| **2a** | C10-H10···N11$^{i}$ | 0.95 | 2.91 | 3.660(4) | 137.0 |
| **3a** | C8-H8···N1$^{ii}$ | 0.95 | 2.72 | 3.624(3) | 160.2 |
| **3a** | C13-H13···N1$^{iii}$ | 0.95 | 2.98 | 3.683(3) | 131.7 |
| **3a** | C3-H3···N3$^{iii}$ | 0.98 | 2.88 | 3.761(4) | 149.4 |
| **4a** | C14-H14···N1$^{iv}$ | 0.95 | 2.75 | 3.593(6) | 148.9 |
| **4a** | C45-H45···N6$^{v}$ | 0.95 | 2.75 | 3.554(6) | 143.4 |
| **4a** | C34-H34···N1$^{ii}$ | 0.95 | 2.84 | 3.522(6) | 129.8 |
| **4a** | C50-H50···N3$^{ii}$ | 0.95 | 2.88 | 3.774(6) | 157.1 |
| **2M** | C43-H43b···N1$^{vi}$ | 0.99 | 2.92 | 3.878(7) | 164.2 |
| **2M** | C62-H62b···N1$^{vii}$ | 0.98 | 2.77 | 3.375(7) | 120.7 |

Symmetry operators: i 1+x, y, z; ii x-1, y, z; iii 1-x, 1-y, 1-z; iv –1-x, 1-y, 1-z; v –x, -y, 1-z; vi x, y+1, z, vii x, y-1, z

**Table 3.9. Crystallographic data**

| Compound | 2a | 3a | 4a | 2M |
|---|---|---|---|---|
| Formula | $C_{20}H_{24}N_2Si_2$ | $C_{25}H_{27}N_3Si_2$ | $C_{31}H_{31}N_3Si_2$ | $C_{50}H_{76}N_2P_4Pt_2$ |
| $M_r$ | 348.59 | 425.68 | 501.77 | 1219.19 |
| Crystal habit | Colourless block | Colourless prism | Colourless plate | Yellow needle |
| Crystal size [mm] | 0.40x0.30x0.20 | 0.28x0.16x0.07 | 0.20x0.18x0.06 | 0.10x0.02x0.01 |
| Crystal system | Monoclinic | Triclinic | Triclinic | Monoclinic |
| Space group | *P2₁/c* | *P-1 (No. 2)* | *P-1 (No. 2)* | *P2₁/c* |
| Cell dimensions | | | | |
| *a* [Å] | 11.024(3) | 6.3543(8) | 11.389(6) | 23.540(7) |
| *b* [Å] | 10.645(4) | 10.844(2) | 13.353(11) | 9.389(3) |
| *c* [Å] | 17.768(4) | 17.722(4) | 19.540(16) | 25.662(7) |
| α [°] | 90 | 84.891(8) | 94.69(3) | 90 |
| β [°] | 92.68(3) | 86.268(10) | 99.71(5) | 116.005(14) |
| γ [°] | 90 | 82.049(10) | 90.48(5) | 90 |
| *U* [Å$^3$] | 2082.8(11) | 1202.8(4) | 2918(4) | 5097(3) |
| *Z* | 4 | 2 | 4 | 4 |
| $\mu$ [mm$^{-1}$] | 1.556 | 0.163 | 0.145 | 5.642 |
| *T* [°C] | -93 | -123 | -93 | -123 |
| $2\theta_{max}$ [°] | 110 | 55 | 45 | 50 |
| Wavelength [Å] | 1.54178 | 0.71073 | 0.71073 | 0.68980 |
| No. of reflections | | | | |
| Measured | 4267 | 7566 | 13311 | 26831 |
| Independent | 2016 | 5373 | 7470 | 9734 |
| $R_{Int}$ | 0.017 | 0.041 | 0.064 | 0.069 |
| Parameters | 223 | 277 | 649 | 535 |
| Restraints | 18 | 14 | 0 | 0 |
| *wR2*(F$^2$, all refl.) | 0.142 | 0.1248 | 0.209 | 0.1508 |
| *R1[F>2σ(F)]* | 0.052 | 0.056 | 0.070 | 0.0611 |
| GoF | 1.079 | 0.937 | 1.024 | 1.286 |

## 3.2.5 Optical Spectroscopy

The results of optical spectroscopy have been carried out by the group of Professor Sir Richard R. Friend and Dr. Anna Köhler from the Cavendish laboratory, University of Cambridge. Their effort in measuring and providing us with these results is gratefully acknowledged. The UV/ visible absorption spectra of these compounds were measured on thin films of thicknesses around 100-150 nm. **Figure 3.7** shows the thin film absorption spectra of the platinum(II) di-ynes **1M-4M** and the corresponding poly-ynes **1P-4P** and all data are summarized in **Table 3.10**. In **1P** and **1M**, the alkynyl groups are at the 5,5′-positions and the compounds are fully conjugated, while in **2P-4P** and **2M-4M**, the alkynyl groups occur at the 6,6′- or 6,6″- positions hindering conjugation between the pyridine rings.

Compared to platinum(II) di-yne and poly-yne with a pyridine spacer where the onset of optical absorption is at 3.3 eV and 3.0 eV, [16] the onset of absorption of **1P** and **1M** is shifted to the red due to the addition of a second pyridine ring by 0.1 and 0.2 eV, respectively, while for **2P-4P** and **2M-4M,** the onset of absorption is blue-shifted by 0.3 and 0.1 eV, respectively. The reason for this may be attributed to the higher conjugation length in the **1P** and **1M** by introducing the second pyridine ring which shifts the energies of transitions to lower values, while in the kinked polymers the number of rings does not compensate the disruption of conjugation and energies were seen to be higher than in the Pt(II) poly-yne with a single pyridine spacer. The onset of absorption in these materials is not as low as in the analogous platinum(II) poly-ynes *trans*-[Pt($P^nBu_3$)$_2$-C≡C-R-C≡C-]$_n$ (R = thiophene-2,5-diyl; 2,2′-bithiophene-5,5′-diyl)[17]. This suggests stronger donor-acceptor interactions in the platinum(II) poly-ynes containing thiophene spacers than for the systems that contain the pyridine spacers.

Comparing the poly-ynes with their corresponding di-ynes, the onset of absorption in **1P** is 0.2 eV lower than in **1M** consistent with the extended conjugation in the poly-yne compared to the di-yne. Similarly, the onset of absorption in **2P-4P** is 0.1 eV lower than in **2M-4M** because even in these kinked poly-ynes, a conjugated segment is still longer than in the di-ynes. The spectral shapes of **1P** and **1M** are very similar to those of the pyridine analogues and the first absorption band at 3 – 3.5 eV is more intense than the higher-lying bands at and above 4 eV. As with the other systems discussed in this thesis, the first absorption band can be assigned to the the $\pi$-$\pi^*$ transition in the organic system, possibly with some admixture of metal d orbitals which may alter the overall energy of the transition.[18] Consequently, the intensity of the first band is reduced in comparison to the higher-lying bands when the conjugation is interrupted by the kinked-spacers in **2P-4P**. The even shorter conjugation length in the di-ynes **2M-4M** further reduces the relative intensity of the first band.

The photoluminescence spectra of the platinum(II) di-ynes **1M-3M** and poly-ynes **1P-3P**, measured at 300, 200, 100, 50 and 10 K are shown in **Figure 3.8**. Two emission bands can be seen with the 0-0 vibrational peaks of the 10 K emissions at 2.91 eV and 2.18 eV for **1P** and at 3.10 eV and 2.22 eV for **1M**. The higher energy emission is fluorescence from the same singlet excited state as the first band in the absorption spectra, and is denoted $S_1$. The lower energy band is attributed to phosphorescence from a triplet excited state $T_1$ as it ha s been

assigned previously to phosphorescence on the basis of lifetime and photoinduced absorption measurements.[19] For **1P**, the low energy band is 0.7 eV below the fluorescence, and the 10 K spectrum shows vibronic structure and a spectral shape similar to the phosphorescence in related compounds[19] which confirms the triplet nature of this transition.

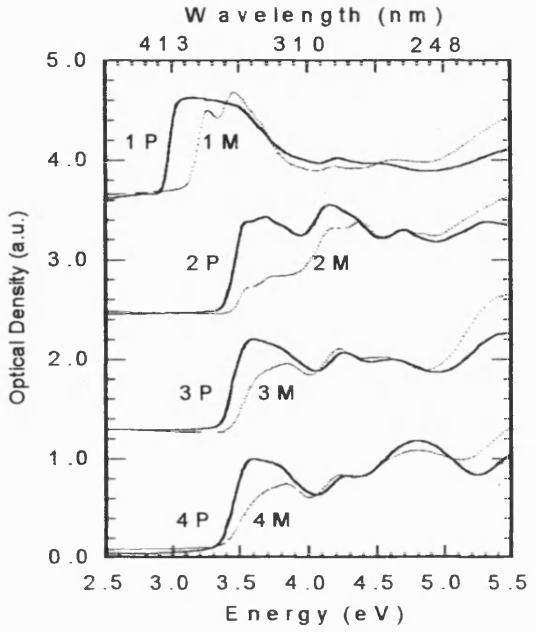


**Figure 3.7: The absorption spectra of films of the Pt(II) poly-ynes 1P-4P (solid lines) and corresponding Pt(II) di-ynes 1M-4M (dotted lines). The spectra are normalised to unity at the peak of the first absorption band.**

For **1M**, the phosphorescence band is at almost the same energy as in **1P**, while the fluorescence is at *ca.* 0.1 eV lower than in **1P**. This is in agreement with previous results that the phosphorescence band ($T_1$) is localised on a single repeat unit while fluorescence band ($S_1$) is extended over a few repeating units. [20]

For the kinked bi- and terpyridine-containing compounds **2P**, **3P**, **2M** and **3M** the observed emission can be attributed to phosphorescence only and this band is still at 0.6 eV below the onset of absorption even though these compounds have their conjugation disrupted by the unfavourable disposition of the alkynyl groups. The reduced conjugation shifts the phosphorescence band to the blue by *ca.* 0.5 eV compared to the linear bipyridine-containing

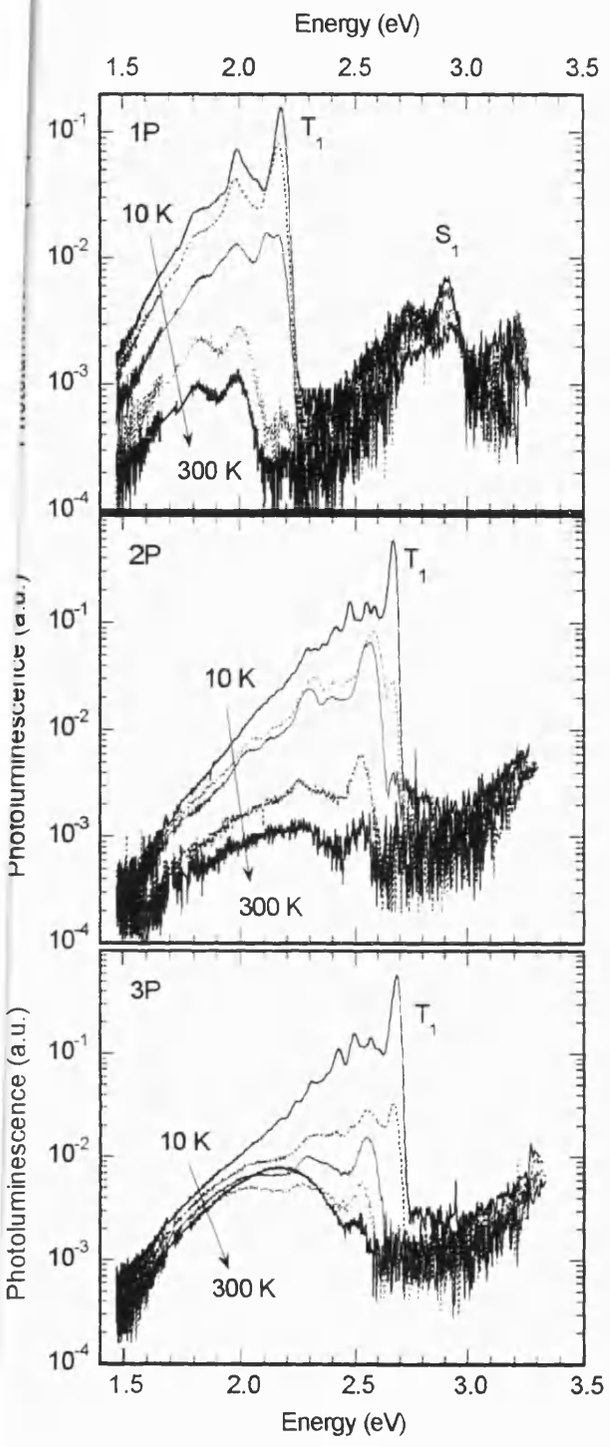


Figure 3.8 (a-c)

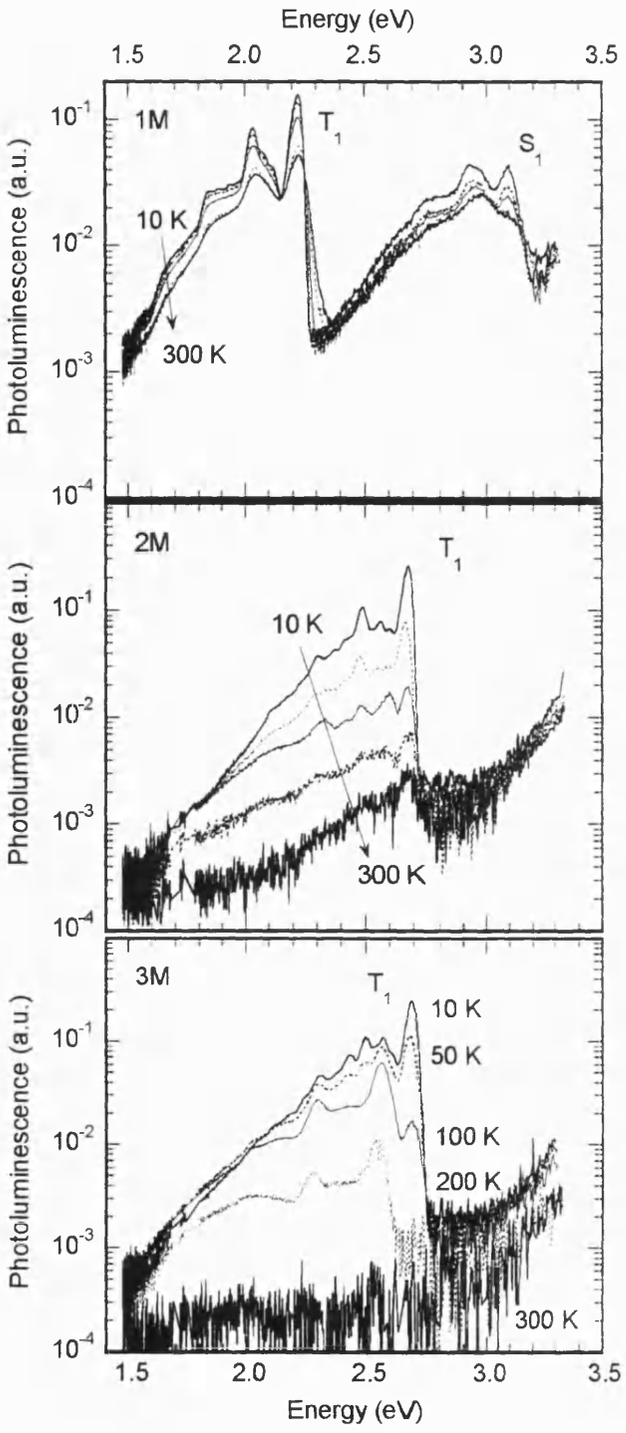


Figure 3.8 (d-f)

**Figure 3.8: The PL spectra of films of the Pt(II) poly-ynes 1P-3P (a-c) and the corresponding Pt(II) di-ynes 1M-3M (d-f) plotted on a logarithmic scale.**

analogues, so that the 0-0 vibrational peaks of the 10 K emissions are located around 2.68 eV. For the Pt(II) poly-ynes and di-ynes with a $T_1$ state at 2.2 eV, or higher, the lifetime of the $T_1$ emission is around or above 100 μs. [19,20] This long lifetime allows for temperature-activated diffusion of the $T_1$ excitation to lower energy sites such as aggregates or excimer sites which are only weakly emissive.[21] From **Figure 3.4**, there is some evidence for such diffusion. For example, for **3P**, the spectrum at 10 K has a well-resolved vibronic structure with most weight in the 0-0 vibrational peak at 2.68 eV. This spectral shape is characteristic of Pt(II) poly-ynes.

In contrast, at room temperature the emission is broad and unstructured. The 0-0 vibrational peak disappears, and the emission is centred further into red at 2.2 eV. This broad, unstructured, red-shifted low-intensity emission is characteristic of an aggregate or excimer site.[21] Similar progressions occur for **1P**, **2P** and, to a lesser extent, for **2M** and **3M**.

In summary, using linear and kinked oligopyridine spacers in the polymer backbone, both red and blue shifts were observed of the $S_1$ and $T_1$ states in platinum(II) di-yne and poly-ynes. The blue shifts are associated with a loss of oscillator strength in the first absorption band. The high energy of the $T_1$ state obtained by using the non-linear linkage in the oligopyridine is expected to be associated with a low non-radiative decay rate from the $T_1$ state. This is desirable for applications that harvest the $T_1$ state for light emission.[22]

**Table 3.10: Optical data for the Pt(II) poly-ynes and di-ynes.**

| Compound | $S_0 \rightarrow S_1$ (Onset) | $S_1 \rightarrow S_0$ (Peak) | $T_1 \rightarrow S_0$ (Peak) | $T_1$-$S_1$ Gap |
|---|---|---|---|---|
| **1M** | 3.10 | 3.0 | 2.22 | 0.78 |
| **2M** | 3.40 | - | 2.68 | - |
| **3M** | 3.40 | - | 2.68 | - |
| **4M** | 3.40 | - | - | - |
| **1P** | 2.90 | 2.91 | 2.18 | 0.73 |
| **2P** | 3.30 | - | 2.68 | - |
| **3P** | 3.30 | - | 2.68 | - |
| **4P** | 3.30 | - | - | - |

## 3.3 Conclusion

The series of **1a-4a** and **1b-4b** acetylide functionalised ligands have been successfully prepared and characterised spectroscopically, and were successfully incorporated into the di-ynes **1M-4M,** and poly-ynes **1P-4P**. The IR spectra show that the stretching frequencies are lower in the di-ynes and poly-ynes compared to that of the metal free lignds. The crystal structures of **2a**, **3a**, **4a** and **2M** were determined in order to confirm the expected structures from the synthetic work and were also compared to other related materials[7-11]. The UV/visible spectroscopy indicated that the linear di-yne, **1M** and poly-yne, **1P** have lower band gaps then the kinked analogues **2M-4M** and **2P-4P**. In the photoluminescence spectra, **1M** and **1P** show an emission band that can be attributed to a singlet excited state (fluorescence) and a lower energy band that can be attributed to a triplet excited state (phosphorescence), while in **2M-4M** and in **2P-4P** the emission observed was only phosphorescence. This might be due to the high radiative decay for the triplet excited state and lower in the siglet excited state which made the detection of such state difficult.

## 3.4 References


1) (a) T. Yamamoto, T. Maruyama, Z.-H. Zhou, T. Ito, T. Fukuda, Y. Toneda, F. Begum, T. keda, S. Sasaki, H. Takezoe, A. Fukuda and K. Kubata, *J. Am. Chem. Soc.* **1994**, 116, 4832; (b) C. Wang, M. Kilitziraki, J.A.H. MacBride, M.R. Bryce, L.E. Horsburgh, A.E. Sheridan, A.P. Monkman and D.W. Samuel, *Adv. Mater.*, **2000**, 12, 217; (c) A.P. Davey, S. Elliott, O. O'Conor and W. Blau, *J. Chem. Soc. Chem. Commun.*, **1995**, 1433; (d) D.A.M Egbe and E. Klemm, *Macromol. Chem. Phys.*, **1998**, 199, 2683; (e) M. Al-Higari, E. Birckner, B. Heise and E. Klemm, *J. Polym. Sci.: Pt. A: Polym. Chem.*, **1999**, 37, 4442.

2) T. Yamamoto, K. Sugiyama, T. Kushida, T. Inoue and T. Kanbara, *J. Am. Chem. Soc.*, **1996**, 118, 3930.

3) (a) A. Harriman, M. Hissler, R. Ziessel, A.De Cian and J. Fisher, *J. Chem. Soc., Dalton Trans.*, **1995**, 4067; (b) K.D. Ley and K.S. Schanze, *Coord. Chem. Rev.*, **1998**, 171, 287.

4) J.E. Parks, B.E. Wagner and R.H. Holm, *J. Organomet. Chem.*, **1973**, 56, 53.

5) T. Yamamoto, T. Maruyama, Z. H. Zhou, T. Ito, T. Fukuda, Yutaka Y. F. Begum, T. Ikeda,S. Sasakil, *J. Am. Chem. Soc.*, **1994**, 116 4832 – 4845

6) E.C. Constable and J. Lewis, *Polyhedron*, **1982**, 1, 303.

7) I.A. Butler and C. Soucy-Breau, *Can. J. Chem.* **1991**, 69, 1117.

8) E.C. Constable, S.M. Elder, J. Healy and D.A. Tocher, *J. Chem. Soc. Dalton Trans.* **1990**, 1669

9) W. Henke, S. Kremer and D. Reinen, *Inorg. Chem.* **1983**, 22, 2858.

10) J. Lewis, N.J. Long, P.R. Raithby, G.P. Shield, W-Y Wong and M. Younus, *J. Chem. Soc. Dalton Trans.*, **1997**, 4283.

11) C.J. Adams, S.L. James, X. Liu, P.R. Raithby and L.J. Yellowlees, *J. Chem. Soc., Dalton Trans.*, **2000**, 63.

12) (a) Z. Berkovitch-Yellin and L. Leiserowitz, *Acta Cryst.* **1984**, B40, 159; (b) F.A. Cotton, L.M. Daniels, G.T. Jordan IV and C.A. Murillo, *J. Chem. Soc. Chem. Commun.* **1997**, 1673; (c) G.A. Jeffrey, *J. Mol. Struct.* **1999**, 485-486, 293.

13) (a) A. Bondi, *J. Phys. Chem.* **1964**, 68, 441; (b) S.C. Nyburg and C.H. Faermann, *Acta Cryst.* **1985**, B41, 274.

14) C.A. Hunter and J.K.M. Sanders, *J. Am. Chem. Soc.* **1990**, 112, 5525.

15) J. Bernstein, R.E. Davis, L. Shimoni and N.-L. Chang, *Angew. Chem. Int. Ed.* **1995,** 34, 1555.

16) N. Chawdhury, A. Köhler, R.H. Friend, M. Younus, N.J. Long, P.R. Raithby and J. Lewis, *Macromolecules*, **1998**, 31, 722.

17) N. Chawdhury, A. Köhler, R.H. Friend, W.-Y. Wong, M. Younus, P.R. Raithby, J. Lewis, T.C. Corcoran, M.R. A. Al-Mandhary and M.S. Khan, *J. Chem. Phys.*, **1999**, 110, 4963.

18) J.S. Wilson, A. Kohler, R.H. Friend, M.K. Al-Suti, M.R.A. Al-Mandhary, M.S. Khan and P.R. Raithby, *J. Chem. Phys.*, **2000**, 113, 7627.

19) J.S. Wilson, N. Chawdhury, M.R.A. Al-Mandhary, M. Younus, M.S. Khan, P.R. Raithby, A. Köhler and R.H. Friend, *J. Am. Chem. Soc.*, **2001**, 123, 9412.

20) N. Chawdhury, A. Köhler, R.H. Friend, W.-Y. Wong, M. Younus, P.R. Raithby, J. Lewis, T.C. Corcoran, M.R. A. Al-Mandhary and M.S. Khan, *J. Chem. Phys.*, **1999**, 110, 4963.

21) M. Pope and C.E. Swenberg, *Electronic Processes in Organic Crystals and Polymers*, 2nd ed., Oxford University Press, Oxford, **1999**.

22) (a) M.A. Baldo, D.F. O'Brien, Y.You, A. Shoustikov, S. Sibley, M.E. Thompson and S.R. Forrest, *Nature*, **1998,395,** 151; (b) M.A. Baldo, M.E. Thompson, and S.R. Forrest, *Nature* **2000**, 403, 750; (c) V. Cleave, G. Yahioglu, P. Lebarny, R.H. Friend, and N. Tessler, *Adv. Mater.* **1999**, 11, 285.

# CHAPTER 4

## Rigid-Rod Pt(II) Poly-ynes and Di-ynes Incorporating Oligothiophene Linker Groups in the Backbone

# 4.1 Introduction

Polythiophenes have sparked particular interest within the area of new opto-electronic materials because of their applications as organic semiconductors for transistor applications[1]. Both fused and non-fused thiophene systems have been the subject of extensive studies because of their potential for these applications[2]. By combining them with the platinum poly-yne systems (**Figures 4.1a, 4.1b**) it is possible to probe, both the singlet and triplet manifolds using conventional spectroscopic techniques, and draw useful comparisons between the two classes of materials.

In fused thiophenes the conjugated ring systems are completely rigid. In comparison, the non-fused thiophenes structures are less rigid and more degrees of freedom are available. In related studies with poly-phenylenes[3] it was found that when poly-phenylenes are linked in a ladder-type structure to give a planar backbone, the conjugation length is increased (and consequently, the optical transitions are lowered), and a similar trend might be expected in the case of fused thiophenes. However, in this chapter, the optical gaps in fused polythiophenes are found to be higher than in non-fused polythiophenes with a comparable number of rings, but the trends can be explained by considering the number of conjugated double bonds in these materials.

Here, the synthesis and characterization of the fused thiophene ligands **4a-5a**, **4b-5b** and that of the di-ynes and poly-ynes, **4M-5M** and **4P-5P** are presented and the results are compared with the previously studied non fused thiophene materials **1M-3M** and **1P-3P**.

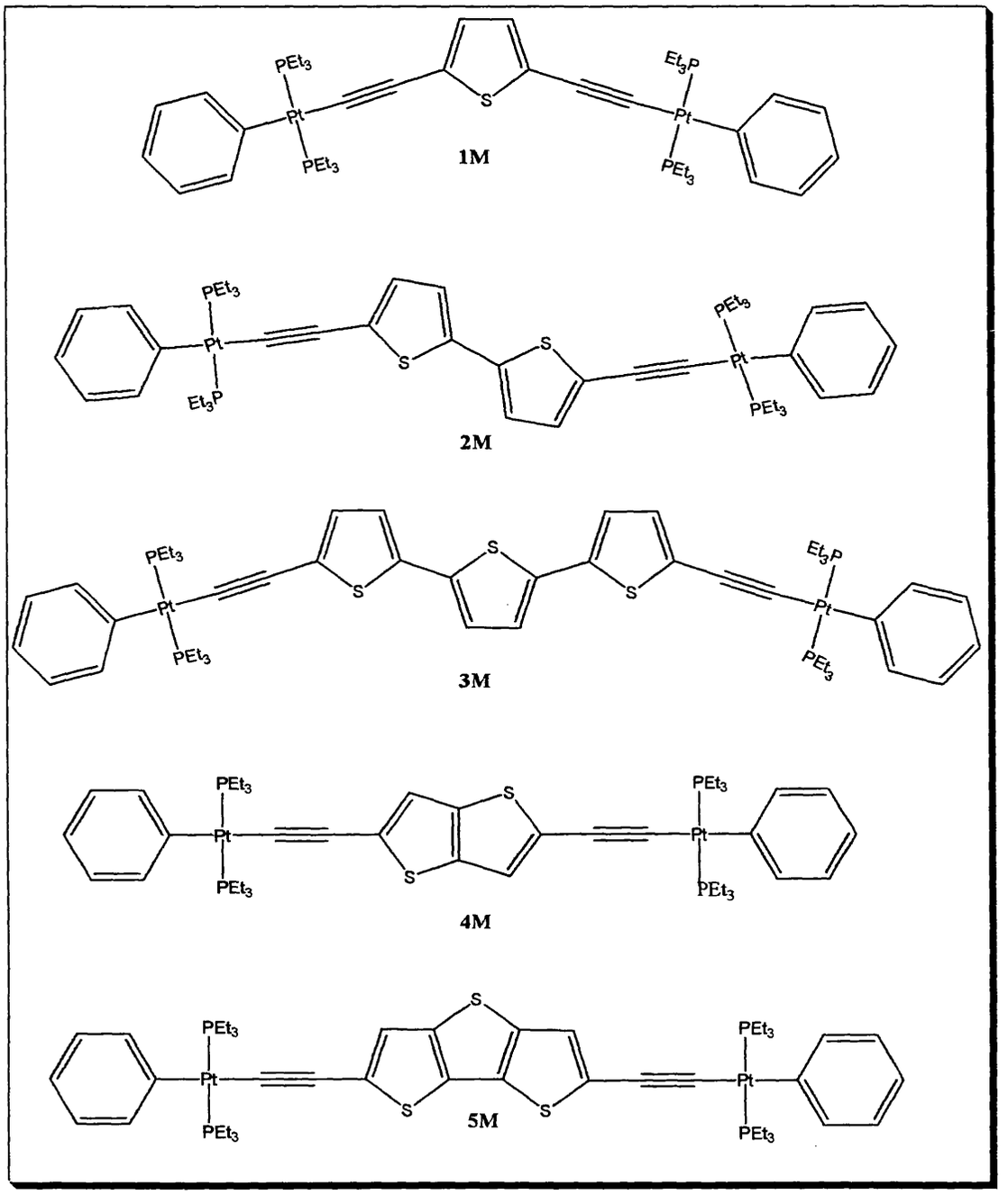


**Figure 4.1a: Pt(II) di-ynes with fused and non-fused thiophene spacers**

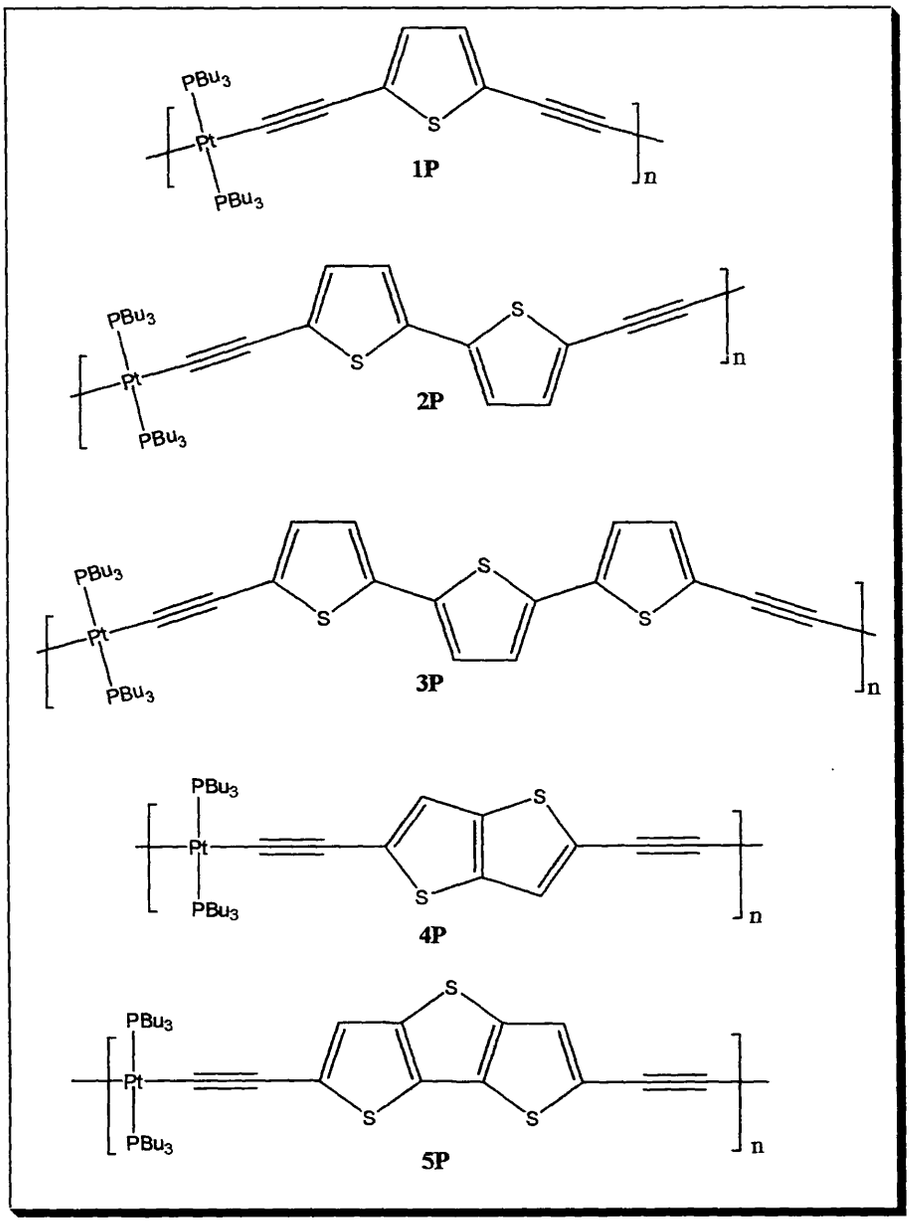


**Figure 4.1b: Pt(II) poly-ynes with fused and non-fused thiophene spacers**

# 4.2 Results and Discussion

## 4.2.1 Synthesis

2,5-Dibromothieno[3,2-*b*]thiophene and 5,5-Dibromodithieno[3,2-*b*:2,3-*d*]thiophene have been prepared by using literature methods[3c,d]. The *bis*-ethynyl ligands **4a-5a** and **4b-5b** were synthesized by a sequence of coupling and proto-desilylation reactons. The protected alkynyl ligand precursors **4a-5a** were prepared by the Sonogashira-Hagihara type cross-coupling reaction involving a palladium(II)/copper(I)-catalysed reactions of trimethylsilylethyne with the dibromo derivatives in $^{i}Pr_2NH$-THF solvent mixture as illustrated in **Scheme 4.1**.

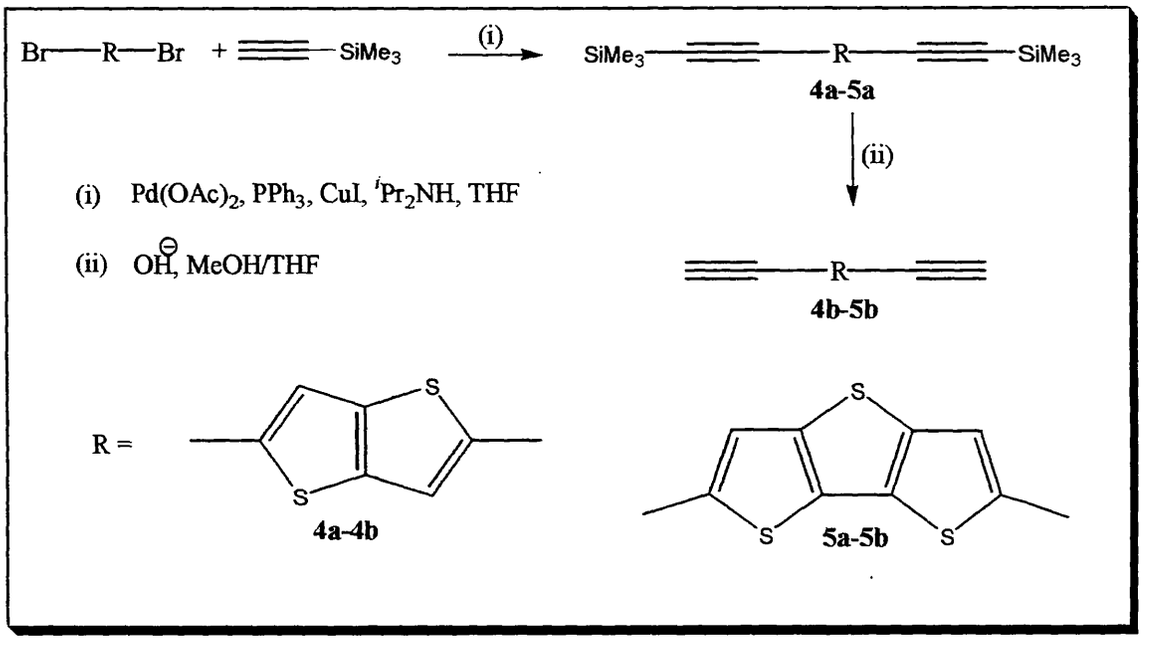


**Scheme 4.1.**

The reactions were monitored by TLC and IR spectroscopy. The IR spectra show a distinctive peak in the region 2140-2145 $cm^{-1}$ due to the acetylenic moieties. Both $^{1}H$ and $^{13}C$ NMR spectra confirm the symmetrical structures in these materials. The $^{1}H$ NMR spectrum of **4a** reveals a singlet peak at 7.27 ppm for the two aromatic protons and a singlet at 0.26 ppm for the 18 methyl protons of the $SiMe_3$ groups, while in **5a** the peaks were at 7.37 and 0.25 ppm, respectively. In the $^{13}C$ NMR spectra, the two acetylenic carbons

appeared at 97 and 100 ppm for both **4a** and **5a**, while in the aromatic region, three signals appeared at 124, 126 and 138 ppm in **4a**, which correspond to the six aromatic carbons of the thienothiophene spacer. In **5a**, four signals for the 8 aromatic carbons of the ditheinothiophene spacer came at 124, 125, 131 and 141 ppm.

Conversion of the protected dialkynes into the diterminal derivatives was accomplished by cleavage of the trimethylsilyl groups with dilute aqueous KOH in MeOH-THF system (**Scheme 4.1**). These diterminal alkynes show distinctive peaks at 2010 $cm^{-1}$ for the acetylenic moieties and at 3300 $cm^{-1}$ for the $C_{sp}$—H bond. It was not possible to collect the NMR spectra of **4b-5b** due to the instability of these materials during the measurements. Both **4a-5a** and **4b-5b** ligands were purified by silica gel column chromatography and isolated in 78–85% yields.

The dehydrohalogenation reactions between *trans*-[(Ph)$(Et_3P)_2PtCl$] and bis(ethynyl) oligothiophenes **4b-5b** (2:1 stoichiometry) in $^{i}Pr_2NH$-$CH_2Cl_2$, in the presence of CuI, at room temperature, afforded the dinuclear platinum(II) diynes **4M-5M** while the polycondensation reactions between *trans*-[$(P^{n}Bu_3)_2PtCl_2$] and **4b-5b** (1:1 equivalent) under similar conditions readily afforded the platinum(II) poly-ynes **4P-5P** (**Scheme 4.2**). The poly-ynes were obtained in yields of 85-90%, pointing to a very high conversion rate. Purification of the platinum(II) diynes was accomplished by silica column chromatography or preparative TLC, while the poly-ynes were purified by chromatography on an alumina column followed by repeated precipitation from dichloromethane into methanol.

Systematic characterization of the platinum(II) diynes and poly-ynes was achieved by spectroscopic methods. The IR spectra show a single sharp $\nu_{C\equiv C}$ absorption at around 2085-2090 $cm^{-1}$ consistent with a *trans*-configuration of the ethynylenic units around the platinum(II) centre. The two aromatic protons in the $^{1}H$ NMR spectra came at range of 6.80-6.90 ppm which is downfield shifted by *ca.* 0.47 ppm from that of the ligands. Gel permeation chromatography (GPC), using a polystyrene (PS) standard shows that the number-average molecular weights of the poly-yne **4P** is 223,200 g $mol^{-1}$ and that of **5P** is 222,300 g $mol^{-1}$, corresponding to degrees of polymerization (*n*) of 284 and 264 repeat units, respectively. The value of poly dispersity index (PDI) varied

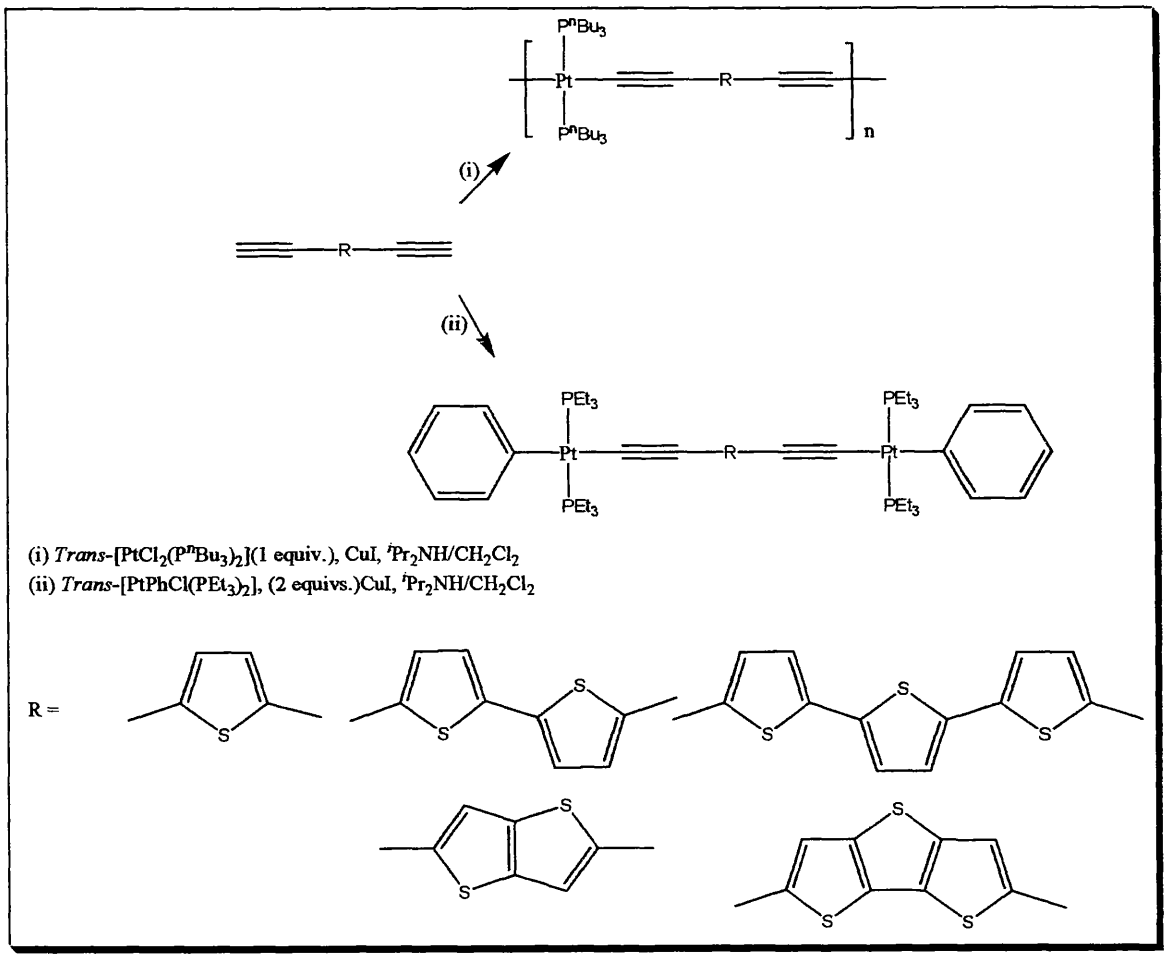


**Scheme 4.2.**

between 1.8 and 1.9. GPC data indicate that the number of repeat unit per chain for the thienothiophene-based platinum(II) poly-yne **4P** is higher than that for the dithienothiophene-based poly-yne **5P** and the degree of polymerization is significantly reduced in both cases as compared to that found for the parent thienylene-based poly-yne **1P** ( $n = 301$) . This result may reflect a decrease in solubility of the larger species.

## 4.2.2 Thermal analysis

The thermal stability was determined by simultaneous differential thermal analysis (DTA) and thermogravemtry (TG) on the fused poly-ynes and di-ynes. The first decomposition step might correspond to the removal of trialkylphosphine groups. TG

traces show that the Pt(II) diynes and poly-ynes have decomposition temperatures of over 300 °C, indicative of excellent thermal stability. Poly-yne **5P** exhibits higher decomposition onset and peak temperatures than **4P**, which in turn, exhibits higher thermal stability than the thiophene-containing poly-yne **1P**. Similar trend in thermal stability was also observed for the platinum(II) di-ynes where **5M** showed the highest and **1M** the lowest onset and peak decomposition temperatures. The diynes exhibited slightly higher onset and peak decomposition temperatures than the corresponding platinum(II) poly-ynes. The results are shown in **Table 4.1**. Decomposition onset was defined as a mass loss of 2%.

**Table 4.1. Decomposition temperatures of 1P, 4P-5P and 1M, 4M-5M all temperatures in °C. Uncertainties are approximately ±8 °C.**

| Compound | $T_{decomp}$ (onset) | $T_{decomp}$ (peak) |
|---|---|---|
| **1P** | 322 | 355 |
| **4P** | 348 | 372 |
| **5P** | 370 | 414 |
| **1M** | 329 | 365 |
| **4M** | 352 | 379 |
| **5M** | 379 | 422 |

## 4.2.3 Crystal structure

The molecular structures of the two ligands **4a** and **5a** and of the two complexes, **4M** and **5M**, were determined in order to establish the exact structures and geometries. The molecular structure of **4a** is illustrated in **Figure 4.2** and selected bond parameters are listed in **Table 4.2.** The thienothiophene unit is planar. Within the thienothiophene unit, the S–C bond lengths (average 1.730 Å) , and the C6–C7 and C8–C8a bond lengths (average 1.395 Å ) are significantly shorter than the C7–C8 bond, 1.444 (3) Å, consistent with the normal bonding picture for thienothiophene, and similar to those found in a

binuclear platinum(II) complex bridged by a thieno[3,2-b]thiophene group[4]. The bond parameters associated with the acetylenic units and the trimethylsilyl groups are similar to those in a number of other bis(trimethylsilyl) substituted diyne compounds[6].

The molecular structure of **5a** is illustrated in **Figure 4.3** and selected bond parameters are listed in **Table 4.3.** The central dithieno[3,2-b:20,30-d]thiophene group is essentially planar and the bond parameters associated with this group are similar to those found in other materials containing this thiophene ring system[5]. The bond parameters for the acetylene groups and the trimethylsilyl ligands are similar to those observed in related compounds[6].

The molecular structure of **4M** is illustrated in **Figure 4.4** and selected bond parameters are listed in **Table 4.4.** The platinum(II) centres are square planar, and the PtCPPC square planes make angles of approximately 60° with the central ring system. The bond parameters within the ethynylenic metal phosphine fragments are similar to those in other crystallographically characterized diplatinum diyne complexes.[6]

The molecular structure of **5M** is illustrated in **Figure 4.5** and selected bond parameters are listed in **Table 4.5.** The central dithienothiphene is ordered and essentially planar, and this group makes dihedral angles of approximately 50° with the planes of the two square planar platinum centres. The bond parameters within the terthiophene unit do not differ significantly from those in the free ligand, and the parameters within the two platinum phosphine acetylide units are similar to those in related structures[6].

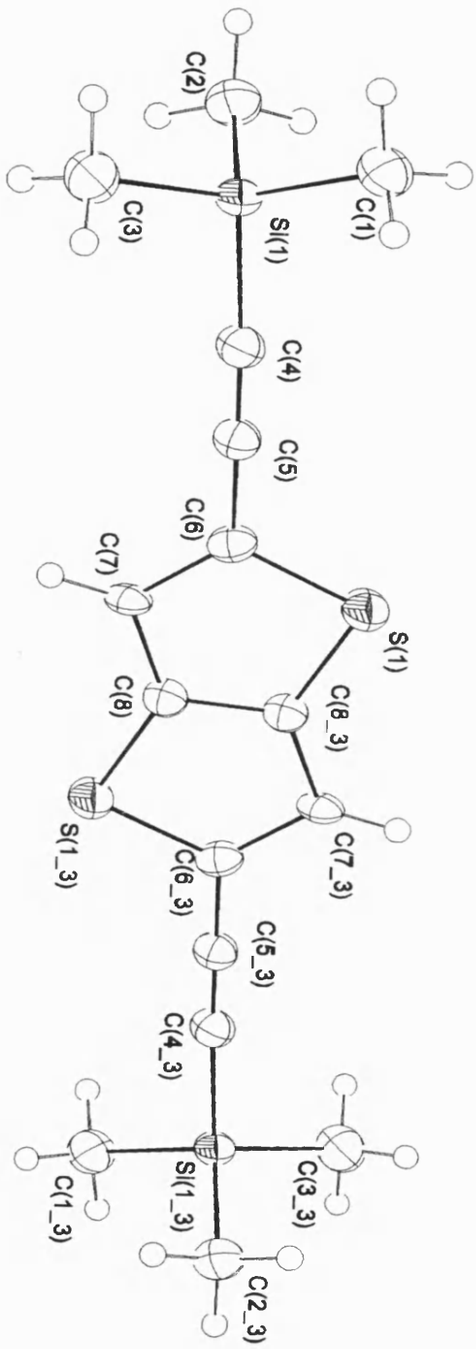


**Figure 4.2. The molecular structure 4a showing the atom numbering scheme adopted**

**Table 4.2. Selected bond lengths (Å) and angles ($^0$) for 4a**

| | | | |
|---|---|---|---|
| S(1)-C(8)#1 | 1.718(2) | C(4)-Si(1)-C(1) | 108.86(12)) |
| S(1)-C(6) | 1.742(2) | C(2)-Si(1)-C(1) | 111.67(12) |
| Si(1)-C(4) | 1.840(2) | C(4)-Si(1)-C(3) | 107.67(11) |
| Si(1)-C(2) | 1.853(3) | C(2)-Si(1)-C(3) | 110.11(13) |
| Si(1)-C(1) | 1.858(3) | C(1)-Si(1)-C(3) | 111.28(13) |
| Si(1)-C(3) | 1.863(3) | C(5)-C(4)-Si(1) | 175.1(2) |
| C(4)-C(5) | 1.207(3) | C(4)-C(5)-C(6) | 179.3(3) |
| C(5)-C(6) | 1.424(3) | C(7)-C(6)-C(5) | 126.2(2) |
| C(6)-C(7) | 1.409(3) | C(7)-C(6)-S(1) | 114.33(16) |
| C(7)-C(8) | 1.444(3) | C(5)-C(6)-S(1) | 119.50(17) |
| C(8)-C(8)#1 | 1.381(4) | C(6)-C(7)-C(8) | 107.8(2) |
| C(8)-S(1)#1 | 1.718(2) | C(8)#1-C(8)-C(7) | 115.1(2) |
| C(8)#1-S(1)-C(6) | 90.76(11) | C(8)#1-C(8)-S(1)#1 | 112.0(2) |
| C(4)-Si(1)-C(2) | 107.07(11) | C(7)-C(8)-S(1)#1 | 132.87(18) |

Symmetry transformations used to generate equivalent atoms:
a -x+1,-y,-z+1

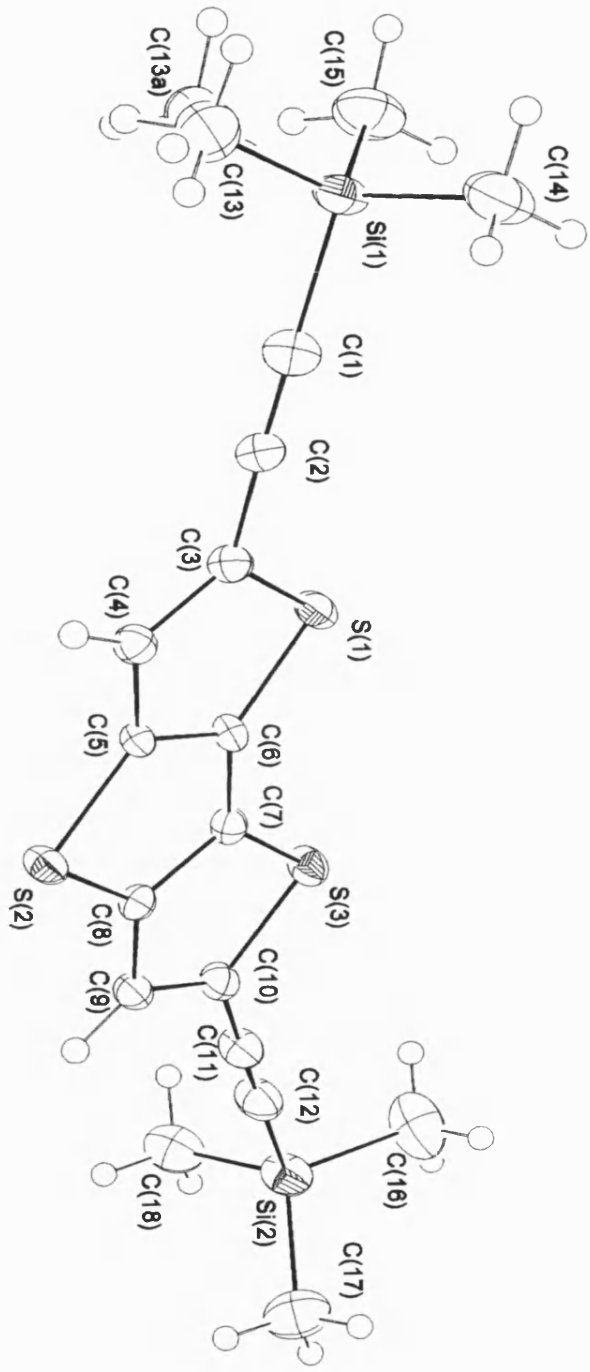


**Figure 4.3. The molecular structure 5a showing the atom numbering scheme adopted**

**Table 4.3. Selected bond lengths (Å) and angles ($^0$) for 5a**

| | | | |
|---|---|---|---|
| Si(1)-C(14) | 1.842(5) | S(3)-C(7) | 1.725(4) |
| Si(1)-C(15) | 1.843(5) | S(3)-C(10) | 1.747(4) |
| Si(1)-C(1) | 1.843(4) | C(1)-C(2) | 1.203(6) |
| Si(1)-C(13) | 1.859(12) | C(2)-C(3) | 1.408(5) |
| Si(1)-C(13') | 1.877(10) | C(3)-C(4) | 1.383(5) |
| Si(2)-C(12) | 1.844(4) | C(4)-C(5) | 1.405(5) |
| Si(2)-C(18) | 1.848(5) | C(5)-C(6) | 1.382(5) |
| Si(2)-C(17) | 1.848(5) | C(6)-C(7) | 1.410(5) |
| Si(2)-C(16) | 1.855(5) | C(7)-C(8) | 1.380(5) |
| S(1)-C(6) | 1.716(4) | C(8)-C(9) | 1.406(5) |
| S(1)-C(3) | 1.739(4) | C(9)-C(10) | 1.356(5) |
| S(2)-C(5) | 1.744(4) | C(10)-C(11) | 1.418(5) |
| S(2)-C(8) | 1.745(3) | C(11)-C(12) | 1.199(5) |

| | | | |
|---|---|---|---|
| C(14)-Si(1)-C(15) | 110.1(2) | C(5)-C(6)-C(7) | 112.7(3) |
| C(12)-Si(2)-C(16) | 107.2(2) | C(7)-C(8)-S(2) | 112.2(3) |
| C(18)-Si(2)-C(16) | 109.7(2) | C(9)-C(8)-S(2) | 133.5(3) |
| C(17)-Si(2)-C(16) | 111.6(3) | C(3)-C(4)-C(5) | 110.8(3) |
| C(6)-S(1)-C(3) | 91.27(18) | C(6)-C(5)-C(4) | 114.5(3) |
| C(5)-S(2)-C(8) | 90.39(17) | C(6)-C(5)-S(2) | 112.1(3) |
| C(7)-S(3)-C(10) | 90.89(17) | C(5)-C(6)-C(7) | 112.7(3) |
| C(2)-C(1)-Si(1) | 177.2(4) | C(10)-C(9)-C(8) | 111.6(3) |
| C(1)-C(2)-C(3) | 175.9(4) | C(9)-C(10)-C(11) | 129.1(4) |
| C(4)-C(3)-C(2) | 128.9(3) | C(9)-C(10)-S(3) | 112.5(3) |
| C(4)-C(3)-S(1) | 112.4(3) | C(11)-C(10)-S(3) | 118.4(3) |
| C(6)-C(7)-S(3) | 136.7(3) | C(12)-C(11)-C(10) | 177.8(4) |
| C(7)-C(8)-C(9) | 114.3(3) | C(11)-C(12)-Si(2) | 179.4(4) |

| | | | |
|---|---|---|---|
| C(14)-Si(1)-C(1) | 109.3(2) | C(12)-Si(2)-C(18) | 107.9(2) |
| C(15)-Si(1)-C(1) | 107.5(2) | C(12)-Si(2)-C(17) | 108.1(2) |
| C(14)-Si(1)-C(13) | 105.7(5) | C(2)-C(3)-S(1) | 118.7(3) |
| C(15)-Si(1)-C(13) | 117.6(5) | C(4)-C(5)-S(2) | 133.4(3) |
| C(1)-Si(1)-C(13) | 106.5(4) | C(5)-C(6)-S(1) | 111.0(3) |
| (14)-Si(1)-C(13') | 116.1(4) | C(7)-C(6)-S(1) | 136.3(3) |
| C(15)-Si(1)-C(13') | 105.1(4) | C(8)-C(7)-C(6) | 112.7(3) |
| C(1)-Si(1)-C(13') | 108.5(4) | C(8)-C(7)-S(3) | 110.7(3) |
| C(13)-Si(1)-C(13') | 13.2(5) | | |

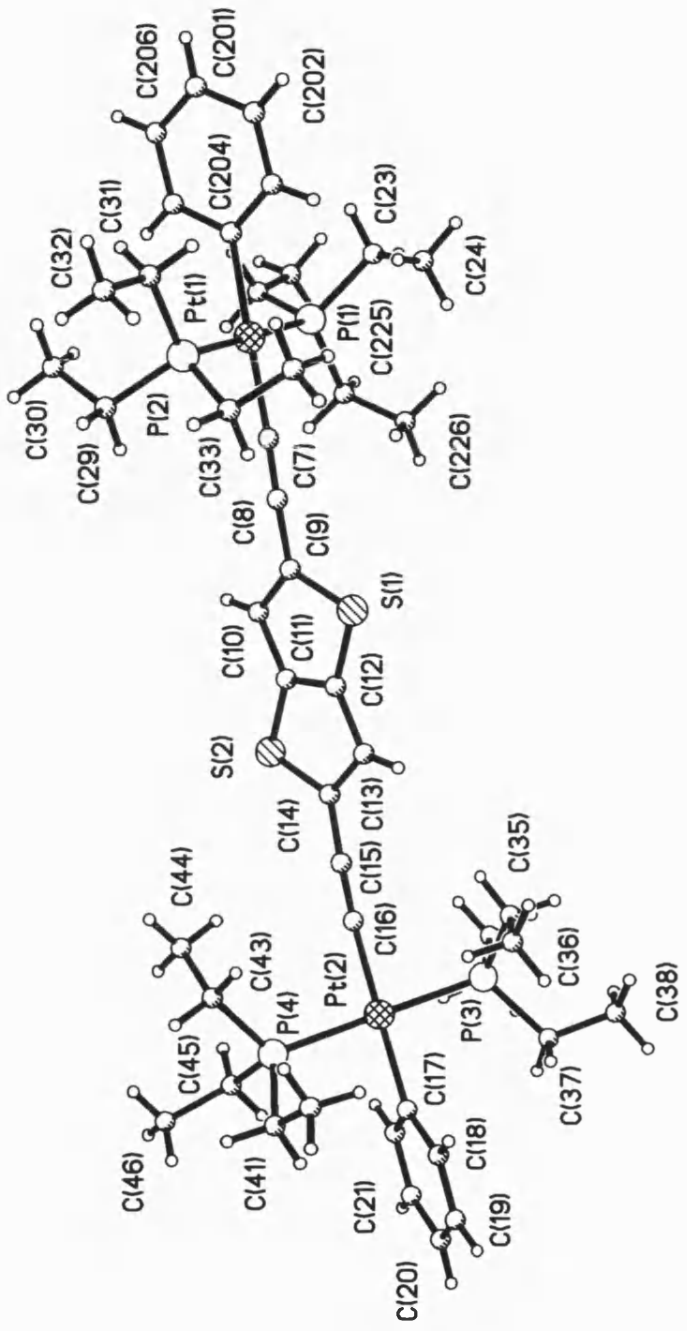


**Figure 4.4. The molecular structure of one of the two independent molecules of 4M showing the atom numbering scheme adopted.**

**Table 4.4. Selected bond lengths (Å) and angles ($^0$) for 4M**

| | | | |
|---|---|---|---|
| C(204)-Pt(1) | 2.048(10) | C(114)-S(102) | 1.719(8) |
| C(7)-C(8) | 1.203(7) | C(115)-C(116) | 1.198(8) |
| C(7)-Pt(1) | 2.011(5) | C(116)-Pt(12) | 2.016(6) |
| C(8)-C(9) | 1.423(7) | C(117)-C(118) | 1.400(7) |
| C(9)-C(10) | 1.462(7) | C(117)-C(122) | 1.409(7) |
| C(9)-S(1) | 1.740(5) | C(117)-Pt(12) | 2.057(5) |
| C(10)-C(11) | 1.482(7) | C(118)-C(119) | 1.387(7) |
| C(11)-C(12) | 1.368(7) | P(1)-Pt(1) | 2.2991(14) |
| C(11)-S(2) | 1.712(5) | P(2)-Pt(1) | 2.2941(13) |
| C(12)-C(13) | 1.459(7) | P(3)-Pt(2) | 2.2956(12) |
| C(12)-S(1) | 1.713(5) | P(4)-Pt(2) | 2.2993(12) |
| C(13)-C(14) | 1.463(7) | P(101)-Pt(11) | 2.2896(13) |
| C(14)-C(15) | 1.423(7) | P(102)-Pt(11) | 2.2967(14) |
| C(14)-S(2) | 1.736(5) | P(103)-Pt(12) | 2.2828(18) |
| C(15)-C(16) | 1.211(7) | P(104)-Pt(12) | 2.2862(17) |
| C(16)-Pt(2) | 2.005(5) | | |
| C(17)-C(22) | 1.399(7) | C(203)-C(204)-Pt(1) | 124.4(9) |
| C(17)-C(18) | 1.404(7) | C(205)-C(204)-Pt(1) | 120.2(9) |
| C(17)-Pt(2) | 2.072(5) | C(8)-C(7)-Pt(1) | 177.2(5) |
| C(104)-Pt(11) | 2.066(4) | C(7)-C(8)-C(9) | 178.2(6) |
| C(107)-C(108) | 1.213(7) | C(8)-C(9)-C(10) | 126.7(5) |
| C(107)-Pt(11) | 2.003(5) | C(8)-C(9)-S(1) | 119.1(4) |
| C(108)-C(109) | 1.421(7) | C(10)-C(9)-S(1) | 114.2(3) |
| C(109)-C(110) | 1.455(8) | C(9)-C(10)-C(11) | 104.7(4) |
| C(109)-S(101) | 1.734(6) | C(12)-C(11)-C(10) | 117.2(4) |
| C(110)-C(111) | 1.498(8) | C(12)-C(11)-S(2) | 111.6(4) |
| C(111)-C(112) | 1.360(9) | C(10)-C(11)-S(2) | 131.2(4) |
| C(111)-S(102) | 1.717(6) | C(11)-C(12)-C(13) | 117.4(4) |
| C(112)-C(113) | 1.479(7) | C(11)-C(12)-S(1) | 111.8(4) |
| C(112)-S(101) | 1.718(6) | C(13)-C(12)-S(1) | 130.8(4) |
| C(113)-C(114) | 1.447(9) | C(12)-C(13)-C(14) | 105.1(4) |
| C(114)-C(115) | 1.434(8) | C(15)-C(14)-C(13) | 125.3(5) |

| | | | |
|---|---|---|---|
| C(11)-C(12)-S(1) | 111.8(4) | C(16)-Pt(2)-C(17) | 177.67(19) |
| C(13)-C(12)-S(1) | 130.8(4) | C(16)-Pt(2)-P(3) | 87.08(14) |
| C(12)-C(13)-C(14) | 105.1(4) | C(17)-Pt(2)-P(3) | 91.79(13) |
| C(15)-C(14)-C(13) | 125.3(5) | C(16)-Pt(2)-P(4) | 93.38(14) |
| | | C(17)-Pt(2)-P(4) | 87.88(13) |
| C(15)-C(14)-S(2) | 120.6(4) | P(3)-Pt(2)-P(4) | 175.94(5) |
| C(13)-C(14)-S(2) | 114.0(3) | C(107)-Pt(11)-C(104) | 175.2(2) |
| C(16)#1-C(15)-C(14) | 175.4(6) | C(107)-Pt(11)-P(101) | 92.66(15) |
| C(15)#2-C(16)-Pt(2) | 176.4(5) | C(104)-Pt(11)-P(101) | 88.58(14) |
| C(22)-C(17)-C(18) | 115.9(4) | C(107)-Pt(11)-P(102) | 90.12(16) |
| C(22)-C(17)-Pt(2) | 120.9(4) | C(104)-Pt(11)-P(102) | 89.06(14) |
| C(18)-C(17)-Pt(2) | 123.2(3) | P(101)-Pt(11)-P(102) | 174.16(5) |
| C(7)-Pt(1)-C(204) | 178.7(4) | C(116)-Pt(12)-C(117) | 179.4(3) |
| C(7)-Pt(1)-C(304) | 170.5(5) | C(116)-Pt(12)-P(103) | 88.9(2) |
| C(204)-Pt(1)-C(304) | 10.7(6) | C(117)-Pt(12)-P(103) | 91.56(16) |
| C(7)-Pt(1)-P(2) | 88.16(15) | C(116)-Pt(12)-P(104) | 87.7(2) |
| C(204)-Pt(1)-P(2) | 91.5(3) | C(117)-Pt(12)-P(104) | 91.86(15) |
| C(304)-Pt(1)-P(2) | 90.4(6) | P(103)-Pt(12)-P(104) | 175.55(6) |
| C(7)-Pt(1)-P(1) | 92.06(15) | C(12)-S(1)-C(9) | 92.1(3) |
| C(204)-Pt(1)-P(1) | 88.3(3) | C(11)-S(2)-C(14) | 91.8(2) |
| C(304)-Pt(1)-P(1) | 89.3(6) | C(112)-S(101)-C(109) | 91.7(3) |
| P(2)-Pt(1)-P(1) | 179.58(5) | C(111)-S(102)-C(114) | 91.7(3) |

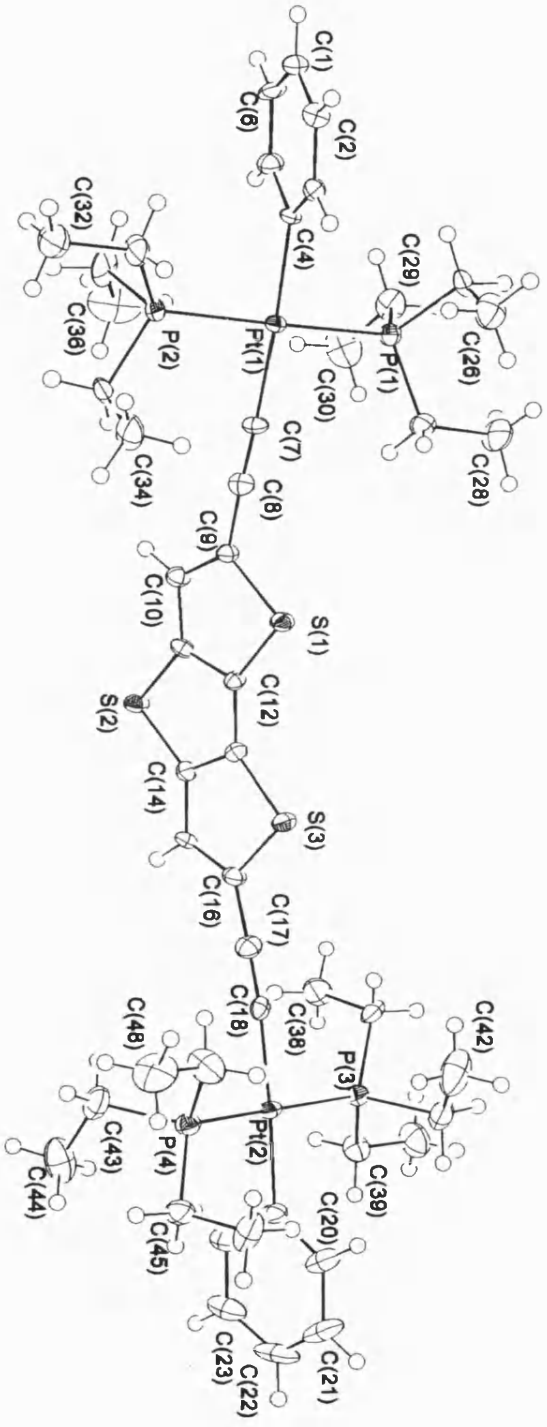


**Figure 4.5. The molecular structure 5M showing the atom numbering scheme adopted.**

**Table 4.5. Selected bond lengths (Å) and angles (°) for 4M**

| | | | |
|---|---|---|---|
| C(4)-Pt(1) | 2.076(9) | C(10)-C(11)-S(2) | 133.3(8) |
| C(7)-C(8) | 1.211(14) | C(11)-C(12)-C(13) | 112.0(9) |
| C(7)-Pt(1) | 2.006(10) | C(11)-C(12)-S(1) | 110.8(7) |
| C(8)-C(9) | 1.414(14) | C(13)-C(12)-S(1) | 137.2(8) |
| C(9)-C(10) | 1.360(15) | C(14)-C(13)-C(12) | 112.6(9) |
| C(9)-S(1) | 1.765(11) | C(14)-C(13)-S(3) | 111.2(8) |
| C(10)-C(11) | 1.412(14) | C(12)-C(13)-S(3) | 136.2(8) |
| C(11)-C(12) | 1.383(14) | C(13)-C(14)-C(15) | 113.9(9) |
| C(11)-S(2) | 1.742(10) | C(13)-C(14)-S(2) | 112.4(8) |
| C(12)-C(13) | 1.426(13) | C(15)-C(14)-S(2) | 133.7(8) |
| C(12)-S(1) | 1.724(10) | C(16)-C(15)-C(14) | 112.6(9) |
| C(13)-C(14) | 1.380(14) | C(16)-C(15)-H(15) | 123.7 |
| C(13)-S(3) | 1.726(10) | C(14)-C(15)-H(15) | 123.7 |
| C(14)-C(15) | 1.410(13) | C(15)-C(16)-C(17) | 130.1(10) |
| C(14)-S(2) | 1.741(10) | C(15)-C(16)-S(3) | 111.1(7) |
| C(15)-C(16) | 1.371(15) | C(17)-C(16)-S(3) | 118.8(9) |
| C(16)-C(17) | 1.417(14) | C(18)-C(17)-C(16) | 179.2(13) |
| C(16)-S(3) | 1.766(11) | C(17)-C(18)-Pt(2) | 173.8(9) |
| C(17)-C(18) | 1.224(15) | C(20)-C(19)-Pt(2) | 125.8(10) |
| C(18)-Pt(2) | 2.005(11) | C(24)-C(19)-Pt(2) | 119.0(9) |
| C(19)-Pt(2) | 2.066(10) | C(7)-Pt(1)-C(4) | 176.1(4) |
| P(1)-Pt(1) | 2.299(3) | C(7)-Pt(1)-P(2) | 89.6(3) |
| P(2)-Pt(1) | 2.287(3) | C(4)-Pt(1)-P(2) | 87.7(3) |
| P(3)-Pt(2) | 2.291(3) | C(7)-Pt(1)-P(1) | 90.4(3) |
| P(4)-Pt(2) | 2.300(3) | C(4)-Pt(1)-P(1) | 92.1(3) |
| | | P(2)-Pt(1)-P(1) | 175.30(11) |
| C(5)-C(4)-Pt(1) | 121.3(7) | C(18)-Pt(2)-C(19) | 174.2(4) |
| C(3)-C(4)-Pt(1) | 122.8(8) | C(18)-Pt(2)-P(3) | 91.2(3) |
| C(8)-C(7)-Pt(1) | 177.4(10) | C(19)-Pt(2)-P(3) | 88.0(3) |
| C(7)-C(8)-C(9) | 176.7(12) | C(18)-Pt(2)-P(4) | 88.4(3) |
| C(10)-C(9)-C(8) | 129.0(10) | C(19)-Pt(2)-P(4) | 93.0(3) |
| C(10)-C(9)-S(1) | 111.5(7) | P(3)-Pt(2)-P(4) | 172.58(11) |
| C(8)-C(9)-S(1) | 119.5(8) | C(12)-S(1)-C(9) | 91.2(5) |
| C(9)-C(10)-C(11) | 112.3(9) | C(14)-S(2)-C(11) | 90.5(5) |
| C(12)-C(11)-S(2) | 112.6(7) | C(13)-S(3)-C(16) | 91.2(5) |

**Table 4.6: Crystallographic data for compounds 4a-5a and 4M-5M**

| Compound | 4a | 5a | 4M | 5M |
|---|---|---|---|---|
| Formula | $C_{16}H_{20}S_2Si_2$ | $C_{18}H_{20}S_3Si_2$ | $C_{42}H_{72}P_4Pt_2S_2$ | $C_{48}H_{72}P_4Pt_2S_3$ |
| $M_r$ | 332.62 | 388.70 | 1203.22 | 1259.30 |
| Crystal habit | Colourless plate | Colourless plate | Pale yellow block | Pale yellow plate |
| Crystal size [mm] | 0.23x0.07x0.04 | 0.07x0.05x0.01 | 0.08x0.04x0.02 | 0.16x0.10x0.01 |
| Crystal system | Monoclinic | Monoclinic | Triclinic | Monoclinic |
| Space group | *$P2_1/c$* | *$P2_1/n$* | *P-1 (No. 2)* | *$P2_1/c$* |
| Cell dimensions | | | | |
| *a* [Å] | 15.173(3) | 6.191(2) | 9.0911(6) | 9.3534(12) |
| *b* [Å] | 5.7317(12) | 28.671(9) | 21.0960(13) | 12.4022(16) |
| *c* [Å] | 10.9836(18) | 12.066(4) | 27.6621(7) | 44.475(6) |
| α [°] | 90 | 90 | 107.3920(10) | 90 |
| β [°] | 108.220(9) | 92.51(2) | 90.6130(10) | 92.129(2) |
| γ [°] | 90 | 90 | 101.5460(10) | 90 |
| *U* [$Å^3$] | 907.3(3) | 2139.7(13) | 4946.1(5) | 5155.7(3) |
| *Z* | 2 | 4 | 4 | 4 |
| $\mu$ [$mm^{-1}$] | 0.415 | 0.455 | 5.894 | 5.697 |
| *T* [°C] | -103 | -123 | -123 | -123 |
| $2\theta_{max}$ [°] | 50.1 | 45.0 | 58.42 | 58.88 |
| Wavelength [Å] | 0.71073 | 0.6887 | 0.69040 | 0.69040 |
| No. of reflections | | | | |
| Measured | 2820 | 11094 | 40214 | 40213 |
| Independent | 1596 | 3062 | 25401 | 13808 |
| $R_{Int}$ | 0.022 | 0.063 | 0.0327 | 0.0376 |
| Parameters | 94 | 224 | 1061 | 514 |
| Restraints | 0 | 105 | 33 | 0 |
| *wR2*($F^2$, all refl.) | 0.1004 | 0.1143 | 0.091 | 0.1660 |
| *R1[F>2σ(F)]* | 0.0365 | 0.0554 | 0.0371 | 0.0788 |
| GoF | 1.051 | 1.166 | 1.025 | 1.394 |

## 4.2.4 Optical Spectroscopy

The results of optical spectroscopy of all the systems described in this thesis have been carried out by the group of Professor Sir Richard R. Friend and Dr. Anna Köhler from the Cavendish Laboratory, University of Cambridge. Their effort in measuring and providing us with these results is gratefully acknowledged. The thin film absorption spectra of **4a-5a**, **4M-5M** and **2P-5P** are shown in **Figure 4.6**. The energies for the onset of absorption are summarized in **Table 4.7**. The spectral shape of the ligand spectra are similar to those of the monomers and polymers, which indicate that the excited state is of predominant by $\pi$–$\pi^*$ character rather then a MLCT transition. The vibronic structures disappear gradually in going from the ligand over the monomer to the polymer. This can be attributed to the small differences in the effective conjugation lengths in the polymer chains and in the di-ynes.

The onset of absorption shifts to the red from ligand to the monomer and polymer due to the increase in conjugation, which extend through the platinum atom, as observed for related compounds[6]. The first absorption band in the compounds based on fused thiophene rings is at higher energy than in the analogous compounds with the non-fused bithiophene and terthiophene spacers[8]. The shifts from ligand to di-ynes and from di-ynes to poly-ynes are comparable in the fused thiophene systems and the non-fused systems suggest similar donor-acceptor interaction strength and degree of conjugation in both cases.

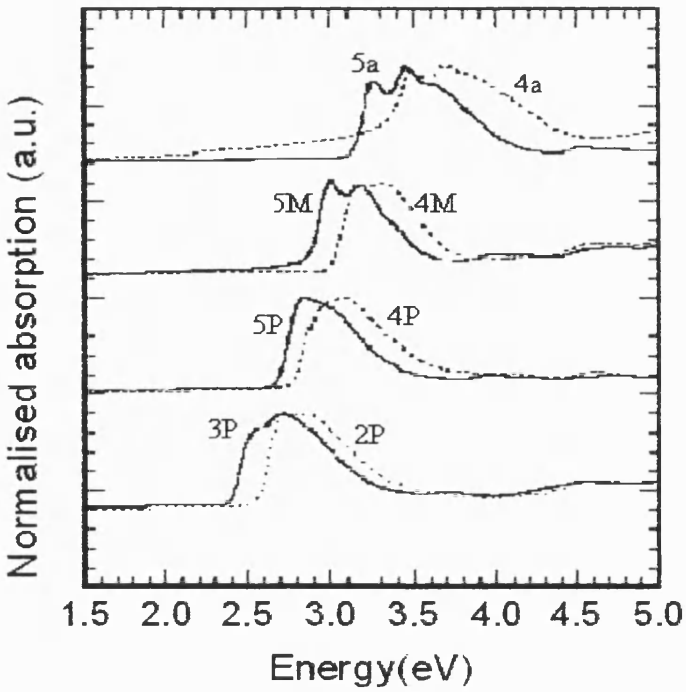


**Figure 4.6 Optical absorption spectra taken from thin films at room temperature of 4a-5a, 4M-5M and 2P-5P.**

The photoluminescence (PL) spectra of the polymers and monomers at 10 K are shown in **Figure 4.7.** The spectra show two emission bands. The emission band at higher energy is attributed to the same singlet state that gives rise to the absorption band in **Figure 4.6**. The lower energy emission is assigned to a triplet excited state (phosphorescence); and its well-resolved vibronic structure is similar to the singlet emission and excludes an excimer origin, it is shifted by about 0.8 eV from the singlet excited state as observed for the analogous compounds.

**Figure 4.8** shows the corresponding spectra at room temperature. At 300K, thermal broadening masks the vibronic structure, and diffusion of the longer-lived triplet excitations to quenching sites along the polymer chain reduces the lifetime and thus the intensity of triplet emission in the polymers.

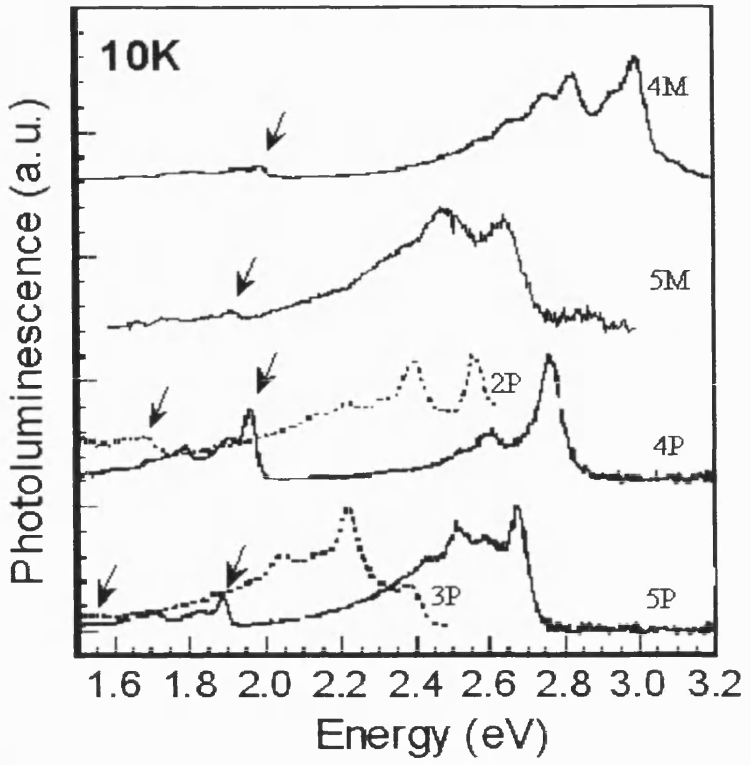


**Figure 4.7. The PL spectra taken from thin films of the monomers 4M and 5M and of the polymers 2P-5P at 10K.**

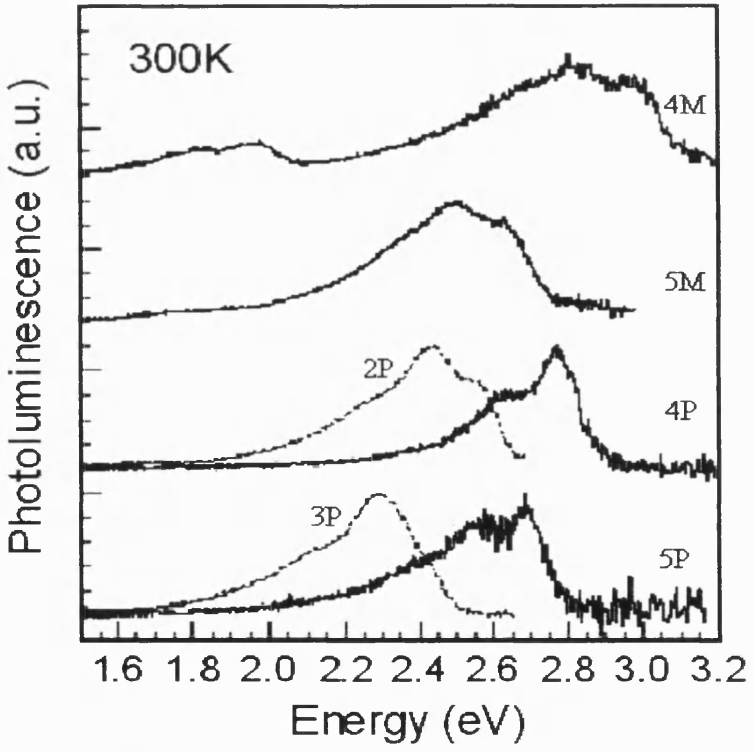


**Figure 4.8. The PL spectra taken from thin films of the monomers 4M and 5M and of the polymers 2P-5P at 300K.**

DFT calculations on the fused and non-fused ligand systems and on the related metal complexes indicate that the factor that determines the energies of the systems, and the HOMO – LUMO gap is related to the level of conjugation within the oligothiophene units, as is illustrated in **Figure 4.9**. The trend in the HOMO – LUMO gap across the series, is related to the number of "formal" double bonds within the systems. Following the schematic in **Figure 4.9**, the linker group in **1M** has two double bonds, the linker group in **4M** has three double bonds, the linker group in **2M** has four double bonds, the linker group in **5M** has also four double bonds, and the linker group in **3M** has six double bonds. Thus, the more double bonds present the lower is the energy gap in the system. When comparing **4P** with **2P** it is evident that fusing the two rings has reduced the number of double bonds present by one.

Reducing the number of double bonds by fusing reduces the conjugation of the system significantly. However, when comparing **5P** and **2P**, which have the same number of double bonds, we still find a higher energy of the optical transitions in the polymer with the fused ring system than in the polymer with the non-fused ring system. The difference might be due to the presence of an additional sulphur atom that affords additional electron density to the bonding orbitals.

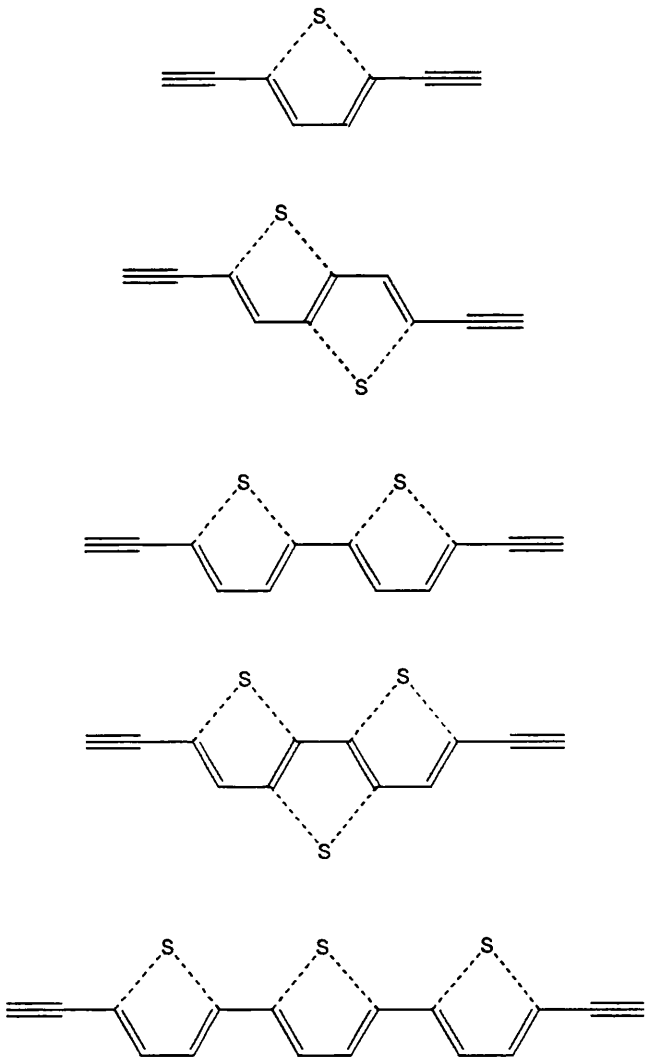

**Figure 4.9: The energy gaps in the fused and non-fused oligothiophene units, showing the level of conjugation within the linker groups.**

**Table 4.7: Energies of the onset of absorption and the 0-0emission peaks for 1M and 4M-5M and of 1P and 4P-5P**

| Compound | Onset of absorption (eV) | Energy of the 0-0 peak in the emission spectra (eV) |
|---|---|---|
| **1M**[9] | 3.14 | 3.10 |
| **4M** | 3.02 | 2.99 |
| **5M** | 2.89 | 2.86 |
| **1P**[8] | 2.86 | 2.85 |
| **4P** | 2.78 | 2.76 |
| **5P** | 2.68 | 2.67 |

# 4.3 Conclusion

The series of **4a-5a** and **4b-5b** acetylide functionalised ligands have been successfully prepared and characterised spectroscopically, and have been successfully incorporated into the di-ynes **4M-5M**, and poly-ynes **4P-5P**. The IR spectra show that the stretching frequencies are lower in the di-ynes and poly-ynes compared to that of the metal free ligands, and also gave evidence for the *trans*-configuration of the actylenic units around the platinum centre. The crystal structures of **4a-5a** and that of **4M** and **5M** have been determined in order to confirm the expected structures from the synthetic work and have also been compared to other related materials. The optical characterisation for the **4M-5M** and **4P-5P** have been established and compared with the related non-fused materials characterised previously. The onset of absorption shifts to the red from ligand to the monomer and polymer due to the increase in conjugation, which extend through the platinum atom. The excited state is predominantly $\pi$–$\pi^*$ in character. The first absorption band in the compounds based on fused thiophene rings is at higher energy than in the analogous non-fused ligands, platinum(II) di-ynes and poly-ynes.

The photoluminescence spectra show two emission bands. The emission band at higher energy is attributed to a singlet state, while the lower energy emission is assigned to a triplet excited state (phosphorescence);

DFT calculations on the fused and non-fused systems indicate that the factor that determines the energies of the systems, and the HOMO – LUMO gap is related to the number of "formal" double bonds within the systems. Reducing the number of double bonds by fusing reduces the conjugation of the system.

## 4.4 References


1) X. C. Li, H. S. Garnier, F. H. Sirringhaus, F. Garnier, A. B. Holmes, S. C. Moratti, N. Feeder, W. Clegg, S. J. Teat, and R. H. Friend., *J .Am. Chem .Soc.* **1998**, *120*, 2206-2207.

2) (a) S. Ledesma, R. Ortiz, D. Ruiz, M. Carmen, V. Yolanda, E. Periz-Inestrosa, J. Casado, V. Hernandez, O. Kim,; J. Lehn, ; N. Lopez, T. Juan; *Chem. A Eur. J.*,**2004**, 10, 16, 3848 (b) M. Mazzeo, V. Vitale, F. S. Della, M. Anni, G. Barbarella, L. Favaretto, G. Sotgiu, R. Cingolani and G. Gigli; **2005**, 17, 1, 34-39. (c) M. Osip, S. Destri, M. Pasini, W. Porzio, K. Pernstich, B. Batlogg; *Syn. Met*, **2004**, 146, 3, 251-257, (d) F. Ciardelli, C. Cellai, A. Pucci,; L. Regoli, G. Ruggeri, N. Tirelli, C. Cardelli, . *Poly. for Adv. Technol.* **2001**, 12(3-4), 223-230.

3) (a) C. Taliani, , R. Zamboni, , R. Damieli, , P. Ostoja, , W. Porzio, , R. Lazzaroni, J. Bredas, *Phys. Scr.* **1989**, *40*, 781.(b) J. Roncali; *Chem. Rev.* **1997**, *97*, 173-205.(c) P. Leriche, J.-M. Raimundo, M. Tarbiez, V. Monroche, M. Allain, F. X. Sauvage, J. Roncali, P. Fr'ere and P. J. Skabara, *J. Mater. Chem.*,**2003**, 13, 1324. (d) R. Rutherford, K Stille, M. C. Elliott and R. V. Reichert; *Macromolecules*, **1992**, 25(9), 2294-306.

4) M. Sato, A. Asami, G. Maruyama, M. Kosuge, J. Nakayama, S. Kumakura, T. Fujihara and K. Unoura, *J. Organomet. Chem*, **2002**, 654, 56-65.

5) (a) J. Frey, A. D. Bond and A. B Holmes, *Chem. Commun.*, **2002**, 2424.

6) (a) M. S. Khan, M. R. A. Al-Mandhary, M. K. Al-Suti, N. Feeder, S. Nahar, A. Köhler, R. H. Friend, P. J. Wilson and P. R. Raithby, *J. Chem. Soc., Dalton Trans.*,

**2002**, 2441-2448; (b) M. S. Khan, M. R. A. Al-Mandhary, M. K. Al-Suti, P. R. Raithby, B. Ahrens, L. Male, R. H. Friend, A. Köhler, J. S. Wilson, *Dalton Trans.* **2003**, 65-73. (c) M. S. Khan, M. R. A. Al-Mandhary, M. K. Al-Suti, A. K. Hisham, P. R. Raithby, B. Ahrens, M. F. Mahon, L. Male, E. A. Marseglia, E. Tedesco, R. H. Friend, A. Köhler, N. Feeder and S. J. Teat, *J. Chem. Soc., Dalton Trans.*, **2002**, 1358; (d) M. S. Khan, M. R. A. Al-Mandhary, M. K. Al-Suti, T. C. Corcoran , J. P. Attfield, N. Feeder, W. I. F. David, K. Shankland, R. H. Friend, A. Köhler, E. A. Marseglia, E. Tedesco, C. C. Tang, P. R. Raithby, J. C. Collings, K. P. Roscoe, A. S. Batsanov, L. M. Stimson and T. B. Marder, *New J. Chem.*, **2003**, 27, 140.

7) P. Li, B. Ahrens, N. Feeder, P. R. Raithby, S. J. Teat and M. S. Khan., *Dalton Trans.*, **2005**, 5, 874-883

8) N. Chawdhury, A. Köhler, R. H. Friend, W. Y. Wong, M. Younus, P. R Raithby, J. Lewis, M. R. A. Al-Mandhury, T. C. Corcoran and M. S. Khan, *J. Chem. Phys.* **1999**, *110*, 4963-4970.

9) N. Chaudhury, A. Köhler, R. H. Friend, M. Younus, N. J. Long, P. R. Raithby, J. Lewis, *Macromolecules,* **1998**, *31*, 722-727.

# CHAPTER 5

## Rigid-Rod Pt(II) Poly-ynes and Di-ynes Incorporating Hetero-Aromatic Linker Groups in the Backbone

# 5.1 Introduction

The synthesis and characterization of a series of new acetylide-functionalised ligands containing some aromatic, hetero-aromatic and mixed heterocyclic spacer units and their platinum(II) di-ynes are discussed in this chapter. A number of these spacers interact strongly with the platinum-containing fragment and the groups act as luminescent chromophores[1]. The di-ynes can be considered as building blocks for the high molecular weight polymers and valuable information concerning their molecular and electronic properties can be obtained through the studies of these model compounds. There is also considerable interest in the solid-state structures of the polymeric materials because of evidence for inter-chain interactions that influence their opto-electronic properties[2].

# 5.2 Results and discussion

## 5.2.1 Syntheses

The synthesis of the aromatic, hetero-aromatic and mixed heterocyclic spacer units is outlined in **Scheme 5.1**. 4,7-Dibromo-2,1,3-benzothiadiazole **A** was synthesised by reaction of 2,1,3-benzothiadiazole with bromine in refluxing 47% HBr[3]. 2,3-Diphenyl-5,8-dibromoquinoxaline **B** was synthesised by condensation reaction of 3,6-dibromo-1,2-phenylenediamine with benzil in refluxing ethanol[4]. 5,8-Diiodoquinoline **C** was prepared by reacting quinoline with $I_2$ in concentrated $H_2SO_4$ in the presence of $Ag_2SO_4$[5]. 1-(2-Ethylhexyl)oxy-4-methoxybenzene was prepared by reacting 4-methoxyphenol with 2-ethylhexylbromide in sodium methoxide solution[6]. The diiodo derivative **D** was then synthesized by reaction with ICl in acetic acid.

These ligands are considered to be electron deficient systems[1] and may interact strongly with Platinum atom in the di-ynes and poly-ynes to yield unique electronic and optical properties. Active materials for light emitting diodes (LEDs) should combine high emission quantum yields, tunable emission properties and high electron affinity to allow electron injection from electrodes. Varying the conjugation length in the metal-

poly-ynes has the effect of controlling the emission wavelength, while the electron affinity could be increased by incorporating electron deficient groups as the spacers[7]. Spacers which are composed of both donor and acceptor moieties have a significant effect in lowering the band gap. Low band gap materials, either conjugated organic or organometallic, may find uses in semiconductor devices.

In order to investigate the electronic properties of spacer groups that contain both electron deficient and electron rich ring systems, the three mixed thienyl-pyridine ring systems, that contain two (**L1**), three (**L2**) and four (**L3**) linked rings, respectively, have been synthesised by coupling reactions of the boronic acid derivatives of thiophene with dibromopyridine/bipyridine precursors[8] (**Scheme 5.1**). Each of the three compounds **L1**, **L2** and **L3**, was then dibrominated using NBS, in DMF, in the absence of light to afford compounds **E**, **F** and **G**.

In the compounds with three **L2** and four rings **L3**, one or two pyridine rings occupy the central positions with a thiophene ring at each end. In each case pyridine rings would act as electron accepting groups and thiophene rings as electron donating groups. Hence, in **L1** there is donor functionality at one end of the spacer and acceptor functionality at the other. In **L2** and **L3** the acceptor group is central with donor groups at either end of the spacer. All the spacer ligands illustrated in **Figure 5.1** have an adequate range of ligand systems to probe the electronic effects of the different spacer groups in the platinum di-yne complexes.

The protected alkynyl ligand precursors, **1a-7a** were prepared by the palladium(II)/copper(I)-catalysed cross-coupling reactions of trimethylsilylethyne with the **A-G** ligands in $^{i}Pr_2NH$-THF solvent mixture as illustrated in **Scheme 5.2**. The protected alkynes are indefinitely stable towards light and air at ambient temperature and show a strong peak in the IR spectra in the region 2144-2159 $cm^{-1}$ due to the presence of acetylenic moieties.

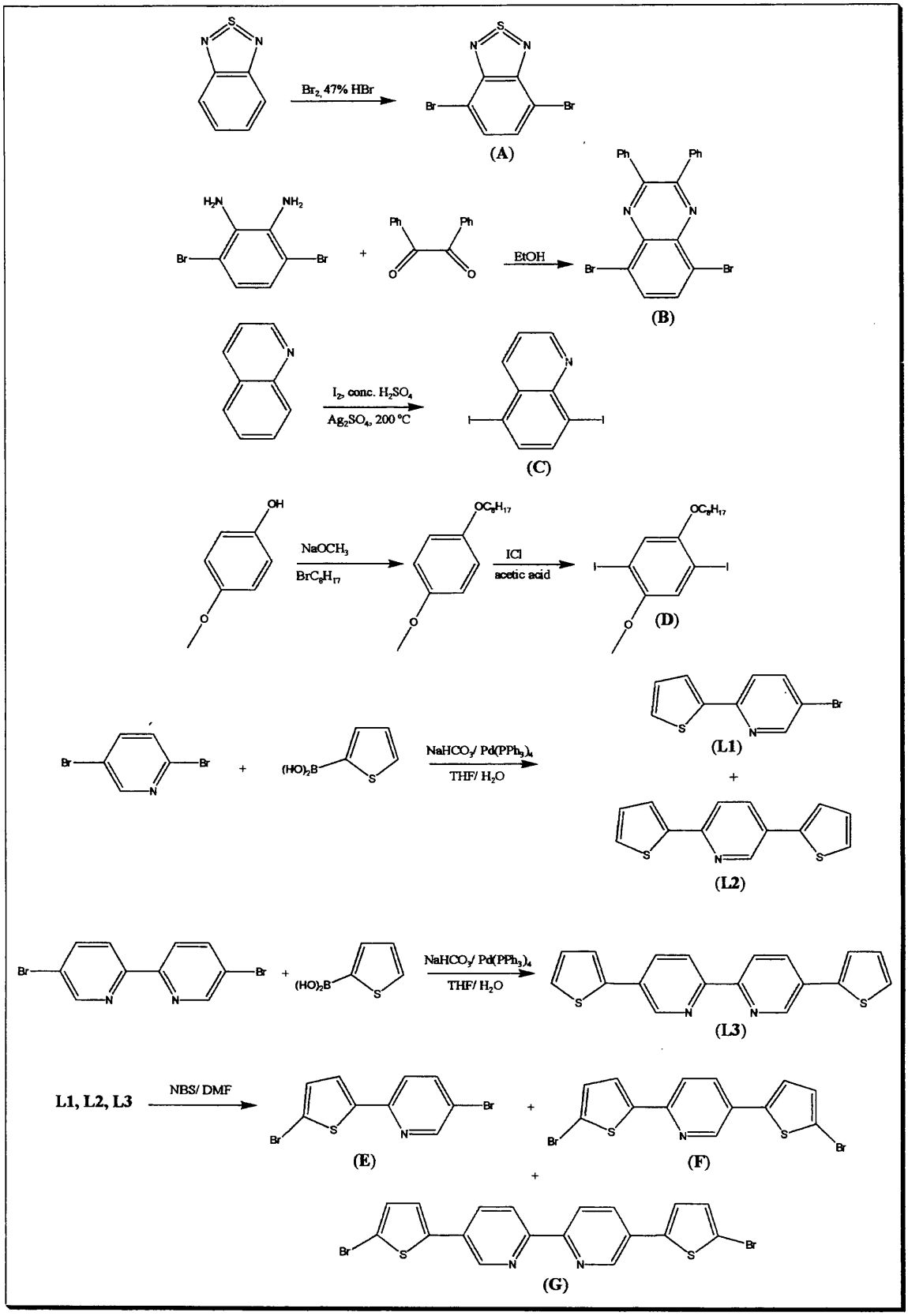


**Scheme 5.1: Synthesis of the dihalo-aromatic, hetero-aromatic and mixed heterocyclic ligands**

Conversion of the protected ligand precursors **1a-7a** into their terminal H derivatives HC≡C-R-C≡CH **1b-7b** was accomplished by smooth removal of the trimethylsilyl protecting groups with dilute aqueous KOH in MeOH/THF (**Scheme 5.2**). The products were purified by silica column chromatography and isolated in 75-90% yield. **Table 5.1** summarizes the synthetic and spectroscopic data of **1a-7a** and **1b-7b**. The diterminal alkynes **2b-4b** are indefinitely stable in air and under light, and could be stored at room temperature while **1b and 5b-7b** are somewhat unstable and long storage times at ambient temperature and under aerobic condition led to the formation of a black tar. All the di-terminal alkynes are significantly less soluble than the trimethylsilyl derivatives, and compound **7b** is only sparingly soluble. The Pt(II) poly-ynes of **1b-4b** ligands have been reported previously[1a]. The Pt(II) poly-yne of **7b** could not be prepared because of the low solubility in organic solvents which made purification difficult, and so it was not possible to obtain an accurate 1:1 reactant ratio needed for the polymerisation reaction.

**Table 5.1: Synthetic and other characterization data for 1a-7a and 1b-7b**

| Compound | Color | Yield (%) | $M^+(gmol^{-1})$ | $\upsilon_{C\equiv C}(cm^{-1})$ ($CH_2Cl_2$) | $\upsilon_{Csp-H}(cm^{-1})$ ($CH_2Cl_2$) |
|---|---|---|---|---|---|
| **1a** | Pale-brown | 75 | 428.6 | 2159 | - |
| **2a** | Off-white | 80 | 321.4 | 2159 | - |
| **3a** | White | 78 | 474.6 | 2159 | - |
| **4a** | Light yellow | 78 | 328.4 | 2159 | - |
| **5a** | Light yellow | 60 | 353.1 | 2144 | - |
| **6a** | Yellow | 67 | 435.1 | 2144 | - |
| **7a** | Bright yellow | 52 | 512.8 | 2144 | - |
| **1b** | Yellow oil | 75 | 284.4 | 2107 | 3299 |
| **2b** | Pale yellow | 85 | 177.2 | 2107 | 3299 |
| **3b** | White | 90 | 330.4 | 2107 | 3299 |
| **4b** | Off-white | 90 | 184.2 | 2107 | 3300 |
| **5b** | Light yellow | 84 | 209.2 | 2102 | 3300 |
| **6b** | Light yellow | 77 | 291.3 | 2101 | 3299 |
| **7b** | Light yellow | ~ 82 | 374 | 2093(Nujol) | 3279(Nujol) |

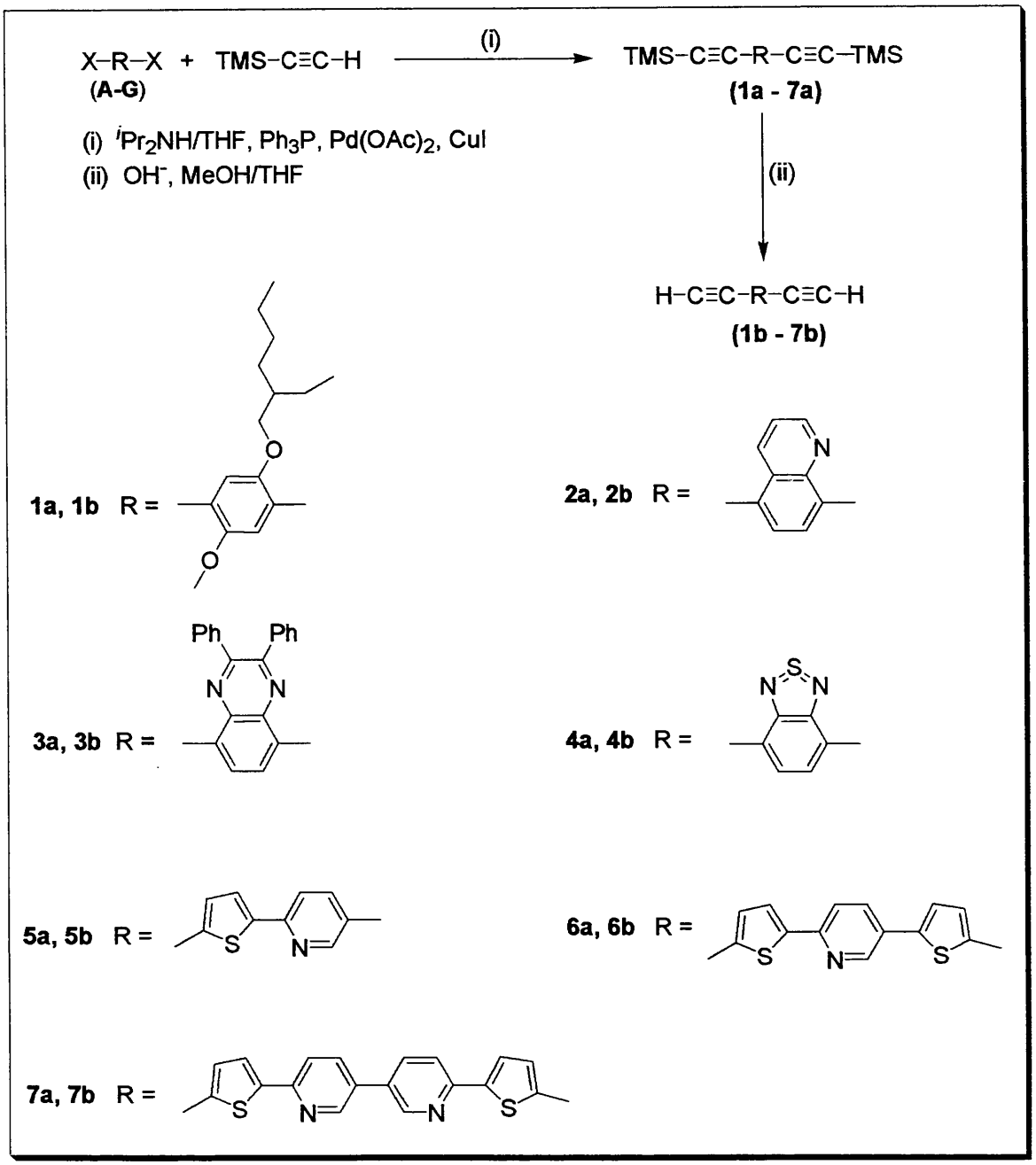


**Scheme 5.2.**

The reaction of **1b-7b** with two equivalents of *trans*-[Pt(Ph)($PEt_3$)$_2$Cl], in $^{i}Pr_2NH/CH_2Cl_2$ solvent mixture, in the presence of CuI, at room temperature, readily affords *trans*-[($Et_3P$)$_2$(Ph)Pt-C≡C-R-C≡C-Pt(Ph)($Et_3P$)$_2$] **1c-7c** in 40-75% yields (**Scheme 5.3** and **Table 5.2**). Purification of the di-ynes was achieved by preparative TLC as well as by silica column chromatography and these complexes exhibited good solubility in common organic solvents.

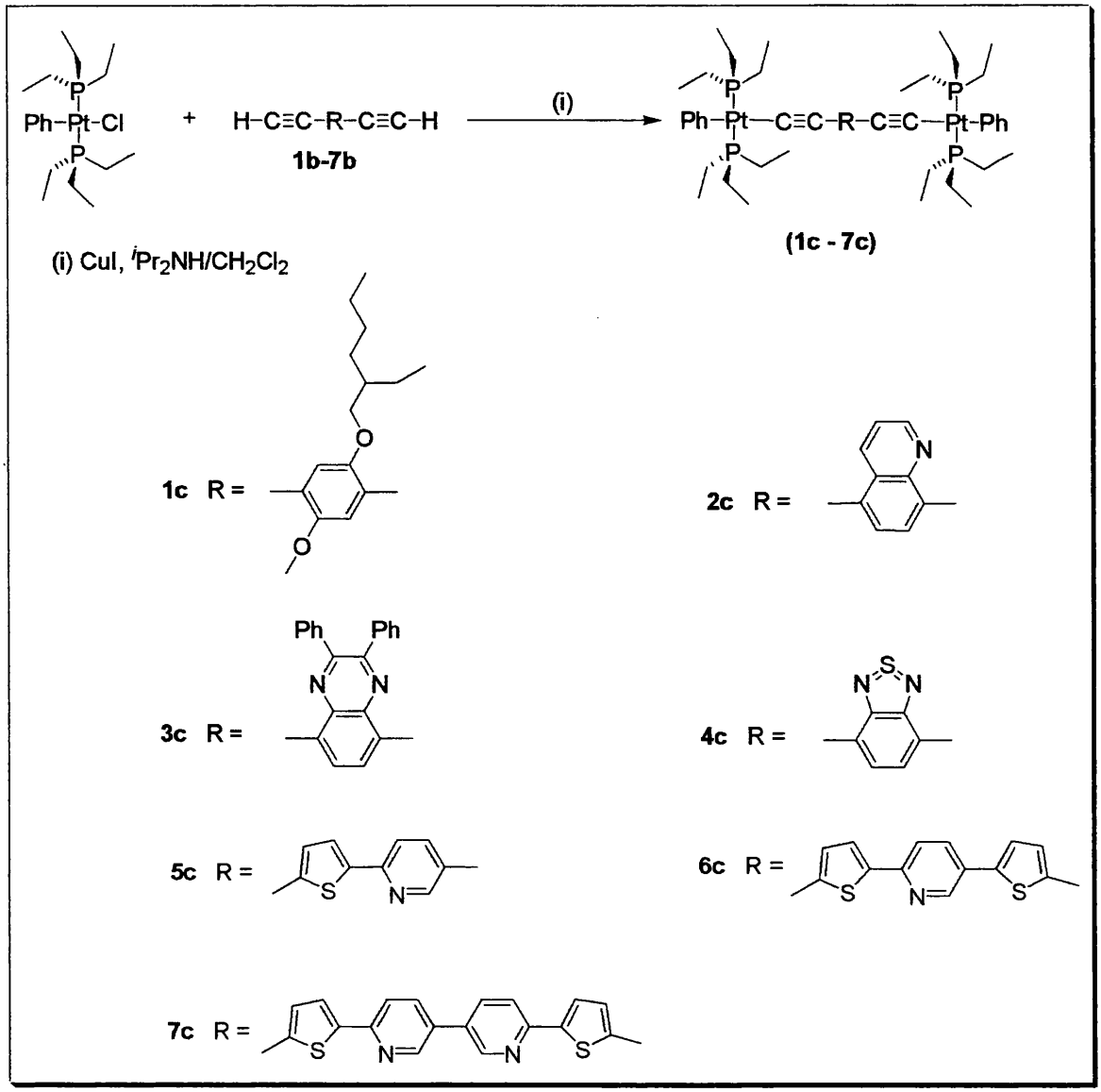


**Scheme 5.3**

Poly-ynes **5P-6P** were also synthesised by the reaction of *trans*-$[PtCl_2(PBu^{n}_3)_2]$ with **5b** and **6b** under similar conditions. The intense yellow products were purified by passing through an alumina column, and obtained as rubbery materials from $CH_2Cl_2$/hexane in yields of 94 and 75%, respectively.

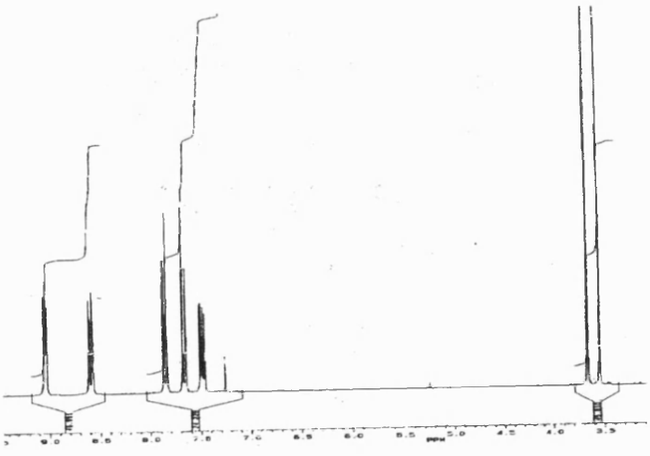

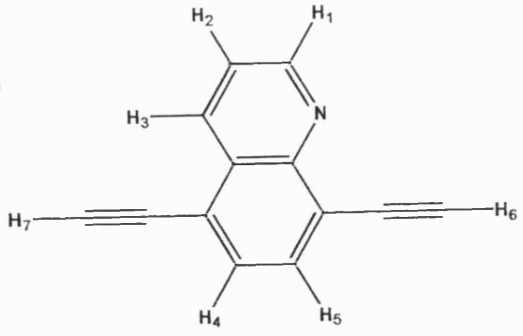


δ: 7.46 ppm (q, 1H, $H_2$)
δ: 7.65 ppm (d, 1H, $H_4$)
δ: 7.84 ppm (d, 1H, $H_5$)
δ: 8.58 ppm (dd, 1H, $H_3$)
δ: 9.03 ppm (dd, 1H, $H_1$)

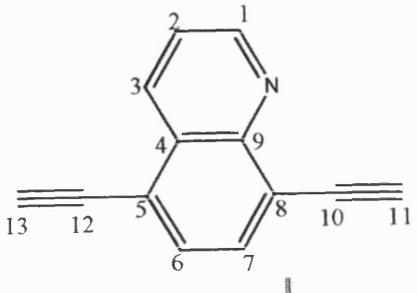


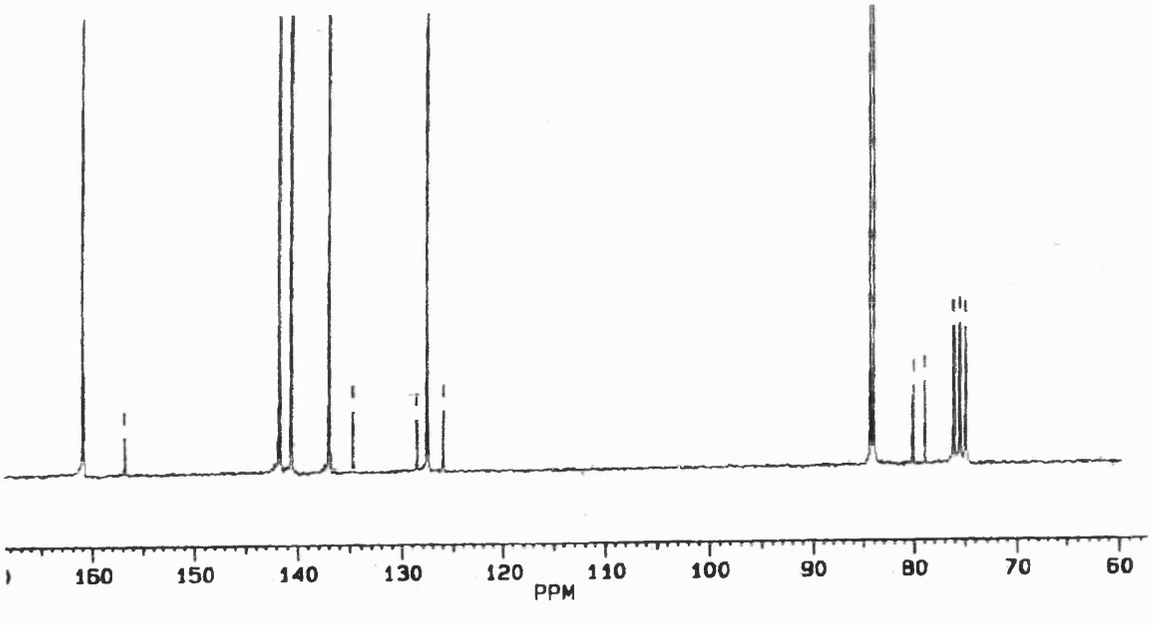


**Figure 5.1: $^{1}H$ and $^{13}C$ NMR spectra of 2b. C1-C9 at 125-165 ppm, while C10-C13 at 77-85 ppm. ~75 ppm is $CHCl_3$ trace in $CDCl_3$ solvent**

The IR spectra of the ligands, di-ynes and poly-ynes exhibited a single strong $\nu_{C\equiv C}$ absorption band consistent with the *trans*-configuration of the acetylenic units. The $^{1}H$ and $^{13}C$ NMR spectra exhibit the expected signals for the individual systems, including resonances for the acetylenic carbons. The example shown in **Figure 5.1** are the $^{1}H$ NMR and $^{13}C$ NMR spectra of **2b**. The aromatic region of the $^{1}H$ NMR spectrum reveals five peaks characteristic for the five different aromatic protons in the quinoline ring, while the acetylenic protons appeared at 3.55 and 3.65 ppm. This reflects the asymmetry of the compound due to the nitrogen atom of the quinoline ring. In the $^{13}C$ NMR spectrum, nine definite peaks are present in the aromatic region for the nine different carbons (**C1-C9**) of quinoline ring between 125-165 ppm. The four acetylenic carbons (**C10-C13**) appeared at 79.0, 80.0, 84.4 and 84.7 ppm.

**Table 5.2: Synthetic and other characterization data for 1c-7c and 1P-2P**

| Compoud | Color | Yield (%) | $M^{+}/M_{w}$ *(gmol$^{-1}$)* | $\upsilon_{C\equiv C}(cm^{-1})$ ($CH_2Cl_2$) | $^{31}P\{^{1}H\}$NMR (ppm) |
|---|---|---|---|---|---|
| **1c** | Light yellow | 75 | 1299.4 | 2096 | −131.25 ($^{1}J_{Pt\text{-}P}$ = 2620 Hz) |
| **2c** | Brownish-yellow | 65 | 1192.2 | 2095 | −131.17 ($^{1}J_{Pt\text{-}P}$ = 2618 Hz) |
| **3c** | Light yellow | 56 | 1321.3 | 2095 | −131.00 ($^{1}J_{Pt\text{-}P}$ = 2621 Hz) |
| **4c** | Bright yellow | 56 | 1199.2 | 2095 | −131.30 ($^{1}J_{Pt\text{-}P}$ = 2619 Hz) |
| **5c** | Bright yellow | 40 | 1224.2 | 2095 | −129.98 ($^{1}J_{Pt\text{-}P}$ = 1311 Hz) |
| **6c** | Bright yellow | 65 | 1306.3 | 2094 | −129.46 ($^{1}J_{Pt\text{-}P}$ = 1313 Hz) |
| **7c** | Bright yellow | 65 | 1383.4 | 2094 | −129.78. ($^{1}J_{Pt\text{-}P}$ = 1312 Hz) |
| **1P** | Deep yellow | 94 | 85,420 | 2095 | −136.48 ($^{1}J_{Pt\text{-}P}$ = 1166 Hz) |
| **2P** | Deep yellow | 75 | 141,467 | 2095 | −136.02 ($^{1}J_{Pt\text{-}P}$ = 1163 Hz) |

## 5.2.2 Crystal structure determinations

The crystal structures of **2c-4c** have been determined by single-crystal X-ray diffraction. Features that can be obtained from the structures are a confirmation of the linearity of the di-yne backbone, a linearity that should be retained in the polymers as well, and the relative

orientations of the square planar platinum(II) centres relative to those of the aromatic spacer groups, The molecular structure of **2c** is shown in **Figure 5.2** while selected bond parameters are listed in **Table 5.3**. The molecular structure is closely related to those reported for the diplatinum thiophenediyl and bithiophenediyl complexes[9] with the *trans*-arrangement of the two 'Pt($PEt_3$)$_2$' groups separated by the aromatic spacer group. The coordination geometry about Pt(1) and Pt(2) is square planar with *cis*-L-Pt-L angles in the range 86.53(14)-91.66(13)°. The two terminal phenyl rings are essentially perpendicular to the planes of the two square planar platinum(II) centres; the dihedral angle between the ring C(101)-C(106) and the plane defined by Pt(1), P(11), P(12), C(101), C(12) is 86.55° and that between the ring C(201)-C(206) and Pt(2), P(21), P(22), C(201), C(42) is 89.04°. The central quinoline group is effectively planar, with a dihedral angle of only 2.16° between the two six-membered rings. The two alkynyl groups are linear with average C-C≡C angles of 176.05° and average Pt-C≡C angles of 176.7° confirming that the whole molecule is linear. The dihedral angle between the C(1), C(2), C(3), C(4), C(5), C(10) ring and the Pt(1) coordination plane {Pt(1), P(11), P(12), C(101), C(12)} is 60.47° and that between the same central ring and the Pt(2) coordination plane { Pt(2), P(21), P(22), C(201), C(42)} is 63.83°. The dihedral angle between the two platinum coordination planes is 56.90° which compares with previous results.

**Table 5.3. Selected bond lengths (Å) and angles (°) for 2c**

| | | | |
|---|---|---|---|
| Pt(1)-P(11) | 2.2868(12) | Pt(2)-P(21) | 2.2936(12) |
| Pt(1)-P(12) | 2.2856(12) | Pt(2)-P(22) | 2.2965(14) |
| Pt(1)-C(12) | 2.007(5) | Pt(2)-C(42) | 2.019(5) |
| Pt(1)-C(101) | 2.061(4) | Pt(2)-C(201) | 2.061(4) |
| C(11)-C(12) | 1.213(7) | C(41)-C(42) | 1.209(7) |
| C(1)-C(11) | 1.435(7) | C(4)-C(41) | 1.437(6) |
| C(1)-C(2) | 1.374(9) | C(3)-C(4) | 1.383(8) |
| C(1)-C(10) | 1.430(9) | C(4)-C(5) | 1.422(8) |
| C(2)-C(3) | 1.421(7) | C(5)-C(10) | 1.417(6) |
| | | | |
| P(12)-Pt(1)-P(11) | 174.83(5) | P(22)-Pt(2)-P(21) | 175.86(6) |
| C(12)-Pt(1)-P(11) | 90.18(14) | C(42)-Pt(2)-P(21) | 87.41(14) |
| C(101)-Pt(1)-P(11) | 91.66(13) | C(201)-Pt(2)-P(21) | 91.03(12) |
| C(12)-Pt(1)-P(12) | 86.53(14) | C(42)-Pt(2)-P(22) | 87.41(14) |
| C(101)-Pt(1)-P(12) | 91.52(13) | C(201)-Pt(2)-P(22) | 87.76(12) |
| C(12)-Pt(1)-C(101) | 177.5(2) | C(42)-Pt(2)-C(201) | 178.22(18) |
| Pt(1)-C(12)-C(11) | 175.4(5) | Pt(2)-C(42)-C(41) | 178.0(5) |
| C(12)-C(11)-C(1) | 175.3(7) | C(42)-C(41)-C(4) | 176.8(6) |

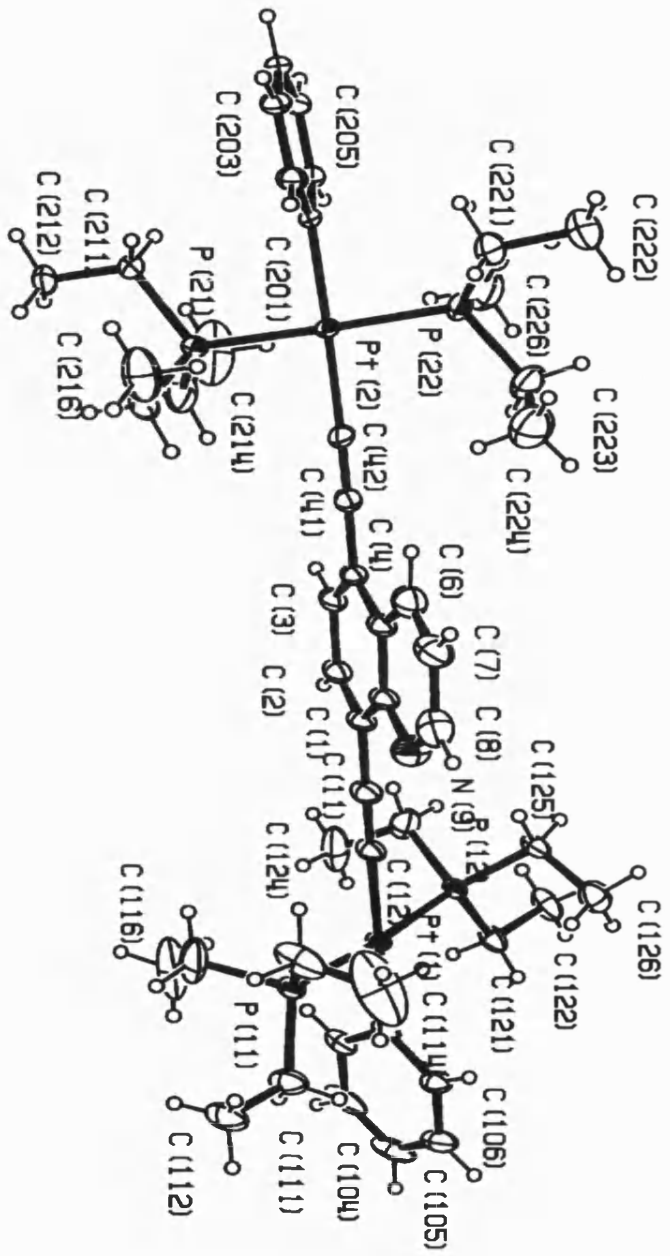


**Figure 5.2: The molecular structure of 2c showing the atom numbering scheme.**

The molecular structure of **3c** is illustrated in **Figure 5.3**, and selected bond parameters are listed in **Table 5.4**. As with **2c** the coordination geometry around the two independent platinum(II) centres is square planar, with *cis*-L-Pt-L angles in the range 86.36(16)-91.57(16)°. The geometry along the backbone is again linear with average Pt-C≡C and C≡C-C angles of 174.5° and 173.6°, respectively. The two terminal arene rings make dihedral angles of 81.47° {for C(1)-C(6) and Pt(1)} and 88.41° {for C(31)-C(36) and Pt(2)} with the two platinum square planes. The quinoxaline group is essentially planar, with a dihedral angle of only 5.79° between the C(9)-C(14) and the N(1)-C(15) rings. The two substituent arene rings make angles of 59.95° {C(17)-C(22)} and 27.42° {C(23)-C(28)} with the N(1)-C(15) ring, and an angle of 64.74° with each other. The dihedral angles between the central C(9)-C(14) ring and the two platinum square planes, that are 32.51° {with Pt(1), P(1), P(2), C(4), C(7)} and 36.82° {with Pt(2), P(3), P(4), C(30), C(31)}. These values are *ca.* 30° lower than the dihedral angles observed in **2c**. The dihedral angle between the two plantinum square planes is only 25.34°, showing that the whole of the central unit, between the two platinum atoms, is significantly closer to planarity.

The average Pt-P, Pt-C(alkynyl) and Pt-C(arene) distances in **3c** at 2.289 Å, 2.018 Å and 2.068 Å, respectively, are similar to those observed in **2c**. The average C≡C bond length of 1.198 Å is also within the expected range.

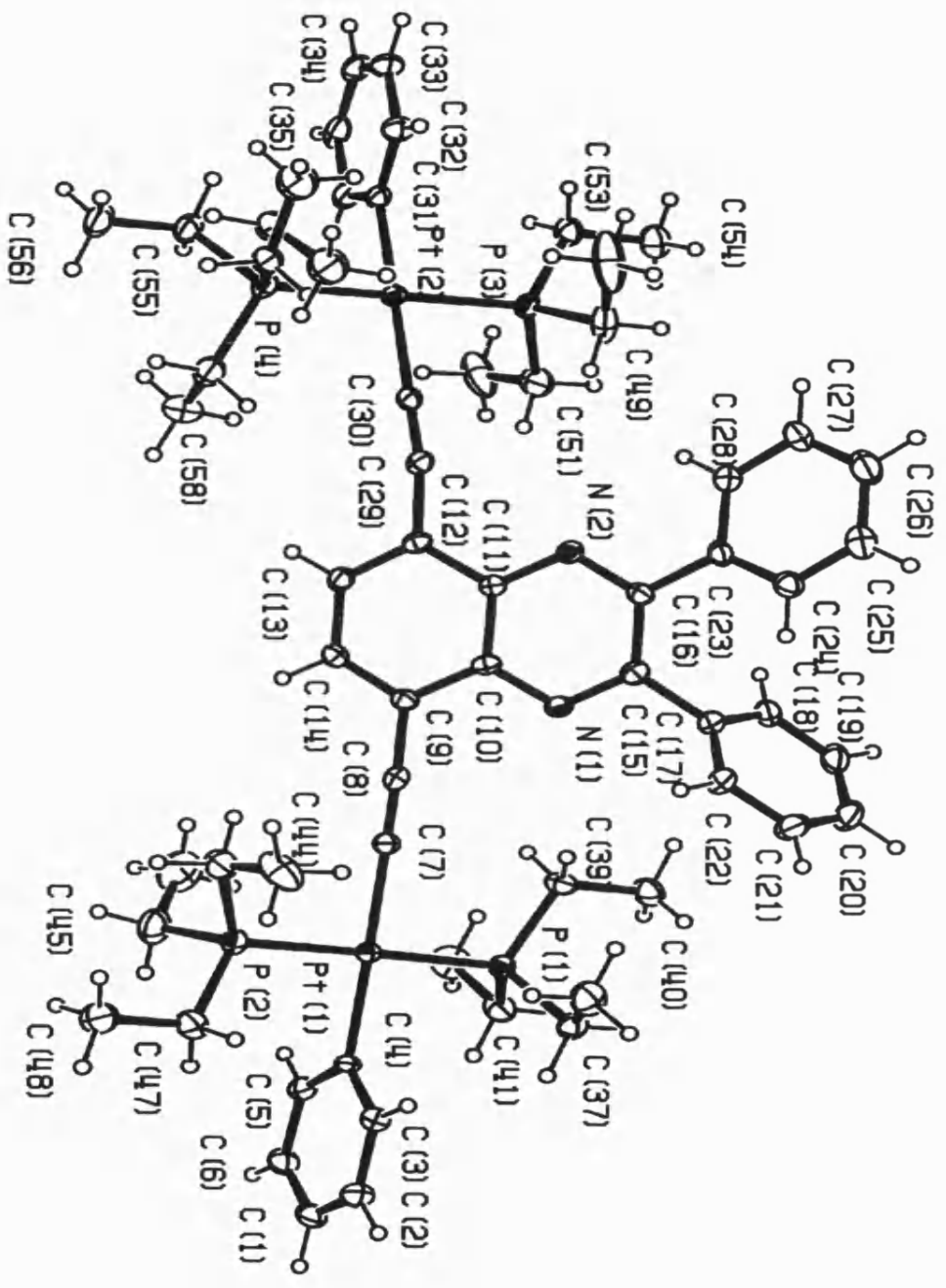


**Figure 5.3: The molecular structure of 3c showing the atom numbering scheme.**

**Table 5.4. Selected bond lengths (Å) and angles (°) for 3c**

| | | | |
|---|---|---|---|
| Pt(1)-P(1) | 2.2873(15) | Pt(2)-P(3) | 2.2874(15) |
| Pt(1)-P(2) | 2.2901(15) | Pt(2)-P(4) | 2.2899(15) |
| Pt(1)-C(7) | 2.017(6) | Pt(2)-C(30) | 2.019(5) |
| Pt(1)-C(4) | 2.075(5) | Pt(2)-C(31) | 2.060(5) |
| C(7)-C(8) | 1.202(7) | C(29)-C(30) | 1.194(7) |
| C(8)-C(9) | 1.443(7) | C(12)-C(29) | 1.453(7) |
| C(9)-C(14) | 1.372(8) | C(12)-C(13) | 1.387(8) |
| C(9)-C(10) | 1.425(8) | C(12)-C(11) | 1.436(7) |
| C(13)-C(14) | 1.403(8) | C(10)-C(11) | 1.435(7) |
| | | | |
| P(1)-Pt(1)-P(2) | 178.46(5) | P(3)-Pt(2)-P(4) | 175.01(6) |
| C(7)-Pt(1)-P(1) | 90.61(16) | C(30)-Pt(2)-P(3) | 86.36(16) |
| C(4)-Pt(1)-P(1) | 89.38(15) | C(31)-Pt(2)-P(3) | 91.41(16) |
| C(7)-Pt(1)-P(2) | 90.65(16) | C(30)-Pt(2)-P(4) | 91.57(16) |
| C(4)-Pt(1)-P(2) | 89.41(15) | C(31)-Pt(2)-P(4) | 91.09(16) |
| C(4)-Pt(1)-C(7) | 177.2(2) | C(30)-Pt(2)-C(31) | 174.0(18) |
| Pt(1)-C(7)-C(8) | 176.1(6) | Pt(2)-C(30)-C(29) | 172.6(5) |
| C(7)-C(8)-C(9) | 177.7(6) | C(30)-C(29)-C(12) | 169.4(7) |

The molecular structure of **4c** is illustrated in **Figure 5.4**, and selected bond parameters are listed in Table **5.5**. Again, the structural diagram confirms the linear nature of the molecular backbone, with average Pt-C≡C and C≡C-C angles of 174.7° and 175.9°, respectively, and the square planar geometry at each of the two platinum(II) centres, with *cis*-L-Pt-L angles in the range 87.7(3) – 93.0(3)°. In this structure the two terminal arene rings make dihedral angles of 84.02° and 86.63° with adjacent platinum square planes, these values lying within the range observed for **2c** and **3c**, 81.47 – 89.04°. The benzothiadiazole ligand is, as expected, planar, with a dihedral angle of only 1.78° between the six- and five-membered rings. The dihedral angles between the central arene ring, C(9)-C(14), and the two platinum square planes are much closer in value to those observed for **2c** than for **3c**, with angles of 60.26° (with the Pt(1) plane) and 69.18° (with the Pt(2) plane). The dihedral angle between the two platinum square planes is only 23.36°. The average Pt-P, Pt-C(alkynyl) and Pt-C(arene) distances in **4c** at 2.292 Å, 2.018 Å and 2.075 Å, respectively, are similar to those observed in **2c** and **3c**, and the average C≡C bond length of 1.209 Å is also not significantly different.

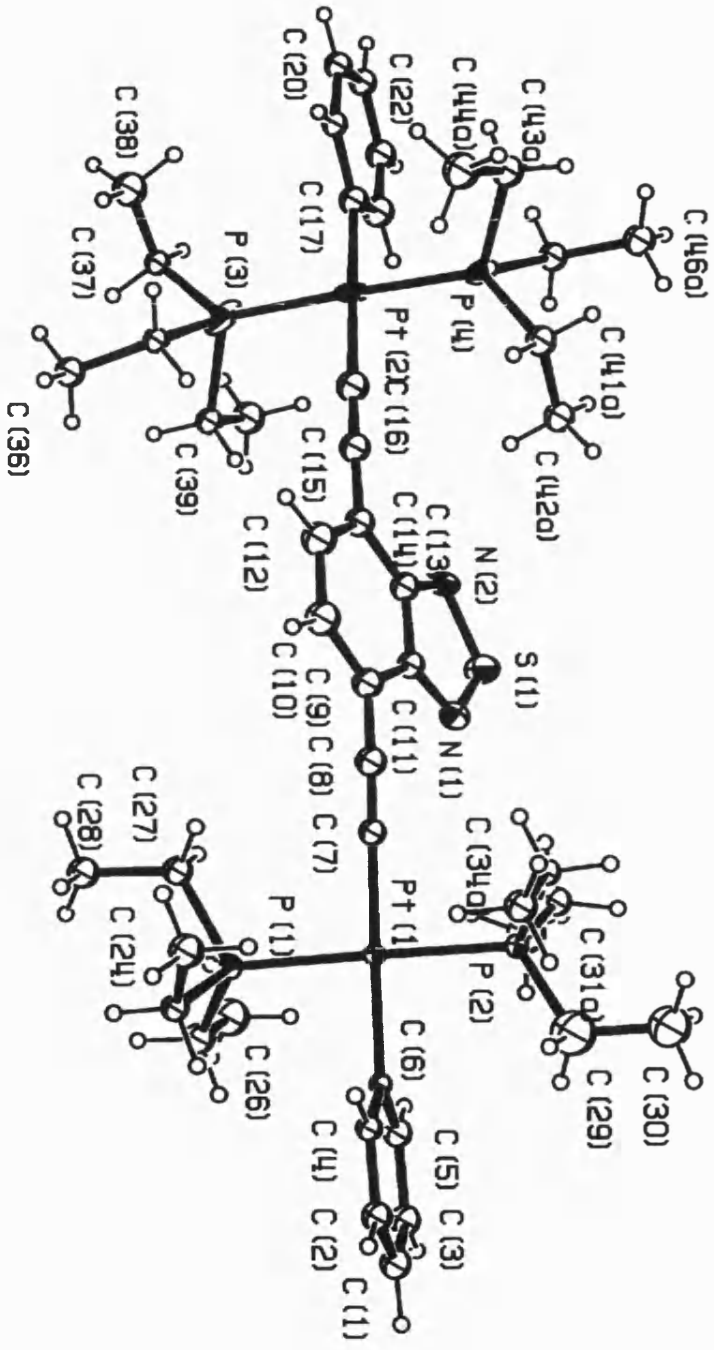


**Figure 5.4: The molecular structure of 4c showing the atom numbering scheme.**

**Table 5.5. Selected bond lengths (Å) and angles (°) for 4c**

| | | | |
|---|---|---|---|
| Pt(1)-P(1) | 2.287(2) | Pt(2)-P(3) | 2.295(4) |
| Pt(1)-P(2) | 2.294(2) | Pt(2)-P(4) | 2.292(3) |
| Pt(1)-C(7) | 2.023(9) | Pt(2)-C(16) | 2.012(11) |
| Pt(1)-C(6) | 2.076(8) | Pt(2)-C(17) | 2.073(10) |
| C(7)-C(8) | 1.208(13) | C(15)-C(16) | 1.209(14) |
| C(8)-C(9) | 1.412(14) | C(14)-C(15) | 1.422(14) |
| C(9)-C(10) | 1.387(14) | C(12)-C(14) | 1.362(14) |
| C(9)-C(11) | 1.425(13) | C(13)-C(14) | 1.433(13) |
| C(10)-C(12) | 1.443(15) | C(11)-C(13) | 1.460(13) |
| N(1)-C(11) | 1.332(12) | N(2)-C(13) | 1.321(12) |
| N(1)-S(1) | 1.607(9) | N(2)-S(1) | 1.619(8) |
| | | | |
| P(1)-Pt(1)-P(2) | 178.38(8) | P(3)-Pt(2)-P(4) | 177.20(13) |
| C(7)-Pt(1)-P(1) | 93.0(3) | C(16)-Pt(2)-P(3) | 87.7(3) |
| C(6)-Pt(1)-P(1) | 88.3(2) | C(17)-Pt(2)-P(3) | 92.3(3) |
| C(7)-Pt(1)-P(2) | 88.1(3) | C(16)-Pt(2)-P(4) | 89.5(3) |
| C(6)-Pt(1)-P(2) | 90.6(2) | C(17)-Pt(2)-P(4) | 90.5(3) |
| C(6)-Pt(1)-C(7) | 176.0(3) | C(16)-Pt(2)-C(17) | 178.7(4) |
| Pt(1)-C(7)-C(8) | 174.9(8) | Pt(2)-C(16)-C(15) | 174.5(9) |
| C(7)-C(8)-C(9) | 174.2(11) | C(16)-C(15)-C(14) | 177.5(11) |

**Table 5.6: Crystallographic data for compounds 2c, 3c and 4c**

| Compound | 2c | 3c | 4c |
|---|---|---|---|
| Molecular formula | $C_{49.5}H_{76}ClNP_4Pt_2$ | $C_{60}H_{82}N_2P_4Pt_2$ | $C_{46}H_{72}N_2P_4Pt_2S$ |
| $M$ | 1234.62 | 1345.34 | 1199.18 |
| Crystal system | Triclinic | Monoclinic | Monoclinic |
| $a$ /Å | 9.1794(1) | 9.3306(1) | 9.2450(1) |
| $b$ /Å | 16.7290(2) | 35.3016(4) | 38.0140(4) |
| $c$ /Å | 18.8959(2) | 18.0831(2) | 14.6550(2) |
| α/ ° | 112.396(1) | 90 | 90 |
| β/ ° | 95.200(1) | 95.793(1) | 105.065(10) |
| γ/ ° | 94.282(1) | 90 | 90 |
| $U$ /Å$^3$ | 2652.93(5) | 5925.88(11) | 4973.33(10) |
| Space group | *P-1 (No. 2)* | $P2_1/c$ | $P2_1/c$ |
| $Z$ | 2 | 4 | 4 |
| $D_c$/Mg m$^3$ | 1.546 | 1.508 | 1.602 |
| μ/mm$^{-1}$ | 5.470 | 4.861 | 5.822 |
| Data collection range/° | $3.53 < \theta < 30.05$ | $2.93 < \theta < 27.46$ | $3.52 < \theta < 27.49$ |
| Reflections measured | 54771 | 30974 | 28015 |
| Independent reflections | 15461 ($R_{int}$ = 0.048) | 12537 ($R_{int}$ = 0.059) | 10244 ($R_{int}$ = 0.070) |
| Parameters, restraints | 534, 0 | 611, 0 | 322, 0 |
| $wR$ 2(all data)§ | 0.1013 | 0.0912 | 0.1383 |
| $R1[I > 2\sigma(I)]$§ | 0.0387 | 0.0450 | 0.0574 |

‡ Data in common: Graphite-monochromated Mo-$K\alpha$ radiation, $\lambda = 0.71073$Å, $T$ = 150(2) K.

§ $R1 = \Sigma\left||F_o| - |F_c|\right| / \Sigma|F_o|$, $wR2 = \left[\Sigma w(F_o^2 - F_c^2)^2 / \Sigma wF_o^4\right]^{\frac{1}{2}}$

## 5.2.3 Optical spectroscopy

The results of optical spectroscopy have been carried out by the group of Professor Sir Richard R. Friend and Dr. Anna Kohler from the Cavendish laboratory, University of Cambridge. Their effort in measuring and providing us with these results is gratefully acknowledged. Figure **5.5** shows the absorption spectra of ligands **1b-4b**, measured in solution together with the absorption spectra of films of the corresponding di-ynes **1c-4c** for comparison. There is similarity in the spectral shape of the first absorption band for the ligands and the di-ynes, suggesting that in the di-ynes this band is mainly due to the $\pi$-$\pi^*$ transition on the ligand, possibly with some admixture of metal d orbitals. There is only a small shift of 0.15 eV between the onset of absorption in the ligand and the di-yne for **1c**, but a large shift of 0.8 eV for complexes **2c-4c**. The large shift observed indicates a substantial donor-acceptor interaction between the platinum(II) centres and the conjugated spacer group.

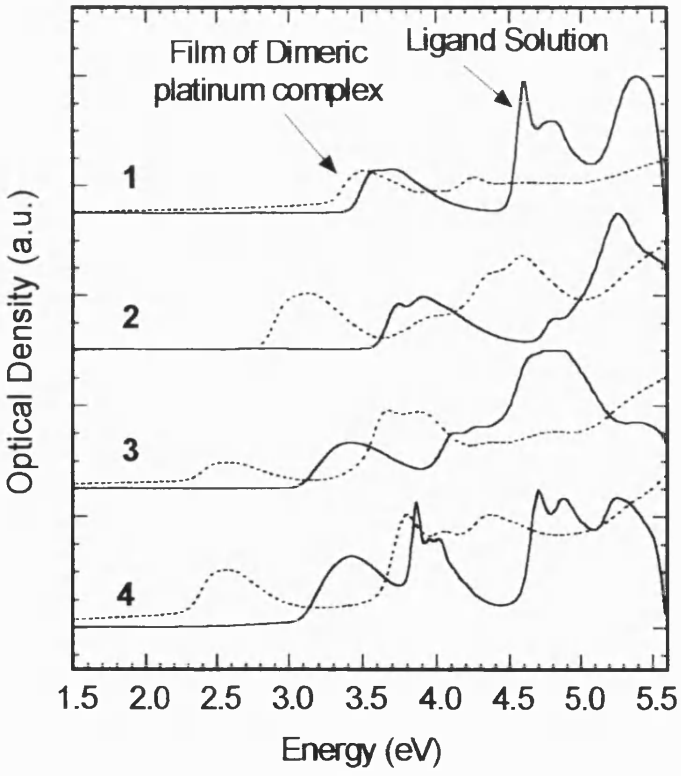


**Figure 5.5**

The solution electronic spectra of the three mixed thienyl-pyridine organic ligands **5a-7a, 5b-7b** as well as **5c-7c** and **5P-6P** were also investigated. All show a strong, relatively low-energy $\pi$-$\pi^*$ transition. There is a shift towards longer wavelength for **5a-7a** when compared to **5b-7b** and there is also a shift to longer wavelength in going from the two-ring compounds to the three and four-ring compounds. These shifts presumably reflect a higher degree of conjugation as the number of rings in the central spacer increases and the energy gap between the HOMO and LUMO levels is reduced. **5c-7c** and **5P-6P** also exhibited absorption spectra that are dominated by $\pi$-$\pi^*$ transitions, and show further red-shifts, such that for ligand **5b**, the absorption ($\lambda_{max}$) occurs at 340 nm, that of **5c** at 393 nm, and that of **5P** at 430 nm, and that for **6b** at 369, **6c** at 420 and **6P** at 453 nm. The observed red shift is consistent with the platinum fragments acting as net electron donors and spacer groups as electron acceptors;[1,7] the results are summarized in **Table 5.7.**

The photoluminescence (PL) spectra of **1c-4c**, measured at room temperature and 10 K, are shown in **Figure 5.6** along with their absorption spectra. All of the spectra (with the exception of that of **4c**) show two characteristic emissions. The higher energy emission is due to the same singlet excited state as the first band in the absorption spectra, and is denoted by $S_1$. The lower energy band is attributed to that of a triplet excited state $T_1$. Both the singlet and triplet emissions can be seen to decrease in energy, along with the absorption. The decreasing intensity of emission from the $T_1$ state along the series has been explained in terms of the energy gap law for non-radiative decay, whereby the non-radiative decay rate increases exponentially with decreasing $T_1$-$S_0$ energy.[10]

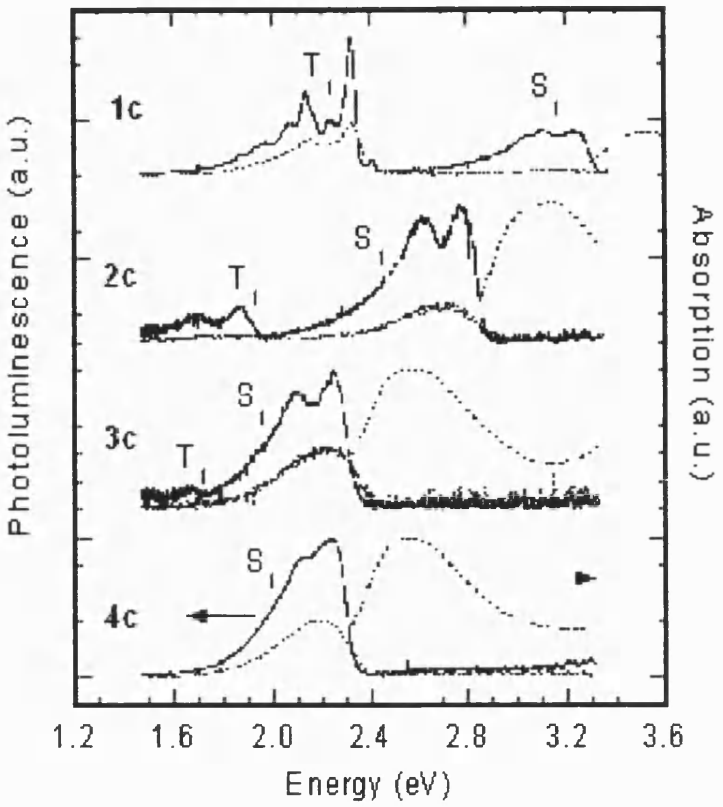


**Figure 5.6.**

The electronic absorption spectra of **5P** and **6P** were also investigated in the solid state and the results are shown in **Figure 5.7,** where **5P** is represented by dotted line and **6P** by solid line. Both spectra show absorption bands in the visible region. A band is observed at 430 nm for **5P** and also for **6P** which possesses an additional higher-energy band centred at *ca* 405 nm. The optical gaps are at 2.67 eV for **5P** and 2.55 eV for **6P**. This compares to the corresponding polymers containing a bithiophene or terthiophene spacer which have optical gaps of 2.55 eV and 2.40 eV.[11] This represents a blue shift of 0.12 and 0.15 eV, respectively.

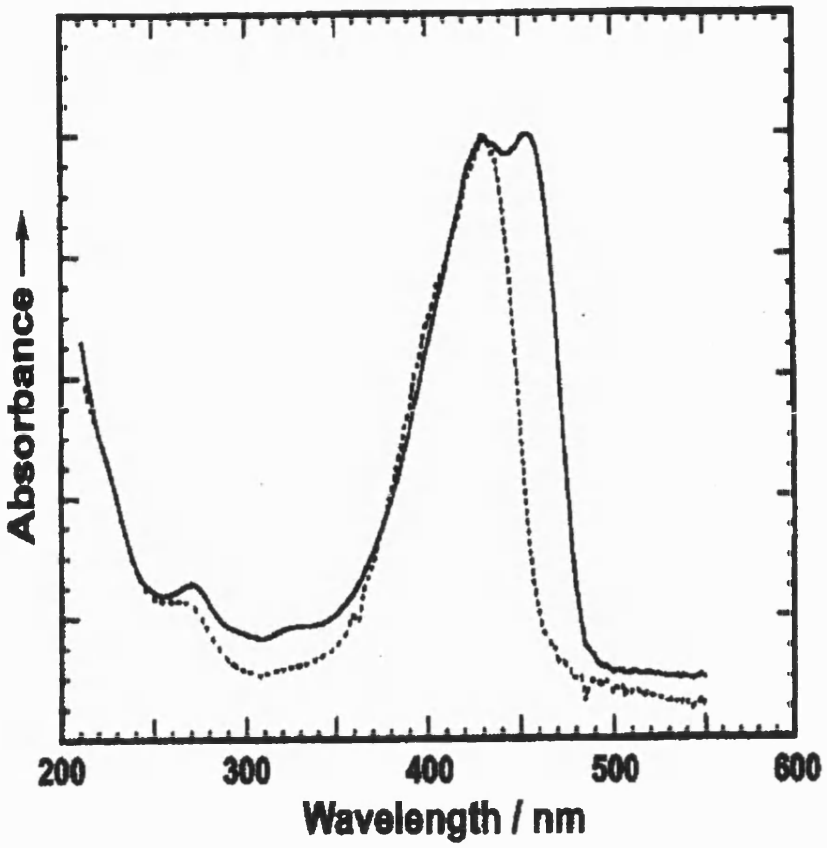


**Figure 5.7**

The solid-state photoluminescence spectra of **5P-6P** as spun films have been recorded at 10 K and room temperature and are illustrated in **Figure 5.8a** for **5P** and **Figure 5.8b** for **6P** and the results are summarized in **Table 5.7**. The low temperature

spectra show two emission bands, one from about 450 to 600 nm, and one from about 630 or 670 to beyond 850 nm. The higher energy band is attributed to emission from the singlet excited state, $S_1$, (fluorescence) while the lower energy band is attributed to emission from the triplet excited state, $T_1$, (phosphorescence) The energetic separation of the peak for the triplet state at 646 nm (1.92 eV) for **5P** and at 691 nm (1.79 eV) for **6P** from the peak for the singlet excited state at 460 nm (2.70 eV) for **5P** and at 485 nm (2.56 eV) for **6P** is 0.77 and 0.78 eV, respectively. These gaps fall in the same range as the values obtained for the $S_1$-$T_1$ energy gaps in related polymeric materials (**See previous chapters**).

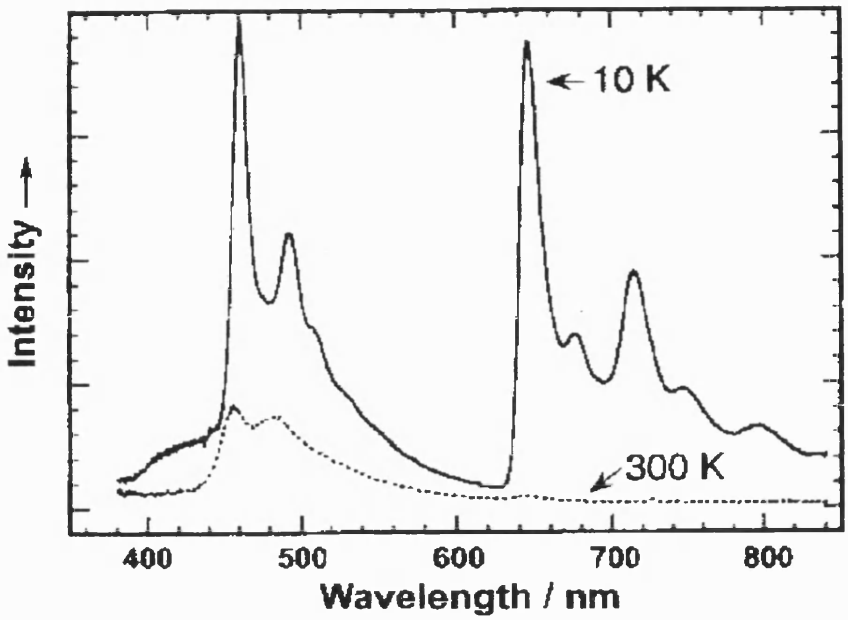


Figure 5.8a

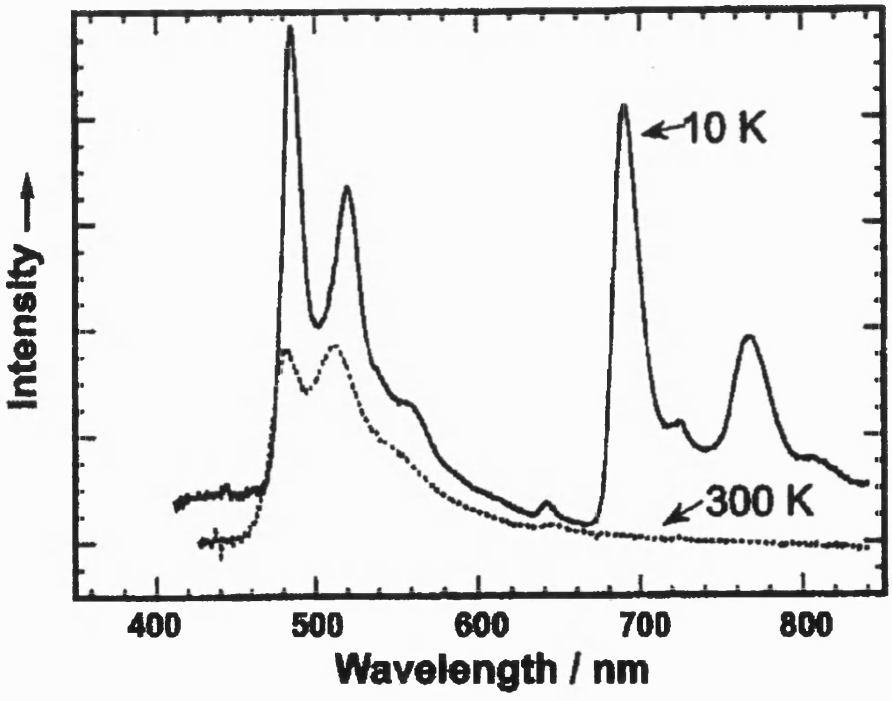


Figure 5.8b

The energies of **5P-6P** are blue-shifted compared to the corresponding bi- and tri-thiophene-containing systems[11]. If there was any charge-transfer-like electronic interaction between the electron-rich thiophene ring and the electron-poor pyridine ring in this system, this should result in increased conjugation and thus lead to a red-shift with respect to an analogous system consisting only of thiophene rings. The observed blue-shift indicates the absence of such a charge-transfer interaction. The exchange of a thiophene ring by a pyridine ring seems to reduce any donor-acceptor interaction between the metal and the ligand. This can be rationalised by considering that the pyridine ring might withdraw electron density from the polymer backbone towards the lone pair. This reduction in electron density compared to a purely thiophene-containing system manifests itself in reduced conjugation and thus results in higher optical gaps.

**Table 5.7: Optical data of the di-ynes and poly-ynes**

| Compound | $S_0 \rightarrow S_1$ (eV) (Onset) | $\lambda_{max}$ (eV) | $S_1 \rightarrow S_0$(eV) (Peak) | $T_1 \rightarrow S_0$(eV) (Peak) | $T_1$-$S_1$ (eV) Gap |
|---|---|---|---|---|---|
| **1c** | 3.25 | 3.50 | 3.20 | 2.35 | 0.85 |
| **2c** | 2.80 | 3.10 | 2.80 | 1.85 | 0.95 |
| **3c** | 2.30 | 2.60 | 2.25 | 1.65 | 0.60 |
| **4c** | 2.30 | 2.60 | 2.25 | - | |
| **5c** | - | 3.16 | - | - | - |
| **6c** | - | 2.95 | - | - | - |
| **7c** | - | 3.01 | - | - | - |
| **1P** | 2.67 | 2.88 | 2.70 | 1.92 | 0.78 |
| **2P** | 2.55 | 2.74 | 2.56 | 1.79 | 0.77 |

# 5.3 Conclusion

The series of **1a-7a**, **1b-7b** ligands as well as di-ynes **1c-7c** and poly-ynes **5P-6P** have been successfully prepared and characterised spectroscopically. The crystal structures of **2c-4c** have been determined. The structures confirm the linear nature of the molecular backbone, and establish that there is a variation in dihedral angle between the platinum(II) square planes and the central aromatic rings of up to 30° depending on the nature of the central ring system. The absorption spectra of the complexes **2c-4c** show substantial donor-acceptor

interaction between the platinum and the conjugated ligands while the mixed thienyl-pyridyl systems showed a reduction in the donor-acceptor interaction between the metal and the ligand as compared with bithiophene and terthiophene Pt-containing poly-ynes[11]. The photoluminescence spectra of **1c-3c** show characteristic singlet ($S_1$) and triplet ($T_1$) emissions. Both the singlet and triplet emissions as well as the absorption decrease in energy with increasing electron withdrawing character of the spacer groups along the series **1c-4c**. The photoluminscence spectra of **1P** and **2P** systems exhibit both triplet (phosphorescence) and singlet (fluorescence) emissions. In both cases the triplet emission is *ca* 0.77 eV below the singlet emission, a feature that has also been observed in the spectra of the related systems.

# 5.4 General conclusion for chapters 2-5.

Extensive studies have been carried out in the last few decades in order to establish the synthetic strategies for obtaining metal-containing conjugated polymers and also in order to explore the origins of electronic transitions that occur upon electrical or optical excitations. In previous work, Pt(II) poly-ynes of the general formula, *trans*-[-Pt($P^nBu_3$)$_2$-C≡C-R-C≡C-]$_n$ (R = aromatic or heteroaromatic spacer group) have been synthesized and characterized with various R groups by the dehydrohalogenation polycondensation reactions of *trans*-[($P^nBu_3$)$_2$$PtCl_2$] with the diterminal alkynes.

In this thesis, the synthetic work has been extended to include a wider range of R groups, including aromatic fused rings spacers, derivatised benzene spacers, oligopyridyl spacers, fused thiophenes spacers and a number of heterocyclic and mixed hererocylic spacers all of which have been incorporated in the backbone of these polymers. The ligand precursors and the model compounds e.g., the Pt(II) di-ynes have all been studied and characterized spectroscopically and crystallographically and were useful in comparing their properties with those of the polymers, which helped to establish the structure-property relationship in these type of materials.

In general, IR spectroscopy was an effective tool for monitoring the reactions and to define the protected, deprotected and also the di-ynes and poly-ynes due to the

characteristic stretching frequencies of the triple bonds. X-ray crystallography studies of some of the ligand precursors and of the Pt(II) di-ynes show the expected linear geometry, and provided the 3-dimensional structure with the associated bond lengths and angles.

Optical spectroscopy studies have shown that some of these materials possess significant increased conjugation upon polymerization than others, and this can be reflected by the decrease of the band gap when moving from the ligand to the di-yne to the poly-yne. From the materials discussed in chapter two, anthracene system showed the lowest band gaps, 2.40 eV for the di-yne and 2.30 for the poly-yne, while substituting the ring with electron withdrawing groups like fluorine and alkoxy groups had a little effect on the optical properties. In the materials discussed in chapter three, with oligo-pyridines as spacers, it was clear that linearity plays a role in increasing the conjugation of the materials while the kinked or bent molecular systems had a negative effect in lowering the energies of transitions. Also, increasing the number of rings proved to be not very efficient for making efficient materials for applications in such systems.

In chapter four, materials based on fused thienothiophene and dithienothiophene systems have been prepared and compared with the previously reported non-fused systems. In was expected that the fused systems would show lower bands gaps and lower emission energies due to the planarity of the rings, which increases the chances of p-p overlap. However, the optical gaps in fused polythiophenes are found to be higher than in non-fused polythiophenes with a comparable number of rings, but the trends can be explained by considering the number of conjugated double bonds in these materials. DFT calculations on the fused and non-fused systems indicate that the factor that determines the energies of the systems, and the HOMO – LUMO gap is related to the number of "formal" double bonds within the systems. Reducing the number of double bonds by fusing reduces the conjugation of the system.

In chapter five, the hetero-aromatic systems show substantial donor-acceptor interaction between the platinum and the conjugated ligands, while the mixed thienyl-pyridyl systems showed a reduction in the donor-acceptor interaction between the metal and the ligand as compared with bithiophene and terthiophene[11].

In all systems, two characteristic emissions were seen at low and/or room temperature, the one just beneath the onset of optical absorption is assigned to emission from the singlet state ($S_1 \rightarrow S_0$), while a lower energy band with a shift from the singlet peak by *ca.*, $0.7 \pm 0.1$ eV was assigned to emission from the triplet excited state. This state has a long lifetime of about 150-160 μs and show temperature dependence more then the singlet emission band. Such studies are important to shine more light on the radiative and non-radiative decay rates and manipulate the efficiency of emission for light emitting diodes (LEDs).

# 5.5 References


1) (a) J.S. Wilson, A. Köhler, R.H. Friend, M. K. Al-Suti, M.R.A. Al-Mandhary, M.S. Khan and P.R. Raithby, *J. Chem. Phys.*, **2000**, 113 7627; (b) J. M. Raimundo, P. Blanchard, H. Brisset, S. Akoudad and J. Roncali, *Chem. Commun.*, **2000**, 939.
2) (a) J. Cornil, D. A. dos Santos, X. Crispin, R. Silbey and J. L. Bredas, *J. Am. Chem. Soc.*, **1998**, 120, 1289; U. H. F. Bunz, V. Enkelmann, L. Kloppenburg, D. Jones, K. D. Shimizu, J. B. Claridge, H.-C. zur Loye and G. Lieser, *Chem. Mater.*, **1999**, 11, 1416.
3) K. Pilgram, M. Zupan and R. Skiles, *J. Heterocycl. Chem.*, **1970**, 7, 629.
4) Y. Tsubata, T. Suzuki, and T. Miyashi, *J. Org. Chem.*, **1992**, 57, 6749.
5) M. Kiamuddin and M.E. Haque, *Chem. Ind.* **1964**, 1753.
6) C.J. Neef and J.P. Ferraris, *Macromolecules*, **2000**, 33, 2311.
7) (a) N. Chawdhury, A. Köhler, R.H. Friend, M. Younus, N.J. Long, P.R. Raithby and J. Lewis, *Macromolecules*, 1998, 31, 722., (b) J.S. Wilson, A.S. Doot, A.J.A.B. Seeley, M.S. Khan, A. Köhler, R.H. Friend, *Nature*, **2002**, 413, 828, (d) W.-Y. Wong, K.-H. Choi, G.-L. Lu and J.-X. Shi, *Macromol. Rapid Commun.* **2001**, 22, 461.
8) (a) Z.-H. Zhou, T. Maruyama, T. Kanbara, T. Ikeda, K. Ichimura, T. Yamamoto and K. Tokuda, *J. Chem. Soc., Chem. Commun.*, **1991**, 1210, (b) I. H. Jenkins, N. G. Rees and P. G. Pickup, *Chem. Mater.*, **1997**, 9, 1213.

9) J. Lewis, N.J. Long, P.R. Raithby, G.P. Shield, W-Y Wong and M. Younus, *J. Chem. Soc., Dalton Trans.*, **1997**, 4283.

10) J.S. Wilson, N. Chawdhury, A. Köhler, R.H. Friend, M.R.A. Al-Mandhary, M.S. Khan, M. Younus and P.R. Raithby, *J. Am. Chem. Soc.*, **2001**, 123, 9412.

11) N. Chawdhury, A. Köhler, R.H. Friend, W.-Y. Wong, M. Younus, P.R. Raithby, J. Lewis, T.C. Corcoran, M. R. A. Al-Mandhary and M.S. Khan, *J. Chem. Phys.*, **1999**, 110, 4963.

# CHAPTER 6

## EXPERIMENTAL

# 6.1 Experimental

## 6.1.1 General

All reactions were performed under a dry argon or nitrogen atmosphere using standard Schlenk techniques. Solvents were pre-dried and distilled before use by standard procedures[1]. All chemicals, except where stated otherwise, were obtained from commercial resources and used as received. The compounds *trans*-$[(Ph)(PEt_3)_2PtCl]$ [2], *trans*-$[(P^nBu_3)_2PtCl_2]$[3], were prepared *via* literature procedures. The NMR spectra were recorded on a Bruker WM-250 or AM-400 spectrometer in $CDCl_3$. The $^1H$ and $^{13}C\{^1H\}$ NMR spectra were referenced to solvent resonances and $^{31}P\{^1H\}$NMR spectra were referenced to external trimethylphosphite or phosphoric acid. Infra red spectra were recorded as $CH_2Cl_2$ solutions, in a NaCl cell, on a Perkin-Elmer 1710 FT-IR spectrometer, mass spectra on a Kratos MS 890 spectrometer by the electron impact (EI) and fast atom bombardment (FAB) techniques. Microanalyses were performed in the Department of Chemistry, University of Bath. Preparative TLC was carried out on commercial Merck plates with a 0.25 mm layer of silica. Column chromatography was performed either on Kieselgel 60 (230 – 400 mesh) silica gel or alumina (Brockman Grade II-III).

## 6.1.2 Thermal characterizations

Thermal analysis (DTA, and TG) was performed simultaneously in a Stanton-Redcroft model STA-780 Simultaneous Thermal Analyser under flowing $N_2$. Sample masses were ~1 mg packed with ~2 mg $Al_2O_3$ in open Inconel crucibles. The reference crucible contained $Al_2O_3$. Samples were heated at 10°C/min to ~ 465°C. The thermocouple readings were calibrated using a series of DTA standard materials: $KNO_3$, In, Sn, $Ag_2SO_4$, and $K_2SO_4$ as well as Pb and Al as secondary standards, using the same heating rates as the samples.

### 6.1.3 X-ray Crystallography

The crystals were mounted in inert oil on a glass fibre. Data were measured using Mo-$K_\alpha$ radiation ($\lambda$ = 0.71073 Å) with a Nonius Kappa area detector or a Bruker AXS SMART CCD area detector on Station 9.8 of the CCLRC Daresbury Laboratory, both fitted with an Oxford Cryo-stream low-temperature attachment. *Structure solution and refinement*: Structures were solved by direct methods and subjected to full-matrix least-squares refinement on $F^2$ (program SHELXL-97). All non-hydrogen atoms were refined anisotropically. Hydrogen atoms were included using rigid methyl groups or a riding model.

**Powder Diffraction**

X-ray diffraction experiment for a polycrystalline sample of **8b** was carried out on Station 2.3 of the Daresbury Synchrotron Radiation Source ($\lambda$=1.2996 Å) using a flat plate geometry, that for **9b** on a Stoe powder X-ray diffractometer equipped with a linear PSD, using Cu-$K\alpha$ radiation ($\overline{\lambda}$ =1.5406 Å) from a sealed-tube source. Both diffraction patterns were indexed using the DICVOL91 programme[33] and each structure solved using the DASH suite of programmes.[34]

### 6.1.4 Molecular weight measurements

Molar masses were determined by Gel permeation chromatography (GPC) using two PL Gel 30 cm, 5 micron mixed C columns at 30 °C running in THF at 1 $cm^3$ $min^{-1}$ with a Roth Mocel 200 high precision pump. A DAWN DSP (Wyatt Technology) Multi-Angle Laser Light Scattering (MALLS) apparatus with 18 detectors and auxiliary Viscotek model 200 differential refractometer/viscometer detectors was used to calculate the molecular weights (referred to GPC LS).

### 6.1.5 Optical characterisation

The thin films were spun from dichloromethane solution onto quartz substrates using a conventional photoresist spin-coater. Films were typically 100-150 nm in thickness

as measured on a Dektak profilometer. The optical absorption was measured with a Hewlett-Packard ultraviolet-visible (UV-VIS) spectrometer. Measurements of photoluminescence (PL) were made with the sample in a continuous-flow Helium cryostat. The temperature was controlled with an Oxford-Intelligent temperature controller-4 (ITC-4) and a calibrated silicon diode adjacent to the sample. For PL measurements, excitation was provided by the UV lines (334-365 nm) of a continuous wave (CW) Argon ion laser. Typical intensities used were a few $mW/mm^2$. The emission spectra were recorded using a spectrograph with an optical fibre input coupled to a cooled charge coupled device (CCD) array (Oriel Instaspec IV).

# 6.2 Synthesis

## 6.2.1 Chapter Two

**1,4-Diiodonaphthalene.** *n*-Butyllithium (8.5 mL, 2.6 M in hexane, 22.1 mmol) was added dropwise over the course of 30 min to a vigorously stirred suspension of 1,4-dibromonaphthalene (2.58 g, 9.0 mmol) in anhydrous diethyl ether (50 $cm^3$). The mixture was stirred for an additional 10 min after which period iodine (7.5 g, 30 mmol) was added in several portions over 5 min. The reaction mixture was stirred for an additional 15 mins. until the colour was a dark brown. The ethereal solution was washed several times with aqueous sodium thiosulfate (25% w/w), dried over anhydrous magnesium sulfate and the solvent removed under vacuum to obtain a pale yellow solid. The crude product was purified by recrystallization from $CCl_4$ (100 $cm^3$) to give off-white solid in 53% yield (1.82 g) identified as 1,4-Diiodonaphthalene compound. $^1H$ NMR (250 MHz, $CDCl_3$) δ: 7.55 (dd, 2H, arom.), 8.55 (dd, 4H, arom.). EI MS: *m/z*: 380.0 ($M^+$). Anal. Calcd for $C_{10}H_6I_2$: C, 31.61; H, 1.59. Found: C, 31.51; H, 1.67%.

**9,10-Diiodoanthracene.** A Similar procedure as described above was adopted using 9, 10-dibromoanthracene (3.0 g, 8.93 mmol) to give 9,10-Diiodoanthracene compound as yellow needles in 50% isolated yield(1.92 g). $^1H$ NMR (250 MHz $CDCl_3$) δ 7.55 (dd, 4H, arom.), 8.55 (dd, 4H, arom.). EI MS: *m/z*: 430.2 ($M^+$). Calcd. for $C_{14}H_8I_2$: C, 39.10; H, 1.88. Found: C, 39.21; H, 1.90%.

**1,4-Bis(trimethylsilylethynyl)naphthalene 2a**. To a solution of 1,4-diiodonapthalene (2.0 g, 5.26 mmol) in $^{i}Pr_2NH$-THF (70 $cm^3$, 1:1 v/v) under nitrogen was added a catalytic mixture of CuI (20 mg), $Pd(OAc)_2$ (20 mg) and $PPh_3$ (60 mg). The solution was stirred for 20 mins. at 50 °C and then trimethylsilylethyne (1.68 g, 17.1 mmol) was added. The reaction mixture was left with stirring for 20h at 75 °C. The completion of the reaction was determined by silica TLC and IR spectroscopy. The solution was allowed to cool down to room temperature, filtered off, and the solvent mixture was removed under reduced pressure. The residue was subjected to silica column chromatography using hexane/$CH_2Cl_2$ (1:1) as eluent to afford **2a** as a salmon coloured crystalline solid in 85 % yield (1.43 g). IR ($CH_2Cl_2$): $\nu/cm^{-1}$ 2155 (-C≡C-). $^1H$ NMR (250 MHz, $CDCl_3$): δ 0.27 (s, 18H, $SiMe_3$), 7.56 (dd, 2H, $H_{6,7}$), 7.64 (s, 2H, $H_{2,3}$), 8.35 (dd, 2H, $H_{5,8}$). $^{13}C$ {$^1H$} NMR (100.6 MHz, $CDCl_3$): δ 0.04 (s, $SiMe_3$), 101.36, 102.81 (C≡C), 121.54, 126.55, 127.24, 129.31, 133.08 (aromatic). EI MS: *m*/z: 320.3 ($M^+$). Calc. for $C_{20}H_{24}Si_2$: C, 74.97; H, 7.55. Found C, 75.03; H, 7.63%.

**1,4-Bisethynylnapthalene 2b.** The bis-trimethylsilylethynyl derivative **2a** (1.0 g, 3.12 mmol) was proto-desilylated in THF-methanol (50 $cm^3$, 4:1 v/v) using aqueous KOH (0.38 g, 6.78 mmol in 1 $cm^3$ $H_2O$). The reaction mixture was stirred at room temperature for 1 h. The solvent was then removed and the crude product was purified by silica column chromatography eluting with hexane/$CH_2Cl_2$ (2:1, v/v). The desired compound **2b** was isolated as an orange-red solid in 80% isolated yield (0.44 g). IR ($CH_2Cl_2$): $\nu/cm^{-1}$ 2107 (-C≡C-), 3299 (C≡C-H). $^1H$ NMR (250 MHz, $CDCl_3$): δ 3.30 (s, 2H, C≡CH), 7.30 (dd, 2H, $H_{6,7}$), 7.56 (s, 2H, $H_{2,3}$) 8.35 (dd, 2H, $H_{5,8}$). $^{13}C$ {$^1H$} NMR (100.6 MHz, $CDCl_3$): δ 101.36, 102.81 (C≡C), 121.54, 126.55, 127.24, 129.31,133.08 (aromatic). EI-MS: *m*/z: 176.2 ($M^+$). Calc. for $C_{14}H_8$: C, 95.43; H, 4.58. Found: C 95.39; H, 4.61%.

**9,10-Bis(trimethylsilylethynyl)anthracene 3a.** 9,10-Diiodoanthracene (2.0 g, 4.6 mmol), trimethylsilylethyne (1.46 g, 14.9 mmol) and $^{i}Pr_2NH$-THF (70 $cm^3$, 1:1 v/v) were mixed with catalytic amounts of CuI (20 mg), $Pd(OAc)_2$ (20 mg) and $PPh_3$ (60 mg). The crude product was worked up, as before, to yield a dark brown residue, which was then applied to a silica column in hexane and eluted with the same solvent. The desired compound **3a** was obtained as a deep red crystalline solid in 78% isolated yield (1.72 g). IR ($CH_2Cl_2$): $\nu/cm^{-1}$ 2152 (-C≡C-). $^1H$ NMR (250 MHz, $CDCl_3$): δ 0.27 (s, 18H, $SiCH_3$),

7.63 (dd, 4H, arom.), 8.44 (dd, 4H, arom.). $^{13}C$ {$^{1}H$} NMR (100.6 MHz, $CDCl_3$): δ 0.20 (s, $SiMe_3$), 101.50, 108.16 (C≡C), 118.44, 127.19, 127.57, 132.36 (arom.). EI-MS: *m*/z 370 ($M^+$). Calc. For $C_{24}H_{26}Si_2$: C, 77.81; H, 7.07. Found: C, 78.04; H 6.98 %.

**9,10-Bisethynylanthracene 3b.** Compound **3a** was proto-desilylated as for **2a** and the crude product was worked up, as before, to yield a dark red solid. Silica column chromatography with hexane-$CH_2Cl_2$ (1:1 v/v) gave a red solid identified as **3b** in 76% yield. IR ($CH_2Cl_2$): ν/$cm^{-1}$ 2107 (-C≡C-), 3299 (C≡C-H). $^{1}H$ NMR (250 MHz, $CDCl_3$): δ 3.30 (s, 2H, C≡CH), 7.63 (dd, 4H, arom.), 8.32 (dd, 4H, arom.). $^{13}C$ {$^{1}H$} NMR (100.6 MHz, $CDCl_3$): δ 101.50, 108.16 (C≡C), 118.44, 127.19, 127.57, 132.36 (arom.). EI-MS: *m*/z 226.3 ($M^+$). Satisfactory microanalysis could not be obtained due to instability of the diterminal alkyne.

**1,4-bis(trimethylsilylethynyl)-2-aminobenzene 4a**. To an ice-cooled solution of 1,4-dibromo-2-aminobenzene (3.01 g, 12 mmol) in diisopropylamine/THF (75 $cm^3$, 1:4 v/v) under nitrogen were added CuI (29 mg, 0.15 mmol), $Pd(OAc)_2$ (27 mg, 0.12 mmol) and $PPh_3$ (157 mg, 0.60 mmol). The solution was stirred for 0.5 h, trimethylsilylethyne (2.95g, 30 mmol) was then added over 10 min to the vigorously stirred solution; during the addition a white precipitate formed. The suspension was stirred for 30 min in an ice-bath before being warmed to room temperature. After reacting for 30 min at room temperature the mixture was heated to 80°C for 20h when TLC and IR spectroscopy indicated that all the starting material had been consumed and the coupling reaction was completed. After being cooled to room temperature, the mixture was filtered to eliminate the ammonium salt and the solvent mixture was removed *in vacuo*.

**1,4-Diethynyl-2-aminobenzene 4b**. The solid residue was dissolved in THF (50 $cm^3$) with stirring. Methanol (15 $cm^3$) and aqueous KOH (1.50 g, 27 mmol in 2 $cm^3$ water) were added at room temperature to the stirred solution. The reaction mixture was stirred for 2 h. The completion of the desilylation reaction was verified by TLC and IR spectroscopy. The mixture was filtered and the solvent was removed under reduced pressure to leave a yellow residue. This residue was dissolved in the minimum amount of dichloromethane and subjected to column chromatography on silica using hexane-dichloromethane (2:1 v/v) as eluant to afford a pale yellow solid.

Recrystallization from hexane with activated charcoal yielded pale yellow micro-crystals (0.62 g, 76% yield). IR ($CH_2Cl_2$): $\nu/cm^{-1}$ 2108 (-C≡C-), 3300 (C≡CH), 3428 (-NH-). $^1H$ NMR (250 MHz, $CDCl_3$): δ 3.12 (s, 1H, C≡C-H), 3.50 (s, 1H, C≡C-H), 4.70 (brs, 2H, $NH_2$), 7.21 (d, 2H, arom.), 7.73 (dd, IH, arom.). $^{13}C$ {$^1H$} NMR (100.6 MHz, $CDCl_3$): δ 78.2, 80.6, 83.1, 84.0 (C≡C), 107.2, 117.5, 121.4, 123.0, 132.2, 148.0, (arom.). EI mass spectrum: m/z 141 ($M^+$). Found: C, 85.03; H, 4.94; N, 9.90; Calc. for $C_{10}H_7N$: C, 85.08; H. 5.00; N, 9.92%.

**1,4-bis(trimethylsilylethynyl)-2-flourobenzene 5a.** To a solution of 1,4-dibromo-2-fluorobenzene (2.5g, 10 mmol) in diisopropylamine/THF (100 $cm^3$, 1:4 v/v) under nitrogen was added a catalyst mixture of CuI (24 mg, 0.13 mmol), $Pd(OAc)_2$ (22 mg, 0.10 mmol) and $PPh_3$ (131 mg, 0.50 mmol). Trimethylsilylethyne (2.45 g, 25 mmol) was then added to the vigorously stirred solution. The reaction mixture was stirred at reflux for 8h and the completion of the reaction was verified by TLC and IR spectroscopy. The reaction mixture was allowed to cool to room temperature and the ammonium iodide precipitate was filtered off. The yellow filtrate was evaporated to dryness.

**1,4-Diethynyl-2-fluorobenzene 5b** Removal of the trimethylsilyl protecting groups was accomplished as for the synthesis of **4b** described above. **5b** was obtained as off-white solid in 82% yield. Good quality crystals were obtained by sublimation (15 mm Hg, ice-water cooled). IR ($CH_2Cl_2$): $\nu/cm^{-1}$ 2107 (-C≡C-) and 3300 (-C≡C-H). $^1H$ NMR (250 MHz, $CDCl_3$): δ 3.21 (s, 1H, C≡C-H), 3.38 (s, 1H, C≡C-H), 7.22 (d, 2H, arom.) and 7.46 (d, 1H, arom.). $^{13}C$ {$^1H$} NMR (100.6 MHz, $CDCl_3$): δ 77.1, 80.2, 81.8, 84.1 (C≡C), 111.51, 119.02, 124.36, 128.10, 134.20 and 162.65. EI mass spectrum: m/z 144 ($M^+$). Found: C, 83.29; H, 3.58. Calc. for $C_{10}H_5F$: C, 83.32; H, 3.50%.

**1,4-Diethynyl-2,5-difluorobenzene 6b** Similar coupling and desilylation procedures as in **5b** were adopted using 1,4-dibromo-2,5-diflurobenzene (2.72 g, 10 mmol) to give **6b** as off-white solid in 95% yield. Good quality crystals were obtained by sublimation (15 mm Hg, ice-water cooled). IR ($CH_2Cl_2$) $\nu/cm^{-1}$: 2107 (-C≡C-) and 3299 (-C≡C-H). $^1H$ NMR (250 MHz, $CDCl_3$): δ 3.41 (s, 2H, C≡CH), 7.24 (d, 2H, arom.), $^{13}C$ {$^1H$} NMR (100.6 MHz, $CDCl_3$): δ 75.7, 85.5 (C≡C), 112.8, 120.2, 158.9

(arom.). EI mass spectrum: m/z 162 ($M^+$). Found C, 74.11; H, 2.45; Calc. for $C_{10}H_4F_2$: C, 74.08; H. 2.49%.

**1,4-Diethynyl-2,3,5,6-tetrafluorobenzene 7b** Similar coupling and desilylation procedures as in **6b** were adopted using 1,4-Diiodo-2,3,5,6-tetrafluorobenzene (4.02 g, 10 mmol) to obtain **7b** as an off-white solid in 82% yield. Good quality crystals were obtained by sublimation (15 mm Hg, ice-water cooled). IR ($CH_2Cl_2$) $\nu/cm^{-1}$: 2106 (-C≡C-) and 3297 (-C≡C-H). $^1H$ NMR (250 MHz, $CDCl_3$): δ 3.72 (s, 2H, C≡CH). $^{13}C$ {$^1H$} NMR (100.6 MHz, $CDCl_3$): δ 68.4, 91.5 (C≡C), 104.5, 147.5 (arom.). EI mass spectrum: m/z 198 ($M^+$). Anal. Found: C, 60.71; H, 1.04; Calc. for $C_{10}H_2F_4$: C, 60.63; H, 1.02%.

**1,4-Diethynyl-2,5-bis(methoxy)benzene 8b** Similar coupling and desilylation procedures as in **7b** using 1,4-diiodo-2,5-bis(methoxy)benzene to yield off-white solid in 86% yield. IR ($CH_2Cl_2$): $\nu/cm^{-1}$ 2107 (-C≡C-) and 3299 (-C≡C-H). $^1H$ NMR (250 MHz $CDCl_3$): δ 3.33 (s, 2H, C≡C-H), 3.92 (s, 6H, $OCH_3$), 7.19 (s, 2H, arom.). $^{13}C$ {$^1H$} NMR (100.6 MHz, $CDCl_3$): δ 69.89 ($OCH_3$), 79.96, 82.57 (C≡C), 113.41, 117.89, 154.14(arom.). EI mass spectrum: m/z 186 ($M^+$). Found: C, 77.46; H, 5.43; Calcd for $C_{12}H_{10}O_2$: C, 77.40; H, 5.41%.

**1,4-Diethynyl-2,5-bis(octyloxy)benzene 9b**. Similar coupling and desilylation procedures as in **8b** were adopted using 1,4-diiodo-2,5-bis(octyloxy)benzene (5.87 g, 10 mmol) to obtain a pale yellow solid in 79% yield. IR ($CH_2Cl_2$): $\nu/cm^{-1}$ 2107 (-C≡C-) and 3299 (-C≡C-H). $^1H$ NMR (250 MHz $CDCl_3$): δ 0.86 (t, 6H, $CH_3$), 1.26, 1.40 (both m, 20H, $CH_2$), 1.78 (m, 4H, $CH_2$), 3.32 (s, 2H, C≡C-H), 3.95 (t, 4H, $OCH_2$), 6.93 (s, 2H, arom.). $^{13}C$ {$^1H$} NMR (100.6 MHz, $CDCl_3$): δ 14.29 ($CH_3$), 22.85, 26.09, 29.31, 29.42, 29.48, 31.99 (all $CH_2$), 69.84 ($OCH_2$), 79.98, 82.60 (C≡C), 113.45, 117.92, 154.18 (arom.). EI mass spectrum: m/z 382 ($M^+$). Found: C, 81.52; H, 10.04; Calc. for $C_{26}H_{38}O_2$: C, 81.63; H, 10.01%.

***Trans*-[(Ph)($Et_3P$)$_2$Pt-C≡C-R-C≡C-Pt($PEt_3$)$_2$(Ph)] (R = benzene-1,4-diyl) 1c.** To a stirred solution of *trans*-[(Ph)($PEt_3$)$_2$PtCl] (0.543 g, 1.0 mmol) and 1,4-bisethynylbenzene (0.063 g, 0.5 mmol) in $^iPr_2NH$-$CH_2Cl_2$ (50 $cm^3$, 1:1 v/v) under nitrogen was added CuI

(5 mg). The yellow solution was stirred at room temperature for 15 h, after which all volatile components were removed under reduced pressure. The residue was dissolved in $CH_2Cl_2$ and passed through a silica column eluting with hexane-$CH_2Cl_2$ (1:1, v/v). Removal of the solvents *in vacuo* gave the title complex as a pale yellow solid in 70% yield (0.40 g). IR ($CH_2Cl_2$): $\nu/cm^{-1}$ 2095 (-C≡C-). $^1H$ NMR (250 MHz, $CDCl_3$): δ 7.35 (d, 4H, $H_{ortho}$ of Ph), 7.13 (s, 4H, phenylene spacer), 6.95(t, 4H, $H_{meta}$ of Ph), 6.78 (t, 2H, $H_{para}$ of Ph), 1.87-1.80 (m, 24H, P-$CH_2$), 1.10 (m, 36H, P-$CH_2CH_3$), $^{13}C\{^1H\}$ NMR (100.6 MHz, $CDCl_3$): δ 156.21, 137.92, 126.93, 125.65, 121.13, 118.68 (aromatic), 112.94, 107.76 (C≡C), 14.92, 7.88 (aliph.). $^{31}P\{^1H\}$-NMR (101.3 MHz, $CDCl_3$): δ –131.17, $^1J_{Pt\text{-}P}$ = 2628 Hz. FAB-MS: *m*/z 1141 ($M^+$). Calc. for $C_{46}H_{74}P_4Pt_2$: C, 48.42; H, 6.54. Found C, 48.48; H, 6.63%.

***Trans*-[(Ph)($Et_3P$)$_2$Pt-C≡C-R-C≡C-Pt($PEt_3$)$_2$(Ph)] (R = napthalene-1,4-diyl) 2c.** This compound was synthesised employing similar reaction conditions to those of **1c** but using **2b** instead of **1b**. The product was purified on preparative TLC plates with hexane-$CH_2Cl_2$ (3:7, v/v) as eluent giving compound **2c** as an orange solid in an isolated yield of 65% (0.39 g). IR ($CH_2Cl_2$): $\nu/cm^{-1}$ 2095 (-C≡C-). $^1H$ NMR (250 MHz, $CDCl_3$): δ 8.34 (dd, 2H, $H_{5,8}$), 7.44 (dd, 2H, $H_{6,7}$), 7.38 (s, 2H, $H_{2,3}$), 7.32 (d, 4H, $H_{ortho}$ of Ph) 6.95 (d, 4H, $H_{meta}$ of Ph), 6.80 (t, 2H, $H_{para}$ of Ph), 1.75 (m, 24H, P-$CH_2$), 1.07 (m, 36H, P-$CH_2CH_3$), $^{13}C\{^1H\}$ NMR (100.6 MHz, $CDCl_3$): δ 156.49, 139.26, 137.29, 133.85, 127.47, 124.91, 123.87, 121.16, 119.22 (aromatics), 111.01, 108.85 (C≡C), 15.22, 7.90 (aliph.). $^{31}P\{^1H\}$-NMR (101.3 MHz, $CDCl_3$): δ –131.17, $^1J_{Pt\text{-}P}$ = 2643 Hz. FAB-MS: *m*/z 1191 ($M^+$). Calc. for $C_{50}H_{76}P_4Pt_2$: C, 50.41; H, 6.43. Found C, 50.69; H, 6.58%.

***Trans*-[(Ph)($Et_3P$)$_2$Pt-C≡C-R-C≡C-Pt($PEt_3$)$_2$(Ph)] (R = anthracene-9,10-diyl) 3c.** Treatment of the freshly prepared diterminal alkyne **3b** (0.113 g, 0.50 mmol) with *trans*-[(Ph)($PEt_3$)$_2$PtCl] (0.543 g, 1.0 mmol) for 15 h at room temperature, in the presence of a catalytic amount of CuI (5 mg) gave the required complex as an orange solid in 65% isolated yield after purification on a silica column using hexane-$CH_2Cl_2$ (3:7, v/v) as eluant. IR ($CH_2Cl_2$): $\nu/cm^{-1}$ 2094 (-C≡C-). $^1H$ NMR (250 MHz, $CDCl_3$): δ 7.72 (dd, 4H, $H_{1,4,5,8}$), 7.40 (dd, 4H, $H_{2,3,6,7}$), 7.25 (d,4H, $H_{ortho}$ of Ph), 6.99 (t, 4H, $H_{meta}$ of Ph), 6.82 (t, 2H, $H_{para}$ of Ph), 1.77 (m, 24H, P-$CH_2$),1.12 (m, 36H, P-$CH_2CH_3$). $^{13}C\{^1H\}$ NMR (100 MHz, $CDCl_3$): δ 139.37, 131.74, 128.45, 127.28, 33,121, 124.16 (arom.), 110.89, 108.68

(C≡C), 15.36 and 8.05 (aliph.). $^{31}$P-NMR (101.3 MHz, $CDCl_3$): δ –131.17, $^1J_{Pt\text{-}P}$ = 2645 Hz. FAB-MS: *m*/z 1241 ($M^+$). Calc. for $C_{54}H_{78}P_4Pt_2$: C, 52.25; H, 6.33. Found C, 52.53; H, 6.28%.

***Trans*-[-$(Bu_3P)_2$Pt-C≡C-R-C≡C-]$_n$, ( R = naphthalene-1,4-diyl) 2d.** CuI (5 mg) was added to a mixture of *trans*-[Pt($PBu^n_3$)$_2Cl_2$] (0.670 g, 1.0 mmol) and **2b** (0.176 g, 1.0 mmol) in $^iPr_2NH$-$CH_2Cl_2$ (50 $cm^3$, 1:1 v/v). The solution was stirred at room temperature for 15 h, after which all volatile components were removed under reduced pressure. The residue was dissolved in $CH_2Cl_2$ and passed through a short alumina column. After removal of the solvents, an off-white film was obtained readily which was then washed with methanol to give the polymer **2d** in 85% isolated yield (0.66 g). Further purification was accomplished by precipitating the polymer solution in methanol from dichloromethane. IR ($CH_2Cl_2$): ν/$cm^{-1}$ 2095 (-C≡C-). $^1$H NMR (250 MHz, $CDCl_3$): δ 8.43 (d, 2H, $H_{5,8}$), 7.36 (d, 2H, $H_{6,7}$), 7.25 (s, 2H, $H_{2,3}$), 2.17 (m, 12H, P-$CH_2$), 1.60 (br, 12H, $CH_2$), 1.41 (sextet, 12H, $CH_2$), 0.92 (t, 18H, $CH_3$), $^{13}$C{$^1$H} NMR (100.6 MHz, $CDCl_3$): δ 133.76, 127.89, 127.48, 124.97, 123.74 (arom.), 112.23, 111.16 (C≡C), 53.38, 26.54, 24.29, 13.84 (aliph.). $^{31}$P{$^1$H}-NMR (101.3 MHz, $CDCl_3$): δ –138.03, $^1J_{Pt\text{-}P}$ = 2363 Hz. Calc. for $(C_{38}H_{60}P_2Pt)_n$: C, 58.97; H, 7.81. Found C, 59.07; H, 7.89 %. GPC (THF): $M_n$ = 41,020 $gmol^{-1}$ (n = 53), $M_w$ = 78,000 $gmol^{-1}$, PDI = 1.9.

***Trans* [-$(Bu_3P)_2$Pt-C≡C-R-C≡C-]$_n$ ( R = anthracene-9,10-diyl) 3d.** This compound was synthesised employing similar reaction conditions to those of **2d** but using **3b** instead of **2b**. Red solid (90% yield). IR ($CH_2Cl_2$): ν/$cm^{-1}$ 2094 (-C≡C-). $^1$H NMR (250 MHz, $CDCl_3$): δ 8.30 (br, 4H, $H_{2,3,6,7}$), 7.51 (br, 4H, $H_{1,4,5,8}$), 2.16 (t, 12H, $PCH_2$), 1.68 (m, 12H, $CH_2$), 1.25 (br, 12H,$CH_2$), 0.88 (t, 18H, $CH_3$), $^{13}$C{$^1$H} NMR (100 MHz, $CDCl_3$): δ 139.37, 131.77, 128.43, 124.46 (arom.), 110.28, 108.39 (C≡C), 50.84, 26.76, 24.34 and 13.85 (aliph.). $^{31}$P{$^1$H}-NMR (101.3 MHz, $CDCl_3$): δ –138.03, $^1J_{Pt\text{-}P}$ = 2373 Hz. Calc. for $(C_{42}H_{62}P_2Pt)_n$: C, 61.22; H, 7.58. Found C, 60.98; H, 7.87%. GPC (THF): $M_n$ = 28,000 $gmol^{-1}$ (n = 34), $M_w$ = 50,500 $gmol^{-1}$, PDI = 1.8.

***Trans*-[Pt($P^nBu_3$)$_2$(-C≡C-$C_6H_3(NH_2)$-C≡C)-]$_n$ 4d** This compound was synthesised employing similar reaction conditions to those of **3d** but using **4b** instead of **3b**. The compound came as off-white and was isolated in 85% yield (0.750 g). IR ($CH_2Cl_2$):

$\nu/cm^{-1}$ 2094 (-C≡C-). $^1H$ NMR (250 MHz, $CDCl_3$): δ 0.87 (t, 18H, $CH_3$), 1.40 (sex, 12H, $CH_2$), 1.65 (brs, 12H, $CH_2$), 2.25 (m, 12H, $PCH_2$), 4.18 (s, 2H, $NH_2$), 6.58 (d, 2H, arom.), 7.12 (d, IH, arom.). $^{31}P\{^1H\}$ NMR (101.3 MHz, $CDCl_3$): δ -138.08, $J_{Pt-P}$ = 2330 Hz. Found: C, 55.17; H, 8.14; Calc. for $(C_{34}H_{59}NP_2Pt)_n$: C, 55.26; H. 8.05%. GPC(THF): $M_n$ = 94700 $g.mol^{-1}$ , $M_w$ = 151,500 $g.mol^{-1}$, polydispersity = 1.6.

***Trans*-[Pt($P^nBu_3$)$_2$(-C≡C-$C_6H_3F$-C≡C)-]$_n$ 5d** This compound was synthesised employing similar reaction conditions to those of **4d** but using **5b** instead of **4b**. Off-white solid (82% yield). IR ($CH_2Cl_2$): $\nu/cm^{-1}$ 2095 (-C≡C). $^1H$ NMR (250 MHz, $CDCl_3$): δ 0.82 (t, 18H, $CH_3$), 1.38 (sex, 12H, $CH_2$), 1.58 (brs, 12H, $CH_2$), 2.29 (m, 12H, $PCH_2$), 7.38 (d, 2H, arom.), 7.28 (d, IH, ar). $^{31}P\{^1H\}$ NMR (101.3 MHz, $CDCl_3$): δ -138.50, $J_{Pt-P}$ = 2330 Hz. Found: C, 55.15; H, 7.74; Calc. for $(C_{34}H_{57}P_2FPt)_n$: C, 55.05; H. 7.76%. GPC(THF): $M_n$ = 94650 $g.mol^{-1}$ (n = 128), $M_w$ = 160,900 $g.mol^{-1}$, polydispersity = 1.7.

***Trans*-[Pt($P^nBu_3$)$_2$(-C≡C-$C_6H_2F_2$-C≡C)-]$_n$ 6d** This compound was synthesised employing similar reaction conditions to those of **5d** but using **6b** instead of **5b**. Off-white solid (78% yield). IR ($CH_2Cl_2$): $\nu/cm^{-1}$ 2094 (-C≡C-). $^1H$ NMR (250 MHz, $CDCl_3$): δ 0.77 (t, 18H, $CH_3$), 1.34 (sex, 12H, $CH_2$), 1.52 (brs, 12H, $CH_2$), 2.20 (m, 12H, $PCH_2$), 7.28 (d, 2H, arom.). $^{31}P\{^1H\}$ NMR (101.3 MHz, $CDCl_3$): δ -138.50, $J_{Pt-P}$ = 2330 Hz. Found: C, 53.65; H, 7.44; Calc. for $(C_{34}H_{56}P_2F_2Pt)_n$: C, 53.74; H. 7.43%. GPC(THF): $M_n$ = 88230 $g.mol^{-1}$ (n = 116), $M_w$ = 158,810 $g.mol^{-1}$, polydispersity = 1.8.

***Trans*-[Pt($P^nBu_3$)$_2$(-C≡C-$C_6F_4$-C≡C-]$_n$ 7d** This compound was synthesised employing similar reaction conditions to those of **6d** but using **7b** instead of **6b**. Off-white solid (72% yield). IR ($CH_2Cl_2$): $\nu/cm^{-1}$ 2095 (-C≡C-). $^1H$ NMR (250 MHz, $CDCl_3$): δ 0.75 (t, 18H, $CH_3$), 1.38 (sex, 12H, $CH_2$), 1.58 (brs, 12H, $CH_2$), 2.20 (m, 12H, $PCH_2$). $^{31}P\{^1H\}$ NMR (101.3 MHz, $CDCl_3$): δ -138.50, $J_{Pt-P}$ = 2330 Hz. Found: C,51.36; H, 6.79; Calc. for $(C_{34}H_{54}P_2F_4Pt)_n$: C, 51.31; H. 6.84%. GPC(THF): $M_n$ = 82,500 $g.mol^{-1}$ (n = 103). $M_w$ = 156,770 $g.mol^{-1}$, polydispersity = 1.9.

***Trans*** **-[Pt(P$^n$Bu$_3$)$_2$(-C≡C-C$_6$H$_4$(OCH$_3$)$_2$-C≡C-]$_n$ 8d.** This compound was synthesised employing similar reaction conditions to those of **7d** but using **8b** instead of **7b** Light yellow solid (85% yield). IR ($CH_2Cl_2$): ν/cm$^{-1}$ 2095 (-C≡C-). $^1$H NMR (250 MHz, $CDCl_3$): δ 0.86 (t, 18H, $CH_3$), 1.38 (sex, 12H, $CH_2$), 1.58 (brs, 12H, $CH_2$), 2.20 (m, 12H, $PCH_2$), 3.70 (s, 6H, $OCH_3$), 7.10 (s, 2H, arom.). $^{31}$P{$^1$H} NMR (101.3 MHz, $CDCl_3$): δ -138.10, $J_{Pt\text{-}P}$ = 2330 Hz. Found: C, 55.22; H, 8.03; Calc. for $(C_{36}H_{62}P_2O_2Pt)_n$: C, 55.16; H. 7.97%. GPC (THF): $M_n$ = 74, 100 g.mol$^{-1}$ (n = 95), $M_w$ = 111,200 g.mol$^{-1}$, polydispersity = 1.5 .

***Trans*****-[Pt(P$^n$Bu$_3$)$_2$(-C≡C-C$_6$H$_4$(OC$_8$H$_{17}$)$_2$-C≡C-]$_n$ 9d** This compound was synthesised employing similar reaction conditions to those of **8d** but using **9b** instead of **8b** Light yellow solid (90% yield). IR ($CH_2Cl_2$): ν/cm$^{-1}$ 2095 (-C≡C-). $^1$H NMR (250 MHz, $CDCl_3$): δ 0.84 (t, 24H, $CH_3$), 1.22-1.38 (m, 32H, $CH_2$), 1.62 (m, 16H, $CH_2$), 2.20 (m, 12H, $PCH_2$), 3.75 (t, 4H, $OCH_2$), 6.82 (s, 2H, arom.). $^{31}$P{$^1$H} NMR (101.3 MHz, $CDCl_3$): δ -138.10, $J_{Pt\text{-}P}$ = 2330 Hz. Found: C, 61.36; H, 9.29; Calc. for $(C_{50}H_{90}P_2O_2Pt)_n$: C, 61.26; H. 9.25%. GPC(THF): $M_n$ = 94,850 g.mol$^{-1}$ (n = 97), $M_w$ = 151,750 g.mol$^{-1}$, polydispersity = 1.6.

## 6.2.2 Chapter Three

**6-Bromo-2-lithiopyridine**[4]. To a slurry of 2,6-dibromopyridine (19.0g, 0.08mol) in ether (150mL) cooled below –60 °C, $^n$BuLi (50mL, 1.6N in hexane) was added at such a rate that the temperature of the reaction mixture did not exceed –60 °C. After addition was complete, the reaction mixture was allowed to warm to –40 °C over a period of 20 minutes, a clear yellow solution resulted. This solution was then used *in situ* for the subsequent steps.

**6,6'-Dibromo-2,2'-bipyridyl**[4]. Anhydrous cupric chloride (3.36g, 0.025mmol) was added to a solution of 6-bromo-2-lithiopyridine (from 11.9g of 2,6-dibromopyridine and 31.3 mL of 1.6N $^n$BuLi in 100mL ether) at –90 °C. The yellow suspension was allowed to warm to –70 °C and stirred for an additional 30 minutes. Oxidation with dry compressed air at –60 °C was carried out for 20 minutes until the brown suspension turned green and led to the precipitation of the product. The product was

hydrolysed with 6M HCl, warmed to room temperature, filtered, dried under anhydrous $Na_2SO_4$ and then it was subjected to silica column chromatography (eluent: hexane/DCM 1:1). The solvent was then evaporated in vacuum resulting in a white compound (9.1 g 60%) yield. m. p. 224-226 ° (Lit. 226-227 °).

**6-Bromo-2-acetylpyridine**[5]. *N,N'*-dimethylacetamide (16.3 mL, 0.13 mol) was added to 6-bromo-2-lithiopyridine ( from 29.7g of 2,6-dibromopyridine and 78.3 mL of 1.6N $^nBuLi$ in 300mL ether) at –80 °C. The solution was allowed to warm to –40 °C and it was stirred for 2 h. It was then hydrolysed with saturated aqueous $NH_4Cl$. The aqueous layer was separated, washed twice with ether and the united ether extracts were dried under $Na_2SO_4$, evaporated to a solid residue which was then subjected to silica column chromatography (eluent: hexane/DCM 1:1). The solvent was then evaporated in vacuum resulting in a white compound (20.2 g, 80%) yield. m. p. 55 °. IR (Nujol): ν(C=O) 1700 $cm^{-1}$.

**1-(2-Bromopyridyl)-3-phenyl-2-propenone**[5]. 6-Bromo-2-acetylpyridine (5.0g, 0.025 mol) and benzaldehyde (10 mL, 0.1 mol) were added to a solution of KOH (1.2g) in $H_2O$ (10 mL). and MeOH (50 mL). The solution obtained was stirred at r.t for 2 h., after which time precipitation of the product was complete (6.64g, 92%). IR: ν(C=O) 1675 $cm^{-1}$.

**1-(2-Bromopyridylcarbonylmethyl)pyridinium iodide**[5]. 6-Bromo-2-acetylpyridine (10.0g, 0.05 mol) and iodine (12.80g , 0.05 mol) were heated to reflux in pyridine (60 mL) for one h. The solution obtained was cooled and the yellow pyridinium salt was separated by filtration yield (15.26g, 75%).

**6,6''-Dibromo-4'-phenyl-2,2':6',2''-terpyridine**[5].1-(2-bromopyridyl)-3-phenyl-2-propenone (5.0g, 0.0174mol), 1-(2-bromopyridylcarbonylmethyl) pyridinium iodide (7.05 g, 0.0174 mol) and ammonium acetate (7.7 g) were heated to reflux in acetic acid (50 mL) for 90 minutes, after which period the pale brown solution was cooled to give the desired compound as off-white needles in 6.96g (86%) yield.

**2-Bromo-6-[3-dimethylamino-1-oxopropyl]pyridinehydrochloride**[5]. 6-bromo-2-acetylpyridine(3.0 g, 15 mmol), dimethylammonium chloride (2.45 g, 30 mmol) and

paraformaldehyde (1.80 g, 60 mmol) were heated to reflux in absolute ethanol (30 mL) containing concentrated HCl (0.05 mL) for 3 h under exclusion of moisture. The reaction mixture became coloured and a pale purple solid began to be deposited, which was then collected by filtration, yield 2.5g, 60%

**6,6''-Dibromo-2,2':6',2''-terpyridine**[5]. 2-bromo-6-[3-dimethylamino-1-oxopropyl] pyridinehydrochloride (0.465g,1.58 mmol),1-(2-bromopyridylcarbonylmethyl) pyridinium iodide (0.620 g, 1.58 mmol) and ammonium acetate (2 g) were heated to reflux in MeOH (20 mL) for 2 h. During this time, the solution darkened in colour and a pale brown solid was deposited. The solid was then collected by filtration and washed several times with cold MeOH. Yield 0.280g, 45%

**5,5'-Dibromo-2,2'-bipyridyl**[6]. This compound was prepared from 2,5-dibromopyridine *via* 5-bromo-2-methylsulfenylpyridine and 5-bromo-2-methylsulfinylpyridine.

To a solution of 2,5-dibromopyridine (17.7 g, 0.074 mmol) in 50 mL of benzene were added the Na salt of methanethiol (15% aqueous solution, 52.3 g, 112 mmol) and tetrabutylammonium bromide (0.68 g, 2.1 mmol) at r.t. the solution was then stirred under reflux for 18 h. The organic layer was then separated, and the aqueous solution was extracted with benzene (120 mL). The combined organic extracts was washed with brine and dried over $MgSO_4$. It was then filtered and the solvent evaporated in *vacuum*. The residue was then subjected to vacuum distillation to give colourless oil of 5-bromo-2-methylsulfenylpyridine which solidified as a white solid at r.t, yield 92% m.p. 45-46 °C.

(13.8 g, 67.7 mmol) of 5-bromo-2-methylsulfenylpyridine in 38 mL of acetic acid was added hydrogen peroxide (30% aqueous solution, 9.21 g, 81.2 mmol) dropwise at 0 °C. The reaction was then stirred at r.t. for 20 h. The solution was then cooled by ice/water bath and neutralised with liquid $NH_3$, extracted with DCM and the combined extracts was washed with water and dried under $MgSO_4$. The solvent was then removed and 5-bromo-2-methylsulfinylpyridine solid was then collected by filteration, yield 80%.

A solution of Grignard reagent EtMgBr, which was prepared from Mg turnings (0.46 g, 19 mmol) and ethylbromide (2.1 g, 19 mmol) in 50 mL THF, was added dropwise to a stirred solution of 5-bromo-2-methylsulfinylpyridine (6.0 g, 27 mmol) in 40 mL THF at –40 °C. The mixture was then warmed to r.t. and stirred overnight. The solvent was then removed under reduced pressure, and the residue was added to 100 mL of water and neutralised with dil. HCl. The compound was then extracted with $CHCl_3$, washed with water, and dried over $Na_2SO_4$. After filtration and concentration the residue was subjected to alumina column chromatography with hexane and then with benzene as eluent yielded 2.6g of white crystals of 5,5'-dibromo-2,2'-bipyridyl. m. p. 224-226 (Lit. m.p. 225-226).

Bis(trimethylsilylethynyl)oligopyridines **1a-4a** were prepared by following a general procedure outlined below for **1a**.

**5,5′-Bis(trimethylsilylethynyl)-2,2′-bipyridine (1a)**. To a solution of 5,5′-dibromo-2,2′-bipyridine (2.0g, 6.37 mmol) in diisopropylamine/THF (60 $cm^3$, 1:1 v/v) under nitrogen was added a catalytic mixture of CuI (15 mg), $Pd(OAc)_2$ (16 mg) and $PPh_3$ (50 mg). The solution was stirred for 20 mins. at 50°C and then trimethylsilylethyne (2.24 $cm^3$, 15.92 mmol) was added and the mixture stirred for another 20 min. The temperature was then raised to 75°C and the reaction left under reflux with stirring for 20h. The completion of the reaction was determined by silica TLC and IR spectroscopy. The solution was allowed to cool down to room temperature, filtered and the solvent mixture was removed. The residue was subjected to silica column chromatography using hexane/$CH_2Cl_2$ (1:2) as eluant to afford **1a** as pale yellow needles (1.77 g, 80% yield). IR ($CH_2Cl_2$): $\nu/cm^{-1}$ 2159 (-C≡C-). $^1H$ NMR (250 MHz, $CDCl_3$): δ 8.70 (dd, 2H, $H_{6,6'}$), 8.34 (t, 2H, $H_{3,3'}$), 7.84 (dd, 2H, $H_{4,4'}$), 0.27(s, 18H, $SiMe_3$x2). $^{13}C$ {$^1H$} NMR (100.6 MHz, $CDCl_3$): δ: 154.18, 152.04, 139.73, 120.44, 120.32 (arom.), 101.75, 99.42 (C≡C), -0.18 ($SiMe_3$). EI-mass spectrum: *m*/z 348 ($M^+$). Calc. for $C_{20}H_{24}Si_2N_2$: C, 68.94; H, 6.94; N, 8.04%. Found: C, 68.88; H, 6.91; N, 7.98%.

**6,6′-Bis(trimethylsilylethynyl)-2,2′-bipyridine (2a)** Off-white solid (72% yield). IR ($CH_2Cl_2$): $\nu/cm^{-1}$2159 $cm^{-1}$ (-C≡C-). $^1H$ NMR (250 MHz, $CDCl_3$): δ 8.40 (2H, dd,

$H_{3,3'}$), 7.74 (t, 2H, $H_{4,4'}$), 7.45 (dd, 2H, $H_{5,5'}$), 0.28(18H, s, $SiMe_3$x2). $^{13}C$ {$^1H$} NMR (100.6 MHz, $CDCl_3$): δ: 155.70, 142.34, 136.91, 127.77, 121.09(arom), 103.95, 94.51 (C≡C), 0.31 ($SiMe_3$). EI-mass spectrum: *m*/z 348 ($M^+$). Calc. for $C_{20}H_{24}Si_2N_2$: C, 68.94; H, 6.94; N, 8.04%. Found: C, 69.10; H, 6.89; N, 8.07%.

**6,6″-Bis(trimethylsilylethynyl)-2,2′:6′,2″-terpyridine (3a)** Off-white solid (75% yield). IR ($CH_2Cl_2$): ν/cm$^{-1}$ 2159 (-C≡C-). $^1H$ NMR (250 MHz, $CDCl_3$): δ 8.53 (dd, 2H, $H_{3,3''}$), 8.51 (d, 2H, $H_{3',5'}$), 7.92 (t, 1H, $H_{4'}$), 7.78 (t, 2H, $H_{4,4''}$), 7.49(dd, 2H, $H_{5,5''}$), 0.28 (s, 18H, $SiMe_3$). $^{13}C$ {$^1H$} NMR (100.6 MHz, $CDCl_3$) δ: 156.29, 154.38, 142.30, 137.67, 136.69, 127.41, 121.67, 120.42 (arom.), 103.84, 94.34 (C≡C), 0.10 ($SiMe_3$). EI-mass spectrum: *m*/z 426 ($M^+$). Calc. for $C_{25}H_{27}N_3Si_2$: C, 70.57; H, 6.40; N, 9.88%. Found: C, 70.42; H, 6.48; N, 9.91%.

**6,6″-Bis(trimethylsilylethynyl)-4′-phenyl-2,2′:6′,2″-terpyridine (4a).** White solid (90% yield). IR ($CH_2Cl_2$): ν/cm$^{-1}$ 2159 (-C≡C-). $^1H$ NMR (250 MHz, $CDCl_3$): δ 8.74 (s, 2H, $H_{3',5'}$), 8.56 (dd, 2H, $H_{3,3''}$), 7.88(td, 2H, $H_{ortho}$ for Ph), 7.80 (t, 2H, $H_{4,4''}$), 7.50 (dd, 2H, $H_{5,5''}$), 7.4-7.5 (m, 3H, H *meta and para* for Ph), 0.39 (s, 18H, $SiMe_3$). $^{13}C$ {$^1H$} NMR (100.6 MHz, $CDCl_3$): δ 156.41, 155.00, 150.43, 142.33, 138.42, 136.80, 128.79, 127.56, 127.35, 121.08, 120.77(arom.), 103.96, 94.47 (C≡C ), -0.30 ($CH_3$). EI-mass spectrum: *m*/z 501 ($M^+$). Calc. for $C_{31}H_{31}N_3Si_2$: C, 74.22; H, 6.23; N, 8.38%. Found: C, 74.19; H, 6.27; N, 8.29%.

Bis(ethynyl)oligopyridines **1b–4b** were prepared by the general procedure outlined below for **1b.**

**5,5′-Bis(ethynyl)-2,2′-bipyridine (1b)** 5,5′-Bis(trimethylsilylethynyl)-2,2′-bipyridine (**1a**) (0.696 g, 2.0 mmol) was desilylated in THF/methanol (50 cm$^3$, 4:1, v/v) using aqueous KOH (0.36 g, 6.6 mmol in 1 cm$^3$ water). The reaction mixture was stirred at room temperature for 2 h during which time IR and TLC showed that all protected compound had been converted to the terminal alkyne. The solvent mixture was then removed and the residue was dissolved in $CH_2Cl_2$ and subjected to column chromatography on silica using hexane/$CH_2Cl_2$ (1:1, v/v) as eluant to afford a white solid identified as **1b** (0.31 g, 76%). IR($CH_2Cl_2$): ν/cm$^{-1}$ 3300 (C≡C-H), 2107 (-C≡C-

). $^1$H NMR (250 MHz, $CDCl_3$) δ: 8.74 (dd, 2H, $H_{6,6'}$), 8.36 (t, 2H, $H_{3,3'}$), 7.88 (dd, 2H, $H_{4,4'}$), 3.16 (s, 2H, C≡C-H). $^{13}$C {$^1$H} NMR (100 MHz, $CDCl_3$): δ 155.66, 152.30, 140.60, 120.79, 120.42 (arom.), 83.14 (C≡C). EI-mass spectrum: *m*/z 204 ($M^+$). Calc. for $C_{14}H_8N_2$: C, 82.33; H, 3.95; N, 13.72%. Found: C, 82.29; H, 3.98; N, 13.69%.

**6,6′-Bis(ethynyl)-2,2′-bipyridine 2b** White solid, 60% yield. IR ($CH_2Cl_2$): ν/cm$^{-1}$ 2107 (-C≡C-), 3299 (C≡C-H). $^1$H NMR (250 MHz, $CDCl_3$) δ: 8.46 (dd, 2H, $H_{3,3'}$), 7.76 (t, 2H, $H_{4,4'}$), 7.50 (dd, 2H, $H_{5,5'}$), 3.16 (s, 2H, C≡C-H). $^{13}$C {$^1$H} NMR (100.6 MHz, $CDCl_3$): δ 155.66, 141.60, 137.11, 127.79, 121.32, 82.94 (C≡C). EI-mass spectrum: *m*/z 204 ($M^+$). Calc. for $C_{14}H_8N_2$: C, 82.33; H, 3.95; N, 13.72%. Found: C, 82.28; H, 3.99; N, 13.76%.

**6,6″-Bis(ethynyl)-2,2′:6′,2″-terpyridine (3b)** White solid, 65% yield. IR($CH_2Cl_2$): ν/cm$^{-1}$ 3298 (C≡C-H), 2105 (-C≡C-). $^1$H NMR (250 MHz, $CDCl_3$): δ 8.56 (dd, 2H, $H_{3,3''}$), 8.54 (d, 2H, $H_{3',5'}$), 7.95 (t, 1H, $H_{4'}$), 7.81 (t, 2H, $H_{4,4''}$), 7.51 (2H, dd, $H_{5,5''}$), 3.2 (s, 2H, C≡C-H). EI-mass spectrum: *m*/z 281($M^+$). Calc. for $C_{19}H_{11}N_3$: C, 81.12; H, 3.94; N, 14.94%. Found: C, 81.09; H, 3.99; N, 14.98%.

**6,6″-Bis(ethynyl)-4′-phenyl-2,2′:6′,2″-terpyridine (4b)** White solid, 85% yield. IR($CH_2Cl_2$): ν/cm$^{-1}$ 3298 (C≡C-H), 2106 (-C≡C-). $^1$H NMR (250 MHz, $CDCl_3$): δ 8.75 (s, 2H, $H_{3',5'}$), 8.61(dd, 2H, $H_{3,3''}$), 7.86 (td, 2H, $H_{ortho}$ for Ph), 7.83 (2H, t, $H_{4,4''}$), 7.52 (2H, dd, $H_{5,5''}$), 7.46-7.44 (3H, m, $H_{meta\ and\ para}$ for Ph), 3.20 (s 2H, C≡C-H). $^{13}$C {$^1$H} NMR (100.6 MHz, $CDCl_3$): δ 156.61, 155.02, 150.63, 141.66, 138.33, 136.98, 128.94, 127.61, 127.46, 121.19, 119.69(arom.), 83.12 (C≡C). EI-mass spectrum: *m*/z 357 ($M^+$). Calc. for $C_{25}H_{15}N_3$: C, 84.01; H, 4.23; N, 11.76%. Found: C, 83.92; H, 4.18; N, 11.81%.

The di-yne complexes **1M-4M** were synthesized by the general procedure outlined below for **1M**.

***Trans*-[(Ph)($Et_3P$)$_2$Pt-C≡C-R-C≡C-Pt($PEt_3$)$_2$(Ph)] (R = 2,2′-Bipyridine-5,5′-diyl), 1M** To a stirred solution *trans*-[($PEt_3$)$_2$(Ph)PtCl] (0.543 g, 1.0 mmol) and 5,5′-bis(ethynyl)-2,2′-bipyridine (**1b**) (0.102 g, 0.50 mmol) in $CH_2Cl_2$/$^i$$Pr_2NH$ (50 cm$^3$, 1:1

v/v) under nitrogen was added a catalytic amount (~5 mg) of CuI. The yellow solution was stirred at room temperature for 15 h, after which all volatile components were removed under reduced pressure. The residue was dissolved in $CH_2Cl_2$ and passed through a silica column eluting with hexane/$CH_2Cl_2$ (1:1, v/v). Removal of the solvents under *vacuo* gave **1M** as an off-white solid (0.43 g, 70%). IR ($CH_2Cl_2$): $\nu/cm^{-1}$ 2093 (-C≡C-). $^1H$ NMR (250 MHz, $CDCl_3$): δ 8.57 (d, 2H, $H_{6,6'}$), 8.18 (dd, 2H, $H_{3,3'}$), 7.60 (dd, 2H, $H_{4,4'}$), 7.31 (t, 4H, $H_{ortho}$ Ph), 6.95 (t, 4H, $H_{meta}$ Ph), 6.80(t, 4H, $H_{para}$ Ph), 1.75 (m, 24H, $PCH_2$), 1.10 [(t, 36H, $P(CH_2)CH_3$)]. $^{13}C$ {$^1H$} NMR (100.6 MHz, $CDCl_3$): δ 155.80, 151.46, 139.02, 137.94, 120.14, 119.80, 117.13(arom), 107.41 (C≡C), 15.08 ($PCH_2CH_3$), 8.00 ($CH_3$).). $^{31}P\{^1H\}$-NMR (101.3 MHz, $CDCl_3$): δ –131.17, $^1J_{Pt\text{-}P}$ = 2677 Hz. FAB-MS: 1219 ($M^+$). Calc. for $C_{50}H_{76}N_2P_4Pt_2$: C, 49.25; H, 6.28; N, 2.30%. Found: C, 49.18; H, 6.34; N, 2.28%.

***Trans*-[(Ph)($Et_3P$)$_2$Pt-C≡C-R-C≡C-Pt($PEt_3$)$_2$(Ph)] (R = 2,2'-Bipyridine-6,6'-diyl) 2M**. Pale yellow solid (70% yield). IR ($CH_2Cl_2$): $\nu/cm^{-1}$ 2095 (-C≡C-). $^1H$ NMR (250 MHz, $CDCl_3$): δ 8.22 (d, 2H, $H_{3,3'}$), 7.56 (t, 2H, $H_{4,4'}$), 7. 33 (d, 4H, $H_{ortho}$ for Ph), 7.16(d, 2H, $H_{5,5'}$), 6.87(t, 4H, $H_{meta}$ Ph), 6.80(t, 2H, $H_{para}$ Ph), 1.79 (m, 24H, $PCH_2$), 1.12 [(t, 36H, $P(CH_2)CH_3$)]. $^{13}C$ {$^1H$} NMR (100.6 MHz, $CDCl_3$) δ: 155.93, 146.72, 139.13, 135.83, 127.32, 125.67, 121.29, 118.13, 117.47 (arom.), 110.40 (C≡C), 13.62 ($PCH_2CH_3$), 8.20($CH_3$)). $^{31}P\{^1H\}$-NMR (101.3 MHz, $CDCl_3$): δ – 131.10, $^1J_{Pt\text{-}P}$ = 2657 Hz. FAB-MS: 1219 ($M^+$). Calc. for $C_{50}H_{76}N_2P_4Pt_2$: C, 49.25; H, 6.28; N, 2.30%. Found: C, 49.18; H, 6.34; N, 2.26%.

***Trans*-[(Ph)($Et_3P$)$_2$Pt-C≡C-R-C≡C-Pt($PEt_3$)$_2$(Ph)] (R = 2,2':6',2''-terpyridine-6,6''- diyl) 3M** Off-white (65% yield). IR ($CH_2Cl_2$): $\nu/cm^{-1}$ 2096 (-C≡C-). $^1H$ NMR (250 MHz, $CDCl_3$): δ 8.48 (d, 2H, $H_{3,3''}$), 8.35 (dd, 2H, $H_{3',5'}$), 7.86 (t,1H, $H_{4'}$), 7.63 (t, 2H, $H_{4,4''}$), 7.33 (dd, 2H, $H_{5,5''}$), 7.21 (dd, 4H, $H_{ortho}$ for Ph), 6.97(t, 4H, $H_{meta}$ for Ph), 6.80 (t, 2H, $H_{para}$ for Ph), 1.82 (m, 24H, $PCH_2$), 1.11 [(t, 36H, $P(CH_2)CH_3$)]. $^{13}C$ {$^1H$} NMR (100.6 MHz, $CDCl_3$) δ: 156.24, 155.59, 146.94, 139.08, 136.77, 127.84, 127.31, 121.87, 120.80 (arom.), 116.60, 111.37 (C≡C), 15.16 (t, $PCH_2CH_3$), 7.87 ($CH_3$). $^{31}P\{^1H\}$-NMR (101.3 MHz, $CDCl_3$): δ –131.27, $^1J_{Pt\text{-}P}$ = 2659 Hz. FAB-MS: 1297($M^+$). Calc. for $C_{55}H_{79}N_3P_4Pt_2$: C, 50.96; H, 6.14; N, 3.24%. Found: C, 51.13; H, 6.21; N, 3.27%.

***Trans*-[(Ph)($Et_3P$)$_2$Pt-C≡C-R-C≡C-Pt($PEt_3$)$_2$(Ph)] (R = 4′-Phenyl-2,2′:6′,2″-terpyridine-6,6″-diyl) 4M** White solid (55% yield). IR ($CH_2Cl_2$): ν/cm$^{-1}$ 2095 (-C≡C-). $^1$H NMR (250 MHz, $CDCl_3$): δ 8.81 (s, 2H, $H_{3',5'}$), 8.40(dd, 2H, $H_{3,3''}$), 7.89(td, 2H, $H_{ortho}$ for ′-Ph), 7.66 (t, $H_{4,4''}$), 7.48(tt, 2H, $H_{meta}$ for 4′-Ph), 7.42(tt, 1H, $H_{para}$ for 4′-Ph), 7.34(d, 2H, $H_{5,5''}$), 7.23 [(dd, 4H, $H_{ortho}$ for Pt(Ph)], 6.97 [(t, 4H, $H_{meta}$ for Pt(Ph)], 6.79 [(t, 2H, $H_{para}$ for Pt(Ph)], 1.8(m, 2H, $PCH_2$), 1.12 [(t, 36H, $P(CH_2)CH_3$)]. $^{13}$C {$^1$H} NMR (100.6 MHz, $CDCl_3$): δ 156.13, 155.67, 149.20, 146.89, 139.27, 136.10, 128.70, 127.20, 125.82, 121.30, 118.77(arom.), 116.54, 111.46 (C≡C), 15.11 (t, $PCH_2CH_3$), 8.06 ($CH_3$). $^{31}$P{$^1$H}-NMR (101.3 MHz, $CDCl_3$): δ –131.12, $^1J_{Pt\text{-}P}$ = 2659 Hz. FAB-MS: 1373 ($M^+$). Calc. for $C_{61}H_{83}N_3P_4Pt_2$: C, 53.38; H, 6.09; N, 3.06%. Found: C, 53.65; H, 5.98; N, 3.03%.

The poly-ynes **1P-4P** were synthesized by the general procedure outlined below for **1P**.

***Trans*-[-($^n$Bu$_3$P)$_2$Pt-C≡C-R-C≡C-]$_n$, (R = 2,2′-Bipyridine-5,5′-diyl) 1P** CuI (5 mg) was added to a mixture of *trans*-[Pt($PBu^n_3$)$_2$$Cl_2$] (0.670 g, 1.0 mmol) and **1b** (0.204 g, 1 mmol) in $^i$$Pr_2NH$/$CH_2Cl_2$ (50 cm$^3$, 1:1 v/v). The solution was stirred at room temperature for 15 h, after which all volatile components were removed under reduced pressure. The residue was dissolved in $CH_2Cl_2$ and passed through an alumina column. After removal of the solvent, an off-white film was obtained readily which was then washed with methanol to give the polymer **1P** in 85% isolated yield (0.680 g). Further purification was accomplished by precipitating the polymer from dichloromethane solution in methanol. IR ($CH_2Cl_2$): ν/cm$^{-1}$ 2096 (-C≡C-). $^1$H NMR (250 MHz, $CDCl_3$): δ 8.54 (s, 2H, $H_{6,6'}$), 8.18 (d, 2H, $H_{3,3'}$), 7.50 (d, 2H, $H_{4,4'}$), 2.13 [m,12H, $PCH_2(CH_2)_2(CH_3)$], 1.64 [(brs, 12H, $PCH_2(CH_2)_2(CH_3)$], 1.44 [(sex,12H, $PCH_2(CH_2)_2(CH_3)$], 0.91 [(t, 18H, $P(CH_2)_3CH_3$]. $^{13}$C {$^1$H} NMR (100.6 MHz, $CDCl_3$): δ 154.86, 151.42, 138.06, 120.61, 120.30 (arom.), 116.68, 108.40 (C≡C), 28.72-23.71 ($PCH_2CH_2CH_2CH_3$), 13.78 ($CH_3$). $^{31}$P{$^1$H}-NMR (101.3 MHz, $CDCl_3$): δ –137.87, $^1J_{Pt\text{-}P}$ = 2353 Hz. Calc. for $(C_{38}H_{60}N_2P_2Pt)_n$: C, 56.91; H, 7.54; N, 3.49%. Found: C, 57.02; H, 7.67; N, 3.52%. GPC (THF): $M_n$ = 68,900 g.mol$^{-1}$ (n = 86), $M_w$ = 89,570 g.mol$^{-1}$, polydispersity = 1.3.

***Trans*-[-($^n$Bu$_3$P)$_2$Pt-C≡C-R-C≡C-]$_n$, (R = 2,2′-Bipyridine-6,6′-diyl) 2P** Off-white solid (85% yield). IR ($CH_2Cl_2$): ν/cm$^{-1}$ 2095 (-C≡C-). $^1$H NMR (250 MHz, $CDCl_3$): δ 8.33 (d, 2H, $H_{3,3'}$), 7.27 (t, 2H, $H_{4,4'}$), 6.98(d, 2H, $H_{5,5'}$), 2.09 [m,12H, $PCH_2(CH_2)_2(CH_3)$], 1.55 [m,12H, $PCH_2(CH_2)_2(CH_3)$], 1.40 [m,12H, $PCH_2(CH_2)_2(CH_3)$], 0.90 [(t, 18H, $P(CH_2)_3CH_3$]. $^{13}$C {$^1$H} NMR (100.6 MHz, $CDCl_3$): δ 155.86, 146.42, 135.69, 125.61, 121.05 (arom.), 116.47, 110.24 (C≡C), 29.72-22.71 ($PCH_2CH_2CH_2CH_3$), 14.13 ($CH_3$). $^{31}$P{$^1$H}-NMR (101.3 MHz, $CDCl_3$): δ −138.07, $^1J_{Pt\text{-}P}$ = 2357 Hz. Calc. for $(C_{38}H_{60}N_2P_2Pt)_n$: C, 56.91; H, 7.54; N, 3.49%. Found: C, 56.82; H, 7.61; N, 3.51%. GPC (THF): $M_n$ = 60,100 g.mol$^{-1}$ (n = 75), $M_w$ = 102,170 g.mol$^{-1}$, polydispersity = 1.7.

***Trans*-[-($^n$Bu$_3$P)$_2$Pt-C≡C-R-C≡C-]$_n$, (R = 2,2′:6′,2″terpyridine 6,6″-diyl) 3P** Off-white product (80% yield). IR ($CH_2Cl_2$): ν/cm$^{-1}$ 2095 (-C≡C-). $^1$H NMR (250 MHz, $CDCl_3$): δ 8.49 (d, 2H, $H_{3',3''}$), 8.37 (d, 2H, $H_{3',5''}$), 7.84 (t, 1H, $H_{4'}$), 7.65 (t, 2H, $H_{4,4''}$), 7.18 (d, 2H, $H_{5,5''}$), 2.25 [m,12H, $PCH_2(CH_2)_2(CH_3)$], 1.67 [m, 12H, $PCH_2(CH_2)_2(CH_3)$], 1.49 [m,12H, $PCH_2(CH_2)_2(CH_3)$], 0.93 [(t, 18H, $P(CH_2)_3CH_3$]. $^{13}$C {$^1$H} NMR (100.6 MHz, $CDCl_3$): δ 155.76, 155.44, 146.70, 137.00, 136.07, 125.86, 120.99, 120.19 (arom.), 116.81, 110.43 (C≡C), 28.14-24.26 ($PCH_2CH_2CH_2CH_3$), 13.85 ($CH_3$). $^{31}$P{$^1$H}-NMR (101.3 MHz, $CDCl_3$): δ −138.28, $^1J_{Pt\text{-}P}$ = 2350 Hz. Calc. for $(C_{43}H_{63}N_3P_2Pt)_n$: C, 58.75; H, 7.22; N, 4.78%. Found: C, 58.86; H, 7.33; N, 4.81%. GPC (THF): $M_n$ = 72,100 g.mol$^{-1}$ (n = 82), $M_w$ = 129,780 g.mol$^{-1}$, polydispersity = 1.8.

***Trans*-[-($^n$Bu$_3$P)$_2$Pt-C≡C-R-C≡C-]$_n$ (R =4′-Phenyl-2,2′:6′,2″-terpyridine-6,6″-diyl) 4P** Off-white product, 70% yield. IR ($CH_2Cl_2$): ν/cm$^{-1}$ 2095 (-C≡C-). $^1$H NMR (250 MHz, $CDCl_3$):): δ 8.76 (s, 2H, $H_{3',5''}$), 8.43 (d, 2H, $H_{3,3'}$), 7.84 (d, 2H, $H_{ortho}$ for Ph), 7.67 (t, 2H, $H_{4,4''}$), 7.49 (t, 2H, H $_{meta}$ for Ph), 7.44 (t, 1H, $H_{para}$ for Ph), 7.24 (d, 2H, $H_{5,5'}$), 2.24 [m,12H, $PCH_2(CH_2)_2(CH_3)$], 1.65 [(brs, 12H, $PCH_2(CH_2)_2(CH_3)$], 1.47 [(sex, 12H, $PCH_2(CH_2)_2(CH_3)$], 0.87 [(t, 18H, $P(CH_2)_3CH_3$]. $^{13}$C {$^1$H} NMR (100.6 MHz, $CDCl_3$): δ 156.07, 155.82, 149.75, 146.75, 139.39, 136.08, 128.70, 127.35, 126.02, 119.05, 117.47 (arom.), 116.78, 109.48 (C≡C), 29.71-24.15

($PCH_2CH_2CH_2CH_3$), 13.83($CH_3$). $^{31}P\{^1H\}$-NMR (101.3 MHz, $CDCl_3$): δ –137.58, $^1J_{Pt\text{-}P}$ = 2357 Hz. Calc. for $(C_{49}H_{67}N_3P_2Pt)_n$: C, 61.61; H, 7.07; N, 4.40%. Found: C, 61.87; H, 6.97; N, 4.37%. GPC (THF): $M_n$ = 86,800 (n = 91), g.mol$^{-1}$ (n = 82), $M_w$ = 156,240 g.mol$^{-1}$, polydispersity = 1.8.

### 6.2.3 Chapter Four

**2,5-Dibromothieno[3,2-*b*]thiophene**[7]**.** A solution of NBS (21.34 g, 0.12 mol) in DMF (150 mL) was added to a stirred and ice-cooled solution of thieno[3,2-*b*]thiophene (8.35 g, 59.58 mmol) in DMF (70 mL). After the mixture was stirred for 3 h under ice cooling, crushed ice was added and the resulting mixture was extracted with $CH_2Cl_2$. The extracts were washed with water, dried over $MgSO_4$, and evaporated. The residue was subjected to alumina column chromatography. $^1H$ NMR (500 MHz, $CDCl_3$) *δ*: 7.62 (s, 2H, thienothiophene). $^{13}C$ NMR (100.6 MHz, $CDCl_3$) *δ*: 124.48, 126.53, 138.67. EIMS (*m/z*): 298.

**5,5'-Dibromodithieno[3,2-*b*:2,3-*d*]thiophene**[7]**.** 0.98 g (5.0 mmol) of dithieno[3,2-*b*:2-3-*d*]thiophene in DMF(20 cm$^3$) was reacted with 2 g (11.2 mmol) of NBS at room temperature overnight. The light yellow suspension was treated with water and filtered off. After silica column chromatography with hexane, 1.7 g (88%) pale greenish crystals was obtained. $^1H$ NMR (*δ* , 500 MHz, $CDCl_3$): 7.27 (s, 2H, thiophenes). $^{13}C$ NMR (100.6 MHz, $CDCl_3$) *δ*: 112.32, 123.17, 130.82, 139.05. EI (*m/z*): 353.8.

**2,5-Bis(trimethylsilylethynyl)thieno[3,2-*b*]thiophene 4a.** To a solution of 2,5-dibromothieno[3,2-*b*]thiophene (2.0 g, 6.71 mmol) in $^iPr_2NH$–THF (70 cm$^3$, 1 : 1 v/v) under nitrogen was added a catalytic mixture of CuI (20 mg), $Pd(OAc)_2$ (20 mg) and $PPh_3$ (60 mg). The solution was stirred for 20 min. at 50 $^0$C and then trimethylsilylethyne (1.64 g, 16.7 mmol) was added. The reaction mixture was left with stirring for 20 h at 75 $^0$C. The completion of the reaction was determined by silica TLC and IR spectroscopy. The solution was allowed to cool down to room temperature, filtered and the solvent mixture removed under reduced pressure. The residue was subjected to silica column chromatography using hexane to afford **4a** as a

colourless solid in 85% yield (1.78 g). IR ($CH_2Cl_2$): $\nu$/cm$^{-1}$ 2141 (–C≡C–). $^1$H NMR (250 MHz, $CDCl_3$)$\delta$: 0.26 (s, 18H, $SiMe_3$), 7.26 (s, 2H, fused bithienyl). $^{13}C\{^1H\}$ NMR (100 MHz, $CDCl_3$) $\delta$: 0.04 (s, $SiMe_3$), 97.68, 101.68 (–C≡C–), 124.60, 126.71, 138.75 (fused bithienyl). EI MS: *m/z*: 332 ($M^+$). Calc. for $C_{16}H_{20}Si_2S_2$: C, 57.80; H, 6.06. Found C, 57.68; H, 6.01%.

**2,5-Bis(ethynyl)thieno[3,2*b*]thiophene 4b.** The bis-trimethylsilylethynyl derivative **4a** (1.0 g, 3.01 mmol) was desilylated in THF–methanol (50 cm$^3$, 4:1 v/v) using aqueous KOH (0.38 g, 6.86 mmol in 1 cm$^3$ $H_2O$). The reaction mixture was stirred at room temperature for 2 h, solvent was then removed and the crude product was purified by silica column chromatography using hexane. **4b** was then isolated as a yellow solid in 95% yield (0.54 g). IR ($CH_2Cl_2$): $\nu$/cm$^{-1}$ 2105 (–C≡C–), 3297 (C≡C–H). $^1$H NMR (500 MHz, $CDCl_3$) $\delta$: 3.50 (s, 2H, C≡CH), 7.25 (s, 2H, thienothiophene). $^{13}C$ $\{^1H\}$ NMR (100.6 MHz, $CDCl_3$) $\delta$,: 79.81, 82.56 (C≡C), 123.88, 133.92, 138.06 (thienothiophene). EIMS (*m/z*): 188 (Calc. *M*r = 188.26).

**5,5'-Bis(trimethylsilylenthynyl)dithieno[3,2-*b*:2,3-*d*]thiophene 5a.** This compound was synthesised by the same method as for **4a** using 1.56 g (4.4 mmol) 5,5'-dibromodithieno[3,2-*b*:2,3-*d*]thiophene. The product was purified by alumina column chromatography with hexane and subsequent recrystallisation from methanol. Yield: 0.91 g (52%) light yellow crystalline solid. IR ($CH_2Cl_2$): $\nu$/cm$^{-1}$ 2141 (–C≡C–). $^1$H NMR (500 MHz, $CDCl_3$) $\delta$: 0.26 (s, 18H, H of TMS), 7.37 (s, 2H, H of thiophenes). $^{13}C$ $\{^1H\}$ NMR (100.6 MHz, $CDCl_3$) $\delta$: 0.25 (s, $SiMe_3$); 97.54, 101.14 (–C≡C–); 124.13, 125.82, 131.15, 141.58 (aromatic C of thiophenes). EIMS (*m/z*): 388.03 (Calc. *M*r = 388.71). Anal. Calc. for $C_{18}H_{20}S_3Si_2$: C, 55.62; H, 5.19. Found: C, 55.85; H, 5.29%.

**5,5-Bis(ethynyl)dithieno[3,2-*b*:2,3-*d*]thiophene 5b.** Compound **5a** was proto-desilylated as **4b** and the crude product was worked up, as before, to yield a red solid in 76% yield. IR ($CH_2Cl_2$): *m*/cm$^{-1}$ 2101 (–C≡C–), 3298 (C≡C–H). $^1$H NMR (500 MHz, CDCl3) $\delta$: 3.50 (s, 2H, C≡CH), 7.31 (s, 2H, dithienothiophene). $^{13}C$ $\{^1H\}$ NMR (100.6 MHz, CDCl3) $\delta$: 79.50, 80.16 (C≡C), 120.73, 126.76, 131.17 141.61 (dithienothiophene). EIMS (*m/z*): 244. (Calc. *M*r = 244.34).

***Trans*-[(Ph)($Et_3P$)$_2$Pt-C≡C-R-C≡C-Pt($PEt_3$)$_2$(Ph)] (R = thieno[3,2b]thiophene-2,5-diyl) 4M.** To a stirred solution of *trans*-[(Ph)($PEt_3$)$_2$PtCl] (0.543 g, 1.0 mmol) and **4b** (0.094 g, 0.5 mmol) in $^{i}Pr_2NH$-$CH_2Cl_2$ (50 $cm^3$, 1:1 v/v) under nitrogen was added CuI (5 mg). The yellow solution was stirred at room temperature for 15 h., after which all volatile components were removed under reduced pressure. The residue was dissolved in $CH_2Cl_2$ and passed through a silica column eluting with hexane-$CH_2Cl_2$ (1:1, v/v). Removal of the solvents *in vacuo* gave **4M** as a pale yellow solid in 70% yield (0.42 g). IR ($CH_2Cl_2$): $\nu/cm^{-1}$ 2085 (-C≡C-). $^1H$ NMR (250 MHz, $CDCl_3$): δ 7.53 (s, 2H, thienothiophene), 7.34 (d, 4H, $H_{ortho}$ of Ph), 6.92(t, 4H, $H_{meta}$ of Ph), 6.77 (t, 2H, $H_{para}$ of Ph), 1.87-1.80 (m, 24H, P-$CH_2$), 1.10 (m, 36H, P-$CH_2CH_3$). $^{13}C\{^1H\}$ NMR (100 MHz, $CDCl_3$): δ 7.82 (P-$CH_2CH_3$), 13.18 (P-$CH_2$), 105.94, 106.76 (C≡C), 126.93, 127.45, 130.85, 132.54, 135.99, 143.52, 150.08 (aromatic and hetero-aromatic). $^{31}P\{^1H\}$-NMR (101.3 MHz, $CDCl_3$): δ –131.17, ($^1J_{Pt-P}$ = 2628 Hz). FABMS: *m*/z 1203 ($M^+$). Calc. for $C_{46}H_{72}P_4S_2Pt_2$: C, 45.92; H, 6.03. Found C, 46.12; H, 5.98%.

***Trans*-[(Ph)($Et_3P$)$_2$Pt-C≡C-R-C≡C-Pt($PEt_3$)$_2$(Ph)] (R = dithieno[3,2-b:2',3'-d]thiophene-5,5'-diyl) 5M.** This compound was synthesized employing similar reaction conditions to those of **4M** but using **5b** instead of **4b**. The product came as yellow solid in an isolated yield of 65%. IR ($CH_2Cl_2$): $\nu/cm^{-1}$ 2083 (-C≡C-). $^1H$ NMR (250 MHz, $CDCl_3$): δ 7.38 (s, 2H, dithienothiophene), 7.32 (d, 4H, $H_{ortho}$ of Ph), 6.95 (d, 4H, $H_{meta}$ of Ph), 6.80 (t, 2H, $H_{para}$ of Ph), 1.75 (m, 24H, P-$CH_2$), 1.07 (m, 36H, P-$CH_2CH_3$). $^{13}C\{^1H\}$ NMR (100.6 MHz, $CDCl_3$): δ 7.90 (P-$CH_2CH_3$), 15.22, (P-$CH_2$), 108.85, 111.01, (C≡C), 126.93, 127.45, 130.85, 132.54, 135.99, 143.52, 150.08, 156.21 (aromatic and hetero-aromatic). $^{31}P\{^1H\}$-NMR (101.3 MHz, $CDCl_3$): δ –131.17, ($^1J_{Pt-P}$ = 2653 Hz). FABMS: *m*/z 1259 ($M^+$). Calc. for $C_{48}H_{72}P_4S_3Pt_2$: C, 50.41; H, 6.43. Found C, 50.69; H, 6.58%.

***Trans*-[-($^{n}Bu_3P$)$_2$Pt-C≡C-R-C≡C-]$_n$, (R =thieno[3,2b]thiophene-2,5-diyl) 4P.** CuI (5 mg) was added to a mixture of *trans*-[Pt($P^{n}Bu_3$)$_2$$Cl_2$] (0.670 g, 1.0 mmol) and **4b** (0.188 g, 1.0 mmol) in $^{i}Pr_2NH$-$CH_2Cl_2$ (50 $cm^3$, 1:1 v/v). The solution was stirred at room temperature for 15 h, after which all volatile components were removed under reduced pressure. The residue was dissolved in $CH_2Cl_2$ and passed through an alumina column.

After removal of the solvents, an orange film was obtained readily which was then washed with methanol to give the polymer **4P** in 85% isolated yield (0.67 g). Further purification was accomplished by precipitating the polymer solution in methanol from dichloromethane. IR ($CH_2Cl_2$): $\nu/cm^{-1}$ 2082 (-C≡C-). $^1H$ NMR (250 MHz, $CDCl_3$): δ 7.21 (s, 1H, thienothiophene), 6.94 (s, 1H, thienothiophene), 2.17 (m, 12H, P-$CH_2$), 1.60 (br, 12H, $CH_2$), 1.41 (sextet, 12H, $CH_2$), 1.08 (t, 18H, $CH_3$). $^{13}C\{^1H\}$ NMR (100 MHz, $CDCl_3$): δ 13.84 ($PCH_2CH_2CH_2CH_3$), 23.76-26.35 ($PCH_2CH_2CH_2$). 111.16, 112.23 (C≡C), 119.48, 132.89, 136.76 (thienothiophene). $^{31}P\{^1H\}$-NMR (101.3 MHz, $CDCl_3$): δ −138.03, ($^1J_{Pt-P}$ = 2363 Hz). Calc. for $(C_{34}H_{56}P_2S_2Pt)_n$: C, 51.96; H, 7.18. Found C, 52.09; H, 7.23 %. GPC (THF): $M_n$ = 223,200 g $mol^{-1}$ (n = 284), $M_w$ = 401,800 g $mol^{-1}$, PDI = 1.8.

***Trans*-[-($^nBu_3P$)$_2$Pt-C≡C-R-C≡C-]$_n$ (R= dithieno[3,2-b:2',3'd]thiophene-5,5'-diyl) 5P.** This compound was synthesized by adopting similar reaction conditions to those of **4P** but using **5b** instead of **4b.** Brown red solid was obtained in 90% yield. IR ($CH_2Cl_2$): $\nu/cm^{-1}$ 2081 (-C≡C-). $^1H$ NMR (250 MHz, $CDCl_3$): δ 7.26 (s, 1H, dithienothiophene), 6.96 (s, 1H, dithienothiophene), 2.12 (t, 12H, $PCH_2$), 1.54 (m, 12H, $CH_2$), 1.48 (br, 12H,$CH_2$), 1.25 (t, 18H, $CH_3$). $^{13}C\{^1H\}$ NMR (100.6 MHz, $CDCl_3$): δ13.84 ($PCH_2CH_2CH_2CH_3$), 23.76-26.35 ($PCH_2CH_2CH_2$). 108.39, 110.28 (C≡C), 120.34, 128.52, 129.40, 139.86 (dithienothiophene). $^{31}P\{^1H\}$-NMR (101.3 MHz, $CDCl_3$): δ −138.03, ($^1J_{Pt-P}$ = 2373 Hz). Calc. for $(C_{36}H_{56}P_2S_3Pt)_n$: C, 51.35; H, 6.70. Found C, 51.69; H, 6.78 %. GPC (THF): $M_n$ = 222,300 $gmol^{-1}$ (n = 264), $M_w$ = 422,400 g $mol^{-1}$, PDI = 1.9.

## 6.2.4 Chapter Five

**4,7-dibromo-2,1,3-benzothiadiazole[8].A** A mixture of 2,1,3-benzothiadiazole (13.6g, 0.1 mol) and 100 mL of 47% HBr was heated to reflux with stirring while 16.5 mL of bromine was added dropwise within 1 h. After 3 h., the mixture was filtered while hot, cooled and filtered again, washed with water and dried to give 30.5g, 98% of the desired product as a white solid m.p. 189-190 $^0$C.

**3,6-dibromo-1,2-phenylenediamine**[9] To a solution of 4,7-dibromo-2,1,3-benzothiadiazole ( 15.3 g, 52 mmol) in absolute EtOH (500 mL) was added portionwise $NaBH_4$ (36.4g, 960 mmol) at 0 $^{o}$C. The mixture was then stirred for 18 hours at r.t. After evaporation of the solvent, 500 mL of water was added and the mixture was extracted three times with ether. The combined extracts was washed with brine and dried over $NaSO_4$. Evaporation of the solvent gave 3,6-dibromo-1,2-phenylenediamine as a pale yellow solid in 12g, 87% yield.

**2,3-Diphenyl-5,8-dibromoquinoxaline**[9] **B** benzil(2g, 9.51 mmol) was added portionwise to a solution of 3,6-dibromo-1,2-phenylenediamine (2.12g, 8.0mmol) in ethanol (50 mL). The reaction mixture was refluxed for 3 h, and then cooled to r.t. a pale yellow precipitate was separated by filtration. It was then subjected to silica column chromatography eluting with hexane/$CH_2Cl_2$ (1:1, v/v) to give the title compound as a pale yellow solid in 60% yield.

**5,8-diiodoquinoline**[10]**.C** Quinoline (12g, 93 mmol) was dissolved in conc. $H_2SO_4$ (200mL, 98%) containing $Ag_2SO_4$ (31g, 99.5 mmol). The mixture was heated at 200 $^{0}$C. $I_2$ (12g,47 mmol) was then added in small quantities and the mixture was stirred for 1 h. It was then basified with NaOH solution, filtered and washed with water and with sodium thiosulfate solution. It was then subjected to silica column chromatography eluting with hexane/$CH_2Cl_2$ (1:1, v/v) to give the title compound as a white solid in 70% yield.

**1-(2-ethylhexyl)oxy-4-methoxybenzene**[11] A solution of 4-methoxyphenol (29.3 g, 236 mmol) in dry methanol (150 mL) was added under Ar to a solution made from Na metal (6.50g, 283 mmol) in 100 mL methanol. The mixture was then heated at reflux for 30 mins. After the reaction mixture was cooled to r.t. a solution of 2-ethylhexylbromide (54.6 g, 284 mmol) was added dropwise and the mixture was then heated at reflux overnight. The solvent was then removed in vacuum and the residue was dissolved in ether (300 mL), washed with dilute aqueous sodium hydroxide (600 mL) and water (600 mL), dried over $MgSO_4$ and concentrated again. It was then subjected to silica column chromatography eluting with hexane/$CH_2Cl_2$ (4:1, v/v) to give the title compound as a yellow viscous liquid in 70% yield.

**2,5-Diiodo-1-(2-ethylhexyl)oxy-4-methoxybenzene D Method A**. ICl (4.46 g, 27.5 mmol) in acetic acid (10 $cm^3$) was added to 1-(2-ethylhexyloxy)-4-methoxybenzene (2.95 g, 12.5 mmol) in acetic acid (15 $cm^3$) . The reaction mixture was heated with stirring at 100 °C for 2h and then cooled to room temperature. Aqueous $Na_2S_2O_4$ (20%) was added until the brown colour of iodine had disappeared, and the reaction mixture was poured into ice water (100 $cm^3$). The organic layer was collected and the aqueous layer was extracted with hexane (3 x 100 $cm^3$). The combined organic layers were dried over $MgSO_4$, and the solvent was removed under *vacuo* to give a brown oil. After column chromatography (silica gel, hexane) the pure product was obtained as a thick yellow liquid (5.18 g, 85%).

**Method B**. 1-(2-Ethylhexyloxy)-4-methoxybenzene (2.95 g, 12.5 mmol), $KIO_4$ (3.45 g, 15 mmol) and iodine (3.8 g, 15 mmol) were added to a stirred solution of acetic acid (22.5 $cm^3$), water (1.75 $cm^3$) and $H_2SO_4$ (0.75 $cm^3$). The resulting solution was stirred for 20 h at 70 °C and then cooled to room temperature. The product was worked up as in method A to obtain a yellow liquid (5.49 g, 90%). $^1H$ NMR (250 MHz, $CDCl_3$): δ 7.15 (s, 1H, $H_6$), 7.14 (s, 1H, $H_3$), 3.85 (d, 2H, $H_{1'}$), 3.80 (s, 3H, O-$CH_3$), 1.72 (m, 1H, $H_{2'}$), 1.50 (m, 4H, $H_{5',2''}$), 1.31 (m, 4H, $H_{3',4'}$), 0.87 (t, 6H, $H_{6',3''}$). $^{13}C\{^1H\}$-NMR (100.6 MHz, $CDCl_3$): δ 153.12 ($C_{1,4}$), 122.44 ($C_6$), 121.56 ($C_3$), 86.12 ($C_2$), 85.41 ($C_5$), 72.36 ($C_{1'}$), 57.10 (O-$CH_3$), 39.46 ($C_{2'}$), 30.51 ($C_{3'}$), 29.05 ($C_{4'}$), 23.95 ($C_{2''}$), 23.03 ($C_{5'}$), 14.10 ($C_{6'}$), 11.22 ($C_{3''}$). EI mass spectrum: m/z 488 ($M^+$). (Found: C, 37.01; H, 4.48. Calc. for $C_{15}H_{22}O_2I_2$: C, 36.91; H, 4.54%).

**2,5-Bis(trimethylsilylethynyl)-1-(2-ethylhexyloxy)-4-methoxybenzene 1a** To a solution of 2,5-diiodo-1-(2-ethylhexyloxy)-4-methoxybenzene (2.00 g, 4.10 mmol) in $^iPr_2NH$/THF (70 $cm^3$, 1:4 v/v) under nitrogen were added catalytic amounts of CuI (10 mg, 0.05 mmol), $Pd(OAc)_2$ (10 mg, 0.04 mmol) and $PPh_3$ (30 mg, 0.11 mmol). The solution was stirred for 30 min at room temperature and then trimethylsilylethyne (1.00 g, 10.18 mmol) was added at room temperature to the vigorously stirred solution; during the addition a white precipitate formed. After the addition was completed, the reaction mixture was stirred at reflux for 2 h. The completion of the reaction was determined by silica TLC and IR spectroscopy. After being cooled to room temperature, the mixture was filtered to eliminate the ammonium salt and the solvent mixture was removed under *vacuo*. The soiled residue was dissolved in

dichloromethane and subjected to silica column chromatography eluting with hexane/$CH_2Cl_2$ (1:2 v/v) to afford **1a** as viscous oil which crystallised as a pale-brown solid (1.32 gm, 75%) on standing overnight. IR ($CH_2Cl_2$): $\nu/cm^{-1}$ 2159 $cm^{-1}$ (C≡C). $^1H$ NMR (250 MHz, $CDCl_3$): δ 6.89 (s, 1H, $H_6$), 6.87 (s, 1H, $H_3$), 3.87 (d, 2H, $H_{1'}$), 3.83 (s, 3H, O-$CH_3$), 1.71 (m, 1H, $H_{2'}$), 1.48 (m, 4H, $H_{5',2''}$), 1.28 (m, 4H, $H_{3',4'}$), 0.86 (t, 6H, $H_{6',3''}$), 0.065 (s, 18H, $SiMe_3$). $^{13}C\{^1H\}$-NMR (100.6 MHz, $CDCl_3$): δ 154.40, 154.08, 116.01, 114.91, 113.39, 112.93, 101.06 (C≡C), 100.19 (C≡C), 71.72, 56.66 (O-$CH_3$), 39.63, 30.57, 29.19, 23.97, 23.13, 14.16, 11.35, -0.002 ($SiMe_3$). EI mass spectrum: m/z 428 ($M^+$). (Found: C, 70.12; H, 9.34. Calc. For $C_{25}H_{40}O_2Si_2$: C, 70.03; H, 9.40%).

**2,5-Bisethynyl-1-(2-ethylhexyloxy)-4-methoxybenzene 1b** Compound **1a** (1.00 g, 2.33 mmol) was proto-desilylated in THF/methanol (50 $cm^3$, 4:1, v/v) using aqueous KOH (0.287 g, 5.12 mmol in 1 $cm^3$ water). The reaction mixture was stirred at room temperature for 2 h during which period IR and TLC showed that all protected compound had been converted to the terminal alkyne ligand. The solvent mixture was then removed and the residue was dissolved in $CH_2Cl_2$ and subjected to column chromatography on silica using hexane/$CH_2Cl_2$ (1:2 v/v) as eluant. The solvent mixture was removed to give **1b** (0.50 g, 75%) as a yellow oil. This compound was somewhat unstable; storage overnight under nitrogen at 4°C resulted in the oil darkening its colour. Long storage times led to the formation of a black tarry liquid that was presumed to be a polymerisation product. This ligand was, therefore, freshly prepared for use in further synthesis. IR ($CH_2Cl_2$): $\nu/cm^{-1}$ 2107 (C≡C), 3299 (C≡C-H). $^1H$ NMR (250 MHz, $CDCl_3$): δ 6.95 (s, 1H, $H_6$), 6.93 (s, 1H, $H_3$), 3.88 (d, 2H, $H_{1'}$), 3.82 (s, 3H, O-$CH_3$), 3.37 (s, 2H, C≡C-H), 1.72 (m, 1H, $H_{2'}$), 1.51-1.25 (m, 8H, $H_{3',4',5',2''}$), 0.86 (t, 6H, $H_{6',3''}$). $^{13}C$ $\{^1H\}$-NMR (100.6 MHz, $CDCl_3$): δ 154.38, 154.24, 117.73, 115.91, 113.37, 112.48, 82.53 (C≡C), 79.74 (C≡C), 72.09, 56.35 (O-$CH_3$), 39.34, 30.46, 29.02, 23.86, 23.01, 14.04, 11.12. EI mass spectrum: m/z 284 ($M^+$).

**5,8-Bis(trimethysilylethynyl)quinoline 2a** 5,8-Diiodoquinoline (2.00 g, 5.24 mmol), trimethylsilylethyne (1.28 g, 13.03 mmol) and $^iPr_2NH$/THF (70 $cm^3$, 1:4 v/v) were mixed with catalytic amounts of CuI (12 mg), $Pd(OAc)_2$ (12 mg) and $PPh_3$ (36 mg). The crude product was worked-up, as before, to yield a pale-brown residue, which

was then applied to a silica column in hexane and eluted with the same solvent. The desired compound **2a** was obtained as an off-white solid in 80% isolated yield. IR ($CH_2Cl_2$): ν/cm$^{-1}$ 2159 cm$^{-1}$ (C≡C). $^1$H NMR (250 MHz, $CDCl_3$): δ 9.02 (dd, 1H, $H_2$), 8.59 (dd, 1H, $H_4$), 7.85 (d, 1H, $H_7$), 7.65 (d, 1H, $H_6$), 7.49 (dd, 1H, $H_3$), 0.32 (t, 18H, $SiMe_3$). $^{13}$C{$^1$H}-NMR (100.6 MHz, $CDCl_3$): δ 151.49, 147.85, 134.97, 134.23, 130.34, 128.67, 124.06, 122.17, 121.63, 102.52 (C≡C), 101.43 (C≡C), 0.53 ($SiMe_3$). EI mass spectrum: m/z 321 ($M^+$). (Found: C, 70.87; H, 7.19. Calc. for $C_{19}H_{23}NSi_2$: C, 70.97; H, 7.21%).

**5,8-Bisethynylquinoline 2b** Compound **2a** was proto-desilylated as in **1a** and the crude product was worked up, as before, to yield a dark-yellow solid. Silica column chromatography with hexane/$CH_2Cl_2$ (1:1 v/v) gave a pale yellow solid identified as **2b**. Yield: 85%. IR ($CH_2Cl_2$): ν/cm$^{-1}$ 2107 (C≡C), 3299 (C≡C-H). $^1$H NMR (250 MHz, $CDCl_3$): δ 9.01 (dd, 1H, $H_2$), 8.57 (dd, 1H, $H_4$), 7.84 (d, 1H, $H_7$), 7.65 (d, 1H, $H_6$), 7.47 (dd, 1H, $H_3$), 3.65 (s, 2H, C≡C-H). $^{13}$C{$^1$H}-NMR (100.6 MHz, $CDCl_3$): δ 151.57, 148.00, 134.83, 133.82, 130.69, 128.67, 123.31, 122.08, 121.00, 84.58 (C≡C), 80.57 (C≡C). EI mass spectrum: m/z 177 ($M^+$). (Found: C, 88.09; H, 4.02. Calc. for $C_{13}H_7N$: C, 88.11; H, 3.98%).

**2,3-Diphenyl-5,8-bis(trimethylsilylethynyl)-quinoxaline 3a** This compound was prepared as described above for **1a** from 2,3-diphenyl-5,8-diiodo-quinoxaline (2.00 g, 3.74 mmol), trimethylsilylethyne (0.92 g, 9.36 mmol), CuI (10 mg), $Pd(OAc)_2$ (10 mg), $PPh_3$ (30 mg) in $^iPr_2NH$/THF (50 cm$^3$, 1:4 v/v). After the usual work-up, the soiled residue was purified by silica column chromatography eluting with dichloromethane-hexane (2:1 v/v) to yield an off-white solid identified as **3a**. Recrystallization from hexane-dichloromethane led to snow-white crystals of **3a** in 78% yield (1.39 g). IR ($CH_2Cl_2$): ν/cm$^{-1}$ 2159 cm$^{-1}$ (C≡C). $^1$H NMR (250 MHz, $CDCl_3$): δ 7.83 (s, 2H, $H_{6,7}$), 7.74 (dd, 4H, $H_{ortho}$ of Ph), 7.37-7.25 (m, 6H, $H_{meta, para}$ of Ph), 0.35 (s, 18H, $SiMe_3$). $^{13}$C{$^1$H}-NMR (100.6 MHz, $CDCl_3$): δ 152.95, 141.02, 138.71-123.46 ($C_{5-8}$ and Ph Cs), 103.71 (C≡C), 101.29 (C≡C), 0.002 ($SiMe_3$). EI mass spectrum: m/z 474 ($M^+$). (Found: C, 75.84; H, 6.28. Calc. for $C_{30}H_{30}N_2Si_2$: C, 75.90; H, 6.37%).

**2,3-Diphenyl-5,8-bisethynylquinoxaline 3b** This compound was synthesized as described above for **1b** from **3a** (1.00 g, 2.1 mmol) and KOH (0.26 g, 4.6 mmol) in THF/methanol (50 $cm^3$, 4:1, v/v). The residue dissolved in $CH_2Cl_2$ was subjected to a silica column and the desired colourless band was collected with the aid of hexane-dichloromethane (1:1 v/v) to afford **3b** (0.63 g, 90%) as a white solid. IR ($CH_2Cl_2$): $\nu/cm^{-1}$ 2107 (C≡C), 3299 (C≡C-H). $^1H$ NMR (250 MHz, $CDCl_3$): δ 7.89 (s, 2H, $H_{6,7}$), 7.58 (dd, 4H, $H_{ortho}$ of Ph), 7.36-7.25 (m, 6H, $H_{meta, para}$ of Ph), 3.62 (s, 2H, C≡C-H). $^{13}C\{^1H\}$-NMR (100.6 MHz, $CDCl_3$): δ 153.83, 141.22, 138.55-123.07 ($C_{5-8}$ and Ph Cs), 85.35 (C≡C), 79.98 (C≡C). EI mass spectrum: m/z 330 ($M^+$). (Found: C, 87.17; H, 4.31. Calc. for $C_{24}H_{14}N_2$: C, 87.25; H, 4.27%).

**4,7-Bis(trimethylsilylethynyl)-2,1,3-benzothiadiazole 4a** This compound was prepared as described above for **1a** from 4,7-dibromo-2,1,3-benzothiadiazole (1.52 g, 5.17 mmol), trimethylsilylethyne ((1.27 g, 12.93 mmol), CuI (10 mg), $Pd(OAc)_2$ (10 mg), $PPh_3$ (30 mg) in $NHPr^i_2$/THF (50 $cm^3$, 1:4 v/v). After the usual work-up, the soiled residue was purified by silica column chromatography eluting with hexane/$CH_2Cl_2$ (1:2 v/v) to yield light yellow solid identified as **4a** in 78% yield (1.32 g). IR ($CH_2Cl_2$): $\nu/cm^{-1}$ 2159 $cm^{-1}$ (C≡C). $^1$HNMR (250 MHz, $CDCl_3$): δ 7.68 (s, 2H, $H_{5,6}$), 0.30 (s, 18H, $SiMe_3$). $^{13}C\{^1H\}$-NMR (100.6 MHz, $CDCl_3$): δ 154.20, 133.09, 117.25, 103.60 (C≡C), 99.98 (C≡C), -0.14 ($SiMe_3$). EI mass spectrum: m/z 328.4 ($M^+$). (Found: C, 58.56; H, 6.16. Calc. for $C_{16}H_{20}N_2Si_2S$: C, 58.49; H, 6.14%).

**4,7-Bisethynyl-2,1,3-benzothiadiazole 4b** This compound was synthesized from **4a** (1.00 g, 3.04 mmol) and KOH (0.375 g, 6.70 mmol). The residue dissolved in $CH_2Cl_2$ was applied to a silica column and the desired light yellow band was collected with the aid of hexane/$CH_2Cl_2$ (1:1 v/v) to afford **4b** (0.51 g, 90%) as an off-white solid. IR ($CH_2Cl_2$): $\nu/cm^{-1}$ 2107 (C≡C), 3300 (C≡C-H). $^1$HNMR (250 MHz, $CDCl_3$): δ 7.64 (s, 2H, $H_{5,6}$), 3.60 (s, 2H, C≡C-H). $^{13}C\{^1H\}$-NMR (100.6 MHz, $CDCl_3$): δ 154.28, 133.17, 116.68, 102.35 (C≡C ), 99.53 (C≡C). EI mass spectrum: m/z 184 ($M^+$). (Found: C, 65.34; H, 2,22. Calc. for $C_{10}H_4N_2S$: C, 65.20; H, 2.19%).

**5,5'-Dibromo-2-(2'-thienyl)pyridine**[12] **E.** In the absence of light, NBS (2.66 g, 15 mmol) was added portionwise at 20 C to a solution of 2-(2'-thienyl)pyridine ( 1.12 g,

7 mmol)) in DMF (25 mL). The reaction mixture was stirred for 3 h, poured onto ice forming a yellow–brown precipitate. The solid was filtered off, washed several times with water and dried *in vacuo* over $P_2O_5$. The crude product was puri.ed by column chromatography on alumina using $CH_2Cl_2$–hexane (4:1 v/v) to yield a yellow solid. Recrystallisation from ethanol afforded 2.12 g (88% yield) as a yellow solid. $^1H$ NMR (250.13 MHz, $CDCl_3$) 8.58 (d, 1H, H-6)7.70 (dd, 1H, H-4), 7.52 (d, 1H, H-3), 7.39 (d, 1H, H-3), 7.20 (d, 1H, H-4). EI-mass spectrum: *m/z* 319.3; Calc. 319.2. Calc for $C_9H_5NSBr_2$: C, 33,86; H, 1.58; N, 4.39. Found: C, 33.91; H, 1.65; N, 4.47%

**5,5'-Dibromo-2,5-bis(2-thienyl)pyridine F.** similar procedure as in **E** was adopted using 2,5-bis(2-thienyl)pyridine instead of 2'-(thienyl)pyridine to afford **F** as a bright yellow solid in 8% yield. $^1H$ NMR (250.13 MHz, $CDCl_3$) δ: (8.74 (d, 1H, H-6), 7.75 (dd, 1H, H-4), 7.60 (dd, 1H, H-3), 7.42 (d, 2H, H-3), 7.21 (d, 2H, H-4). EI-mass spectrum: *m/z* 401.3; Calc. 401.3. Calc for $C_{13}H_7NS_2Br_2$: C, 38.90; H, 1.76; N, 3.49. Found: C, 38.98; H, 1.74; N, 3.53%.

**5,5-Dibromo-6,6-bis(2-thienyl)-3,3-bipyridine G.** similar procedure as in **E** was adopted using 6,6-bis(2-thienyl)-3,3-bipyridine instead of 2'-(thienyl)pyridine to afford **G** as a bright yellow solid in 76% yield. $^1H$ NMR (250.13 MHz, $CDCl_3$): δ 8.78 (dd, 2H, H-2), 8.01 (dd, 2H, H-4), 7.82 (dd, 2H, , H-5), 7.46 (d, 2H, H-3), 7.25 (d, 1H, H-4). EI-mass spectrum: *m/z* 478.5; Calc. 478.4. Calc for $C_{18}H_{10}N_2S_2Br_2$: C, 45.19; H, 2.11; N, 5.86. Found: C, 45.23; H, 2.14; N, 5.95%.

**5,5′-Bis(trimethylsilylethynyl)-2-(2′-thienyl)-pyridine 5a**: Similar procedures as for **4a** were adopted using 5,5′-dibromo-2-(2′-thienyl)-pyridine (2.0 g, 6.27 mmol) to produce a light yellow trimethylsilylethynyl-derivative **5a** in 60% yield (0.66 g). Calc. for $C_{19}H_{23}Si_2SN$**:** C, 64.50; H, 6.6; N, 3.96. Found: C, 64.47; H, 6.61; N, 3.93.

**5,5′- Di(ethynyl) -2- (2′-thienyl)-pyridine 5b**:Compound **5b** was synthesised from **5a** adopting a similar procedure to that described above for **4b**. The product was obtained as a pale yellow solid in 84% yield after purification using silica column and $CH_2Cl_2$/hexane (1:2) as eluent. Calc. for $C_{13}H_7SN$: C,74.6; H, 3.37; N, 6.69. Found: C, 74.58; H,3.50; N, 6.60.

**5′,5′′-Bis(trimethylsilylethynyl)-2,5-bis(2′-thienyl)-pyridine 6a** Similar procedures as for **4a** were adopted using 5′,5′′-Dibromo-2,5-bis(2′-thienyl)-pyridine (3g, 7.48 mmol). The product eluted as a bright yellow band from the column chromatrography which was further purified by recrystallisation from warm 2:1 toluene / $CH_2Cl_2$ as a glistering yellow flakes in 67% yield (2.2 g). Calc. for $C_{23}H_{25}Si_2S_2N$: C, 63.4; H, 5.78; N, 3.21. Found: C, 61.9; H, 5.62; N, 3.03.

**5′,5′′-Di(ethynyl)-2,5-bis(2′-thienyl)-pyridine 6b**: Compound **6b** was synthesised from **6a** adopting a similar procedure to that described above for **4b**. The product was obtained as a pale yellow solid in 84% yield after purification using silica column and $CH_2Cl_2$/hexane (1:2) as eluent. Calc. for $C_{17}H_9S_2N$: C, 70.10; H, 3.11; N, 4.81. Found: C, 68.96; H, 3.43; N, 4.47.

**5′′,5′′-Bis(trimethylsilylethynyl)-6,6′-bis(2′′-thienyl)-3,3′-bipyridine 7a** :Similar procedures as for **4a** were adopted using 5′,5′′-Dibromo-6,6′-Bis(2′′-thienyl)-3,3′-bipyridine (1.2 g, 2.51 mmol) to produce a bright yellow trimethylsilylethynyl-derivative **7a** in 52% yield (0.66 g). Calc. for $C_{28}H_{28}Si_2S_2N_2$: C, 65.50; H, 5.50; N, 5.46. Found: C, 64.10; H, 5.22; N, 5.29.

**5′′,5′′-Di(ethynyl)-6,6′-Bis(2′′-thienyl)-3,3′-bipyridine 7b**: Compound **7b** was synthesised from **7a** adopting the similar procedure as above for **4b**. However, the product **7b** was only sparingly soluble in organic solvents and that made purification difficult. It was sparingly soluble in THF, and was purified by passing a THF solution through a silica column and washing the residue with hexane. The product, after work up, was not sufficiently pure to proceed to the organometallic polymerisation reaction where an accurate 1:1 ratio is required.

***Trans*-[$(Et_3P)_2$PhPt-C≡CRC≡C-PtPh$(PEt_3)_2$] 1c (R = 1-(2-ethylhexyloxy)-4-methoxy-benzene-2,5-diyl).** To a stirred solution of *trans*-[$(PEt_3)_2$(Ph)PtCl] (0.598 g, 1.10 mmol) and **1b** (0.142 g, 0.50 mmol, freshly prepared from **1a**) in $^iPr_2NH/CH_2Cl_2$

(50 $cm^3$, 1:1 v/v) under nitrogen was added CuI (5 mg). The yellow solution was stirred at room temperature for 15 h, after which all volatile components were removed under reduced pressure. The residue was dissolved in $CH_2Cl_2$ and passed through a silica column eluting with hexane/$CH_2Cl_2$ (1:1 v/v). Removal of the solvents under *vacuo* gave **1c** as a light yellow solid in 75% yield (0.49 g). IR ($CH_2Cl_2$): $\nu/cm^{-1}$ 2096 (C≡C). $^1H$ NMR (250 MHz, $CDCl_3$): δ 7.33 (s, 1H, $H_6$), 7.32 (s, 1H, $H_3$), 6.94 (dd, 4H, $H_{ortho}$ of Ph), 6.78 (dd, 4H, $H_{meta}$ of Ph), 6.73 (s, 2H, $H_{para}$ of Ph), 3.88 (d, 2H, $H_{1'}$), 3.75 (s, 3H, O-$CH_3$), 1.80-1.76 (m, 24H, P-$CH_2$), 1.72 (m, 1H, $H_{2'}$), 1.51 -1.09 (m, 8H, $H_{3'}$, $_{4'}$, $_{5'}$, $_{2''}$), 1.07 (m, 36H, P-$CH_2CH_3$), 0.89 (t, 6H, $H_{6'}$, $_{3''}$). $^{13}C\{^1H\}$-NMR (100.6 MHz, $CDCl_3$): δ 153.79 ($C_4$), 153.15 ($C_1$), 139.32-120.99 (Ph Cs), 117.42 ($C_6$), 116.84 ($C_3$), 116.41 ($C_2$), 115.96 ($C_5$), 106.57, 106.29 (C≡C), 72.05 ($C_{1'}$), 56.53 (O-$CH_3$), 39.18 ($C_{2'}$), 30.19 ($C_{3'}$), 29.00 ($C_{4'}$), 23.47($C_{2''}$), 23.19 ($C_{5'}$), 15.10 (P-$CH_2$), 14.14 ($C_{6'}$), 10.88 ($C_{3''}$), 8.02 (P-$CH_2CH_3$). $^{31}P\{^1H\}$-NMR (101.3 MHz, $CDCl_3$): δ −131.25, $^1J_{Pt\text{-}P}$ = 2620 Hz. FAB-MS: 1299 $M^+$. (Found: C, 50.75; H, 7.17. Calc. for $C_{55}H_{92}O_2P_4Pt_2$: C, 50.84; H, 7.13%.

***Trans*-[$(Et_3P)_2$PhPt-C≡CRC≡C-PtPh$(PEt_3)_2$] 2c (R = quinoline-5,8-diyl).** This was prepared as in **1c** but using **2b** instead of **1c** affording the required complex as a brownish-yellow solid in 65% isolated yield (0.386 g). IR ($CH_2Cl_2$): $\nu/cm^{-1}$ 2095 (C≡C). $^1H$ NMR (250 MHz, $CDCl_3$): δ 8.83 (dd, 1H, $H_2$), 8.76 (dd, 1H, $H_4$), 7.55 (d, 1H, $H_7$), 7.36 (d, 1H, $H_6$), 7.32 (dd, 1H, $H_3$), 6.96 (dd, 4H, $H_{meta}$ of Ph), 6.89 (dd, 4H, $H_{ortho}$ of Ph), 6.81 (dd, 2H, $H_{para}$ of Ph), 1.76 (q, 24H, P-$CH_2$), 1.09 (t, 36H, P-$CH_2CH_3$). $^{13}C\{^1H\}$-NMR (100 MHz, $CDCl_3$): δ 150.62 ($C_2$), 147.97 (d, $C_9$), 139.37-120.08 ($C_3$, $C_4$, $C_7$, $C_{10}$, $C_8$, $C_6$, $C_5$, and Ph Cs), 103.47, 103.19 (C≡C), 15.19 (t, P-$CH_2$), 7.89 (q, $CH_3$). $^{31}P\{^1H\}$-NMR (101.3 MHz, $CDCl_3$): δ −131.17, $^1J_{Pt\text{-}P}$ = 2618 Hz. FAB-MS: 1192 ($M^+$). (Found: C, 49.52; H, 6.28. Calc. for $C_{49}H_{75}NP_4Pt_2$: C, 49.37; H 6.34%).

***Trans*-[$(Et_3P)_2$PhPt-C≡CRC≡C-PtPh$(PEt_3)_2$] 3c (R = 2,3-diphenyl-quinoxaline-5,8-diyl).** This complex was synthesized employing the similar reaction conditions described for **2c** but **3b** was used instead of **2b**. The product was purified on preparative TLC plates with hexane/$CH_2Cl_2$ (1:1 v/v) as eluant giving compound **3c** as pale yellow micro-crystals in an isolated yield of 56%. IR ($CH_2Cl_2$): $\nu/cm^{-1}$ 2095

(C≡C). $^1$H NMR (250 MHz, $CDCl_3$): δ 7.60 (s, 2H, $H_{6,7}$), 7.47 (dd, 4H, $H_{ortho}$ of Ph (quinoxaline), 7.33 (dd, 4H, $H_{ortho}$ of Ph (Pt)), 7.26-7.25 (m, 6H, $H_{meta, para}$ of Ph (quinoxaline), 6.95 (dd, 4H, $H_{meta}$ of Ph (Pt), 6.79 (dd, 2H, $H_{para}$ of Ph (Pt), 1.78 (m, 24H, P-$CH_2$),1.02 (q, 36H, P-$CH_2CH_3$). $^{13}C\{^1H\}$-NMR (100.6 MHz, $CDCl_3$): δ 156.92 ($C_{9,10}$) 151.72 ($C_{2,3}$), 142.42 - 121.87 ($C_{5-8}$ and Ph Cs), 107.88 (C≡C), 15.10 (P-$CH_2$), 121.87 (P-$CH_2CH_3$). $^{31}P\{^1H\}$-NMR (101.3 MHz, $CDCl_3$): δ –131.00, $^1J_{Pt-P}$ = 2621 Hz . FAB-MS: 1321.3 ($M^+$). (Found: C, 52.68; H, 6.19. Calc. for $C_{58}H_{82}N_2P_4Pt_2$: C, 52.70; H, 6.26%).

***Trans*-[$(Et_3P)_2$PhPt-C≡CRC≡C-PtPh$(PEt_3)_2$] 4c (R = 2,1,3-benzothiadiazole-4,7-diyl).** Similar procedures as for complex **3c** were adopted using **4b** to produce bright yellow solid in 56% yield. IR ($CH_2Cl_2$): ν/cm$^{-1}$ 2095 (C≡C). $^1$HNMR (250 MHz, $CDCl_3$): δ 7.32 (s, 4H, $H_{ortho}$ of Ph), 7.25 (s, 2H, $H_{5,6}$), 6.96 (t, 4H, $H_{meta}$ of Ph), 6.79 (t, 2H, $H_{para}$ of Ph), 1.87-1.80 (m, 24H, P-$CH_2$), 1.10 (m, 36H, P-$CH_2CH_3$). $^{13}C\{^1H\}$-NMR (100.6 MHz, $CDCl_3$): δ 156.46 ($C_{8,9}$), 139.18 ($C_{5,6}$), 130.30-121.18 (Ph Cs), 119.09 ($C_{4,7}$), 107.48 (C≡C), 15.14 (P-$CH_2$), 8.07 (P-$CH_2CH_3$). $^{31}P\{^1H\}$-NMR (101.3 MHz, $CDCl_3$): δ –131.30, $^1J_{Pt-P}$ = 2619 Hz . FAB-MS: 1199 ($M^+$). Found: C, 46.07; H, 6.12. Calc. for $C_{46}H_{72}N_2P_4SPt_2$: C, 46.07; H, 6.05%.

***Trans*-[$(Et_3P)_2$(Ph)Pt-C≡C-R-C≡C-Pt(Ph)$(PEt_3)_2$] [R = 2-(2′-thienyl)-pyridine] 5c:** Similar procedures as for complex **4c** were adopted using **5b** to produce a bright yellow solid in 39% yield. Calc. for $C_{49}H_{75}P_4Pt_2SN$: C, 48.07; H, 6.18; N, 1.14. Found: C, 48.67; H, 6.13; N, 1.44%.

***Trans*-[$(Et_3P)_2$(Ph)Pt-C≡C-R-C≡C-Pt(Ph)$(PEt_3)_2$] [R =2,5-bis(2′-thienyl)-pyridine 6c :** Complex **6c** was synthesised using the same conditions as described for **5c** by the reaction of **6b**. Calc. for $C_{53}H_{77}P_4Pt_2S_2N$: C, 48.7; H, 5.94; N, 1.07. Found: C, 48.98; H, 5.91; N, 1.04%.

***Trans*-[$(Et_3P)_2$PhPt-C≡C-L3-C≡C-PtPh$(PEt_3)_2$] 7c:** Complex **7c** was synthesised using the similar method to that described for **5c** using **7b** (55.9 mg, 0.15 mmol) and *trans*-[PtPh(Cl)$(PEt_3)_2$] (165 mg, 0.303 mmol) in THF/$NHPr^i_2$ (80 cm$^3$, 1:1 v/v)

because of limited solubility of **7b** in $CH_2Cl_2$. Calc. for $C_{58}H_{80}P_4Pt_2S_2N_2$: C, 50.35; H, 5.83; N, 2.02. Found: C, 49.33; H, 5.22; N, 2.79%.

***Trans*-[–Pt(PBu$_3^n$)$_2$–C≡C–L1–C≡C–]$_n$ 5P:** To a mixture of *trans*-[Pt(PBu$_3^n$)$_2$Cl$_2$] (0.19 g, 0.28 mmol) and one equivalent of **5b** (59.3 mg, 0.28 mmol) in $CH_2Cl_2$/$^i$Pr$_2$NH (60 cm$^3$, 1:1 v/v) was added CuI (3 mg). The mixture was stirred at room temperature for 18 h, after which all volatile components were removed under reduced pressure. The residue was redissolved in $CH_2Cl_2$ and filtered through a short alumina column. After removal of solvent on a rotary evaporator, a yellow residue was obtained which was purified by precipitation from $CH_2Cl_2$/hexane to produce a deep yellow polymer **5P** in 94% yield (0.2 g). Calc. for $[C_{37}H_{59}SNP_2Pt]_n$: C, 59.65; H, 7.98: N, 1.88. Found: C, 54.76; H, 7.35; N, 1.76%.

***Trans*-[–Pt(PBu$_3^n$)$_2$–C≡C–L2–C≡C–]$_n$ 6P:** The diterminal diyne **6b** (17.3 mg, 0.06 mmol) was dissolved in 100 ml $^i$Pr$_2$NH and heated at 95°C for 30 min. *Trans*-[Pt(PBu$_3^n$)$_2$Cl$_2$] (39.8 mg, 0.06 mmol) was added followed by CuI (2 mg). The reaction mixture was then heated under reflux for a further 24 h, after which all volatile components were removed under reduced pressure. The mixture was worked up as described for **5P** to produce a deep yellow rubbery polymer **6P** in 75% yield (0.04 g). Calc. for $[C_{41}H_{61}S_2NP_2Pt]_n$: C, 55.38; H, 6.92: N, 1.57. Found: C, 53.51; H, 6.64: N, 1.46%.

# 6.3 References


1) W. L. F. Armarego, D. D. Perrin, Purification of Laboratory Chemicals, 4$^{th}$ edn, Butterworth-Heinemann, Guildford, UK , **1996**.
2) K. Siegmann, P.S. Pregosin and L.M. Venanzi, *J. Organomet. Chem.*, **1989**, 8, 2659.
3) G.B. Kaufmann and L.A. Teter, *Inorg. Synth.*, **1963**, 7, 248.
4) J.E. Parks, B.E. Wagner and R.H. Holm, *J. Organomet. Chem.*, **1973**, 56, 53.
5) (a) F.M. Romero and R. Ziessel, *Tet. Lett.*, **1995**, 36, 6471.(b) E.C. Constable and J. Lewis, *Polyhedron*, **1982**, 1, 303.
6) (a) T. Kanbara N. Saito, T. Yamammoto, K. Kubota, *Macromolecules*, **1991**, 24, (b) T. Yamamoto, T. Maruyama, Z. Zhen-H; Ito, T. F. Takayori,

Y. Yoneda, F. Begum, T. Ikeda,; S. Sasaki, *J. Am. Chem. Soc.*, **1994**, 116(11), 4832-45.

7) (a) P. Li, B. Ahrens, N. Feeder,; P. R. Raithby, S. Teat, M. S. Khan., *Dalton Transactions* **2005**, (5), 874-883. (b) D. R. Rutherford, J. K. Stille, M. C. Elliott, V. R. Reichert., **1992**, 25(9), 2294-306.

8) K. Pilgram, M. Zupan and R. Skiles, *J. Heterocycl. Chem.*, **1970**, 7, 629.

9) Y. Tsubata, T. Suzuki, and T. Miyashi, *J. Org. Chem.*, **1992**, 57, 6749.

10) M. Kiamuddin and M.E. Haque, *Chem. Ind.* **1964**, 1753.

11) C.J. Neef and J.P. Ferraris, *Macromolecules*, **2000**, 33, 2311.

12) Z.-H. Zhou, T. Maruyama, T. Kanbara, T. Ikeda, K. Ichimura, T. Yamamoto and K. Tokuda, *J. Chem. Soc. Chem. Commun.*, **1991**, 1210. (b) I. H. Jenkins, N. G. Rees and P. G. Pickup, *Chem. Mater.*, **1997**, 9, 1213.

Papers published as a result of the work carried out in this thesis

1) "Structural characterisation of a series of acetylide-functionalised oligopyridines and the synthesis, characterisation and optical spectroscopy of platinum di-ynes and poly-ynes containing oligopyridyl linker groups in the backbone", M. S. Khan, M. R. A. Al-Mandhary, M. K. Al-Suti, A. Hisahm, P. R. Raithby, B. Ahrens, M. F Mahon, L. Male, E. A. Marseglia, E. Tedesco, R. H Friend, A. Koehler, N. Feeder and S. J Teat, *Dalton Transactions*, **2002**, 7, 1358-1368.

2) "Synthesis, characterization and electronic properties of a series of platinum(II) poly-ynes containing novel thienyl-pyridine linker groups", M. S. Khan, M. R. A. Al-Mandhary, M. K. Al-Suti, N. Feeder,; S. Nahar,; A. Koehler, R. H. Friend, P. J Wilson and P. R Raithby., *Dalton Transactions*, **2002**, 12, 2441-2448.

3) "Synthesis and characterization of new acetylide-functionalized aromatic and hetero-aromatic ligands and their dinuclear platinum complexes", M. S. Khan, M. K. Al-Suti, M. R. A. Al-Mandhary, B. Ahrens, J. K. Bjernemose, M. F Mahon, L. Male, P. R. Raithby, R. H. Friend, A. Koehler and J. S. Wilson., *Dalton Transactions*, **2003**, 1, 65-73.

4) "Synthesis and optical characterisation of platinum(II) poly-yne polymers incorporating substituted 1,4-diethynylbenzene derivatives and an investigation of the intermolecular interactions in the diethynylbenzene molecular precursors", M. S. Khan, M. R. A. Al-Mandhary, M. K. Al-Suti, T. C Corcoran, Y. Al-Mahrooqi, P. J. Attfield, N. Feeder, W. I. F David, K. Shankland, R. H Friend, A. Koehler, E. A Marseglia, E. Tedesco, C. C. Tang, P. R. Raithby, J. C. Collings, K. P. Roscoe, A. S Batsanov, L. M. Stimson and T. B. Marder., *New Journal of Chemistry*, **2003**, 27(1), 140-149.

5) "Synthesis, characterization and optical spectroscopy of platinum(II) di-ynes and poly-ynes incorporating condensed aromatic spacers in the backbone", M. S. Khan, M. R. A. Al-Mandhary, M. K. Al-Suti, F. R Al-Battashi, S. Al-Saadi, B. Ahrens, J. K. Bjernemose, M. F Mahon, P. R. Raithby, M. Younus, N. Chawdhury, A. Koehler, E. A. Marseglia, E. Tedesco, N. Feeder and S. J. Teat., *Dalton Transactions*, **2004**, 15, 2377-2385.

# APPENDIX B

## CRYSTALLOGRAPIC DATA